Antibodies against *P. falciparum* glycosylphosphatidylinositol epitopes

Inaugural-Dissertation

to obtain the academic degree

Doctor rerum naturalium (Dr. rer. nat.)

submitted to the Department of Biology, Chemistry and Pharmacy

of Freie Universität Berlin

by

Jonnel Anthony Jaurigue

2019

The presented work was performed

at the Max Planck Institute of Colloids and Interfaces

in the Department of Biomolecular Systems

and at Freie Universität Berlin

in the Department of Biology, Chemistry and Pharmacy

under the supervision of Prof. Dr. Peter H. Seeberger

between June 15th 2015 and June 14th 2019

1st Reviewer: Prof. Dr. Peter H. Seeberger

2nd Reviewer: Prof. Dr. Kevin Pagel

date of defense: 27th November 2019

Acknowledgements

First and foremost I thank my supervisor Prof. Dr. Peter Seeberger for his guidance and inspirational leadership throughout my doctoral study. I am honoured to be part of the Seeberger family.

I thank Prof. Dr. Kevin Pagel for kindly agreeing to review this thesis.

I thank all members of the Vaccine group, particularly Dr. Felix Bröcker, Paulina Kaplonek, Bruna Seco, Katrin Sellrie, and Annette Wahlbrink. I especially want to thank Dr. Andreas Geißner for all his expertise and fruitful discussions.

I thank the rest of the past and present Arnimallee crew, particularly Magdalena Zaslona, Adam Peters, Felix Gördeler, Sana Khilji, Jost Lühle, Prof. Dr. Bernd Lepenies, Dr. Fridolin Steinbeis, and Dr. Falko Schirmeister. I especially want to thank Dr. Oren Moscovitz and Dr. Christian Roth for sharing their extensive experience regarding scientific thinking, writing, and presentation.

I thank the rest of the Biomolecular Systems department, particularly Dr. Ankita Malik and Dr. Daniel Varón Silva for their synthetic chemistry expertise.

I thank PD Dr. med. Florian Kurth and Dr. Clemens Kocken for providing valuable samples.

Finally, I thank Dr. Lina Jaurigue for all of her support.

Contents

Acknowledgements iii

Contents 1

List of abbreviations 7

List of monosaccharides 9

Lists of tables and figures 11

Summary 25

Zusammenfassung 27

1 Introduction 29

1.1 Malaria 29

Prevalence 29

Lifecycle 30

Evasion mechanisms 33

1.2 Malaria disease 34

Signs and symptoms 34

Severe malaria pathogenesis 35

Acquired immunity 37

1.3 Malaria treatment 39

Current measures 39

Mass drug treatment 39

Drug resistance 40

1.4 Malaria vaccine development 40

Current status 40

Liver stage vaccines 41

Blood stage vaccines 42

1.5 GPIs as vaccine antigens 44

Attractive targets 44

Structure and function 44

Signalling and inflammation 45

Naturally occurring antibodies against GPI 46

Synthetic GPI 46

1.6 Aim of this study 49

2 Materials & Methods 51

2.1 Glycoconjugate preparation 51

Preparation of minimal epitope antigen glycoconjugates 51

Sodium dodecyl sulfate polyacrylamide gel electrophoresis 51

Formulation with adjuvant 52

Adsorption determination.....52

2.2 Immunisation model 52

Animal experiments.....52

Immunisation regime 53

2.3 Challenge model with *P berghei* ANKA 54

Preparation of parasite stabilates 54

Infection with parasite.....54

2.4 Synthetic GPI epitope libraries.....55

Preparation of microarray slides.....55

Glycan microarray analysis for epitope mapping.....56

2.5 Cell culture techniques.....57

P. falciparum 3D7 cell culture 57

Monoclonal hybridoma production 57

RAW 264.7 macrophage cell culture.....58

2.6 *In vitro* analysis techniques 59

Fluorescent microscopy of *P. falciparum* 3D7.....59

Flow cytometry of *P. falciparum* 3D7.....59

Fluorescent microscopy of *L. mexicana* 60

TNF- α release of RAW 264.7 macrophages assay 60

Merozoite invasion-inhibition assay 61

Western blot with isolated *P. falciparum* GPI 61

3 Results and Discussion 63

3.1 Elucidating immunogenic GPI residues 63

Profiling antibodies induced by various synthetic GPI fragments 63

Profiling of previously published monoclonal antibodies 69

3.2 Design of synthetic minimal epitope fragments 72

Rationale for design 72

Profiling induced antibodies against minimal epitope fragments 75

3.3 Elucidating whether synthetic GPI fragments are a proxy for native GPI 81

Profiling pooled sera antibodies 81

Profiling individual infected monkey sera antibodies 84

Profiling antibodies in individual human sera 90

3.4 Inducing antibodies to epitopes of the GPI terminus 100

Minimum dose of glycoconjugate required 100

Preparation of glycoconjugates using the minimal epitope antigens 103

Profiling antibodies induced by minimal epitope antigens 105

Isotype ratios to determine Th1 or Th2 biases 110

3.5 ECM challenge study 112

Immunisation did not affect experiment cerebral malaria outcome 112

3.6 *In vitro* analysis of terminal epitope-specific antibodies 115

Binding of antibodies to *P. falciparum* 115

Effect of antibodies on merozoite-induced TNF-α release 119

Binding of antibodies to *L. mexicana* 121

3.7 Monoclonal antibody specific to the GPI terminus 123

Immunisation of mice and subsequent antibody profiling 123

mAb binds to the minimal epitope 126

Effect of mAb on *in vitro* parasitemia and TNF-α release 130

Binding of mAb to *L. mexicana* 132

4 Conclusions & Outlook 137

Bibliography 141

Publications 157

Scientific articles 157

Conferences 157

Research Training Group presentations 158

Appendix 161

Minimal dosing test for glycoconjugates of 2 and 5 161

MALDI-TOF spectra for glycoconjugates of 7 and 8 163

Determining that the stabilates mice work only from Janvier mice 165

Determining that glycoconjugates remain intact after freezing 167

Preliminary immunisation study for glycoconjugates of 7 and 8 169

Immunisation with a synthetic hexasaccharide glycoconjgugate 172

Additional glycan array data during the immunisation study 174

Additional mouse data during the ECM challenge study 198

Curriculum Vitae 199

List of abbreviations

ACT	artemisinin-based combination therapy
Alum	aluminium hydroxide
AMA-1	apical membrane antigen 1
ANKA	NK for New York-Katanga, ANKA for Antwerpen-Kasapa
BSA	bovine serum albumin
CFA/IFA	complete and then incomplete Freund's adjuvant
CRM	cross-reacting material
CSP	circumsporozoite protein
Da	dalton
DTT	Dithiothreitol
ECM	experimental cerebral malaria
ELISA	enzyme-linked immunosorbent assay
FBS	foetal bovine serum
FITC	fluorescein isothiocyanate
GlcN	glucosamine
GLURP	Glutamate-Rich Protein
GPI	glycosylphosphatidylinositol
IFN	interferon
Ig	immunoglobulin
IL	interleukin
InoP	myo-inositol-2-phosphate
iRBC	infected red blood cell
LPS	lipopolysaccharide
mAb	monoclonal antibodies
MALDI-TOF	matrix-assisted laser desorption/ionization, time-of-flight

Man	mannose
MFI	mean fluorescence intensity
MSP	merozoite surface protein
PBS	Dulbecco's phosphate buffered saline
PEtN	phosphoethanolamine
RBC	red blood cell
RT	room temperature
SBAP	succinimidyl 3-(bromoacetamido)propionate
SDS-PAGE	sodium dodecyl sulfate polyacrylamide gel electrophoresis
TCEP	Tris(2-carboxyethyl)phosphine
TLR	toll-like receptor
WHO	World Health Organisation

List of monosaccharides

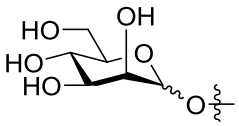

D-Mannose (Man)

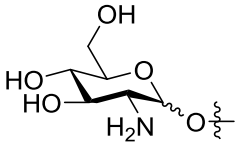

D-Glucosamine (GlcN)

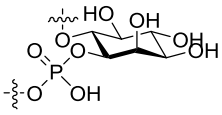

myo-inositol-2-phosphate (InoP)

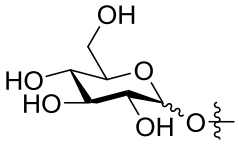

D-Glucose (Glc)

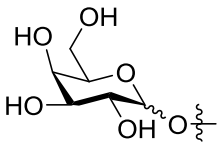

D-Galactose (Gal)

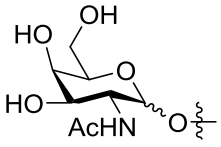

D-*N*-Acetylgalactosamine (GalNAc)

Lists of tables and figures

Table 1: General timeline of the immunisation regime. 54

Table 2: Shorthand notation of structures listed in graphed results. Longer structure names (especially for glycan fragments based on GPI from other organisms) use shorthand notation for ease of visualisation. 66

Table 3: Adsorption values for glycoconjugates of **7** and **8**. 104

Table 4: Adsorption values for glycoconjugates of **1 – 6**. 168

Figure 1: Countries with malaria transmission. Image taken from *World Malaria Report 2018* (WHO 2018). 30

Figure 2: Blood stage merozoite representations. a) Illustration of major organelles. **b)** A *P. falciparum* merozoite in the process of invading a human red blood cell. Scale bar = 200 nm. Image composite taken from *The cellular and molecular basis for malaria parasite invasion of the human red blood cell* (Cowman, Berry et al. 2012). 32

Figure 3: Model for merozoite invasion. Scale = 0.5 µM. Image composite taken from *Super-Resolution Dissection of Coordinated Events during Malaria Parasite Invasion of the Human Erythrocyte* (Riglar, Richard et al. 2011). 32

Figure 4: The complete P. falciparum lifecycle. Image taken from *Malaria* (White, Pukrittayakamee et al. 2014). 33

Figure 5: Overview of disease pathogenesis. Lifecycle context and consequent symptoms of disease are also shown. Image taken from *Innate sensing of malaria parasites* (Gazzinelli, Kalantari et al. 2014). 37

Figure 6: Lifelong exposure confers protection to severe malaria. This is followed by immunity to febrile, uncomplicated malaria, and finally to parasitemia. Image taken from *Malaria* (White, Pukrittayakamee et al. 2014). 38

Figure 7: Targeted stages of the parasite lifecycle. The stage targeted in a malaria vaccine reflects the type of protective effect the vaccine would have. Human liver stage vaccines would combat infection and transmission of the vaccine, while human blood stage vaccines would combat disease symptoms and associated mortality and morbidity. Image taken from *PATH Malaria Vaccine Initiative*. 41

Figure 8: The modes of action of merozoite antigen-specific antibodies. Functions include interfering with red blood cell invasion, disrupt intracellular replication, target iRBCs for destruction, or neutralize the parasite inflammatory toxins. Image taken from *Functional Antibodies and Protection against Blood-stage Malaria* (Teo, Feng et al. 2016). 43

Figure 9: The P. falciparum GPI anchor. The Man IV residue is absent in free GPI. .. 45

Figure 10: A selection of synthetic GPI fragments. These were printed on glycan arrays, and glycoconjugates thereof were used to immunise mice. **(1-3)** Fragments with a trimannose backbone. **1)** PEtN-Man_3-GlcN-InoP. Note the displacement of PEtN to Man-II. **2)** PEtN-Man_3-GlcN. **3)** Man_3-GlcN. **(4-6)** Fragments with a tetramannose backbone. **4)** PEtN-Man_4-GlcN-InoP. **5)** PEtN-Man_4-GlcN. **6)** Man_4-GlcN. 66

Figure 11: IgG titres against synthetic GPI fragments in sera at day 42. Group size n=15, classified by the immunising glycoconjugate. **Top panel (a-c)** IgG titres after immunisation with glycoconjugates of **1-3** lacking the fourth Man. **Bottom panel (d-f)** IgG titres after immunisation with glycoconjugates of **4-6** containing the fourth Man. 67

Figure 12: IgM titres against synthetic GPI fragments in sera at day 42. Group size n=15, classified by the immunising glycoconjugate. **Top panel (a-c)** IgM titres after immunisation with glycoconjugates of **1-3** lacking the fourth Man. **Bottom panel (d-f)** IgM titres after immunisation with glycoconjugates of **4-6** containing the fourth Man. ... 67

Figure 13: IgG titres against synthetic GPI in other organisms in sera at day 42. Group size n=15, classified by the immunising glycoconjugate. **Top panel (a-c)** IgG titres after immunisation with glycoconjugates of **1-3** lacking the fourth Man. **Bottom panel (d-f)** IgG titres after immunisation with glycoconjugates of **4-6** containing the fourth Man. 68

Figure 14: IgM titres against synthetic GPI in other organisms in sera at day 42. Group size n=15, classified by the immunising glycoconjugate. **Top panel (a-c)** IgM titres after immunisation with glycoconjugates of **1-3** lacking the fourth Man. **Bottom panel (d-f)** IgM titres after immunisation with glycoconjugates of **4-6** containing the fourth Man. 68

Figure 15: The synthetic Man4-GlcN-InoP- fragment used to generate mAb. Note the inclusion of the InoP residue and absence of the PEtN moiety. 71

Figure 16: MTG mAb binding profiles. Top panel (a-c) IgG3 titres against synthetic *P. falciparum* GPI. **Bottom panel (d-f)** IgG3 titres against synthetic GPI from other organisms. 71

Figure 17: The minimal epitope antigens. The full GPI is shown in grey for context. **7)** PEtN-Man_3 focuses on the non-reducing terminus of free GPI. **8)** PEtN-Man_4 includes the fourth mannose specific to *P. falciparum* GPI. 74

Figure 18: The minimal GPI epitope for naturally-occurring antibodies. PEtN-Man3 minimal epitope antigen (black) is smaller than the pentasaccharide epitope containing GlcN-InoP (blue). The full GPI is shown in grey for context. 74

Figure 19: IgG1 titres against synthetic GPI fragments in sera at day 42. Group size n=15, classified by the immunising glycoconjugate. **Top panel (a-c)** IgG1 titres after immunisation with glycoconjugates of **1-3** lacking the fourth Man. **Bottom panel (d-f)** IgG1 titres after immunisation with glycoconjugates of **4-6** containing the fourth Man....77

Figure 20: IgG2a titres against synthetic GPI fragments in sera at day 42. Group size n=15, classified by the immunising glycoconjugate. **Top panel (a-c)** IgG2a titres after immunisation with glycoconjugates of **1-3** lacking the fourth Man. **Bottom panel (d-f)** IgG2a titres after immunisation with glycoconjugates of **4-6** containing the fourth Man..77

Figure 21: IgG3 titres against synthetic GPI fragments in sera at day 42. Group size n=15, classified by the immunising glycoconjugate. **Top panel (a-c)** IgG3 titres after immunisation with glycoconjugates of **1-3** lacking the fourth Man. **Bottom panel (d-f)** IgG3 titres after immunisation with glycoconjugates of **4-6** containing the fourth Man....78

Figure 22: IgM titres against synthetic GPI fragments in sera at day 42. Group size n=15, classified by the immunising glycoconjugate. **Top panel (a-c)** IgM titres after immunisation with glycoconjugates of **1-3** lacking the fourth Man. **Bottom panel (d-f)** IgM titres after immunisation with glycoconjugates of **4-6** containing the fourth Man. ... 78

Figure 23: IgG1 titres against synthetic GPI fragments in other organisms in sera at day 42. Group size n=15, classified by the immunising glycoconjugate. **Top panel (a-c)** IgG1 titres after immunisation with glycoconjugates of **1-3** lacking the fourth Man. **Bottom panel (d-f)** IgG1 titres after immunisation with glycoconjugates of **4-6** containing the fourth Man. 79

Figure 24: IgG2a titres against synthetic GPI fragments in other organisms in sera at day 42. Group size n=15, classified by the immunising glycoconjugate. **Top panel (a-c)** IgG2a titres after immunisation with glycoconjugates of **1-3** lacking the fourth Man. **Bottom panel (d-f)** IgG2a titres after immunisation with glycoconjugates of **4-6** containing the fourth Man. 79

Figure 25: IgG3 titres against synthetic GPI fragments in other organisms in sera at day 42. Group size n=15, classified by the immunising glycoconjugate. **Top panel (a-c)** IgG3 titres after immunisation with glycoconjugates of **1-3** lacking the fourth Man. **Bottom panel (d-f)** IgG3 titres after immunisation with glycoconjugates of **4-6** containing the fourth Man. 80

Figure 26: IgM titres against synthetic GPI fragments in other organisms in sera at day 42. Group size n=15, classified by the immunising glycoconjugate. **Top panel (a-c)** IgM titres after immunisation with glycoconjugates of **1-3** lacking the fourth Man. **Bottom panel (d-f)** IgM titres after immunisation with glycoconjugates of **4-6** containing the fourth Man. 80

Figure 27: Antibody titres against synthetic GPI from pooled sera. Top panel (a-c) IgG titres. Profiles of **a) 10-198** pooled sera from Kenya, **b) 09-222** pooled sera control, **c) 99-706** pooled sera control. **Bottom panel (d-f)** IgM titres. Profiles of **d) 10-198** pooled sera from Kenya, **e) 09-222** pooled sera control, **f) 99-706** pooled sera control. 83

Figure 28: Antibody titres against synthetic GPI in other organisms from pooled sera. Top panel (a-c) IgG titres. Profiles of **a) 10-198** pooled sera from Kenya, **b) 09-222**

pooled sera crol, **c) 99-706** pooled sera control. **Bottom panel (d-f)** IgM titres. Profiles of **d) 10-198** pooled sera from Kenya, **e) 09-222** pooled sera control, **f) 99-706** pooled sera control.....83

Figure 29: IgG titres against synthetic *P. falciparum* GPI fragments in sera from monkeys experiencing controlled infection. Pre- (serum timepoint 0) and post-infection (serum timepoint 4) IgG titres in sera of monkeys (n=6) were compared using paired T-test. Significant differences ($p<0.05$) indicate that antibodies cross-reactive to the synthetic GPI fragment were induced after infection.. 86

Figure 30: IgG titres against synthetic GPI fragments from other organisms in sera from monkeys experiencing controlled infection. Pre- (serum timepoint 0) and post-infection (serum timepoint 4) IgG titres in sera of monkeys (n=6) were compared using paired T-test. Significant differences ($p<0.05$) indicate that antibodies cross-reactive to the synthetic GPI fragment were induced after infection.. 87

Figure 31: IgM titres against synthetic *P. falciparum* GPI fragments in sera from monkeys experiencing controlled infection. Pre- (serum timepoint 0) and post-infection (serum timepoint 4) IgM titres in sera of monkeys (n=6) were compared using paired T-test. Significant differences ($p<0.05$) indicate that antibodies cross-reactive to the synthetic GPI fragment were induced after infection.. 88

Figure 32: IgG titres against synthetic GPI fragments from other organisms in sera from monkeys experiencing controlled infection. Pre- (serum timepoint 0) and post-infection (serum timepoint 4) IgG titres in sera of monkeys (n=6) were compared using paired T-test. Significant differences ($p<0.05$) indicate that antibodies cross-reactive to the synthetic GPI fragment were induced after infection. 89

Figure 33: IgG titres in sera from naïve patients experiencing primary infection against synthetic *P. falciparum* **GPI fragments.** Early and late IgG titres in sera of patients (n=16) were compared using paired T-test. Significant differences ($p<0.05$) indicate that antibodies cross-reactive to the synthetic GPI fragment were induced after infection.....92

Figure 34: IgG titres in sera from naïve patients experiencing primary infection against synthetic GPI fragments from other organisms. Early and late IgG titres in sera

of patients (n=16) were compared using paired T-test. Significant differences ($p<0.05$) indicate that antibodies cross-reactive to the synthetic GPI fragment were induced after infection. 93

Figure 35: IgG titres in sera from patients with previous exposure against synthetic *P. falciparum* GPI fragments. Early and late IgG titres in sera of patients (n=6) were compared using paired T-test. Significant differences ($p<0.05$) indicate that antibodies cross-reactive to the synthetic GPI fragment were induced after infection. 94

Figure 36: IgG titres in sera from patients with previous exposure against synthetic GPI fragments from other organisms. Early and late IgG titres in sera of patients (n=6) were compared using paired T-test. Significant differences ($p<0.05$) indicate that antibodies cross-reactive to the synthetic GPI fragment were induced after infection. 95

Figure 37: IgM titres in sera from naïve patients experiencing primary infection against synthetic *P. falciparum* GPI fragments. Early and late IgM titres in sera of patients (n=16) were compared using paired T-test. Significant differences ($p<0.05$) indicate that antibodies cross-reactive to the synthetic GPI fragment were induced after infection. 96

Figure 38: IgM titres in sera from naïve patients experiencing primary infection against synthetic GPI fragments from other organisms. Early and late IgM titres in sera of patients (n=16) were compared using paired T-test. Significant differences ($p<0.05$) indicate that antibodies cross-reactive to the synthetic GPI fragment were induced after infection. 97

Figure 39: IgM titres in sera from patients with previous exposure against synthetic *P. falciparum* GPI fragments. Early and late IgM titres in sera of patients (n=6) were compared using paired T-test. Significant differences ($p<0.05$) indicate that antibodies cross-reactive to the synthetic GPI fragment were induced after infection. 98

Figure 40: IgM titres in sera from patients with previous exposure against synthetic GPI fragments from other organisms. Early and late IgM titres in sera of patients (n=6) were compared using paired T-test. Significant differences ($p<0.05$) indicate that antibodies cross-reactive to the synthetic GPI fragment were induced after infection. 99

Figure 41: IgG titres against synthetic GPI fragments in sera at day 42. Group size n=3, classified by glycan antigen dose. **Top panel (a-c)** IgG titres after immunisation with glycoconjugates of **1-3** lacking the fourth Man. **Bottom panel (d-f)** IgG titres after immunisation with glycoconjugates of **4-6** containing the fourth Man. 102

Figure 42: IgM titres against synthetic GPI fragments in sera at day 42. Group size n=3, classified by glycan antigen dose. **Top panel (a-c)** IgM titres after immunisation with glycoconjugates of **1-3** lacking the fourth Man. **Bottom panel (d-f)** IgM titres after immunisation with glycoconjugates of **4-6** containing the fourth Man. 102

Figure 43: SDS-PAGE analysis of glycoconjugates of 7 & 8. Bands are compared to non-conjguated **CRM197** and molecular weight **ladder**. Numbers to the right indicate the molecular weight of marker bands in kDa. 104

Figure 44: Antibody titres against synthetic *P. falciparum* GPI fragments in sera at day 42. Group size n=10, immunised with glycoconjugate of **7**. **Top panel (a-b)** IgG1 and IgG2a titres. **Bottom panel (c-d)** IgG3 and IgM titres. 107

Figure 45: Antibody titres against synthetic *P. falciparum* GPI fragments in sera at day 42. Group size n=10, immunised with glycoconjugate of **8**. **Top panel (a-b)** IgG1 and IgG2a titres. **Bottom panel (c-d)** IgG3 and IgM titres. 107

Figure 46: Antibody titres against synthetic GPI fragments from other organisms in sera at day 42. Group size n=10, immunised with glycoconjugate of **7**. **Top panel (a-b)** IgG1 and IgG2a titres. **Bottom panel (c-d)** IgG3 and IgM titres. 108

Figure 47: Antibody titres against synthetic GPI fragments from other organisms in sera at day 42. Group size n=10, immunised with glycoconjugate of **8**. **Top panel (a-b)** IgG1 and IgG2a titres. **Bottom panel (c-d)** IgG3 and IgM titres. 108

Figure 48: Antibody titres in sera from mice immunised with 7 [green], 8 [orange], or CRM197 only [blue]. IgM titres increase early, while IgG titres arise later, typical of a primary antibody response. **Top panel (a-c)** Antibody titres against fragment **7**. **Bottom panel (d-f)** Antibody titres against fragment **8**.....109

Figure 49: IgG1/IgG2a titre ratios in sera at day 42. Top panel (a-f) Average titre ratios after immunisation with glycoconjugates **1-6**. **Bottom panel (g-h)** Average titre ratios after immunisation with glycoconjugates of **7** and **8** suggest an IgG1 bias. 111

Figure 50: ECM challenge shows no difference between immunised groups. a) Glycoconjugate immunisation did not affect development of neurological symptoms compared to CRM197 control group. **b)** Glycoconjugate immunisation did not affect the disease score during infection compared to CRM197 control group. Mice were euthanized at a cumulative disease score of 3, and were assigned a score of 4 thereafter, increasing the disease score..... 114

Figure 51: Parasitemia of mice at day 6 post-infection. A significant difference between mice immunised with glycoconjugate of **8** and CRM197 only was observed... 114

Figure 52: Binding of IgG against merozoites of iRBCs. Fixed iRBCs were incubated with pooled mouse sera and then labelled to show DNA [blue] and bound IgG [red]. **a)** Day 0, before glycoconjugate of **7** immunisation. **b)** Day 42, after glycoconjugate of **7** immunisation. **c)** Day 0, before glycoconjugate of **8** immunisation. **d)** Day 42 after glycoconjugate of **8** immunisation. **e)** Day 0 before CRM197 control immunisation. **f)** Day 42 after CRM197 control immunisation. 117

Figure 53: Binding of IgG against merozoites. Mice immunised with glycoconjugate of **7** [orange], **8** [blue], or CRM197 control [grey] were compared in flow cytometry. Increased titre of bound IgG to iRBCs is represented by an increased APC-A peak shift away from day 7 baseline [grey bar]. **a)** Day 7, early after immunisation. **b)** Day 35, late after immunisation. 118

Figure 54: TNF-α concentrations in reaction wells with pooled sera of mice before and after immunisation at varying dilutions. Sera from mice at day 0 before immunisation (grey) were compared to sera from mice at day 42 after immunisation (black). Dotted line indicates the lowest level of TNF-α release achieved. Error bars indicate 95% CI. **a)** Group immunised with glycoconjugate **7**. **b)** Group immunised with glycoconjugate **8**. **c)** Group immunised with CRM197 control. 120

Figure 55: Binding of IgG against *L. mexicana*. Fixed *L. mexicana* parasites were incubated with pooled mouse sera and then labelled to show DNA [blue] and bound IgG

[red]. **a)** Day 0, before glycoconjugate of **7** immunisation. **b)** Day 42, after glycoconjugate of **7** immunisation. **c)** Day 42, after CRM197 control immunisation. 122

Figure 56: Antibody titres in sera at day 35 against synthetic *P falciparum* GPI fragments. Top panel (a-d) Antibody titres after immunisation with glycoconjugate of **7**. **Bottom panel (e-h)** Antibody titres after immunisation with glycoconjugate of **2**. 124

Figure 57: Antibody titres in sera at day 35 against synthetic GPI fragments from other organisms. Top panel (a-d) Antibody titres after immunisation with glycoconjugate of **7**. **Bottom panel (e-h)** Antibody titres after immunisation with glycoconjugate of **2**. 125

Figure 58: Monoclonal antibody binding specificities in sera at day 35 against synthetic *P falciparum* GPI fragments. (a-b) Antibody titres after immunisation with glycoconjugate of **7**. **(c)** Antibody titres after immunisation with glycoconjugate of **2**. ..128

Figure 59: 2D10D2C6 mAb titres against synthetic GPI fragments. Top panel (a-c) mAb binding against *P. falciparum* GPI. **a)** 40 µg/mL **b)** 1.25 µg/mL **c)** 0.0391 µg/mL. **Bottom panel (d-f)** mAb binding against GPI from other organisms. **d)** 40 µg/mL **e)** 1.25 µg/mL **f)** 0.0391 µg/mL. 128

Figure 60: Binding concentration curves of mAb against specific GPI fragments. Top panel (a-c) mAb binding against *P. falciparum* GPI. **a)** Fragment **7**. **b)** Fragment **2**. **c)** Fragment **1**. **Bottom panel (d-f)** mAb binding against GPI from other organisms. **d)** Fragment **Tgon1.1**. **e)** Fragment **Tgon1.2**. **f)** Fragment **Mamm1.1**.....129

Figure 61: mAb raised by glycoconjugate of 7 bind to GPI isolated from *P. falciparum*. Image courtesy of S. Khilji. 129

Figure 62: Parasitemia in cell culture with varying amounts of 2D10D2C6 mAb. a) After 1 cycle, at 48 hours. **b)** After 2 cycles, at 96 hours. 131

Figure 63: Dose-dependent TNF-α release. Concentration of 2D10D2C6 mAb, up to 40 µg/mL, compared to TNF-α concentration in cell culture. 131

Figure 64: Binding of mAb against *L. mexicana*. Fixed *L. mexicana* amastigotes expressing DsRed [orange] were incubated with 2D10D2C6 mAb and then labelled to

show DNA [blue] and bound IgM [red]. 2D10D2C6 mAb added at **a)** 10 µg/mL, **b)** 1 µg/mL, **c)** 0.1 µg/mL, **d)** 0.01 µg/mL. 133

Figure 65: Binding of control IgM mAb against *L. mexicana*. Fixed *L. mexicana* amastigotes expressing DsRed [orange] were incubated with control IgM mAb and then labelled to show DNA [blue] and bound IgM [red]. Control IgM mAb added at **a)** 10 µg/mL, **b)** 1 µg/mL, **c)** 0.1 µg/mL. **d)** No mAb added. 134

Figure 66: Binding of mAb against *L. mexicana*. Fixed *L. mexicana* promastigotes were incubated with 2D10D2C6 mAb and then labelled to show DNA [blue] and bound IgM [red]. 2D10D2C6 mAb added at **a)** 10 µg/mL, **b)** 1 µg/mL, **c)** 0.1 µg/mL, **d)** 0.01 µg/mL. 135

Figure 67: Binding of control IgM against *L. mexicana*. Fixed *L. mexicana* promastigotes were incubated with control IgM mAb and then labelled to show DNA [blue] and bound IgM [red]. Control IgM mAb added at **a)** 10 µg/mL, **b)** 1 µg/mL, **c)** 0.1 µg/mL. **d)** No mAb added. 136

Figure 68: Antibody titres against synthetic GPI fragments in sera at day 35. Group size n=4. **Top panel (a-c)** IgG isotype titres of mice immunised with glycoconjugate of **2**. **Bottom panel (d-f)** IgG isotype titres of mice immunised with glycoconjugate of **5**. 161

Figure 69: Antibody titres against synthetic GPI fragments in other organisms in sera at day 35. Group size n=4. **Top panel (a-c)** IgG isotype titres of mice immunised with glycoconjugate of **2**. **Bottom panel (d-f)** IgG isotype titres of mice immunised with glycoconjugate of **5**. 162

Figure 70: MALDI-TOF spectra for glycoconjugate of 7. a) Activated CRM197 before conjugation to fragment **7**. Mass reported as 60054 Da. **b)** Activated CRM197 conjugated to fragment **7.** Mass reported as 63958 Da. 163

Figure 71: MALDI-TOF spectra for glycoconjugate of 8. a) Activated CRM197 before conjugation to fragment **8**. Mass reported as 60804 Da. **b)** Activated CRM197 conjugated to fragment **8**. Mass reported as 66623 Da. 164

Figure 72: ECM challenge shows mice develop neurological symptoms. a) Inoculation leads to development of neurological symptoms. **b)** Inoculation leads to a rise in disease

score. Mice were euthanized at a cumulative disease score of 3, and were assigned a score of 4 thereafter, increasing the disease score. 165

Figure 73: Mass of mice during challenge. Consistent with the model, mice lost weight after the challenge inoculation. Mice that were euthanised mice were as a result of neurological symptom development, before the other endpoint of extreme weight loss occurred. 166

Figure 74: Parasitemia of mice after inoculation. Parasitemia confirms that injection with the stabilates lead to infection. 166

Figure 75: SDS-PAGE analysis of glycoconjugates of 1 – 6. Bands are compared to non-conjguated **CRM197** and molecular weight **ladder**. Numbers indicate the molecular weight of marker bands in kDa. Samples from left to right as follows: **3**, **2**, **6**, **5**, CRM197, ladder, **1**, **4**. 168

Figure 76: Antibody titres in sera at day 35 against synthetic GPI fragments. Group size n=4, immunised with glycoconjugate **7**. **Top panel (a-b)** IgG1 and IgG2a titres. **Bottom panel (c-d)** IgG3 and IgM titres. 170

Figure 77: Antibody titres in sera at day 35 against synthetic GPI fragments. Group size n=4, immunised with glycoconjugate **8**. **Top panel (a-b)** IgG1 and IgG2a titres. **Bottom panel (c-d)** IgG3 and IgM titres. 170

Figure 78: Antibody titres in sera at day 35 against synthetic GPI fragments in other organisms. Group size n=4, immunised with glycoconjugate **7**. **Top panel (a-b)** IgG1 and IgG2a titres. **Bottom panel (c-d)** IgG3 and IgM titres. 171

Figure 79: Antibody titres in sera at day 35 against synthetic GPI fragments in other organisms. Group size n=4, immunised with glycoconjugate **8**. **Top panel (a-b)** IgG1 and IgG2a titres. **Bottom panel (c-d)** IgG3 and IgM titres. 171

Figure 80: The hexasaccharide antigen. The full GPI is shown in grey for context. ...173

Figure 81: MALDI-TOF spectra for glycoconjugate of hexasaccharide. Observed change is 5098 Da. 173

Figure 82: IgG1 titres against synthetic GPI fragments in sera of mice immunised with glycoconjugate of 7. Group size n=10, classified by the immunising glycoconjugate. Titres at day **a)** 0, **b)** 7, **c)** 14, **d)** 21, **e)** 28, **f)** 35, **g)** 42..... 174

Figure 83: IgG1 titres against synthetic GPI fragments in sera of mice immunised with glycoconjugate of 8. Group size n=10, classified by the immunising glycoconjugate. Titres at day **a)** 0, **b)** 7, **c)** 14, **d)** 21, **e)** 28, **f)** 35, **g)** 42..... 175

Figure 84: IgG1 titres against synthetic GPI fragments in sera of mice immunised with CRM197 control. Group size n=10, classified by the immunising glycoconjugate. Titres at day **a)** 0, **b)** 7, **c)** 14, **d)** 21, **e)** 28, **f)** 35, **g)** 42..... 176

Figure 85: IgG2a titres against synthetic GPI fragments in sera of mice immunised with glycoconjugate of 7. Group size n=10, classified by the immunising glycoconjugate. Titres at day **a)** 0, **b)** 7, **c)** 14, **d)** 21, **e)** 28, **f)** 35, **g)** 42..... 177

Figure 86: IgG2a titres against synthetic GPI fragments in sera of mice immunised with glycoconjugate of 8. Group size n=10, classified by the immunising glycoconjugate. Titres at day **a)** 0, **b)** 7, **c)** 14, **d)** 21, **e)** 28, **f)** 35, **g)** 42..... 178

Figure 87: IgG2a titres against synthetic GPI fragments in sera of mice immunised with CRM197 control. Group size n=10, classified by the immunising glycoconjugate. Titres at day **a)** 0, **b)** 7, **c)** 14, **d)** 21, **e)** 28, **f)** 35, **g)** 42..... 179

Figure 88: IgG3 titres against synthetic GPI fragments in sera of mice immunised with glycoconjugate of 7. Group size n=10, classified by the immunising glycoconjugate. Titres at day **a)** 0, **b)** 7, **c)** 14, **d)** 21, **e)** 28, **f)** 35, **g)** 42..... 180

Figure 89: IgG3 titres against synthetic GPI fragments in sera of mice immunised with glycoconjugate of 8. Group size n=10, classified by the immunising glycoconjugate. Titres at day **a)** 0, **b)** 7, **c)** 14, **d)** 21, **e)** 28, **f)** 35, **g)** 42..... 181

Figure 90: IgG3 titres against synthetic GPI fragments in sera of mice immunised with CRM197 control. Group size n=10, classified by the immunising glycoconjugate. Titres at day **a)** 0, **b)** 7, **c)** 14, **d)** 21, **e)** 28, **f)** 35, **g)** 42..... 182

Figure 91: IgM titres against synthetic GPI fragments in sera of mice immunised with glycoconjugate of 7. Group size n=10, classified by the immunising glycoconjugate. Titres at day **a)** 0, **b)** 7, **c)** 14, **d)** 21, **e)** 28, **f)** 35, **g)** 42. 183

Figure 92: IgM titres against synthetic GPI fragments in sera of mice immunised with glycoconjugate of 8. Group size n=10, classified by the immunising glycoconjugate. Titres at day **a)** 0, **b)** 7, **c)** 14, **d)** 21, **e)** 28, **f)** 35, **g)** 42. 184

Figure 93: IgM titres against synthetic GPI fragments in sera of mice immunised with CRM197 control. Group size n=10, classified by the immunising glycoconjugate. Titres at day **a)** 0, **b)** 7, **c)** 14, **d)** 21, **e)** 28, **f)** 35, **g)** 42. 185

Figure 94: IgG1 titres against synthetic GPI fragments from other organisms in sera of mice immunised with glycoconjugate of 7. Group size n=10, classified by the immunising glycoconjugate. Titres at day **a)** 0, **b)** 7, **c)** 14, **d)** 21, **e)** 28, **f)** 35, **g)** 42. 186

Figure 95: IgG1 titres against synthetic GPI fragments from other organisms in sera of mice immunised with glycoconjugate of 8. Group size n=10, classified by the immunising glycoconjugate. Titres at day **a)** 0, **b)** 7, **c)** 14, **d)** 21, **e)** 28, **f)** 35, **g)** 42. 187

Figure 96: IgG1 titres against synthetic GPI fragments from other organisms in sera of mice immunised with CRM197 control. Group size n=10, classified by the immunising glycoconjugate. Titres at day **a)** 0, **b)** 7, **c)** 14, **d)** 21, **e)** 28, **f)** 35, **g)** 42. 188

Figure 97: IgG2a titres against synthetic GPI fragments from other organisms in sera of mice immunised with glycoconjugate of 7. Group size n=10, classified by the immunising glycoconjugate. Titres at day **a)** 0, **b)** 7, **c)** 14, **d)** 21, **e)** 28, **f)** 35, **g)** 42. 189

Figure 98: IgG2a titres against synthetic GPI fragments from other organisms in sera of mice immunised with glycoconjugate of 8. Group size n=10, classified by the immunising glycoconjugate. Titres at day **a)** 0, **b)** 7, **c)** 14, **d)** 21, **e)** 28, **f)** 35, **g)** 42. 190

Figure 99: IgG2a titres against synthetic GPI fragments from other organisms in sera of mice immunised with CRM197 control. Group size n=10, classified by the immunising glycoconjugate. Titres at day **a)** 0, **b)** 7, **c)** 14, **d)** 21, **e)** 28, **f)** 35, **g)** 42. 191

Figure 100: IgG3 titres against synthetic GPI fragments from other organisms in sera of mice immunised with glycoconjugate of 7. Group size n=10, classified by the immunising glycoconjugate. Titres at day **a)** 0, **b)** 7, **c)** 14, **d)** 21, **e)** 28, **f)** 35, **g)** 42….. 192

Figure 101: IgG3 titres against synthetic GPI fragments from other organisms in sera of mice immunised with glycoconjugate of 8. Group size n=10, classified by the immunising glycoconjugate. Titres at day **a)** 0, **b)** 7, **c)** 14, **d)** 21, **e)** 28, **f)** 35, **g)** 42….. 193

Figure 102: IgG3 titres against synthetic GPI fragments from other organisms in sera of mice immunised with CRM197 control. Group size n=10, classified by the immunising glycoconjugate. Titres at day **a)** 0, **b)** 7, **c)** 14, **d)** 21, **e)** 28, **f)** 35, **g)** 42….. 194

Figure 103: IgM titres against synthetic GPI fragments from other organisms in sera of mice immunised with glycoconjugate of 7. Group size n=10, classified by the immunising glycoconjugate. Titres at day **a)** 0, **b)** 7, **c)** 14, **d)** 21, **e)** 28, **f)** 35, **g)** 42….. 195

Figure 104: IgM titres against synthetic GPI fragments from other organisms in sera of mice immunised with glycoconjugate of 8. Group size n=10, classified by the immunising glycoconjugate. Titres at day **a)** 0, **b)** 7, **c)** 14, **d)** 21, **e)** 28, **f)** 35, **g)** 42….. 196

Figure 105: IgM titres against synthetic GPI fragments from other organisms in sera of mice immunised with CRM197 control. Group size n=10, classified by the immunising glycoconjugate. Titres at day **a)** 0, **b)** 7, **c)** 14, **d)** 21, **e)** 28, **f)** 35, **g)** 42….. 197

Figure 106: Mass of mice a) during immunisation and b) during challenge. Consistent with the model, mice lost weight after the challenge inoculation. Mice that were euthanised mice were as a result of neurological symptom development, before the other endpoint of extreme weight loss occurred. 198

Figure 107: Parasitemia of mice at day 9 post-infection. Parasitemia appears lower at day 9 post-infection for surviving mice immunised with glycoconjugate of **7** and **8** compared to mice immunised with CRM197 only, however not enough mice are sampled to draw a conclusion. 198

Summary

Severe malaria is a life threatening disease caused by *Plasmodium falciparum.* Glycosylphosphatidylinositol (GPI) glycolipids specific to *P. falciparum* are abundant on the parasite surface and are implicated as a toxin in severe malaria. Glycoconjugate vaccines that induce GPI-specific antibodies are predicted to ameliorate the hyper-inflammatory response against the native GPI toxin and protect against severe malaria. Here, I disclose the immunogenic properties of designed synthetic GPI glycoconjugates.

Binding specificities of polyclonal and monoclonal antibodies induced by various synthetic GPI glycoconjugates were profiled using microarrays displaying synthetic GPI epitopes. This profiling gave detailed insight about how residues of the GPI core backbone affect the specificity of the induced antibodies. Based on the derived antibody specificity profile, synthetic GPI antigens PEtN-Man3 and PEtN-Man4 were designed to induce antibodies recognizing the non-reducing terminus of the core GPI backbone. I reasoned that antibodies against this terminal epitope, specific to *P. falciparum* GPI, may protect against the toxic hyper-inflammatory response implicated in severe malaria. Since GPIs are inflammatory only in the context of the full glycolipid, with the reducing end masked by the lipid tail, binding to the terminal non-reducing epitope may be enough to stop inflammation. Also, these antibodies would share epitope specificities with naturally occurring GPI-specific antibodies.

As predicted, immunisation with both glycoconjugates reproducibly induced high antibody titres recognising the targeted terminal epitope. Monoclonal antibodies against the target epitope were also generated after immunisation. Though the current glycoconjugate formulation did not protect against neurological symptoms in the mouse model of experimental cerebral malaria, it may be protective in other malaria models if a Th2 bias is needed. Furthermore, different glycoconjugate formulations can also be investigated to balance Th1/Th2 responses. Serendipitously, I discovered that the antibodies were cross-reactive with *L. mexicana*, so possible protective effects of immunisation against other protozoan diseases may be explored. This thesis demonstrates that reliable and effective strategies for glycoconjugate vaccine design are strengthened by glycan microarray profiling. Designed antigens can be further formulated into glycoconjugates to produce poly- and monoclonal antibodies specific to targeted epitopes.

Zusammenfassung

Schwere Malaria ist eine durch den Parasiten *P. falciparum* ausgelöste lebensbedrohliche Krankheit. Die Parasiten tragen an der Oberfläche ein Kohlenhydratlipid, das Glycophosphatidylinositol (GPI), das in seiner freien Form als mögliches Toxin in der schweren Form der Malaria identifiziert wurde. Glycokonjugatimpfstoffe die Antikörper gegen GPI induzieren, sollten diesen toxischen Effekt der GPI's neutralisieren oder zumindest abschwächen und somit die Entzündungseffekte reduzieren. In dieser Arbeit habe ich die immunogenen Eigenschaften verschiedener synthetischer GPI-Kohlenhydrat analysiert, um die Impfstoffentwicklung voran zu treiben.

Hierfür wurden die Bindungseigenschaften verschiedener polyklonaler und monoklonaler Antikörper, die in mit synthetischen GPI-Derivaten geimpften Mausseren zu finden waren, mittels Mikroarrays bestimmt. Die Analyse zeigte auf, wie einzelne Strukturelemente der GPI-Kernstruktur die Spezifität der induzierten Antikörper beeinflusst. Auf Basis dieser Analyse konnten zwei optimierte synthetische Glykokonjugate, PetMan3 und PetMan4, entwickelt werden. Beide Strukturen zielten darauf ab, Antikörper mit einer Spezifität für das nicht reduzierte Ende der GPI-Kernstruktur zu bekommen, da diese Spezifität auch für Antikörper in Patienten mit schwerer Malaria gefunden wurde. Diese Antikörper sollten dann auch die Entzündungsreaktion des Körpers gegen die GPI-Struktur effektiv unterdrücken.

Im Einklang mit meiner Hypothese, haben beide Strukturen reproduzierbar eine starke Immunantwort mit einhergehender Überproduktion von Antikörpern hervorgerufen. Wir konnten ebenfalls einen Antikörper des IgM-Typs mit einer Spezifität gegen PEtN-Man3 als monoklonalen Antikörper rekombinant herstellen und in reinigen. Versuche einer aktiven Immunisierung mit den entwickelten Glykoknjugatimpfstoffen im Maus-Modell für experimentelle zerebrale Malaria zeigte jedoch keinen Effekt. Unsere entwickelten Impfstoffe führten reproduzierbar zu einer Th2-basierten Immunantwort, welche im Falle unseres Malariamodells die falsche ist und eine Aktivierung der Th1- basierten Immunantwort wünschenswert wäre. Daher sollten noch weitere Malariamodelle getestet werden, bei denen bekannt ist, dass eine Th2 basierte Immunantwort von Vorteil ist. Alternativ könnte ebenfalls durch Modifizierung der Glykokonjugatimpfstoffformulierung eine bessere Balance zwischen der TH1- und Th2-basierten Immunantwort erhalten

werden, um so doch noch einen Impfschutz in dem von uns benutzten Mausmodell zu beobachten.

Zufällig hat sich gezeigt, dass die hier erhaltenen Antikörper ebenfalls GPI-Strukturen des Parasiten *L. mexicana* erkennen. Daher ergibt sich die Möglichkeit die entwickelten Glykoknjugatimpfstoffe zur Immunisierun gegen andere durch Parasiten hervorgerufenen Krankheiten einzusetzten.

Zusammengenommen zeige ich in meiner Arbeit, dass die Entwicklung von Kohlenhydrat basierten Impfstoffen durch gezielte Charakterisierung der Immunantwort gegen verschiedene strukturell verwandte Strukturen verbessert und beschleunigt werden kann. Dadurch können immunodominante Strukturen schnell und zuverlässig identifiziert werden. Gleichzeitig können in weiteren Schritten Impfstoffformulierungen bei minimalen Aufwand optimiert werden.

1 Introduction

"This year's report shows that after an unprecedented period of success in global malaria control, progress has stalled. Data from 2015–2017 highlight that ***no significant progress in reducing global malaria cases*** *was made in this period. There were an estimated 219 million cases and 435 000 related deaths in 2017." Text taken from* World Malaria Report 2018 *(WHO 2018).*

1.1 Malaria

Prevalence

Malaria is a blood-borne parasitic disease caused by *Plasmodium* protozoan species and is among the most devastating infectious diseases of human history. Today, over 3.3 billion people across 97 countries are at risk of infection and developing disease, with 1.2 billion at high risk for infection [**Figure 1**] (WHO 2013, WHO 2014). Latest data from 2017 indicate an increased disease burden compared to recent years, with an estimated 219 million new cases of disease and 435,000 related deaths (WHO 2018). Over 90% of these deaths occur in sub-Saharan Africa mostly as a result of severe malaria, with remaining cases mostly in South-East Asia, India, and South America (WHO 2013). Upper estimates of severe disease-related deaths are as high as 1.2 million (Murray, Rosenfeld et al. 2012).

Humans today are infected by five *Plasmodium* species. The most common species to infect humans is *P. falciparum* that is most prevalent on the African continent and is responsible for most malaria-associated death (WHO 2014). *P. falciparum* is the focus of this thesis due to its ability to cause severe malaria. *P. vivax*, the second most common malaria parasite, has a wider geographical distribution due to its ability to survive cooler climates (WHO 2014) and infects over 70 million people per year mainly in Asia and South America (Mendis, Sina et al. 2001, Gething, Elyazar et al. 2012). *P. ovale* and *P. malariae* also cause human infection (White 2011), with the monkey malaria parasite *P. knowlesi* causing relatively uncommon zoonotic infection (Antinori, Galimberti et al. 2013, WHO 2014).

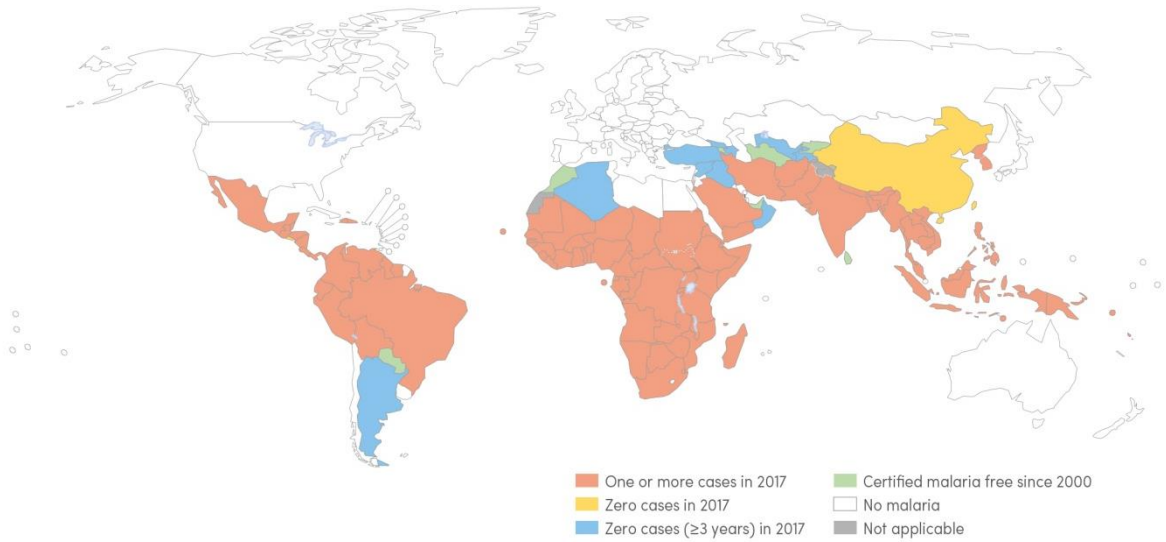

Figure 1: Countries with malaria transmission. Image taken from *World Malaria Report 2018* (WHO 2018).

Lifecycle

The *P. falciparum* lifecycle takes place across two hosts. The *Anopheles gambiae* mosquito is the definitive host required for sexual replication, while the human host is where asexual replication occurs.

Infected female mosquitoes infect humans with motile sporozoites during a blood meal. Within an hour, at least one sporozoite migrates through the bloodstream to the liver and invades a hepatocyte. During this liver stage, sporozoites remain within the hepatocyte for about a week until about 30,000 daughter parasites are produced. Parasite-filled vesicles called merosomes detach from the hepatic schizont and enter circulation (Sturm, Amino et al. 2006). The merosomes rupture, and matured daughter parasites enter the systemic circulation as merozoites (White, Pukrittayakamee et al. 2014, Hoffman, Vekemans et al. 2015).

Merozoites are responsible for clinical symptoms, and are the focus of many intervention strategies. This non-motile blood-stage parasite is the smallest cell in the *Plasmodium* lifecycle and one of the smallest eukaryotic cells known (~1–2 µm). It is characterised by an apical complex of micronemes and rhoptries which contain protein adhesins facilitating erythrocyte adherence and protein invasins essential for invasion [**Figure 2a**] (Cowman,

Berry et al. 2012). Merozoites reversibly adhere to red blood cells (RBCs) upon initial contact, presumably via protein-protein interactions (Hodder, Czabotar et al. 2012). The apical complex aligns (Dvorak, Miller et al. 1975, Gilson and Crabb 2009) and binds irreversibly via a tight junction before releasing rhoptry invasins. Merozoites propel into the established parasitophorous vacuole, shedding their surface coat and sealing the RBC membrane behind them [**Figure 3**] (Riglar, Richard et al. 2011). Attachment, invasion, and sealing takes place over ~27 seconds (Dvorak, Miller et al. 1975).

The intraerythrocytic merozoite develops through ring, trophozoite, and schizont stages, while imparting changes in the RBC membrane for rigidity and nutrient metabolism (Maier, Rug et al. 2008). After 48 hours the infected RBC (iRBC) contains a schizont replete with 6-30 daughter merozoites (Radfar, Mendez et al. 2009, Hoffman, Vekemans et al. 2015). Schizont rupture is then sudden and explosive, propelling non-motile merozoites back into circulation. Liberated merozoites attach to new erythrocytes within 60 seconds after release (Dvorak, Miller et al. 1975) for repeated cycles of reinfection and asexual replication, culminating into billions of merozoites in the bloodstream (White, Pukrittayakamee et al. 2014). One week after the first merozoites emerged from the liver, or two weeks after the inoculating mosquito bite, parasite densities in the blood are high enough for detection methods such as blood-smear microscopy (WHO 2013, White, Pukrittayakamee et al. 2014).

Some merozoites will mature into sexual-form gametocytes in the bloodstream. These long-lived gametocytes are taken up by a female mosquito during their next blood meal and fuse to become zygotes in the mosquito gut. The zygote develops into an ookinete, and then an oocyst that migrates to the salivary gland. Sporozoites are produced in the salivary gland, to be injected into the next human host upon the mosquito's next blood meal, completing the lifecycle [**Figure 4**] (Cowman and Crabb 2006, White, Pukrittayakamee et al. 2014, Hoffman, Vekemans et al. 2015).

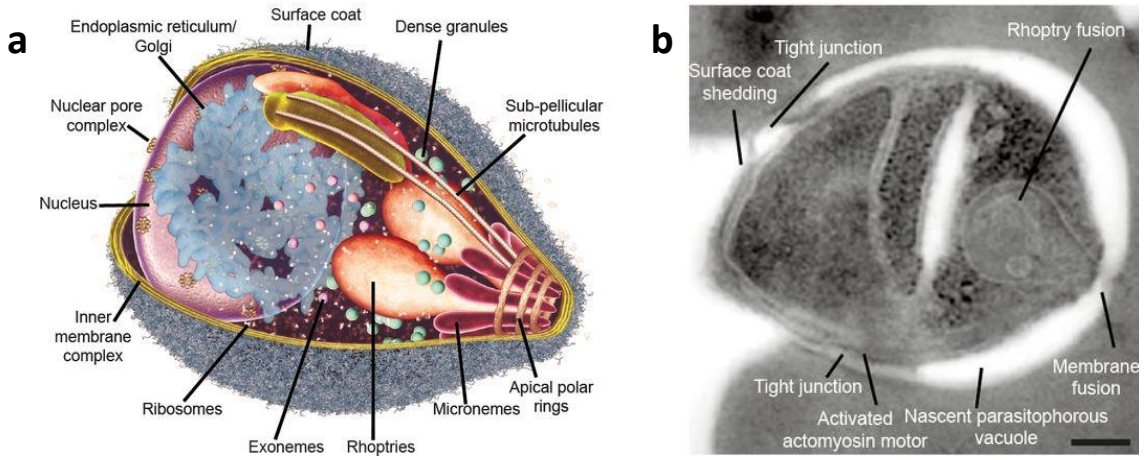

Figure 2: Blood stage merozoite representations. a) Illustration of major organelles. **b)** A *P. falciparum* merozoite in the process of invading a human red blood cell. Scale bar = 200 nm. Image composite taken from *The cellular and molecular basis for malaria parasite invasion of the human red blood cell* (Cowman, Berry et al. 2012).

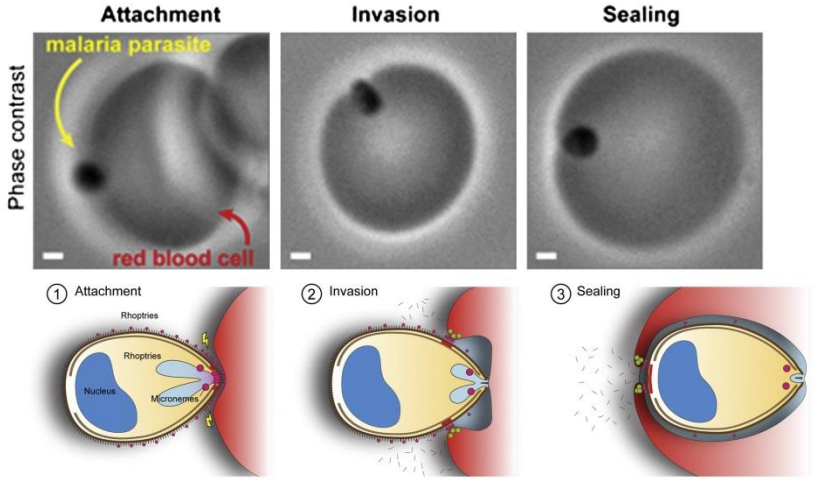

Figure 3: Model for merozoite invasion. Scale = 0.5 μM. Image composite taken from *Super-Resolution Dissection of Coordinated Events during Malaria Parasite Invasion of the Human Erythrocyte* (Riglar, Richard et al. 2011).

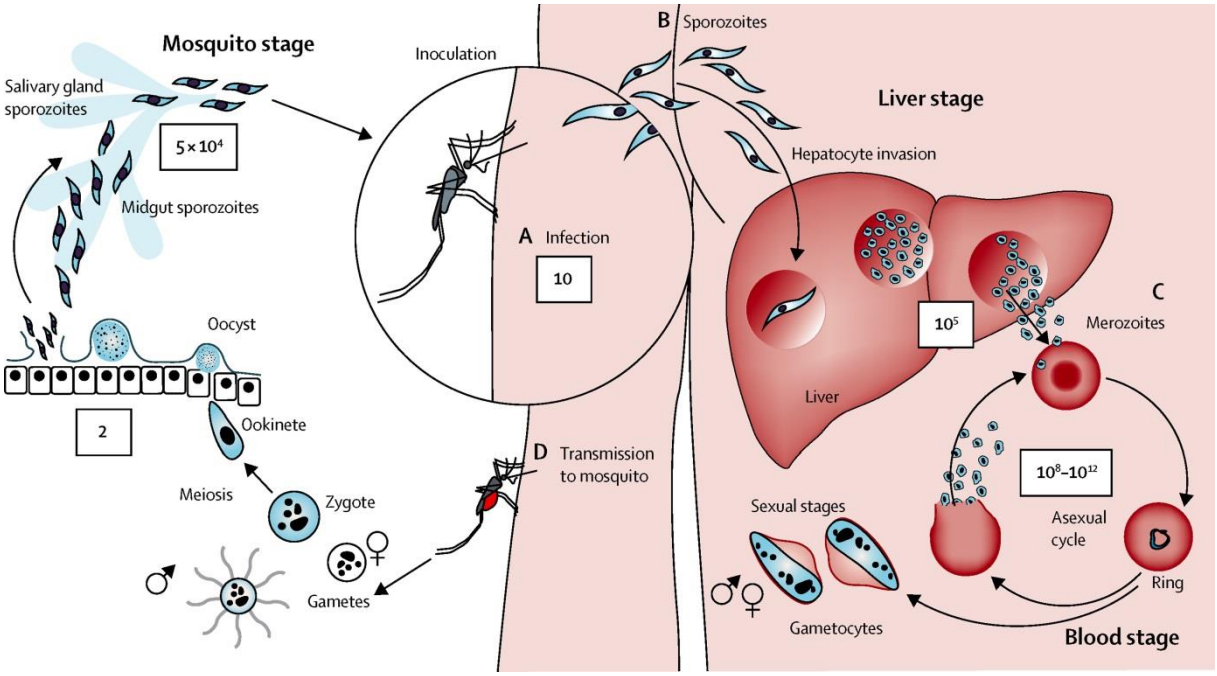

Figure 4: The complete *P. falciparum* lifecycle. Image taken from *Malaria* (White, Pukrittayakamee et al. 2014).

Evasion mechanisms

Malaria has infected mammals for over 150 million years (Carter and Mendis 2002). Over time, the free-floating *P. falciparum* has evolved ways to evade host immune mechanisms at all stages of its lifecycle. For example, gametocytes assimilate host proteins to evade complement after blood meal uptake (Simon, Lasonder et al. 2013). Polymorphisms in sporozoite proteins, e.g. CSP, are shown to limit effective cellular immune responses and efficacy as vaccine antigens (Plebanski, Lee et al. 1999, Neafsey, Juraska et al. 2015). Proteins required for merozoite invasion of erythrocytes, e.g. AMA1, are targets of naturally acquired antibody induction, but are also highly polymorphic, limiting their viability as vaccine antigens (Drew, Wilson et al. 2016). Merozoite antigens on the surface of iRBCs e.g. PfEMP1, are also highly polymorphic, and their expression switches between replication cycles (Roberts, Craig et al. 1992). Variant, redundant invasion strategies employed by merozoites also suggests a means to evade protective antibodies (Persson, McCallum et al. 2008). Additionally, proteins essential for invasion are exposed only when needed, limiting the time for potential immune detection (Cowman, Berry et al. 2012).

A “smoke screen” strategy, wherein parasites divert antibody induction to non-protective epitopes, is also hypothesised to explain the heavy investment in diverse surface antigens, however more evidence is needed (Cowman, Berry et al. 2012, Renia and Goh 2016).

1.2 Malaria disease

Signs and symptoms

The first symptoms of malaria are generally non-specific and flu-like. Common symptoms include fever, headache, chills, coughs, malaise, weakness, gastrointestinal complaints, and neurological complaints such as seizures and coma (White, Pukrittayakamee et al. 2014, WHO 2015, CDC 2019). There is no combination of signs or symptoms that reliably distinguishes malaria from other causes of fever (WHO 2015), so infection is usually confirmed by laboratory diagnosis through microscopic examination of sample blood smears (CDC 2019), with detection kits and PCR methods to detect species-specific antigens (WHO 2015). Patients with mild, uncomplicated malaria infection can expect rapid, full recovery with effective antimalarial treatment (WHO 2015, CDC 2019).

P. falciparum infections carry a risk of progressing to severe malaria within hours after early infection, especially if antimalarial treatment is delayed or of low-quality (WHO 2015). Severe malaria is the deadliest form of infection that approaches 100% mortality rate when poorly treated (WHO 2015). It develops in 5% of cases (WHO 2015) and accounts for 98% of all malaria-related deaths. Over 90% of these deaths occur in sub-Saharan Africa, with remaining cases mostly in South-East Asia, India, and South America (WHO 2013). Young children, infants, and those experiencing infection for the first time are at risk for developing this condition, and malaria-related deaths are mostly in young children under five years of age (WHO 2018).

Severe malaria is usually defined by three major clinical syndromes that can manifest: severe malarial anaemia, respiratory distress, and cerebral malaria consisting of multiple daily seizures, coma, and other neuropathologies. Other diagnostic symptoms include renal impairment, pulmonary oedema, lactic acidosis, and a general shock-like syndrome

with hypotension, hypoglycaemia and poor tissue perfusion. In children, severe malarial anaemia and hypoglycaemia are common. In adults, renal impairment and pulmonary oedema are more common (Miller, Baruch et al. 2002, Dondorp, Lee et al. 2008, Gazzinelli, Kalantari et al. 2014, White, Pukrittayakamee et al. 2014, WHO 2015).

Severe malaria pathogenesis

The underlying causes of severe malaria syndromes are not fully known, but is currently understood to be a combination of complications arising from merozoite infection **[Figure 5]**. Cerebral malaria is thought to arise, in part, from the interference of the brain microcirculatory system (Pongponratn, Turner et al. 2003, Cowman, Berry et al. 2012). Here, parasite-induced expression of adherence proteins causes iRBC rigidity and adherence to receptors on endothelial walls of veins and capillaries. This leads to their sequestration in the brain, and other vital organs including the liver, lungs, spleen, intestine, and kidney (Hommel 1993, Fried and Duffy 1996, Miller, Baruch et al. 2002, White, Pukrittayakamee et al. 2014).

Merozoite-derived molecules, called malaria toxins, may also induce immune responses contributing to severe malaria susceptibility. Here, the sequestration and subsequent rupture of iRBCs in vital organs leads to the efficient, concentrated release of malaria toxins that induce the excessive production of pro-inflammatory cytokines TNF-α, IL-1, IL-6, IL-12, and IFN-γ (Gowda 2007). This hyper-inflammatory response leads to adverse effects such as endothelial cell dysfunction, leukocyte tissue infiltration, blood cell destruction, and vascular leakage, resulting in metabolic damage and organ dysfunction associated with severe malaria (Clark and Rockett 1994, Day, Hien et al. 1999, Torre, Speranza et al. 2002, Schofield and Grau 2005, Ayimba, Hegewald et al. 2011, Gazzinelli, Kalantari et al. 2014, White, Pukrittayakamee et al. 2014).

A plausible malaria toxin is the biocrystal hemozoin produced by the intraerythrocytic merozoite. During asexual replication amino acids are acquired through haemoglobin metabolism. The resultant heme is catabolised into hemozoin which is a safe by-product for the growing merozoite. Hemozoin is released upon schizont rupture, and is recognized by circulating host immune cells as pathogen-associated molecular pattern molecules (Renar, Iskra et al. 2016). The stimulated immune cells internalise the hemozoin and

produce excess IL-1β, a pro-inflammatory cytokine that often acts in concert with TNF-α during severe malaria (Kalantari, DeOliveira et al. 2014).

P. falciparum-specific glycosylphosphatidylinositol (GPI) is also hypothesised to be a major malaria toxin (Schofield, Novakovic et al. 1996, Tachado, Gerold et al. 1997, de Souza and Riley 2002, Schofield and Grau 2005). GPIs are the major carbohydrate modifications for *P. falciparum* proteins (Gowda, Gupta et al. 1997). Upon schizont rupture, immune cells recognise these GPI molecules and release excess amounts of pro-inflammatory cytokines such as TNF-α, IL-6, & IL-1β associated with severe malaria (Boutlis, Gowda et al. 2002, Krishnegowda, Hajjar et al. 2005, Patel, Lu et al. 2007).

Other pathogenic components of *P. falciparum* that may contribute to severe malaria are described. These include parasite membrane-derived microparticles that stimulate macrophages (Couper, Barnes et al. 2010), RESA protein exported to iRBC membranes which affect microcirculation (Diez-Silva, Park et al. 2012), protein DNA complexes that activate dendritic cells (Wu, Gowda et al. 2010), and uric acid that induces inflammatory cytokine production (Orengo, Leliwa-Sytek et al. 2009).

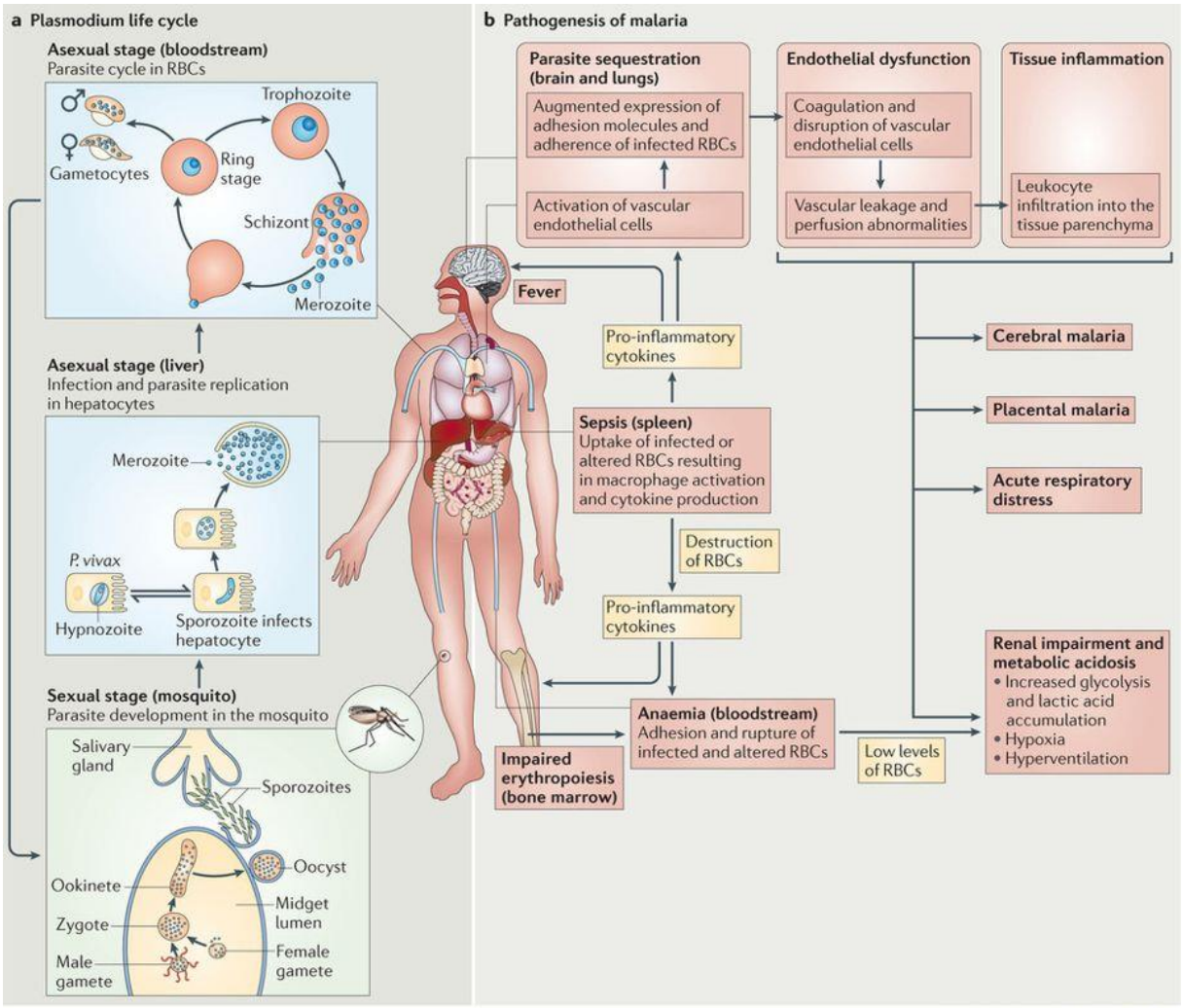

Figure 5: Overview of disease pathogenesis. Lifecycle context and consequent symptoms of disease are also shown. Image taken from *Innate sensing of malaria parasites* (Gazzinelli, Kalantari et al. 2014).

Acquired immunity

In malaria-endemic areas virtually all individuals are infected by early childhood (WHO 2015). In these areas infants and young children under five years of age disproportionally account for 77% of malarial disease-related deaths due to severe malaria (WHO 2013). Conversely, those ≥12 years of age have immunity to severe malaria acquired over lifelong parasite exposure [**Figure 6**]. Uncomplicated malaria is also rarely seen in adults with acquired immunity. Later in life, acquired immunity protects against high parasitemia (White, Pukrittayakamee et al. 2014).

Acquiring this immunity is still unclear, as an individual's age and exposure rate in non-endemic areas may affect its development (Doolan, Dobano et al. 2009). It is also unclear whether acquired immunity persists after cessation of chronic exposure, with studies indicating that it does persist (Castelli, Matteelli et al. 1999, Jelinek, Schulte et al. 2002, Bouchaud, Cot et al. 2005, Phillips, Bassett et al. 2009, Pistone, Diallo et al. 2014) contradicted by studies indicating it does not (Bunn, Escombe et al. 2004, Jennings, De Souza et al. 2006, Farnert, Wyss et al. 2015). Given that acquired immunity tends to lower the occurrence of severe malaria (Doolan, Dobano et al. 2009), a vaccine that can induce a similar immune status in children and other at-risk groups, including non-immune travellers, is a highly desirable treatment.

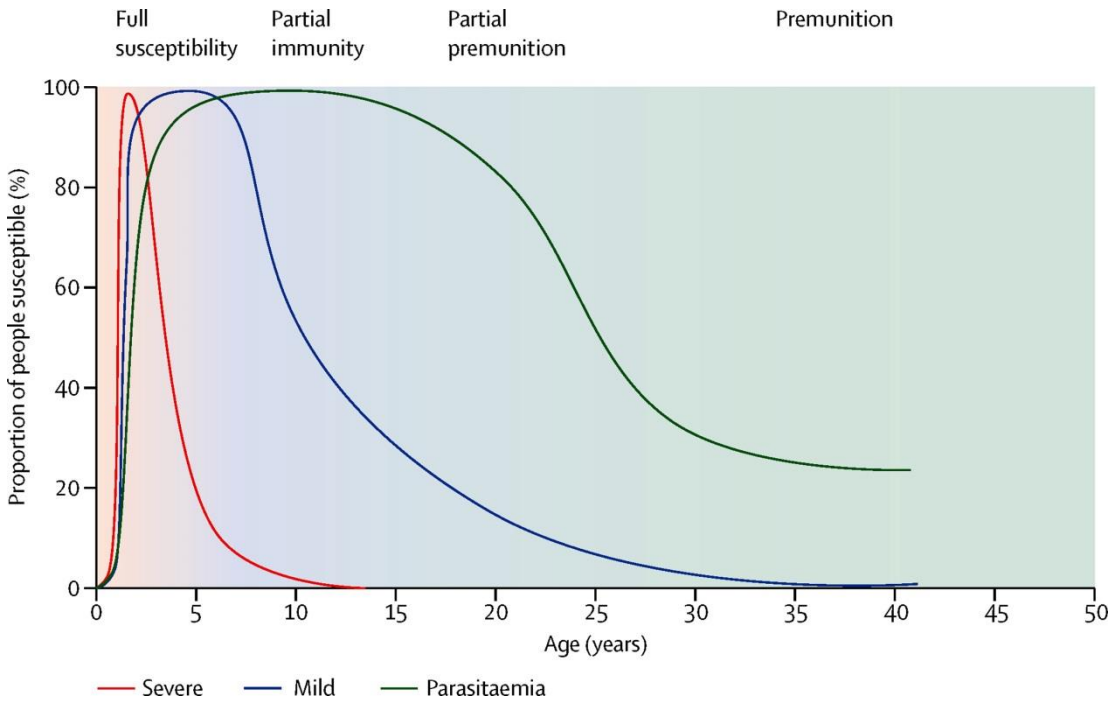

Figure 6: Lifelong exposure confers protection to severe malaria. This is followed by immunity to febrile, uncomplicated malaria, and finally to parasitemia. Image taken from *Malaria* (White, Pukrittayakamee et al. 2014).

1.3 Malaria treatment

Current measures

At least €2.4 billion are spent annually on malaria control programs (WHO 2013, WHO 2015). For lowering exposure rates in countries with malaria transmission bed nets and insecticides are employed (WHO 2015). For managing disease, uncomplicated malaria is treated with artemisinin-based combination therapy (ACT) to prevent progression to severe malaria. ACT is generally administered orally over three days, corresponding to two asexual replication cycles, and consists of an artemisinin derivative for rapid parasite clearance combined with a longer-acting partner drug to clear remaining parasites (WHO 2015). Increased access to ACTs in malaria-endemic countries has been integral to reducing global malaria burden (WHO 2018).

The primary focus for treating severe malaria is to prevent patient death. Severe malaria fatality can occur within hours and the risk of death is greatest in the first day, so it is essential that antimalarial drugs are promptly administered. The treatment of choice is intravenous or intramuscular artemisinin derivative administered for at least 24 hours, given to all patients suffering from severe malaria including infants, pregnant women, and lactating women (WHO 2015, WHO 2018). Oral ACT is administered as a follow-up treatment with additional palliative care. Ultimately, effective drug treatment can reduce severe malaria mortality from 100% down to 10-20% (WHO 2015, CDC 2019).

Mass drug treatment

Mass drug treatments aim to cure all symptomatic and asymptomatic infections from a population, eliminating malaria from the area. A mass drug treatment campaign eliminated malaria incidence in the long term on the island of Vanuatu (Kaneko, Taleo et al. 2000). However, other attempts generally resulted in only transient reduction (von Seidlein and Greenwood 2003, Newby, Hwang et al. 2015). Since mass treatment campaigns require extensive community engagement for any chance of success, compounded with the lack of clarity on benefits and risks such as drug selection pressure (von Seidlein and Dondorp 2015), mass drug treatment strategies are rarely used (WHO 2015).

Drug resistance

Partial artemisinin resistance and consequent drug treatment failure is observed in the Greater Mekong Subregion of Southeast Asia. Partial artemisinin resistance typically refers to delayed parasite clearance following administration of artemisinin-derived drugs. However it is resistance to longer-lasting ACT partner drugs that leads to treatment failure, possibly facilitated by partial artemisinin resistance (WHO 2018). Despite growing drug resistance, ACT remains the frontline choice for treatment. However, other approaches to control disease, including vaccines, should be considered.

1.4 Malaria vaccine development

Current status

Vaccines against malaria should reduce morbidity and mortality. To this end, vaccines in development aim to decrease parasite load during transmission and liver stages, or reduce disease symptoms during the blood stage [**Figure 7**]. Regrettably, vaccines are not part of any control programs since no routine vaccine against malaria exists (Nyame, Kawar et al. 2004, Astronomo and Burton 2010, Hoffman, Vekemans et al. 2015).

Complex biology and evasion hampers parasite vaccine development, compared to vaccine development in bacteria and viruses. However, a malaria vaccine should be possible considering that naturally acquired immunity to disease symptoms develops over time. Malaria vaccines at the most advanced stages of development aim to induce protective immune responses during the human liver stage of disease through the induction of antibody-mediated and cell-mediated responses against *P. falciparum* (Hoffman, Vekemans et al. 2015).

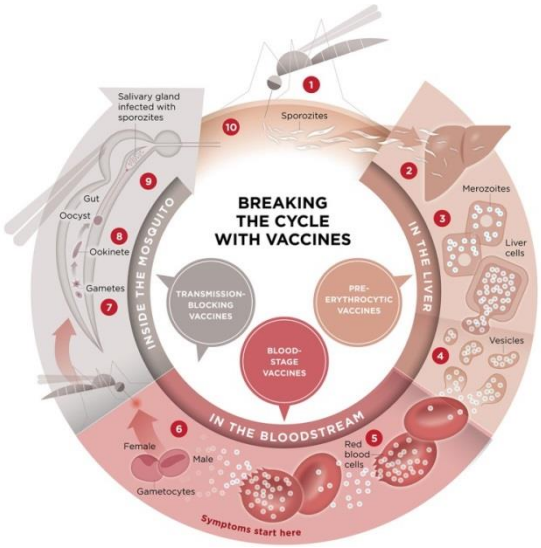

Figure 7: Targeted stages of the parasite lifecycle. The stage targeted in a malaria vaccine reflects the type of protective effect the vaccine would have. Human liver stage vaccines would combat infection and transmission of the vaccine, while human blood stage vaccines would combat disease symptoms and associated mortality and morbidity. Image taken from *PATH Malaria Vaccine Initiative.*

Liver stage vaccines

Liver stage vaccines aim to inhibit disease transmission by blocking liver stage development of the parasite. Downstream pathology would also be reduced by preventing blood stage progression.

Whole organism vaccines using radiation-attenuated sporozoites were early strategies for inducing adaptive immune responses against liver stage parasites (Clyde, Mccarthy et al. 1975). A modern radiation-attenuated sporozoite vaccine has shown to protect vaccinated individuals from controlled malaria infection in field trials, presumably by inducing CD8 T cell responses to liver stage parasite antigens (Seder, Chang et al. 2013). However, whole organism vaccines have a number of key challenges to overcome. These include scaling up of the product, cryopreservation of the vaccine, route of administration, and dosing strategies (Pinder, Moorthy et al. 2010, Hoffman, Vekemans et al. 2015).

Liver stage antigen vaccines, as opposed to whole organism vaccines, are considered a viable alternative in terms of production and distribution. RTS,S is the most advanced liver stage antigen vaccine. It targets the abundant GPI-anchored circumsporozoite protein (CSP) which is involved in liver cell adherence. CSP-specific antibodies are associated with protection from disease (John, Tande et al. 2008) and RTS,S raises CSP-specific

antibodies reported to interfere with parasite homing to the liver. However, distinguishing protective and non-protective CSP-specific antibodies is considered (Charoenvit, Sedegah et al. 1990). Ultimately, the efficacy of the RTS,S/AS01 formulation is greatly contested based on the results of a 2009-2014 phase III trial. The vaccine did not significantly protect against cases of severe malaria in the target groups of infants and young children, and protection against clinical malaria symptoms waned over time (Tinto, D'Alessandro et al. 2015, Gosling and von Seidlein 2016). Phase 4 studies vaccinating up to 40,000 children to further evaluate safety is currently planned by Glaxo-Smith-Kline (WHO 2016).

Blood stage vaccines

It is now understood that antibodies play a role in protection during the blood stage of malaria through many different effects depending on the targeted antigen [**Figure 8**]. Vaccines aimed at ameliorating blood stage disease symptoms could raise such antibodies. Merozoite-specific antibodies are believed to interfere with red blood cell invasion, disrupt intracellular replication, target iRBCs for destruction, or neutralise parasite inflammatory toxins (Teo, Feng et al. 2016). These antibodies were initially thought to play a relatively unimportant part in acquired immunity against severe malaria before early studies indicated a protective role. Passive transfer of immunity was reported when IgG injections from semi-immune adults led to clinical improvement of infected, non-immune patients (Cohen, Carrington et al. 1961, Bouharountayoun, Attanath et al. 1990). Today, the most advanced blood stage vaccine is GMZ2, which raises MSP3 & GLURP-specific IgG and induces memory B-cell responses (Esen, Kremsner et al. 2009). Apical membrane antigen 1 (AMA1) is another malaria antigen currently in blood stage vaccine development. AMA1-specific antibodies are reported to inhibit asexual replication, highlighting its vaccine potential (Remarque, Faber et al. 2008).

Combining antigens from both the blood and liver stages of disease are also being actively developed into vaccine formulations. A combination of the blood stage antigen AMA1 and CSP is the strategy currently employed by all multi-stage vaccines (Okitsu, Silvie et al. 2007, Thompson, Porter et al. 2008, Sedegah, Tamminga et al. 2011). Field studies of these vaccines look to measure both sterile immunity and clinical protection from disease.

A subset of blood stage vaccines may not directly target the parasite. Instead, toxic molecules released by the parasite during cycles of asexual replication could be targeted in order to reduce disease symptoms. This concept is proven by successful tetanus and diphtheria toxoid vaccines targeting the bacterial toxins that cause disease (Playfair, Taverne et al. 1990, Schofield 2007). A similar vaccine approach for malaria could work by blocking toxins such as GPI in order to ameliorate downstream manifestation of severe malaria.

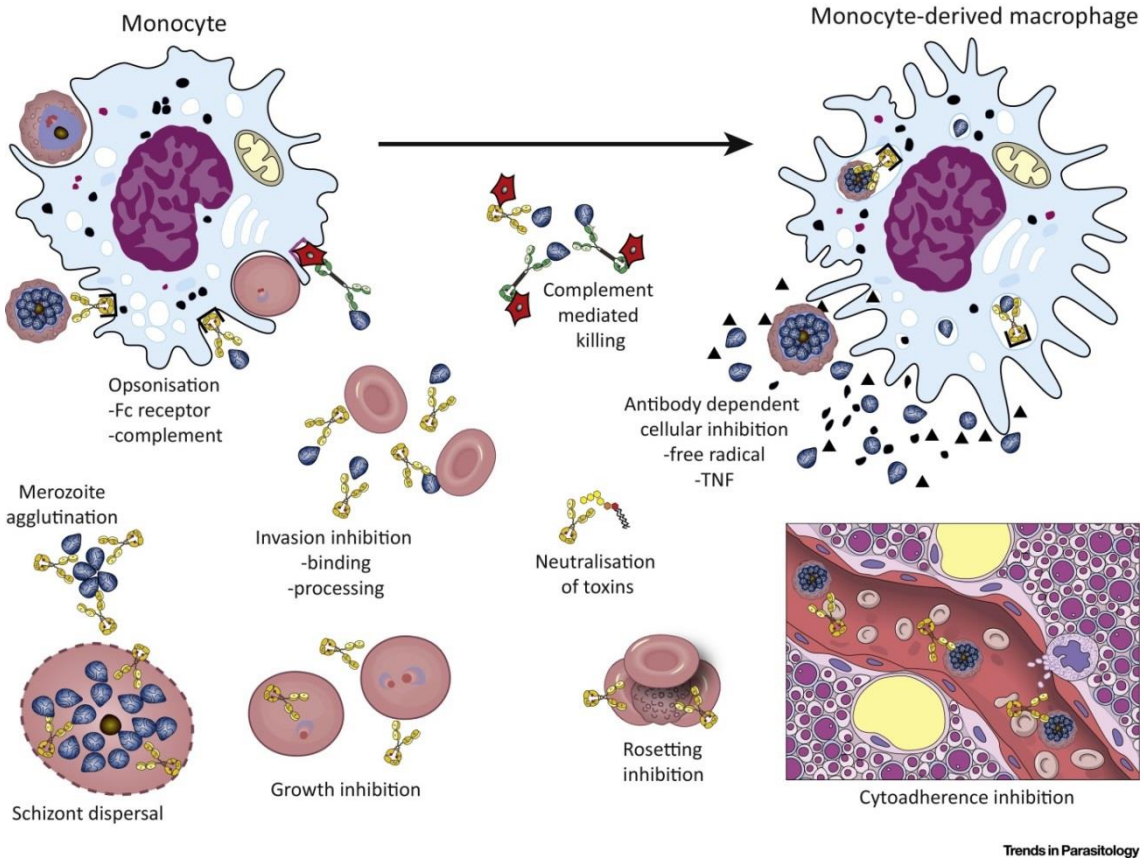

Figure 8: The modes of action of merozoite antigen-specific antibodies. Functions include interfering with red blood cell invasion, disrupting intracellular replication, targeting iRBCs for destruction, or neutralising parasite inflammatory toxins. Image taken from *Functional Antibodies and Protection against Blood-stage Malaria* (Teo, Feng et al. 2016).

1.5 GPIs as vaccine antigens

Attractive targets

GPIs, compared to proteins, are attractive candidates as malaria vaccine antigens. Glycan biosynthesis is a complex, multi-enzymatic process compared to protein synthesis (Delorenzi, Sexton et al. 2002) such that random gene point mutations are unlikely to confer a change in the GPI glycan structure without lethal consequences for the parasite. Since parasite evasion mechanisms rely on antigen variation and polymorphism, targeting invariant glycan antigens on GPI could overcome these mechanisms. Indeed, an essential merozoite adhesin with limited polymorphism is currently being developed as a promising vaccine candidate (Douglas, Baldeviano et al. 2015). Moreover, GPI is conserved across *P. falciparum* strains (Berhe, Schofield et al. 1999). As a result, parasite resistance to vaccines using carbohydrate antigens would be hindered. In fact, microbial resistance to glycoconjugate vaccines currently on the market has not yet developed.

Structure and function

After their first complete characterisation (Ferguson, Homans et al. 1988) GPIs were shown to be ubiquitous, modifying up to 1% of all eukaryotic proteins (Eisenhaber, Bork et al. 2001). They are usually expressed at low levels on the plasma membrane but are expressed at relatively high levels in parasitic protozoa (Gowda 2002), including *Plasmodium* (Schofield and Hackett 1993, Gowda 2007). GPIs cover the merozoite surface and are released into circulation at schizont rupture (Gilson, Nebl et al. 2006). They are the major carbohydrate modifications for blood stage proteins, compared to O-glycosylation and N-glycosylation which are virtually absent or only at very low levels (Gowda, Gupta et al. 1997).

GPI glycolipids typically act as protein anchors by embedding their lipid tail in the hydrophobic membrane [**Figure 9**]. The glycan backbone of GPI is attached to the lipid tail via a *myo*-inositol-2-phosphate (InoP) residue that extends with one glucosamine (GlcN) and three mannose (Man) residues Man-I, Man-II, and Man-III. Proteins are attached to the non-reducing terminus of this core GPI backbone via a phosphoethanolamine (PEtN) bridge. A fourth Man extends the core GPI backbone

(PEtN-6-[Man-(α1-2)-]Man-(α1-2)-Man-(α1-6)-Man-(α1-4)-GlcN-(α1-6)-InoP while abundant free GPI that cover the parasite surface lack protein as well as the additional Man residue (Gowda 2002, Tsai, Liu et al. 2012). Molecular dynamics modelling suggests that the glycan backbone of the GPI anchor interacts strongly with lipid head groups on the outer leaflet of the cell membrane, partially embedding the glycan residues. As a result, proteins anchored by GPI reside close to the lipid bilayer (Banerjee, Wehle et al. 2018). While it has been reported that the GPI molecule is conserved across different geographical isolates of *P. falciparum* (Berhe, Schofield et al. 1999) the GPI structures for non-lethal human *Plasmodium* species have not been published.

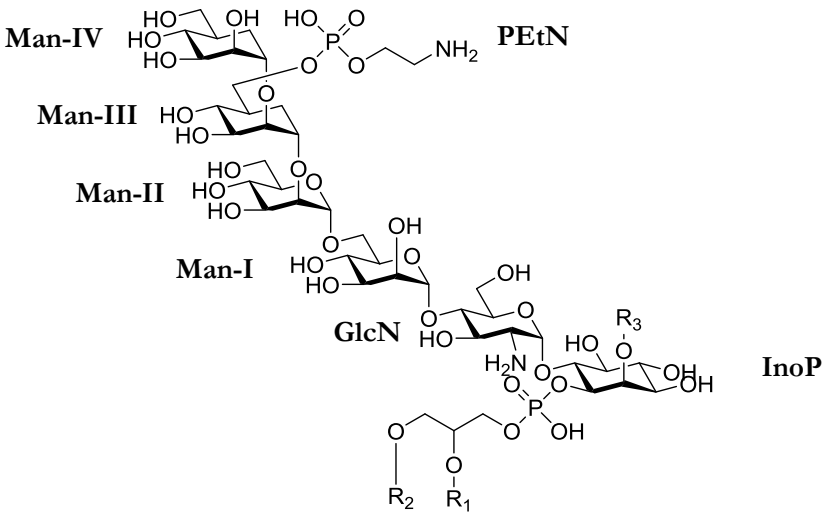

Figure 9: The *P. falciparum GPI* anchor. The Man IV residue is absent in free GPI.

Signalling and inflammation

GPI toxic effects are comparable to those induced by lipopolysaccharide (LPS) (Jakobsen, Baek et al. 1988, Caro, Sheikh et al. 1996). Innate immune system toll-like receptor (TLR) TLR2 and TLR4, which recognise lipoproteins and LPS, bind to GPIs present either on merozoites or those released as soluble molecules after schizont rupture (Krishnegowda, Hajjar et al. 2005, Panda, Das et al. 2016). Host immune cells such as macrophages are activated by the TLR-dependent signalling cascades leading to the production of inflammatory cytokines TNF-α (Grau, Piguet et al. 1989, Day, Hien et al. 1999, Hunt and Grau 2003) and IL-6 (Molyneux, Taylor et al. 1991, Clark and Rockett 1994, Sarthou, Angel et al. 1997, Day, Hien et al. 1999, Hunt and Grau 2003, Zhu, Krishnegowda et al.

2005). IL-1β and nitric oxide are also released. The outcome is a hyper-inflammatory response associated with severe malaria (Boutlis, Gowda et al. 2002, Krishnegowda, Hajjar et al. 2005, Patel, Lu et al. 2007).

Isolated GPI can also produce TNF-α, IL-1 and IFN-γ in macrophages, as well as replicate acute disease symptoms in mice in the absence of the whole malaria parasite (Schofield, Vivas et al. 1993). GPI can also increase expression of cell adhesion molecules on macrophages and vascular endothelial cells (Schofield, Novakovic et al. 1996). Isolated GPI is also sufficient to induce nitric oxide release in macrophages and vascular endothelial cells (Tachado, Gerold et al. 1996, Tachado, Gerold et al. 1997). Notably, the entire, intact GPI glycolipid is required to induce cytokine and nitric oxide production. Separated GPI glycan and lipid do not lead to cytokine production (Tachado, Gerold et al. 1997, Vijaykumar, Naik et al. 2001).

Naturally occurring antibodies against GPI

GPI-specific antibodies from natural infection are suggested to provide protection against severe malaria by neutralizing the toxic activity of GPIs. However, it is still up for debate whether elevated levels of naturally acquired GPI-specific antibodies are protective against severe malaria. Relatively high levels of GPI-specific antibodies in patients who did not present with severe malaria have been reported in malaria-endemic areas in Africa (Naik, Branch et al. 2000, Perraut, Diatta et al. 2005) and Indonesia (Keenihan, Ratiwayanto et al. 2003). These findings that suggest an association between GPI-specific antibody titre, age, and protection from severe malaria are balanced by studies that find no such association (Boutlis, Gowda et al. 2002, de Souza, Todd et al. 2002, Cissoko, Daou et al. 2006, Gomes, Totino et al. 2013, Mbengue, Niang et al. 2016). However, GPI-specific antibodies are reported to show relevant action in modulating immune responses by protecting immune cells against severe *P. falciparum*-induced inflammatory responses *in-vitro* (Schofield, Vivas et al. 1993, de Souza, Runglall et al. 2010).

Synthetic GPI

Epitope mapping using synthetic glycans has been applied to antibodies against microbial pathogens (Oberli, Tamborrini et al. 2010, Martin, Broecker et al. 2013, Broecker, Aretz

et al. 2014, Götze, Azzouz et al. 2014, Broecker, Martin et al. 2016, Geissner, Pereira et al. 2016, Schumann, Hahm et al. 2017). Synthetic glycans are ideal for epitope analysis in microarrays, and overcome the challenges associated with isolating carbohydrates from biological sources, limited to organisms that can be grown in culture, that typically yield heterogeneous antigens (Seeberger and Werz 2007, Hecht, Stallforth et al. 2009, Lepenies and Seeberger 2010, Jaurigue and Seeberger 2017, Geissner, Reinhardt et al. 2019).

Synthetic GPIs have been used to investigate the role of naturally-occurring antibodies in malaria, particularly elucidating the specific GPI epitopes that naturally-occurring antibodies bind to. Since GPI epitope fragments are synthesised directly, a larger library of fragments can be created, compared to what can be obtained by chemically modifying isolated GPI (Tachado, Gerold et al. 1997). Studies employing these synthetic GPI microarrays found that naturally-occurring GPI-specific antibodies mainly recognise synthetic fragments containing Man_3-GlcN-InoP without the fourth Man (Naik, Branch et al. 2000, Naik, Krishnegowda et al. 2006). Titres are highest in sera of healthy individuals followed by those with uncomplicated malaria (Kamena, Tamborrini et al. 2008, Tamborrini, Liu et al. 2010), and are also induced in malaria-naïve individuals after parasite infection (Kamena, Tamborrini et al. 2008).

Antibodies recognising synthetic fragments containing Man_3-GlcN-InoP with the fourth Man are highest in sera from individuals with severe malaria, followed by healthy individuals (Kamena, Tamborrini et al. 2008, Tamborrini, Liu et al. 2010). These antibodies may also be induced by infection with other parasites or fungi, which can account for their presence in malaria-naïve individuals (Kamena, Tamborrini et al. 2008, Tamborrini, Liu et al. 2010). The fourth Man was described as a key recognition element for *P. falciparum* GPI-specific antibodies (Kamena, Tamborrini et al. 2008), while elsewhere it was described as contributing only marginally to immunogenicity (Naik, Krishnegowda et al. 2006).

The potential of synthetic GPI vaccines against severe malaria disease was demonstrated in a glycoconjugate shown to ameliorate blood stage toxicity. Synthetic *P. falciparum* GPI hexasaccharide antigen, PEtN-6-[Man-(α1-2)-]Man-(α1-2)-Man-(α1-6)-Man-(α1-4)-GlcN-(α1-6)-Ino-cyclic-phosphate, was conjugated to KLH carrier protein and emulsified in complete and then incomplete Freund's adjuvant (CFA/IFA). C57BL/6 mice were

immunised with this glycoconjugate to induce GPI-specific antibody production. The mice were subsequently challenged with experimental cerebral malaria (ECM) via infection with *P. berghei* ANKA. Significant protection from cerebral syndrome and fatality was likely due to the induction of GPI-specific antibodies that ameliorated the hyper-inflammatory response against the native free GPI toxin (Schofield, Hewitt et al. 2002).

1.6 Aim of this study

The aim of this dissertation was to identify a glycoconjugate that induces protective GPI-specific antibodies that ameliorate the toxic effects of GPI in *P. falciparum* infection. Immunisation would essentially induce a semi-immune status in immunised individuals. The GPI antigen I planned to design should be the minimum epitope required to raise protective GPI-specific antibodies.

To achieve that goal various biological and biochemical techniques, including microarrays furnished with synthetic carbohydrates, the use of glycoconjugates containing synthetic GPI, and animal models to determine outcomes of immunisation and infection, were used to address the current questions on the role of GPIs in malaria:

- Do residues in synthetic GPI antigens affect the epitope specificity of antibodies induced after immunisation?
- Do residues in synthetic GPI antigens affect the isotype of antibodies induced after immunisation?
- Can an understanding of residue immunogenicity aid antigen design against GPI epitopes?
- Can antigens be designed to facilitate the generation of monoclonal antibodies specific to target GPI epitopes?
- What are the similarities/differences between antibodies induced by synthetic GPI antigens versus natural infection?
- Are antibodies that are specifically induced against a target GPI epitope protective against severe malaria?
- Do antibodies specific for the targeted GPI epitopes cross-react with GPI from other organisms?

Ultimately, this thesis aimed to demonstrate that reliable and effective strategies for glycoconjugate vaccine design are strengthened by glycan microarray profiling and the use of synthetic antigens. Taken together this should lead to the development of glycoconjugates and monoclonal antibodies that protect against severe malaria.

2 Materials & Methods

2.1 Glycoconjugate preparation

Preparation of minimal epitope antigen glycoconjugates

Synthesis of PEtN-Man_3 and PEtN-Man_4 was accomplished by Dr. Ankita Malik (MPIKG) according to published procedures (Tsai, Götze et al. 2013). The glycan antigens were synthesized with a C6 thiol linker. For conjugation, the thiol glycans were conjugated to CRM197 carrier protein (purchased from Pfēnex Inc.). Here, the glycans were reduced with Tris(2-carboxyethyl)phosphine (TCEP) before incubating with succinimidyl 3-(bromoacetamido)propionate (SBAP) activated CRM197. After quenching, the glycoconjugates were characterized with matrix-assisted laser desorption/ionization (MALDI) and sodium dodecyl sulfate polyacrylamide gel electrophoresis (SDS-PAGE). Glycan loading was calculated as: ([mass $_{\text{activated CRM197}}$] − [mass $_{\text{activated CRM197 with glycan}}$]) / [mass $_{\text{glycan}}$]. For long term storage, conjugates were frozen at -80°C [**Appendix, Figure 75 & Table 4**].

Sodium dodecyl sulfate polyacrylamide gel electrophoresis

Sodium dodecyl sulfate polyacrylamide gel electrophoresis (SDS-PAGE) (Laemmli 1970) was performed using a MiniProtean system (Bio-Rad, Hercules, USA). An alkaline separating gel (255 mM Tris/HCl pH 8.8, 10 to 12% (w/v) of a 29:1 acrylamide/bisacrylamide mixture) and an acidic stacking gel (125 mM Tris/HCl pH 6.8, 4% (w/v) of a 29:1 acrylamide/bisacrylamide mixture), polymerized by spiking with TEMED and 10% (w/v) ammonium peroxodisulfate, were prepared. Glycoproteins (~1 mg protein per lane) were boiled at 95°C for 5 minutes with 6x Laemmli sample buffer (75mM Tris pH 6.8, 150 mg/mL SDS, 750 µg/mL bromophenol blue, 116 mg/ml DTT, 59% (v/v) glycerol), and then run on the gel with limits set at 200 V and 35 mA for approximately 1 hr. Gels were stained using Coomassie G-250.

Formulation with adjuvant

Glycoconjugate or carrier protein solutions were pre-adsorbed to aluminium hydroxide (Alum) adjuvant (Alhydrogen, Brentage, Denmark) by adding to an equal volume of glycoconjugate solution to adjuvant in a microcentrifuge tube on the day before scheduled injection. The solution was then left for 18 hr at 4°C on a rotating mixer. Each 100 µL injection volume was formulated to contain a pre-set amount of glycan. Therefore, the glycoconjugates were diluted accordingly with sterile Dulbecco's phosphate buffered saline (PBS) before adsorption. Moreover, the amount of carrier protein varied between glycoconjugate formulations depending on the loading of the antigen to the carrier protein.

Adsorption determination

The adsorption of antigen was evaluated by determination of the free glycoprotein level in the supernatant (Broecker, Martin et al. 2016). After absorption, glycoconjugate in adjuvant formulations were centrifuged (10 mins at 3000 rcf) to pellet the adjuvant. Supernatant containing non-adsorbed glycoconjugate was analysed via the Micro BCA™ Protein Assay Kit (#23235, Thermo Fisher Scientific, MA, USA) according to the manufacturer's protocol. The amount of absorbed antigen was calculated by comparing the protein concentration of the supernatant to the protein concentration of glycoconjugate solution without added adjuvant.

2.2 Immunisation model

Animal experiments

All experiments were carried out under approval number G0239/14, with additional addenda, granted by the Office for Health and Social Affairs Berlin (LAGeSo, Berlin, Germany). Animal suffering was minimised, and mice were euthanised as necessary according to humane experimental endpoints. Mice were housed in individually-ventilated cages under specific pathogen-free conditions in the animal facility of the Federal Institute for Risk Assessment (BfR, Berlin, Germany). Mice were provided food and water *ad libitum*. Mice used for immunisations were female C57BL/6 mice, 6-8 weeks old,

corresponding to late puberty/early adulthood (Dutta and Sengupta 2016) at the time of the prime immunisation. Mice were either from in-bred strains at the BfR animal facility or sourced from Janvier Labs (Saint-Berthevin, France). When the mice were sourced from outside the BfR facility then the mice were allowed to rest for 7 days upon delivery to the BfR animal facility before the prime immunisation.

Immunisation regime

Glycoconjugate formulation of 100 µL was injected into the mice subcutaneously above the shoulders, into loose skin over the neck using a syringe with a 27G needle. The glycoconjugate formulation was allowed to warm to RT before injection to minimise discomfort. A total of three injections were administered every two weeks constituting a prime-boost-boost regime in order to generate the antigen-specific antibody response. Thus, mice were immunised on days 0, 14, and 21, roughly human equivalent to two years between boosts (Dutta and Sengupta 2016).

Serum samples were collected from each mouse for downstream profiling of the induced antibody response. Serum samples were collected on the day of the prime injection, day 0, and every week thereafter on days 7, 14, 21, and day 35. Day 42 sera may also be collected. To obtain sera, the mice were placed in a restrainer. Blood was sampled from the tail-tip, with no more than 25 µL being collected per bleed. The blood was left to coagulate for at least 30 min at RT and then centrifuged at 2000 rcf to pellet the blood cells and separate the serum. Serum was aspirated, and an additional centrifugation step was repeated to clean the serum from remaining blood cells. Serum was frozen at -80°C until further use. Mice were additionally weighed on these days to ensure they did not experience unexpected weight loss as a possible consequence of glycoconjugate immunisation.

Day	Protocol
0	Prime, serum collection, weigh
7	Serum collection, weigh
14	Boost 1, serum collection, weigh
21	Serum collection, weigh
28	Boost 2, serum collection, weigh
35	Serum collection, weigh
42	Serum collection, weigh

Table 1: General timeline of the immunisation regime.

2.3 Challenge model with *P berghei* ANKA

Preparation of parasite stabilates

P. berghei ANKA MRA-671 (Malaria Research and Reference Reagent Resource Center, Manassas, VA, US) stabilates were prepared at the Immunology Unit & Research Center for Emerging Infections and Zoonoses (University of Veterinary Medicine Hannover, 30559 Hannover, Germany). BALB/c mice were infected with *P. berghei* ANKA. At 10-20% parasitemia, mice were anaesthetised before blood was drawn from the mouse via cardiac puncture. Blood was enriched for infected schizonts using magnetic bead separation, pooled into heparinised tubes and resuspended to a concentration of 10^8 cells/mL in 0.9% (w/v) NaCl, 4.6% (v/v) sorbitol, 35% (v/v) glycerol. Aliquots of 250 µL containing 2×10^7 cells/mL were flash frozen in liquid nitrogen and stored at -80°C until use.

Infection with parasite

At the completion of the immunisation schedule on day 42, mice were challenged with parasite stabilate, corresponding to day 0 post-infection. Parasite stabilates of 250 µL were quickly thawed by resuspension with sterile 750 µL PBS at RT. The stabilate solution was taken up into a syringe with a 27G needle. To each mouse a 100 µL volume of thawed stabilate was injected intraperitoneally, corresponding to 1×10^6 iRBCs. Up to 10 mice were injected within 10 minutes of the stabilate being thawed to ensure that mice were injected with viable parasites, at which point another stabilate was prepared. Mice were

randomized prior to infection, so that one mouse out of each group was infected using the stabilate. To confirm that the inoculation was successful, a small drop of blood was taken by tail-vein bleed on day 6, day 9 and day 12 post-infection. The blood was directly dropped onto a glass side, smeared and stained for the presence of parasites.

Infected mice typically develop neurological symptoms from day 6 onwards after challenge, and mice are observed twice daily from day 5 onwards for signs of discomfort and disease. During the crucial time period from day 6 to 9, mice were observed three times daily. Symptoms generally appearing in order of severity are ruffled fur, hunching, wobbly gait, limb paralysis, convulsions, and coma. Each symptom is one point of disease score (Amante, Stanley et al. 2007). Cumulative disease scores ≥3 indicate the animal has succumbed to experimental cerebral malaria and is immediately euthanised, at which point she is given a disease score of 4. Other humane endpoints for the infection course are severe weight loss (≥20%), excessive parasitemia (≥20%) or 12 days after infection.

2.4 Synthetic GPI epitope libraries

Preparation of microarray slides

All synthetic GPI substructures used for this study were synthesized with a C6 thiol linker, allowing for conjugation to 3D-Maleimide glass slides (PolyAn GmbH, Berlin, Germany). Additional C6 thiol linked synthetic glycan fragments were sourced from the glycan array database (Biomolecular Systems, MPIKG) in order to map the epitopes that were immunogenic on the synthetic GPI antigen.

Lyophilised synthetic GPI substructures were resuspended to a stock concentration of 10 mM using 50 mM sodium phosphate buffer, pH 8.5. Working solutions were prepared at 1 mM, 0.2 mM, and 0.05 mM concentrations. The solutions were spiked with equimolar amounts of concentrated TCEP before spotting in triplicate onto microarray slides using an S3 piezoelectric spotting device (Scienion, Berlin, Germany) optimised for delivering a 0.5 nL drop volume to the slide. Spotted slides were incubated in a humidified chamber for 18 hr to complete coupling reactions before quenching with 0.1% (v/v) 2-mercaptoethanol in PBS for 1 hr at RT. Slides were rinsed with ultrapure water, dried by

centrifugation and stored at 4 °C until use. Glycan array spots using 0.2 mM concentrations were used for the subsequent antibody profiling analysis.

Glycan microarray analysis for epitope mapping

Epitope-specific antibody profiles of sera from immunised mice were characterised on the glycan microarray. Glycan microarray slides displaying the GPI epitope library were blocked with 1% (w/v) bovine serum albumin (BSA) in PBS for 1 hr at RT, rinsed with ultrapure water and dried by centrifugation. 64-well incubation chambers (Grace Bio-Laboratories, Bend, OR, USA) were applied to the microarray slides. 25 µL sera diluted 1:50 in PBS were added to each well for incubation overnight at 4°C in a humidified chamber. Following incubation, sera were discarded and wells rinsed with 0.05% (v/v) Tween-20 in PBS. Anti-mouse secondary antibodies were added to each well (Invitrogen, Waltham, MA, USA) diluted 1:400 with 1% (w/v) BSA, 0.05% (v/v) Tween-20 in PBS and incubated on the microarray slides for 1 hr at RT. For isotype titre analysis, combinations of goat anti-mouse IgG2a Alexa Fluor 647 (#A21241, Invitrogen), goat anti-mouse IgG1 Alexa Fluor 594 (#A21125, Invitrogen), goat anti-mouse IgG3, Alexa Fluor 488 (#A21151, Invitrogen), and goat anti-mouse IgM, Alexa Fluor 546 (#A21045, Invitrogen) at 1:400 dilution were used. For total IgG analysis, goat anti-mouse IgG (H+L) Alexa Fluor 635 (#A31574, Invitrogen) with goat anti-mouse IgM (µ-chain) Alexa Fluor 594 (#715-585-020, Dianova, Hamburg, Germany) was used. For monoclonal antibody analysis goat anti-mouse IgM (µ-chain) Alexa Fluor 647 (#A21238, Invitrogen) was used. For human antibody analysis goat anti-human IgG (H+L) Alexa Fluor 546 (#A21089, Invitrogen) and goat anti-Human IgM (Heavy chain) Alexa Fluor 647 (#A21249, Invitrogen) at 1:400 dilution were used. For monkey antibody analysis goat anti-monkey IgG (Fc specific) FITC (#GAMon/IgG(Fc)/FITC, Nordic-Mubio, Susteren, The Netherlands) and goat anti-monkey IgM (Fc specific) TRITC (# GAMon/IgM(Fc)/TRITC, Nordic-MUbio) at 1:200 dilution were used.

Microarray slides were rinsed with 0.1% (v/v) Tween-20 in PBS, PBS only, ultrapure water, and then dried by centrifugation. Microarray slides were scanned with a GenePix 4300A microarray scanner (Molecular Devices, Sunnyvale, CA, USA). Background-subtracted mean fluorescence intensity (MFI) values reflected the antibody titre present in the sera. These data were exported to R for analysis and visualisation.

2.5 Cell culture techniques

P. falciparum 3D7 cell culture

All cell culture work was conducted in a laminar flow sterile workbench. *P. falciparum* 3D7 synchronised cell culture was carried out with standard protocols (Radfar, Mendez et al. 2009), with modifications for growing parasites to high parasitemia with a reasonable daily workload. Parasites were grown in RPMI-1640 (P04-17500, Aidenbach, Germany) supplemented with 5 mM HEPES, 0.5% (w/v) AlbuMAX™ II Lipid-Rich BSA (#10624053, Thermo Fisher Scientific, MA, USA), 2mM L-glutamine, 28 µg/mL hypoxanthine, 50 µg/mL gentamycin, and 1% (v/v) human RBCs, at 5% CO_2 at 37°C. Parasitemia was checked daily via peripheral smear, and cultures >10% parasitemia were split to 2% parasitemia to avoid acidification of the cell culture media. Cultures were synchronised via sorbitol treatment (Radfar, Mendez et al. 2009) at least once per week.

To prepare infected cells for in vitro analysis, iRBCs were pelleted and washed in PBS to remove excess media before fixation with 4% (v/v) paraformaldehyde (diluted from 37% paraformaldehyde solution), 0.0075% glutaraldehyde in PBS for 1 hour at 37°C. iRBCs were washed and resuspended in PBS and kept at 4°C until use.

Monoclonal hybridoma production

Hybridoma monoclonal antibody fusion (Kohler and Milstein 1975) was based on a protocol outlined by BM Condimed H1 (#11088947001, Roche Diagnostics GmbH, Mannheim, Germany). Once a strong antibody response against the PEtN-Man epitope was confirmed by glycan microarray analysis, the selected mouse was given a final boost four days before it was sacrificed and splenic tissue was collected. Under sterile conditions, the collected tissue was dissociated into single cell suspension. Myeloma cells X63-Ag8 (previously maintained in active growth phase in IMDM or RPMI (PAN-Biotech, Aidenbach, Germany) supplemented with 2 mM L-glutamine, 0.05 mg/mL gentamycin, 1% penicillin & streptomycin, 10% (v/v) foetal bovine serum (FBS) (heat inactivated at 56°C, 45 min), 1% non-essential amino acids, 1% sodium pyruvate) and spleen cells are pelleted to facilitate good cell-cell contact (Greenfield 2018). Cells were slowly resuspended in polyethelene glycol 1500 (#10783641001, Roche Diagnostics GmbH) to fuse the membranes.

After fusion, hybridoma cells were transferred to cell culture for clonal expansion. Cells were grown in IMDM (PAN-Biotech) supplemented with 2 mM L-glutamine, 1% penicillin & streptomycin, 0.05 mg/mL gentamycin, 1% non-essential amino acids, 1% sodium pyruvate, and 0.1% 2-mercaptoethanol. Additional supplementation of aminopterin with hypoxanthin/thymidin selected for fused cells only. FBS (10% (v/v), heat inactivated at 56°C, 45 min) and 10% BM Condimed (#10663573001, Roche, Basel, Switzerland) were additionally added as needed to facilitate growth. Hybridoma clones for final expansion were selected by glycan microarray analysis using goat anti-mouse IgG, and goat anti-mouse IgM. Isotype analysis was carried out with a Mouse Isotyping Test (#RAP-4461, DRG Instruments GmbH, Marburg, Germany). Selected clones were expanded, with FBS content in the growth media gradually reduced to 0% to promote antibody production.

Monoclonal IgM with κ light chain was purified from cell culture supernatant using a Pierce™ Protein L Chromatography Cartridge (#89928, Thermo Fisher Scientific, MA, USA) on the NGC Discover Pro Chromatography System (Bio-Rad Laboratories Inc., Hercules, CA, USA). Binding buffer was PBS, elution buffer was 0.1M glycine, pH 2.5, HCl adjusted, and neutralisation buffer was 1 M Tris, pH 8.0, HCl adjusted.

RAW 264.7 macrophage cell culture

All cell culture work was conducted in a laminar flow sterile workbench. Murine (Balb/c) macrophages RAW 264.7 were handled according to standard protocols (Bowdish Lab, McMaster University, Hamilton, ON, Canada). When cells were needed for assays, they were quickly thawed in a 37°C water bath then transferred to 10 mL pre-warmed RPMI media with 10% (v/v) FBS, 2 mM L-glutamine, 1% penicillin & streptomycin. Cells were pelleted at 300 rcf and then resuspended with fresh media to remove the freezing medium. Cells were grown in 75 cm^2 flasks and propagating cells were allowed to grow to 60-75% confluence (no higher) before subculturing. Cells were dislodged from the flask using the cell scraper method, pelleted at 300 rcf before splitting 1:3 to new flasks and fresh media. To freeze cells, up to 2×10^7 cells were resuspended in 3.6 mL culture media. To this, 400 µL DMSO are added dropwise before 1 mL aliquots are added to cryovials. Aliquots are stored overnight in a freezing container at -80°C, and then transferred to liquid nitrogen for long term storage.

2.6 *In vitro* analysis techniques

Fluorescent microscopy of *P. falciparum* 3D7

To determine binding of antibodies from sera of immunised mice via fluorescent microscopy, fixed iRBCs were blocked with 3% (v/v) FBS in PBS for 1 hr at RT then rinsed with PBS. Pooled sera of mice diluted in PBS was added as primary antibody and incubated for 1 hr at RT. Following incubation, primary antibody solutions were discarded and iRBCs rinsed with 0.05% (v/v) Tween-20 in PBS. Goat anti-mouse IgG (H+L) Alexa Fluor 635 (#A31574, Invitrogen), diluted 1:1000 with 0.05% (v/v) Tween-20 in PBS, was incubated with the iRBCs for 1 hr at RT. iRBCs were rinsed with 0.05% (v/v) Tween-20 in PBS, then with PBS. iRBCs were mounted onto a glass microscope slide (#1010412, Paul Marienfeld GmbH & Co. KG, Lauda-Königshofen, Germany) using Fluoromount-G™, with DAPI (#00495952, Invitrogen).

Flow cytometry of *P. falciparum* 3D7

To determine binding of antibodies from sera of immunised mice via flow cytometry, pelleted schizonts were incubated with 0.1% saponin for 10 min on ice to lyse iRBCs. Liberated merozoites were washed by repeated cycles of pelleting at 2000 rcf and resuspension with PBS. Merozoites were blocked with 3% (v/v) FBS in PBS for 1 hr at RT then rinsed with PBS. Pooled sera of mice diluted 1:50 in PBS was added as primary antibody and incubated for 1 hr at RT. Following incubation, goat anti-mouse IgG (H+L) Alexa Fluor 635 (#A31574, Invitrogen), diluted 1:400 with 0.05% (v/v) Tween-20 in PBS, was incubated with the merozoites for 1 hr at RT. Merozoites were rinsed with 0.05% (v/v) Tween-20 in PBS, then with PBS. Merozoites were suspended in solution containing 1:1000 dilution of SYBR safe DNA gel stain 10,000x (#S33102, Invitrogen) in PBS. Merozoites were subjected to flow cytometry (FACSCanto™ II, Becton Dickinson, Franklin Lakes, NJ, USA). Voltage parameters were set at: FSC=280, SSC=300, FITC=380, APC=380. Merozoites were gated on FSC-A (logscale) versus SSC-A (logscale). Single merozoites were further gated on FSC-A (logscale) versus FSC-H (logscale).

Fluorescent microscopy of *L. mexicana*

Axenic *L. mexicana* DsRed amastigotes or promastigotes were fixed on 13 mm circular glass coverslips in 4% paraformaldehyde (v/v) in PBS. Fixed cells were blocked with 3% (v/v) FBS in PBS for 1 hr at RT then rinsed with PBS. Monoclonal antibody or IgM isotype control (#M5909, Sigma-Aldrich, St. Louis, MO, USA) diluted in PBS, in a range of 10 µg/mL to 0.01 µg/mL, was added as primary antibody and incubated overnight at 4°C in a humidified chamber. Following incubation, primary antibody solutions were discarded and fixed cells rinsed with 0.05% (v/v) Tween-20 in PBS. Goat anti-Mouse IgM, Alexa Fluor 647 (#A21238, Invitrogen), diluted 1:1000 with 0.05% (v/v) Tween-20 in PBS, was incubated on the fixed cells coverslips for 1 hr at RT. Fixed cells were rinsed with 0.05% (v/v) Tween-20 in PBS, then with PBS, before mounting onto a glass microscope slide (#1010412, Paul Marienfeld GmbH & Co. KG, Lauda-Königshofen, Germany) using Fluoromount-G™, with DAPI (#00495952, Invitrogen).

TNF- α release of RAW 264.7 macrophages assay

RAW 264.7 at 50-75% confluence, in 10 mL culture media within a 75 cm2 flask, gave ~5 x 10^5 cells/mL after resuspension. In a reaction well, 100 µL culture media containing 4 x 10^5 RAW 264.7 cells are left to settle for 1 hr at 37°C/5% CO_2. In the meantime, 2.5 x 10^5 merozoites are incubated with endotoxin-free sera diluted in PBS in a maximum volume of 5 µL for 1 hr at RT. After incubation, the merozoite/sera solution is added to the cell culture reaction wells. The final reaction wells contain 2.5 x 10^5 merozoites and 4 x 10^5 RAW 264.7 cells. The reaction wells are left to incubate for 18 hr at 37°C/5% CO_2. The following morning, cell culture supernatant is aspirated from each well and stored at -20°C until use.

To determine the TNF-α concentration in the supernatant the Murine TNF-α Mini TMB ELISA kit was employed (900-TM54, PeproTech Germany, 22081 Hamburg, Germany). The assay was carried out according to the manufacturer's instructions on MaxiSorp™ Nunc-immuno plates (#442404, Nunc, Roskilde, Denmark).

Merozoite invasion-inhibition assay

Synchronised trophozoites were diluted to 0.5% parasitemia, and 100 µL added to reaction wells of an untreated 96-well plate. Stock sample solutions were diluted to 50 µg/mL, and doubling dilutions were prepared. Sample dilutions were added at 5 µL volumes in triplicate wells containing 100 µL cell culture, giving 2.5 µg/mL for the highest concentration. To test for parasitemia levels after 48 hours, 40 µL parasite soup was added to 400 µL SYBR Green I nucleic acid gel stain (S7563, Invitrogen, Waltham, MA, USA) diluted 1:10,000 in PBS and parasitemia was determined by flow cytometry. For two cycle assays add 20 µL fresh medium to each well and then repeat flow cytometry again at 96 h. As a control for mAb, IgM Isotype Control (M5909, Sigma-Aldrich, St. Louis, MO, USA) was used.

Western blot with isolated *P. falciparum* GPI

P. falciparum 3D7 synchronised cell culture was sourced for GPI. Late-stage merozoites were isolated using sorbitol treatment, washed with PBS, and lyophilized (Radfar, Mendez et al. 2009). GPI was isolated using chloroform/methanol extraction. The merozoite pellet was sonicated in 6 mL Chloroform:Methanol (2:1). Supernatant was collected and dried, then sonicated in 6 mL Chloroform:Methanol:Water (10:10:3). Supernatant was collected and dried, then sonicated in 10 mL saturated butanol. Water was added and the upper organic phase containing lipids was collected then dried. The lipids were resuspended in Chloroform:Methanol (1:1) and GPI was fractionated using a column loaded with Sephadex LH-20 resin washed in Chloroform:Methanol:Water (3:3:1).

To confirm the presence of GPI, fractions were stained for the presence of glycans then confirmed in NMR. Isolated GPI was conjugated to polypeptide with an Amine Coupling kit [#BR-1000-50, Biacore, Uppsala, Sweden]. The polypeptide was stabilised with sulfo-NHS before addition of NHS/EDC reagent. GPI was incubated with the polypeptide and then quenched with ethanolamine.

GPI-polypeptide conjugate was transferred to a membrane using the Trans-Blot® Turbo™ Transfer System (BioRad, Hercules, CA, USA). Western blot was blocked with 5% (w/v) BSA 0.1% (v/v) Tween 20% in TBS for 1 hr at RT. Antibodies were diluted in 0.1% (w/v) BSA 0.1% (v/v) Tween 20% and incubated for 1 hr at RT. Monoclonal antibody was

added at 1.8 µg/ml. After washing, goat anti-mouse IgM HRP (#M31507, Invitrogen) was added at 1:1000 dilution. Western blot was developed with ECL™ Western Blotting Reagents kit (#RPN2106, GE Healthcare, Chicago, IL, USA).

3 Results and Discussion

3.1 Elucidating immunogenic GPI residues

Profiling antibodies induced by various synthetic GPI fragments

A glycoconjugate that protects against severe malaria requires the selection of an epitope that is presumably the target epitope of protective antibodies. After epitope selection, a synthetic antigen needs to be designed that facilitates the induction of these epitope-specific antibodies, when formulated as part of an immunising glycoconjugate. To aid in the antigen design, an understanding of how certain GPI residues affect the epitope specificity of induced antibodies is required.

In order to investigate how the inclusion or omission of residues on GPI antigens could direct antibody specificities I utilised synthetic glycan fragments **1-6** [**Figure 10**] based on *P. falciparum* GPI, which were previously synthesised in our lab. Microarrays were furnished with these fragments, along with other control oligosaccharides, to create a library of GPI epitopes allowing the multiplexed detection of glycan-specific antibodies (Geissner, Anish et al. 2014). Additionally, I employed the sera of C57BL/6 mice previously immunised with glycoconjugates of **1-6** containing 5 µg of synthetic GPI. I screened these sera (diluted 1:100) at day 42 post-prime immunisation (n=15 per group, classified by the immunising glycoconjugate) on the GPI epitope microarray to profile epitope-specific antibody titres and evaluate how induced antibody titres are affected by residues within various carbohydrate antigens.

Immunisation with glycoconjugates of **1-6** induced various class-switched IgG, indicative of T cell dependent immunity [**Figure 11**], and also IgM [**Figure 12**]. Immunisation with glycoconjugates of **1** and **4** containing InoP induced antibodies predominantly against fragments containing InoP, and to a lesser extent GlcN, independent of PEtN or Man [**Figure 11a & d** and **Figure 12a & d**]. Fragments lacking GlcN or InoP were not recognized. This suggests that InoP and GlcN are immunodominant residues facilitating the induction of antibodies specific to the GlcN-InoP epitope. The immunogenicity of InoP was similarly reported when InoP-specific antibodies were induced in mice immunised with glycoconjugates of synthetic Man4-GlcN-InoP antigen (Tamborrini

2009). The immunogenicity of InoP may have also contributed to the specificity of antibodies induced by glycoconjugates of synthetic *T. gondii* GPI containing InoP (Götze, Reinhardt et al. 2015). Interestingly, naturally occurring GPI-specific antibodies can recognise synthetic GPI fragments containing GlcN-InoP epitopes when presented in conjunction with the intact *P falciparum*-specific core Man backbone. However, these naturally-induced antibodies do not recognise the non-specific GlcN-InoP fragments on their own (Kamena, Tamborrini et al. 2008). Therefore, InoP and GlcN are immunodominant residues when included in synthetic GPI fragments that are used for immunisation, but do not appear similarly immunodominant as a part of native GPI antigen.

Immunisation with glycoconjugates of **2** and **5** lacking InoP induced antibodies directed mainly toward Man and GlcN, with further improvement when PEtN was present [**Figure 11b & e** and **Figure 12b & e**]. However, the antibodies also bound to fragments lacking PEtN, indicating that PEtN is not the immunodominant epitope. The antibodies do not recognize the Man2-GlcN-InoP fragment similar to naturally occurring GPI-specific antibodies (Kamena, Tamborrini et al. 2008) suggesting that antigens lacking InoP could induce antibodies more akin to naturally occurring GPI-specific antibodies.

Immunisation with glycoconjugates of **3** and **6**, lacking PEtN on Man-III, show decreased immunogenicity compared to their counterparts with PEtN [**Figure 11c & f** and **Figure 12c & f**]. In larger glycoconjugates containing all three immunogenic groups, the induced antibodies preferentially recognize and bind InoP and GlcN. Thus, inclusion of PEtN is important for antibody induction, if immunodominant groups like GlcN and InoP are missing. PEtN has been reported to contribute to immunogenicity in synthetic glycan antigens based on *C. difficile* PSII cell wall polysaccharide (Adamo, Romano et al. 2012) and lipoteichoic acid (Broecker, Martin et al. 2016). PEtN on these synthetic glycan antigens were also shown to be crucial in inducing antibodies with similar binding properties to antibodies induced by native PSII (Adamo, Romano et al. 2012).

For antibody titres against GPI from other organisms, immunisation with glycoconjugate of **2** induced high IgG and IgM titres to *T. gondii* and mammalian GPI [**Figure 13b** and **Figure 14b**]. Interestingly, immunisation with glycoconjugate of **5** did not induce this non-specific binding [**Figure 13e** and **Figure 14e**] suggesting that the fourth Man induces

antibody profiles specific to *P. falciparum* GPI. This finding supports previous reports describing the fourth Man as a key recognition element (Kamena, Tamborrini et al. 2008).

Immunisation with glycoconjugates of **3** and **6** show little binding to GPI from other organisms [**Figure 13c & f** and **Figure 14c & f**], supporting the notion that PEtN is important for antibody induction if immunodominant groups like GlcN and InoP are missing. Finally, immunisation with glycoconjugates of **1** and **4** induces IgG and IgM to non-*P. falciparum* GPI [**Figure 13a & d** and **Figure 14a & d**], likely mediated by InoP.

Taken together, we observe that InoP and GlcN are immunogenic residues of synthetic GPI antigens. PEtN is also immunogenic, and should be included if immunodominant groups like GlcN and InoP are missing. These results also suggest that antigens designed to induce antibodies mimicking the epitope binding profile of naturally occurring antibodies would likely require the omission of InoP.

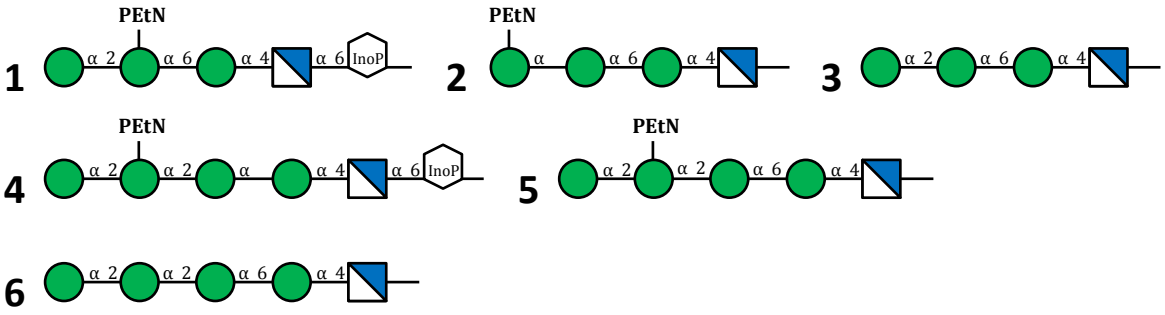

Figure 10: A selection of synthetic GPI fragments. These were printed on glycan arrays, and glycoconjugates thereof were used to immunise mice. **(1-3)** Fragments with a trimannose backbone. **1)** PEtN-Man_3-GlcN-InoP. Note the displacement of PEtN to Man-II. **2)** PEtN-Man_3-GlcN. **3)** Man_3-GlcN. **(4-6)** Fragments with a tetramannose backbone. **4)** PEtN-Man_4-GlcN-InoP. **5)** PEtN-Man_4-GlcN. **6)** Man_4-GlcN.

Shorthand	Full name of structure
Pfal2.1	PEtN-Man3- (fragment **7**)
Pfal2.2	PEtN-Man4- (fragment **8**)
Tgon1.1	Glc-GalNAc-[PEtN-Man2-]Man-GlcN-InoP-
Tgon1.2	GalNAc-[PEtN-Man2-]Man-GlcN-InoP-
Tgon1.3	GalNAc-[Man2-]Man-GlcN-InoP-
Tbru1.1	Gal-Man-
Tbru1.2	Gal2-Man-
Tbru1.3	PEtN-[Gal-]Man-[Gal-]Man2-
Mamm1.1	GalNAc-[PEtN-Man2-]Man-2-PEtN-GlcN-InoP-

Table 2: Shorthand notation of structures listed in graphed results. Longer structure names (especially for glycan fragments based on GPI from other organisms) use shorthand notation for ease of visualisation.

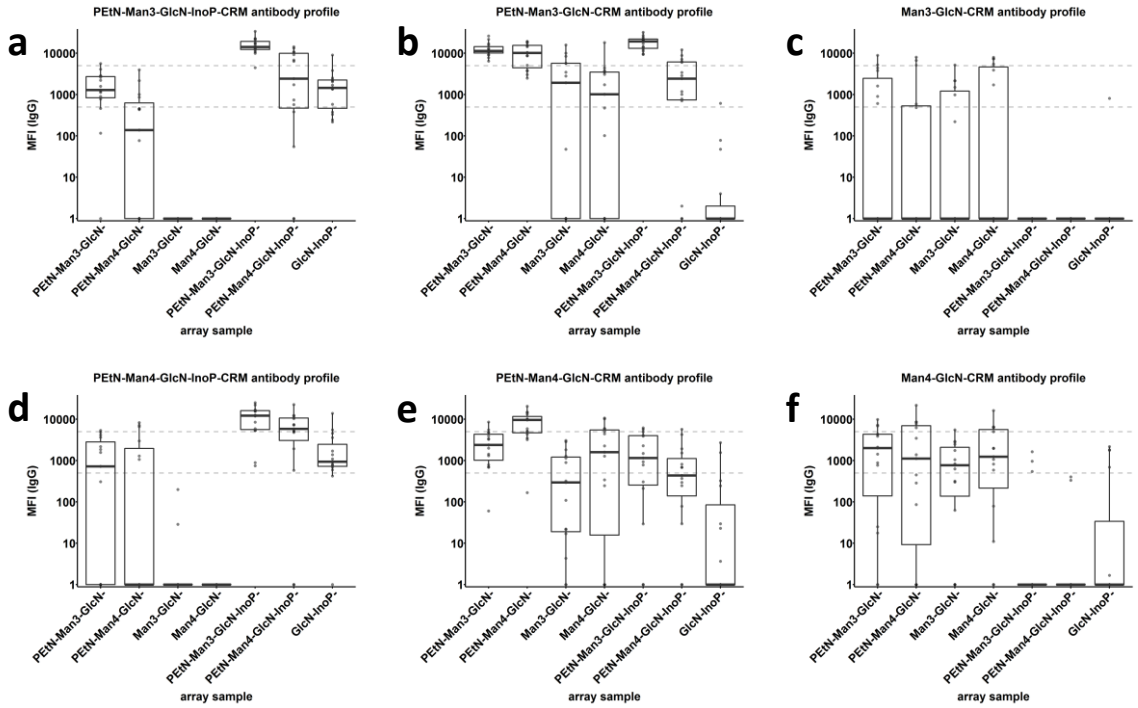

Figure 11: IgG titres against synthetic GPI fragments in sera at day 42. Group size n=15, classified by the immunising glycoconjugate. **Top panel (a-c)** IgG titres after immunisation with glycoconjugates of **1**-**3** lacking the fourth Man. **Bottom panel (d-f)** IgG titres after immunisation with glycoconjugates of **4**-**6** containing the fourth Man.

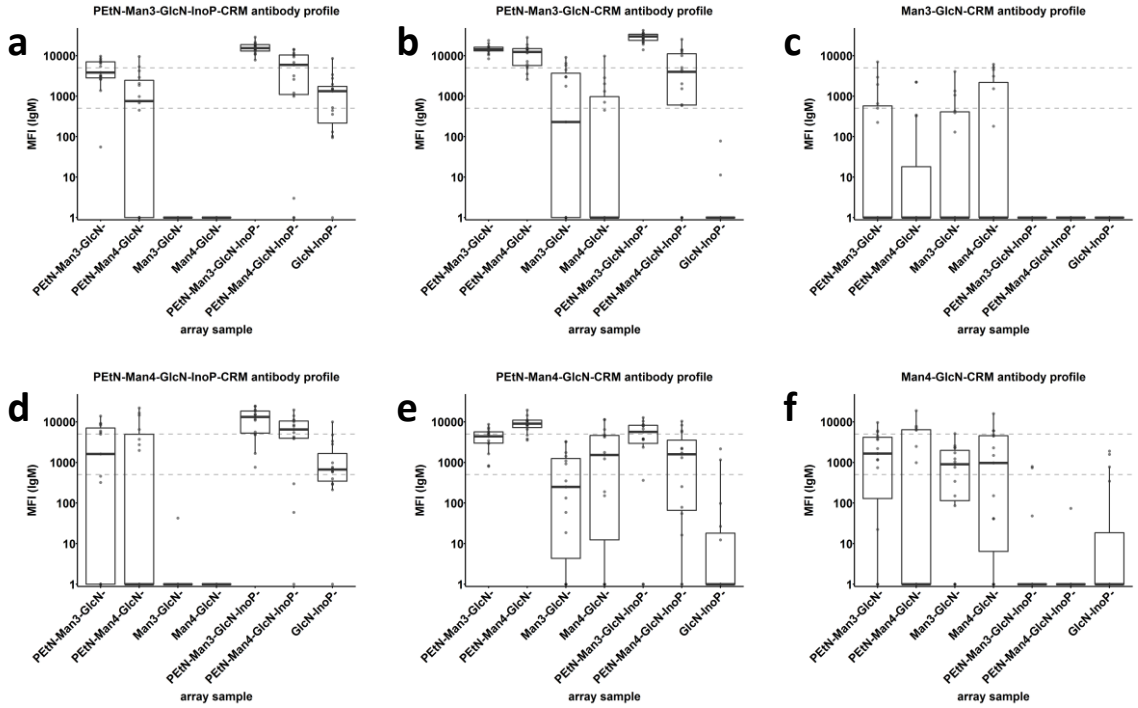

Figure 12: IgM titres against synthetic GPI fragments in sera at day 42. Group size n=15, classified by the immunising glycoconjugate. **Top panel (a-c)** IgM titres after immunisation with glycoconjugates of **1**-**3** lacking the fourth Man. **Bottom panel (d-f)** IgM titres after immunisation with glycoconjugates of **4**-**6** containing the fourth Man.

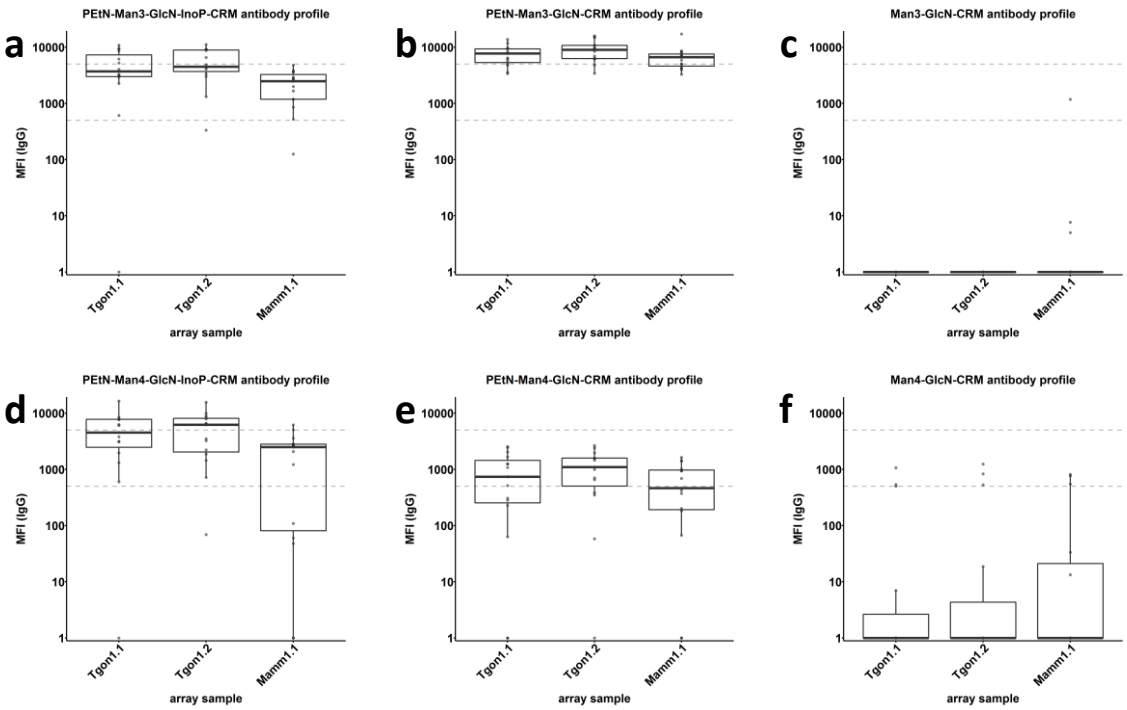

Figure 13: IgG titres against synthetic GPI in other organisms in sera at day 42. Group size n=15, classified by the immunising glycoconjugate. **Top panel (a-c)** IgG titres after immunisation with glycoconjugates of **1**-**3** lacking the fourth Man. **Bottom panel (d-f)** IgG titres after immunisation with glycoconjugates of **4**-**6** containing the fourth Man.

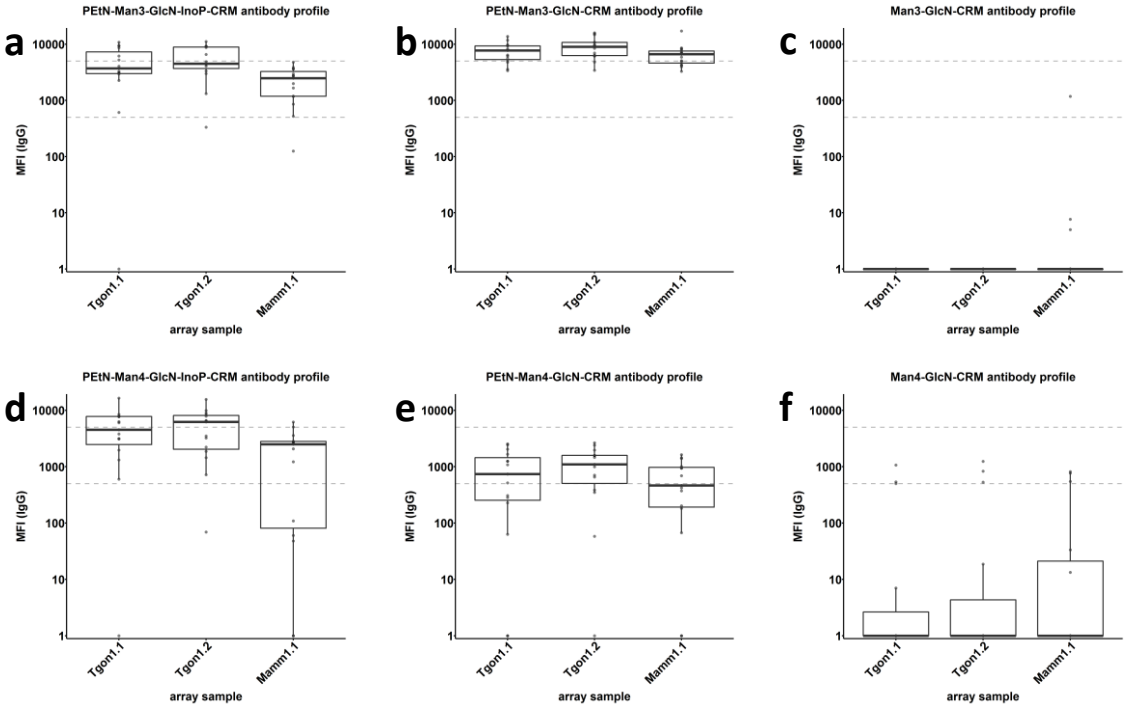

Figure 14: IgM titres against synthetic GPI in other organisms in sera at day 42. Group size n=15, classified by the immunising glycoconjugate. **Top panel (a-c)** IgM titres after immunisation with glycoconjugates of **1**-**3** lacking the fourth Man. **Bottom panel (d-f)** IgM titres after immunisation with glycoconjugates of **4**-**6** containing the fourth Man.

Profiling of previously published monoclonal antibodies

I found that InoP is immunodominant in synthetic GPI fragments used for immunisation. Therefore, antibodies induced by InoP-containing glycoconjugates should be directed to the immunodominant InoP epitope. To further validate this finding, I analysed the binding profile of published monoclonal antibodies (mAb) derived from InoP-containing glycoconjugate immunisation. Previously, mice were immunised with synthetic GPI Man4-GlcN-InoP- [**Figure 15**] conjugated to KLH carrier protein in order to induce GPI-specific antibodies. Three mAbs MTG4, MTG5, and MTG6 were generated from the immune cells of these immunised mice (Tamborrini 2009). The mAbs were then screened against a published epitope library of synthetic GPI fragments truncated from the non-reducing terminus, all containing InoP (Tamborrini, Liu et al. 2010). To elucidate the mAb specificity, or lack thereof, to GPI residues other than InoP I screened the mAbs against the current epitope library containing synthetic GPI fragments lacking InoP.

Preserved stocks of monoclonal hybridoma cells expressing MTG4, MTG5, or MTG6 mAb were cultured. The individual cell culture supernatants (diluted 1:100) were screened on the synthetic GPI library to evaluate mAb specificity. The mAbs MTG5 and MTG6 exclusively recognise fragments containing a GlcN-InoP epitope [**Figure 16b & c**]. MTG4 was also able to recognise GPI fragments containing the GlcN-InoP epitope [**Figure 16a**] in addition to GPI fragments containing a Man4-GlcN epitope, independent of InoP and PEtN. Fragments without the fourth Man were not recognised, indicating that the fourth Man is required for recognition, possibly in combination with the GlcN residue.

MTG4 and MTG5 also bind to *T. gondii* and mammalian GPI fragments [**Figure 16d** and **Figure 16e**]. MTG6 also shows binds to GPI from other organisms to a lesser extent [**Figure 16f**]. One can presume this cross-specific binding is facilitated by the GlcN-InoP epitope contained in the GPI fragments from other organisms.

Microarray profiling of the mAbs confirms their specificity to InoP. It can then be presumed that the mouse from which these mAbs were derived had high numbers of antibody-producing cells producing Ig of this specificity (French, Fischberg et al. 1986). Induction of cells producing InoP-specific antibodies was likely facilitated by immunisation with the glycoconjugate containing InoP, confirming the immunogenicity of InoP when used in synthetic GPI antigens.

A hexasaccharide was also synthesised and conjugated to CRM197 carrier protein [**Appendix**, **Figure 80 & Figure 81**]. This hexasaccharide was similar to previously published glycoconjugates containing InoP. Mice were immunised in order to determine induced antibody specificities. It was revealed that this glycoconjugate did not induce antibody production against the synthetic GPI epitopes. As the glycoconjugate was not immunogenic, further work with this glycoconjugate was not pursued.

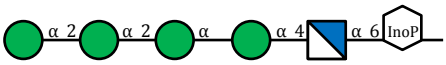

Figure 15: The synthetic Man4-GlcN-InoP- fragment used to generate mAb. Note the inclusion of the InoP residue and absence of the PEtN moiety.

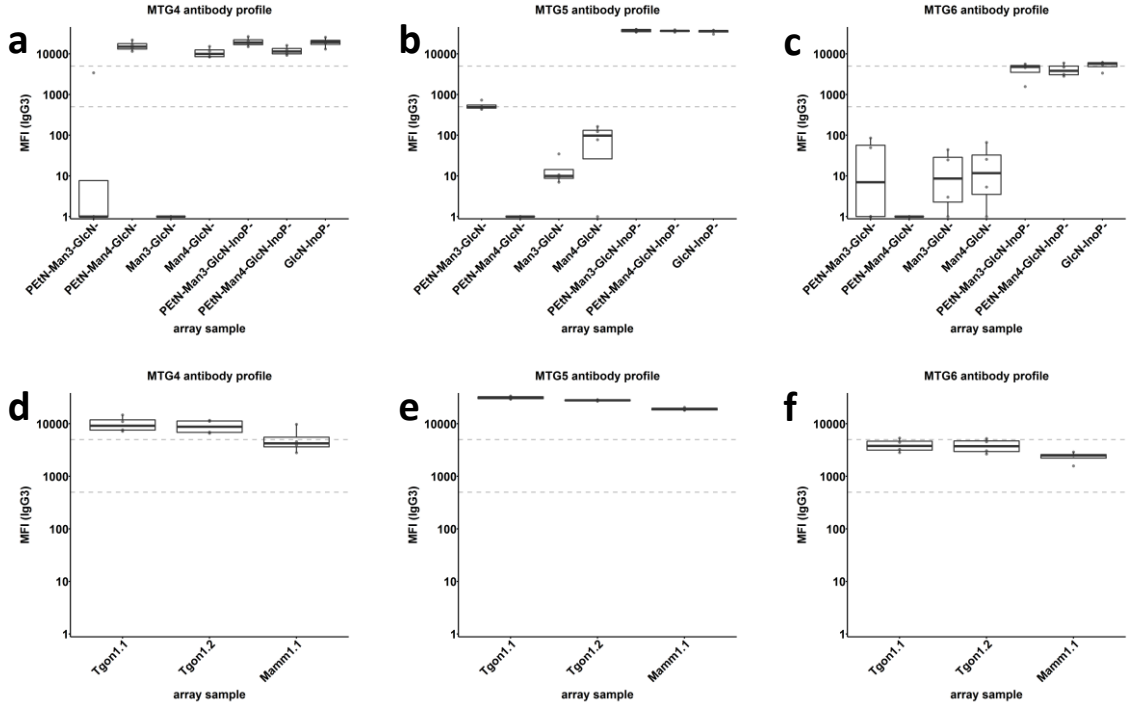

Figure 16: MTG mAb binding profiles. Top panel (a-c) IgG3 titres against synthetic *P. falciparum* GPI. **Bottom panel (d-f)** IgG3 titres against synthetic GPI from other organisms.

3.2 Design of synthetic minimal epitope fragments

Rationale for design

With an understanding of how certain residues on synthetic GPI affect the subsequent immune response, the next step was to consider which epitope on GPI would be the target of induced antibodies. Ideally, antibodies specific to this epitope would be protective against the toxic effects of GPI. To this end, minimal epitope fragments were designed [**Figure 17**]. PEtN-Man_3 (**7**) is based on free GPI, and PEtN-Man_4 (**8**) is based on GPI anchors attached to merozoite invasion proteins (Gerold, Dieckmann-Schuppert et al. 1994) considered prime vaccine candidates (Cowman, Berry et al. 2012). These minimal epitope antigens lack the immunodominant GlcN and InoP residues. Since larger glycans are usually more immunogenic than smaller oligosaccharides (Martin, Broecker et al. 2013, Broecker, Martin et al. 2016) we retain the immunogenic PEtN moiety on Man-III. PEtN should also facilitate the induction of antibodies specific to epitopes on the non-reducing terminus of GPI, distal to the phospholipid.

I reasoned that antibodies specific to this terminal epitope may protect against the toxic hyper-inflammatory response implicated in severe malaria. The linear structure without further modification is specific to *P. falciparum* GPI, avoiding structurally similar GPI epitopes found on host cells that possibly retard the induction of effective immune responses (Cowman, Berry et al. 2012). Since GPIs are inflammatory only in the context of the full glycolipid (Vijaykumar, Naik et al. 2001), with the reducing end masked by the lipid tail, binding to the terminal non-reducing epitope may be enough to stop inflammation. More recently, human liver-plasma protein C1INH was shown to neutralize GPI-induced inflammation presumably by binding GPI glycan residues (Mejia, Diez-Silva et al. 2016).

The antigens, lacking InoP, could induce antibodies more akin to naturally occurring GPI-specific antibodies (Kamena, Tamborrini et al. 2008). Indeed, the minimal epitope antigens are part of experimentally determined epitopes for antibodies isolated from individuals with malaria [**Figure 18**], excluding the GlcN-InoP epitope (Naik, Branch et al. 2000, Naik, Krishnegowda et al. 2006, Kamena, Tamborrini et al. 2008, Tamborrini, Liu et al. 2010).

Antigen diversion was previously observed when functional antibodies were blocked by antibodies competing for different epitopes on the same merozoite antigen (Guevara-Patino, Holder et al. 1997). The minimal epitope antigens are expected to exclusively induce the production of antibodies specific to the terminal epitope, avoiding competition with other GPI-specific antibodies. If these terminal epitope-specific antibodies are protective, then our minimal epitope antigens could "tip the balance" to their production via glycoconjugate immunisation (Renia and Goh 2016).

Variants of the minimal epitope with or without this the fourth Man aim to further clarify the role of this residue thought to confer specificity towards *P. falciparum*, though conflicting results are reported (Naik, Krishnegowda et al. 2006, Kamena, Tamborrini et al. 2008). Surprisingly, antibodies specific to core GPI with the additional fourth Man have also been isolated from uninfected individuals, which might have been induced due to infections with unrelated fungi or parasites (Kamena, Tamborrini et al. 2008, Tamborrini, Liu et al. 2010).

Finally, these antigens could induce epitope-specific antibodies that have likely not been induced by earlier glycoconjugates of synthetic GPI. Analysis of GPI residue immunogenicity suggests that the previously published glycoconjugates of synthetic GPI containing InoP (Schofield, Hewitt et al. 2002, Tamborrini 2009) likely lead to the production of antibodies predominantly against InoP. Facilitating the induction of antibodies specific to epitopes of the non-reducing terminus of GPI would allow the characterisation of antibodies as yet unexplored.

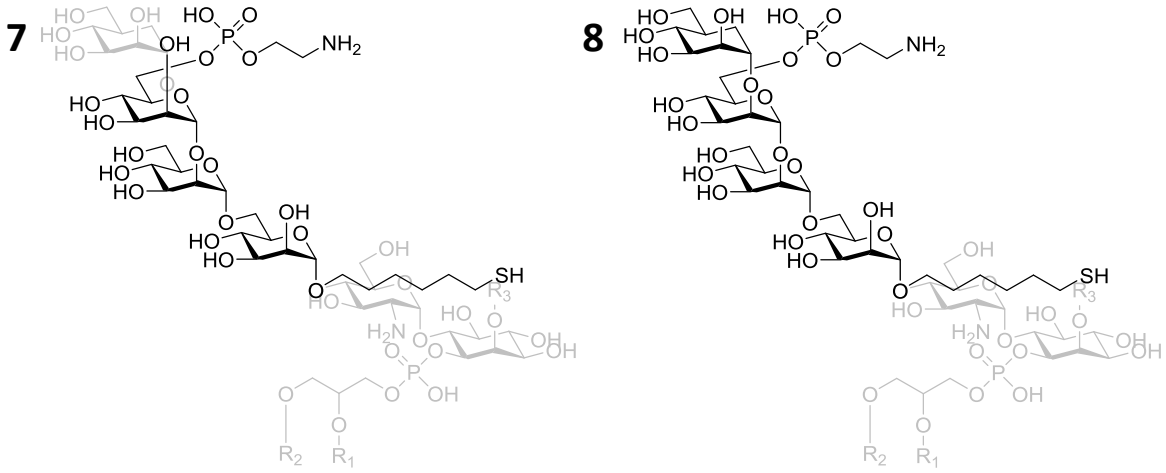

Figure 17: The minimal epitope antigens. The full GPI is shown in grey for context. **7)** PEtN-Man$_3$ focuses on the non-reducing terminus of free GPI. **8)** PEtN-Man$_4$ includes the fourth mannose specific to *P. falciparum* GPI.

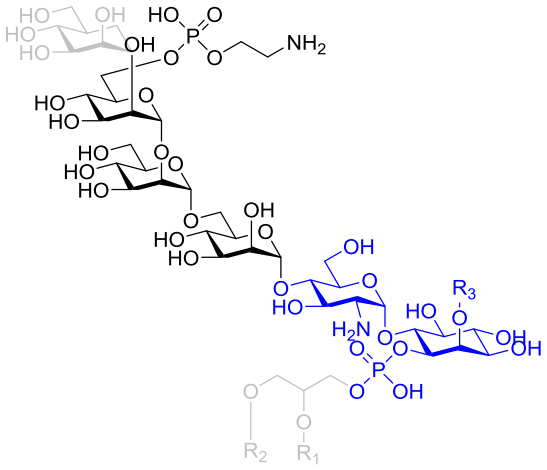

Figure 18: The minimal GPI epitope for naturally-occurring antibodies. PEtN-Man3 minimal epitope antigen (black) is smaller than the pentasaccharide epitope containing GlcN-InoP (blue). The full GPI is shown in grey for context.

Profiling induced antibodies against minimal epitope fragments

Minimal epitope fragments **7** and **8** were synthesised according to published procedures (Tsai, Götze et al. 2013). The synthetic minimal epitope fragments **7** and **8** were printed onto microarrays to expand the GPI epitope library. Truncated GPI substructures lacking Man residues were also added. Specific IgG isotype titres in the sera of mice that were immunised with glycoconjugates of **1**-**6** were then profiled on this expanded microarray. In this way, we could determine whether immunisation with glycoconjugates of **1-6** induced antibodies specific to the target terminal epitope. Additionally, we could observe possible IgG isotype biases elicited by the various glycoconjugates.

I screened sera (diluted 1:100) at day 42 post-prime immunisation (n=15 per group, classified by the immunising glycoconjugate). Class-switched IgG1 [**Figure 19**] and IgG2a [**Figure 20**] titres were consistently higher than IgG3 [**Figure 21**]. Isotype IgG1 is of high affinity and limits inflammatory responses. Isotype IgG2a is associated with cellular toxicity, complement fixation, and antigen clearance. Though it is difficult to draw direct comparisons to human IgG isotypes, mouse IgG1 can be considered similar to Ig4 while mouse IgG2a is similar to human IgG1, based on function and receptor binding (Vidarsson, Dekkers et al. 2014, Collins 2016).

Immunisation with glycoconjugates of **1** and **4** induced high IgG1 and IgG2a titres against fragments containing InoP structures, including truncated GPI fragments lacking Man, as observed with total IgG [**Figure 19a & d** and **Figure 20a & d**]. Negligible IgG1 and IgG2a titres against minimal epitope fragments **7** and **8** were observed.

Immunisation with glycoconjugates of **2** and **5** lacking InoP induce low IgG1 and IgG2a titres against fragments **7** and **8** [**Figure 19b & e** and **Figure 20b & e**] compared to fragments with additional GlcN, supporting the evidence that GlcN is immunogenic and potentially induces antibodies away from the terminal epitope. There is, however, a lack of binding to the Man-truncated fragment, suggesting that the intact core GPI Man backbone is required for binding.

Immunisation with glycoconjugates of **3** and **6** did not induce antibodies against the minimal epitopes [**Figure 19c & f** and **Figure 20c & f**]. Titres were also lower compared to other glycoconjugates, likely due to the absence of PEtN on Man-III.

Across all glycoconjugates, the IgG3 titre is generally low, except against fragment **1**. The PEtN on Man-II (non-natural position) for fragment **1** could contribute to this preferred binding over other fragments [**Figure 21**]. IgM shows specificity to fragment **7**, in addition to other fragments lacking InoP. This suggests that class-switching to IgG skews the specificity of antibodies away from terminal GPI epitopes [**Figure 22a, b, d, & e**].

IgG1 and IgG2a titres were generally low for GPI fragments from other organisms [**Figure 23** and **Figure 24**]. However, moderate IgG3 titres to *T. gondii* and mammalian GPI are detected after immunisation with glycoconjugate of **2**. [**Figure 25b**]. Binding to synthetic *T. brucei* GPI is low across all isotypes [**Figure 25**], likely due to the absence of GlcN and InoP.

Based on this analysis, antibodies induced by glycoconjugates of **1-6** did not induce class-switched antibodies with a preferred specificity to the minimal epitope fragments **7** and **8**.

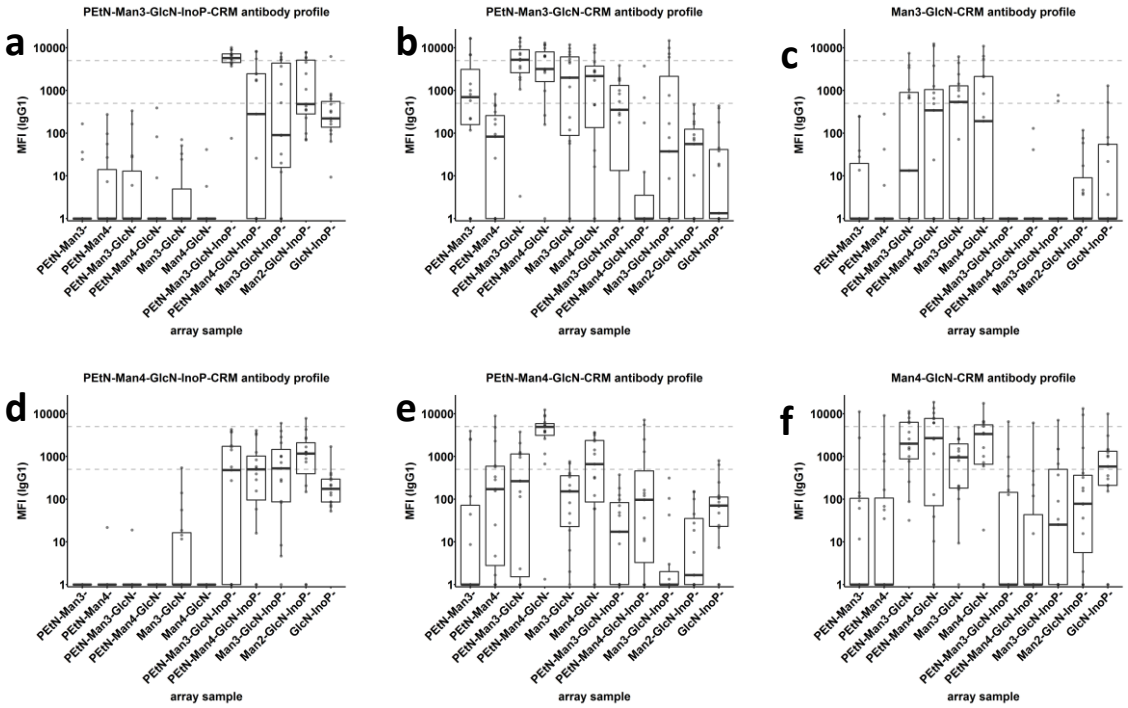

Figure 19: IgG1 titres against synthetic GPI fragments in sera at day 42. Group size n=15, classified by the immunising glycoconjugate. **Top panel (a-c)** IgG1 titres after immunisation with glycoconjugates of **1**-**3** lacking the fourth Man. **Bottom panel (d-f)** IgG1 titres after immunisation with glycoconjugates of **4**-**6** containing the fourth Man.

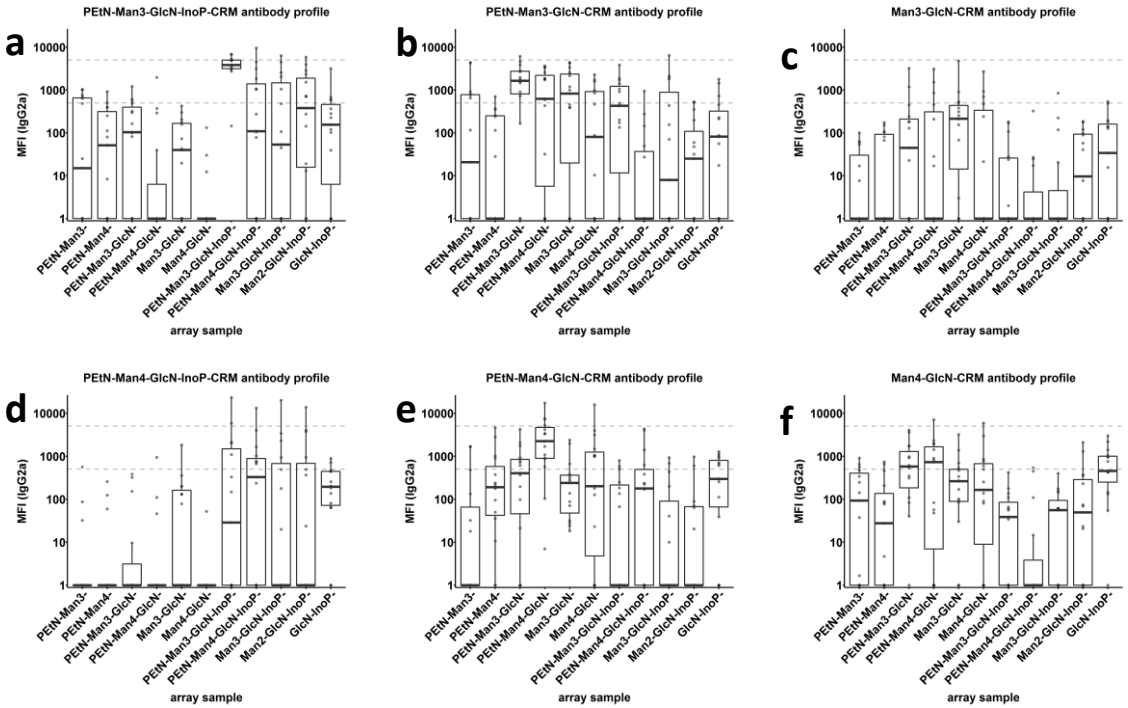

Figure 20: IgG2a titres against synthetic GPI fragments in sera at day 42. Group size n=15, classified by the immunising glycoconjugate. **Top panel (a-c)** IgG2a titres after immunisation with glycoconjugates of **1**-**3** lacking the fourth Man. **Bottom panel (d-f)** IgG2a titres after immunisation with glycoconjugates of **4**-**6** containing the fourth Man.

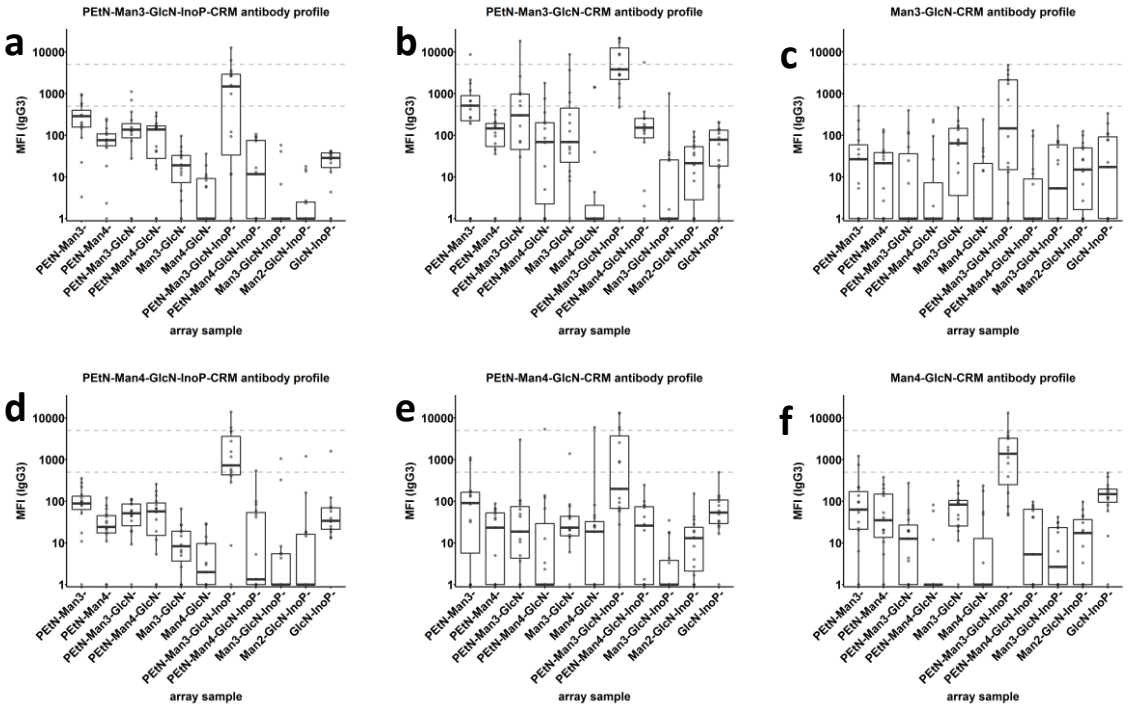

Figure 21: IgG3 titres against synthetic GPI fragments in sera at day 42. Group size n=15, classified by the immunising glycoconjugate. **Top panel (a-c)** IgG3 titres after immunisation with glycoconjugates of **1**-**3** lacking the fourth Man. **Bottom panel (d-f)** IgG3 titres after immunisation with glycoconjugates of **4**-**6** containing the fourth Man.

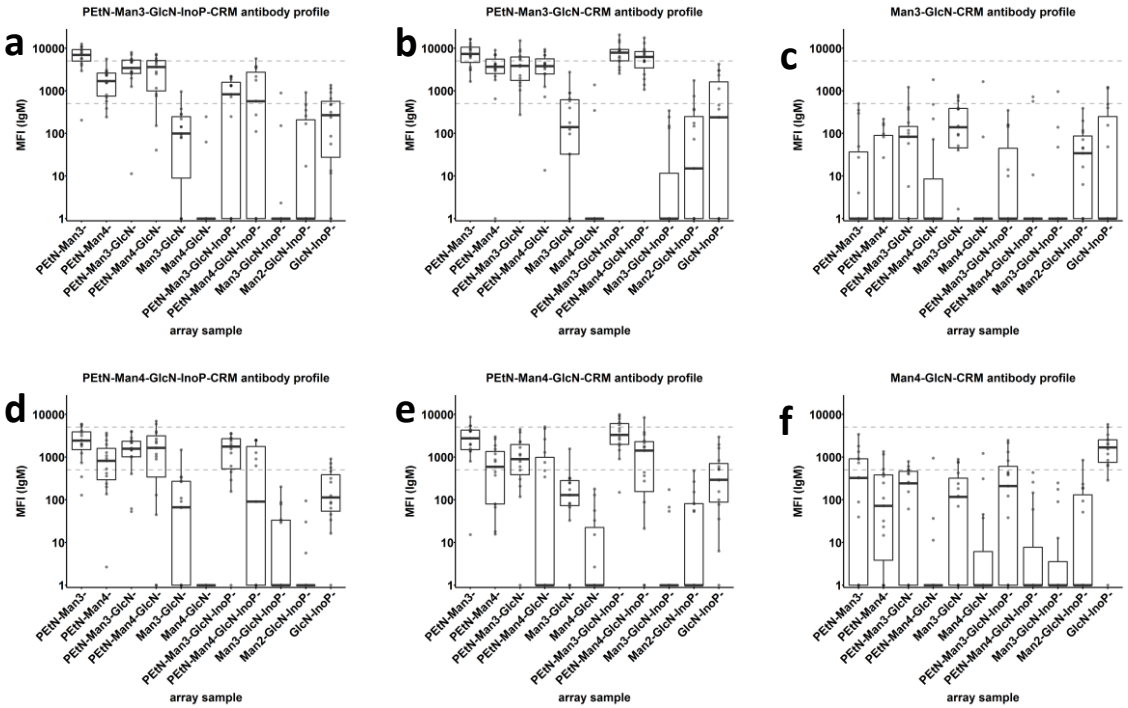

Figure 22: IgM titres against synthetic GPI fragments in sera at day 42. Group size n=15, classified by the immunising glycoconjugate. **Top panel (a-c)** IgM titres after immunisation with glycoconjugates of **1**-**3** lacking the fourth Man. **Bottom panel (d-f)** IgM titres after immunisation with glycoconjugates of **4**-**6** containing the fourth Man.

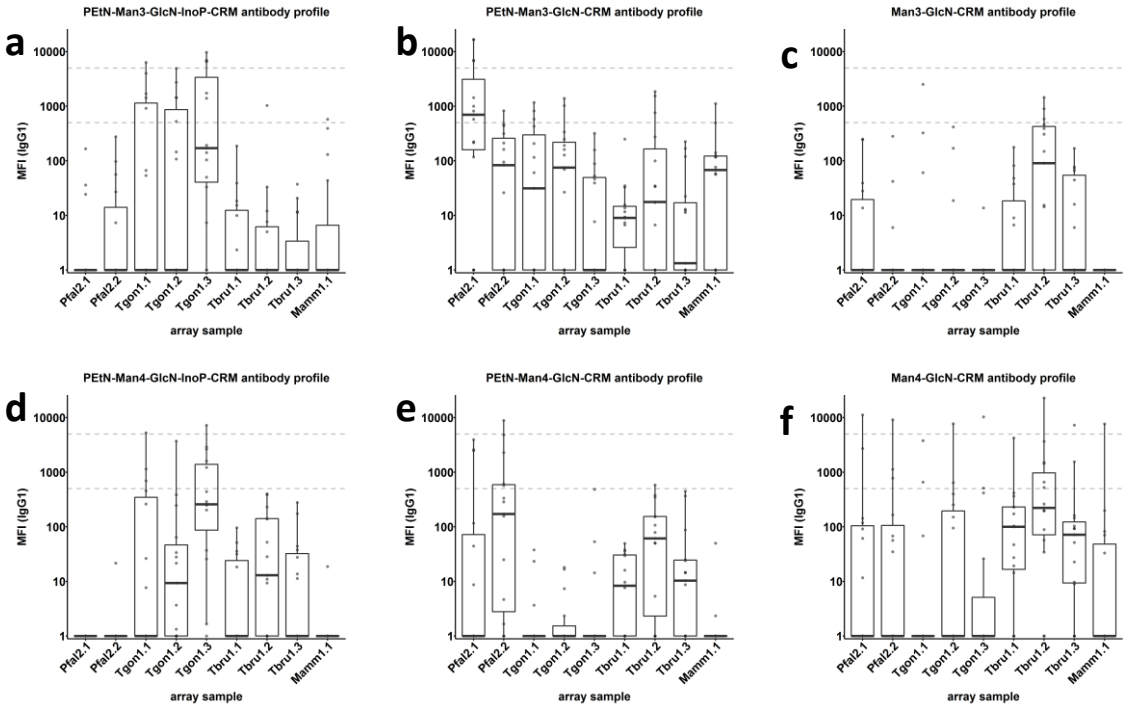

Figure 23: IgG1 titres against synthetic GPI fragments in other organisms in sera at day 42. Group size n=15, classified by the immunising glycoconjugate. **Top panel (a-c)** IgG1 titres after immunisation with glycoconjugates of **1**-**3** lacking the fourth Man. **Bottom panel (d-f)** IgG1 titres after immunisation with glycoconjugates of **4**-**6** containing the fourth Man.

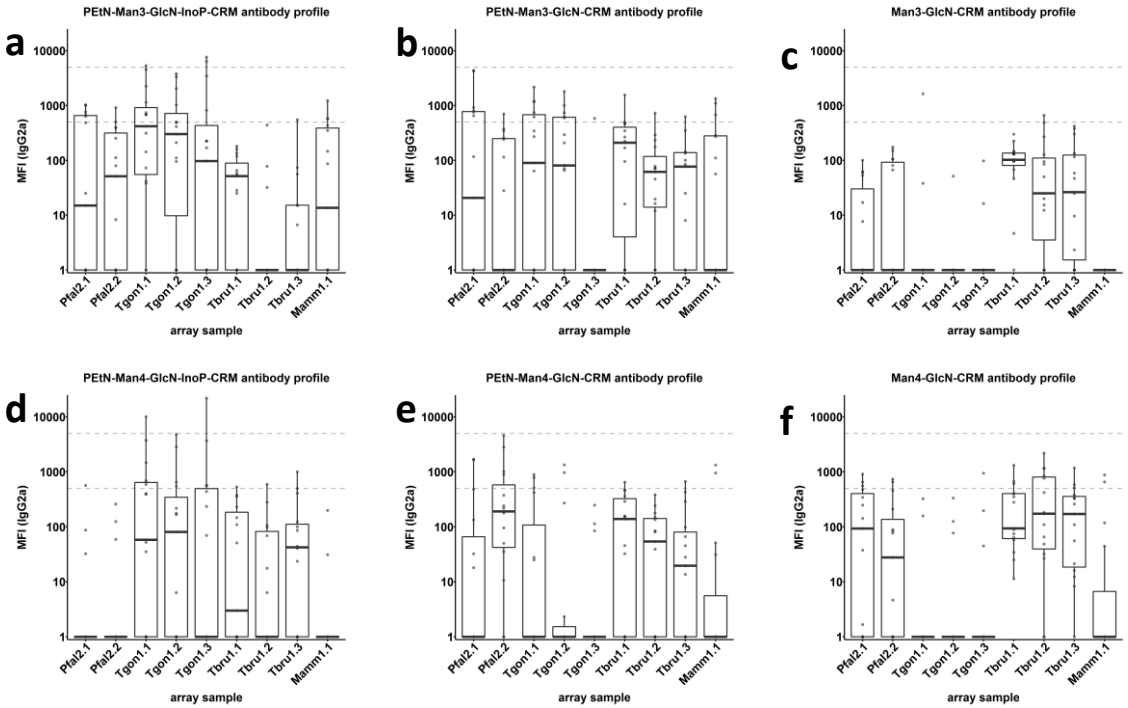

Figure 24: IgG2a titres against synthetic GPI fragments in other organisms in sera at day 42. Group size n=15, classified by the immunising glycoconjugate. **Top panel (a-c)** IgG2a titres after immunisation with glycoconjugates of **1**-**3** lacking the fourth Man. **Bottom panel (d-f)** IgG2a titres after immunisation with glycoconjugates of **4**-**6** containing the fourth Man.

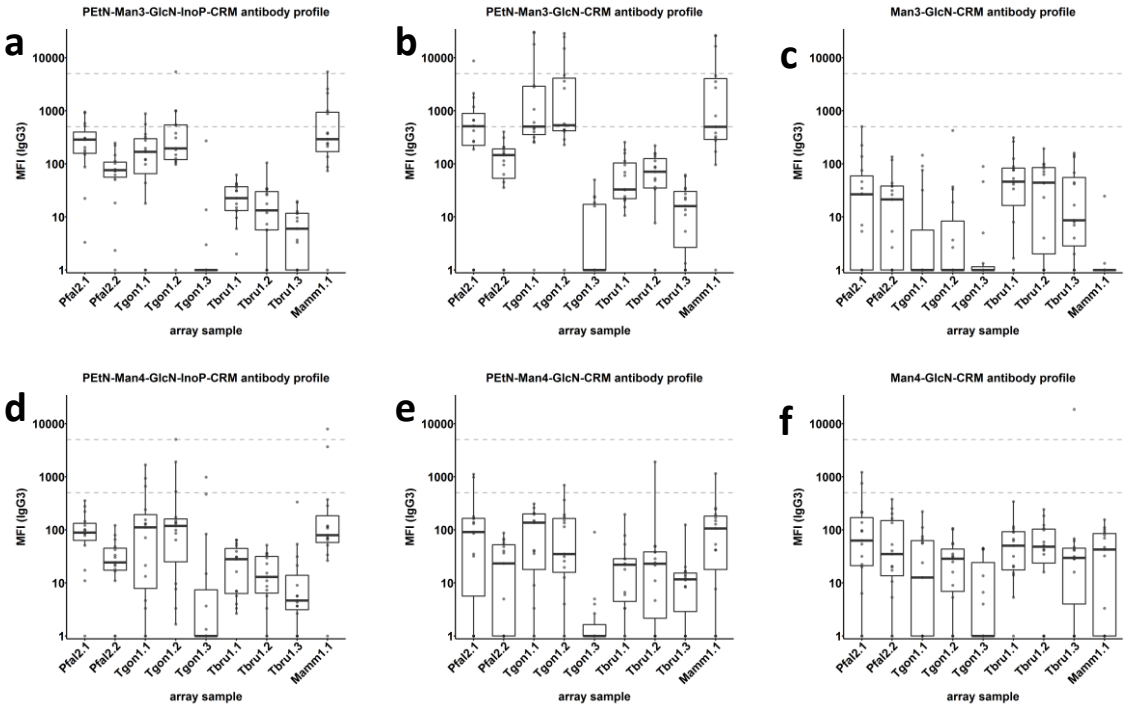

Figure 25: IgG3 titres against synthetic GPI fragments in other organisms in sera at day 42. Group size n=15, classified by the immunising glycoconjugate. **Top panel (a-c)** IgG3 titres after immunisation with glycoconjugates of **1**-**3** lacking the fourth Man. **Bottom panel (d-f)** IgG3 titres after immunisation with glycoconjugates of **4**-**6** containing the fourth Man.

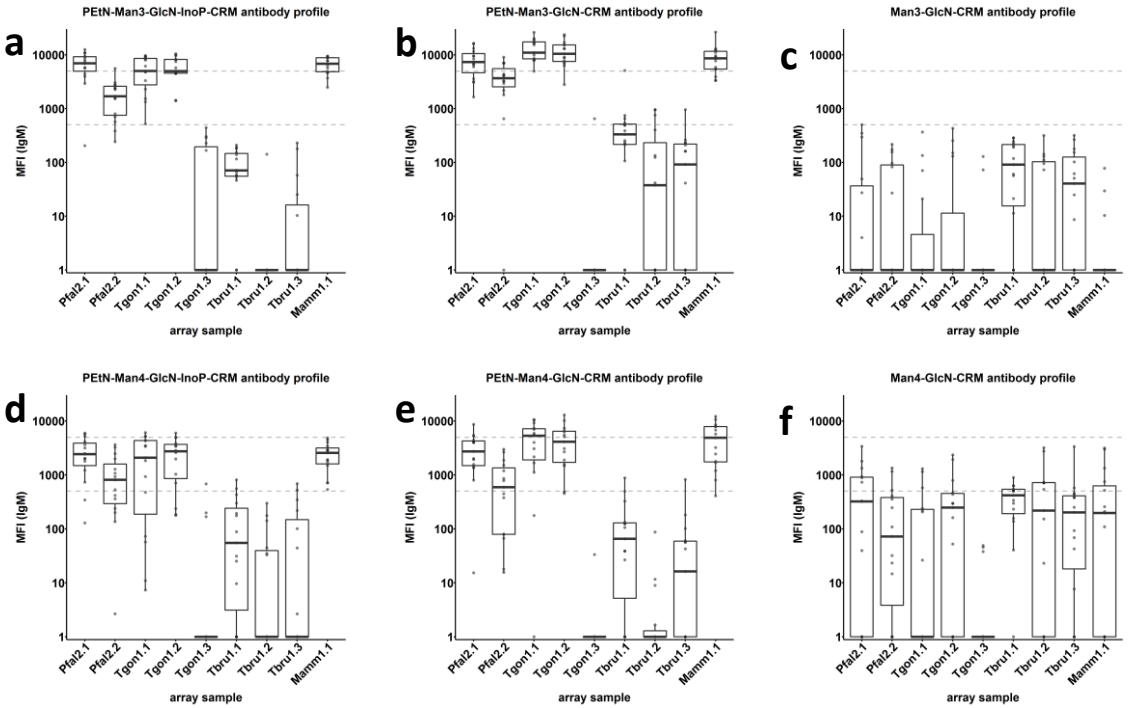

Figure 26: IgM titres against synthetic GPI fragments in other organisms in sera at day 42. Group size n=15, classified by the immunising glycoconjugate. **Top panel (a-c)** IgM titres after immunisation with glycoconjugates of **1**-**3** lacking the fourth Man. **Bottom panel (d-f)** IgM titres after immunisation with glycoconjugates of **4**-**6** containing the fourth Man.

3.3 Elucidating whether synthetic GPI fragments are a proxy for native GPI

Synthetic GPI fragments are considered a suitable representation of native GPI, and have been used to map the epitope specificities of naturally-occurring antibodies (Kamena, Tamborrini et al. 2008, Tamborrini, Liu et al. 2010). The various synthetic fragments on the current GPI epitope library, which includes the newly designed minimal epitope antigens, are also expected to be suitable representations of native GPI, however this was not yet confirmed. Various individual and pooled serum samples from infected individuals were profiled against the current GPI epitope library. This was to determine whether the fragments are cross-reactive to naturally-occurring GPI-specific antibodies, suggesting that the synthetic GPI fragments are a proxy for native GPI.

Profiling pooled sera antibodies

Pooled sera originating from a malaria-endemic area in Kenya (NIBSC code #10-198), and non-endemic areas in the United Kingdom (NIBSC code #09-222 and #99-706) were purchased from vendors. I screened these sera (diluted 1:50) on the GPI epitope microarray to profile epitope-specific antibody titres. When comparing the binding profiles between the samples of pooled sera, I expected to see higher antibody titres recognising synthetic GPI fragments in sera from the malaria-endemic area.

When comparing IgG titres against the synthetic GPI fragments [**Figure 33a-c**], there are very similar profiles between pooled sera **10-198** (from Kenya) and **09-222** (from the United Kingdom). Highest titres are against structures containing the fourth Man, with highest binding to fragment **6**. Highest IgG titres are also against fragment **6** for sera **99-706** (from the United Kingdom).

When comparing IgM titres against the synthetic GPI fragments [**Figure 33d-f**], there are again very similar profiles between pooled sera **10-198** and **09-222**. However, **09-222** stands out for having very high IgM titre against fragment **6** compared to **10-198** and **99-706**. Highest titres for all pooled sera samples are against GlcN-InoP epitope.

When profiling IgG and IgM titres against GPI from other organisms [**Figure 28**], a similar binding profile between **10-198** and **09-222** is observed again, with overall lower titres observed for **99-706.**

It can be confirmed from this analysis that the current synthetic GPIs are cross-reactive to naturally-occurring antibodies. However, the increased antibody titres against *P falciparum* fragments were not observed in the pooled **10-198** sera when compared to control sera **09-222**. The binding profiles in both sera samples were not only similar, but oftentimes higher in **09-222**. Given that a clear difference in binding profile is not observed between sera from individuals in malaria endemic and non-endemic areas, it remains to be seen whether the synthetic GPIs, including the minimal epitope antigens, are specific to native *P. falciparum* GPI. Screening of individual serum samples may be required to determine whether the synthetic GPIs are indicative of natural infection.

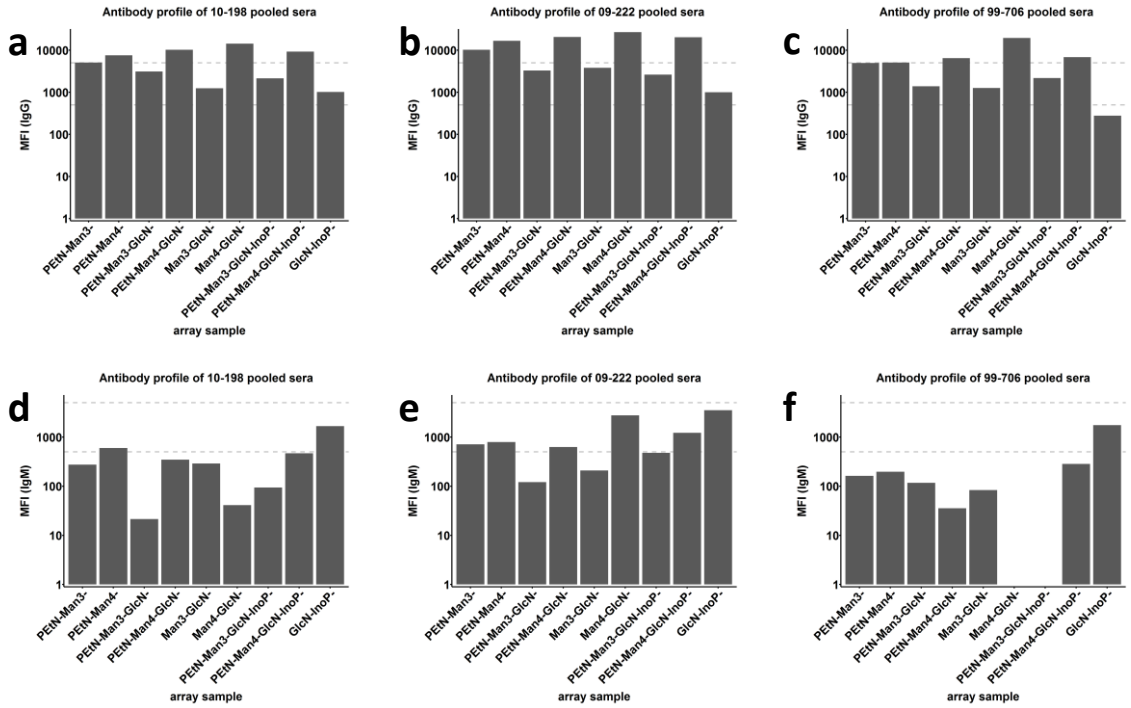

Figure 27: Antibody titres against synthetic GPI from pooled sera. Top panel (a-c) IgG titres. Profiles of **a) 10-198** pooled sera from Kenya, **b) 09-222** pooled sera control, **c) 99-706** pooled sera control. **Bottom panel (d-f)** IgM titres. Profiles of **d) 10-198** pooled sera from Kenya, **e) 09-222** pooled sera control, **f) 99-706** pooled sera control.

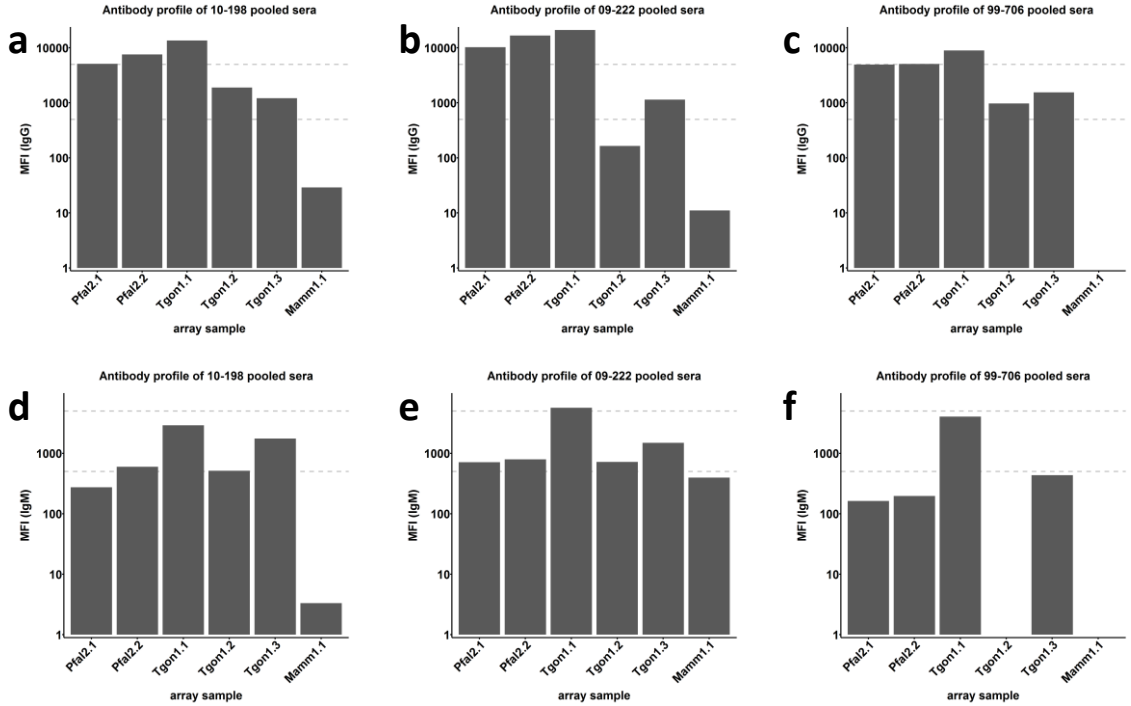

Figure 28: Antibody titres against synthetic GPI in other organisms from pooled sera. Top panel (a-c) IgG titres. Profiles of **a) 10-198** pooled sera from Kenya, **b) 09-222** pooled sera control, **c) 99-706** pooled sera control. **Bottom panel (d-f)** IgM titres. Profiles of **d) 10-198** pooled sera from Kenya, **e) 09-222** pooled sera control, **f) 99-706** pooled sera control.

Profiling individual infected monkey sera antibodies

I confirmed that the synthetic GPI fragments are cross-reactive to naturally occurring antibodies. To test whether the synthetic GPI fragments based on *P. falciparum* are specific to antibodies induced by malaria infection, serum samples collected before and after controlled infection were screened. Here, primate sera were sourced from the Biomedical Primate Research Centre (Department of Parasitology, Rijswijk, The Netherlands). Sera were collected from rhesus monkey before and after the 4th round of *P. knowlesi* infection. Sera (diluted 1:50) were screened on the glycan microarray, and for each GPI fragment the IgG and IgM titres before and after infection were compared using paired T-test. A significantly higher titre after the 4th infection timepoint would suggest that the GPI fragment binds to antibodies induced as a result of controlled *P. knowlesi* infection. I expect only *P. falciparum* GPI fragments to show a significant difference indicating IgG induction. Conversely, GPI from other organisms should not show this significant difference. For fragments showing low Ig titres (MFI <500) across all of the serum samples, the T-test analysis was not carried out.

Monkey sera generally do not show any significant differences ($p < 0.05$) in IgG titre against *P. falciparum* GPI fragments before and after the 4th infection round [**Figure 29**]. The only significant difference observed was for IgG against fragment **6** however a decrease, rather than increase in IgG titre, was observed [**Figure 29f**]. Monkey sera generally do not show any significant differences in IgG titre against GPI fragments from other organisms before and after the 4th infection round [**Figure 30**].

For IgM titres against *P. falciparum* GPI fragments, monkey sera generally do not show any significant differences before and after the 4th infection round [**Figure 31**]. However, there is a significant increase observed for IgM against fragment **5** [**Figure 31d**]. Monkey sera generally do not show any significant differences in IgM titre against GPI fragments from other organisms before and after the 4th infection round [**Figure 38**].

The general lack of antibody induction observed in these sera may be explained by the fact that this approach uses controlled *P. knowlesi* infection as a model of natural *P. falciparum* infection. The structure of *P.falciparum* GPI has been well characterised and is known to be conserved across *P falciparum* strains (Berhe, Schofield et al. 1999).

However, the structure of GPI in other *Plasmodium spp.* has not been published. Thus, the lack of antibody induction against the synthetic GPI fragments may be due to the fact that antibodies were induced against *P. knowlesi* GPI rather than *P. falciparum* GPI.

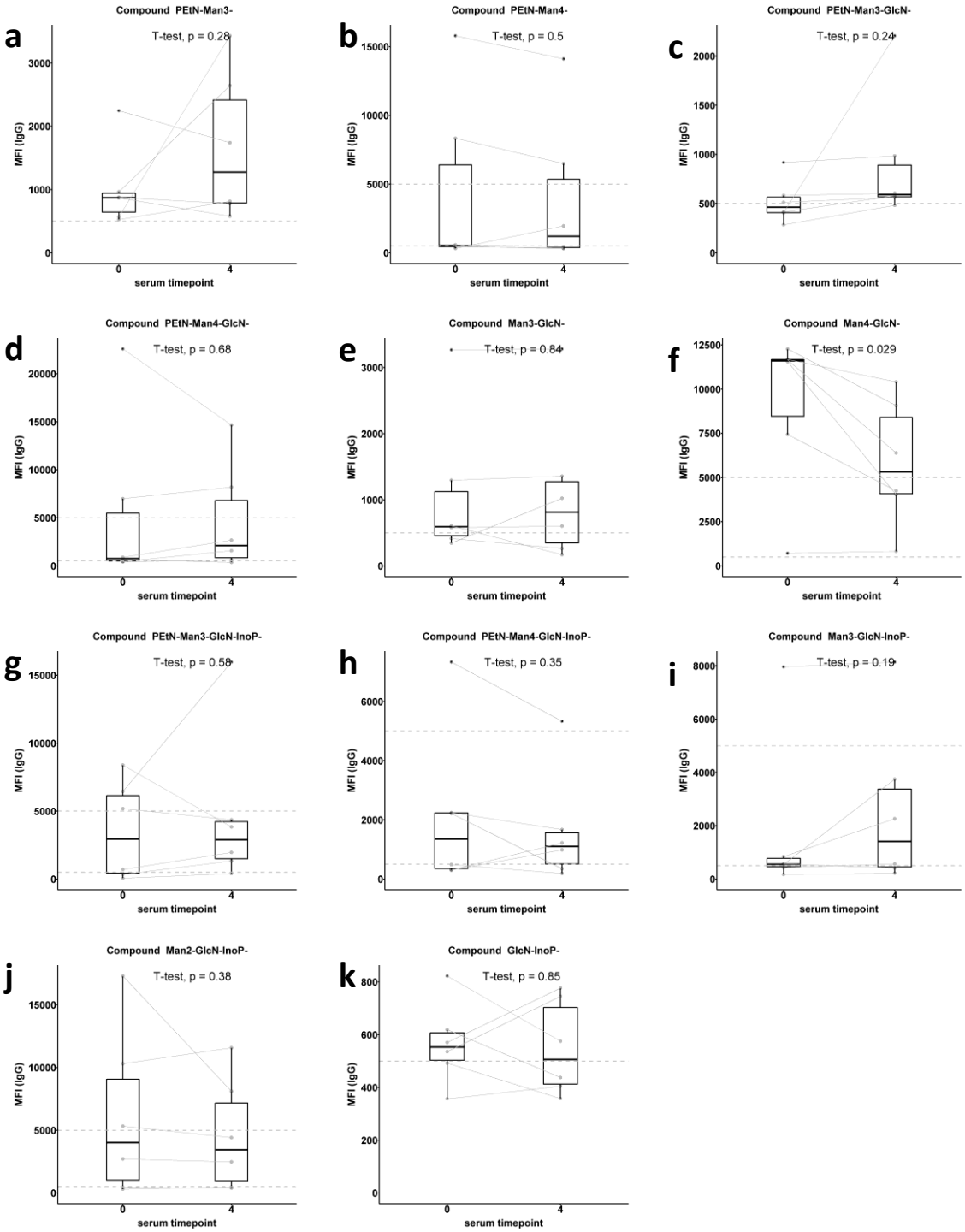

Figure 29: IgG titres against synthetic *P. falciparum* GPI fragments in sera from monkeys experiencing controlled infection. Pre- (serum timepoint 0) and post-infection (serum timepoint 4) IgG titres in sera of monkeys (n=6) were compared using paired T-test. Significant differences ($p<0.05$) indicate that antibodies cross-reactive to the synthetic GPI fragment were induced after infection.

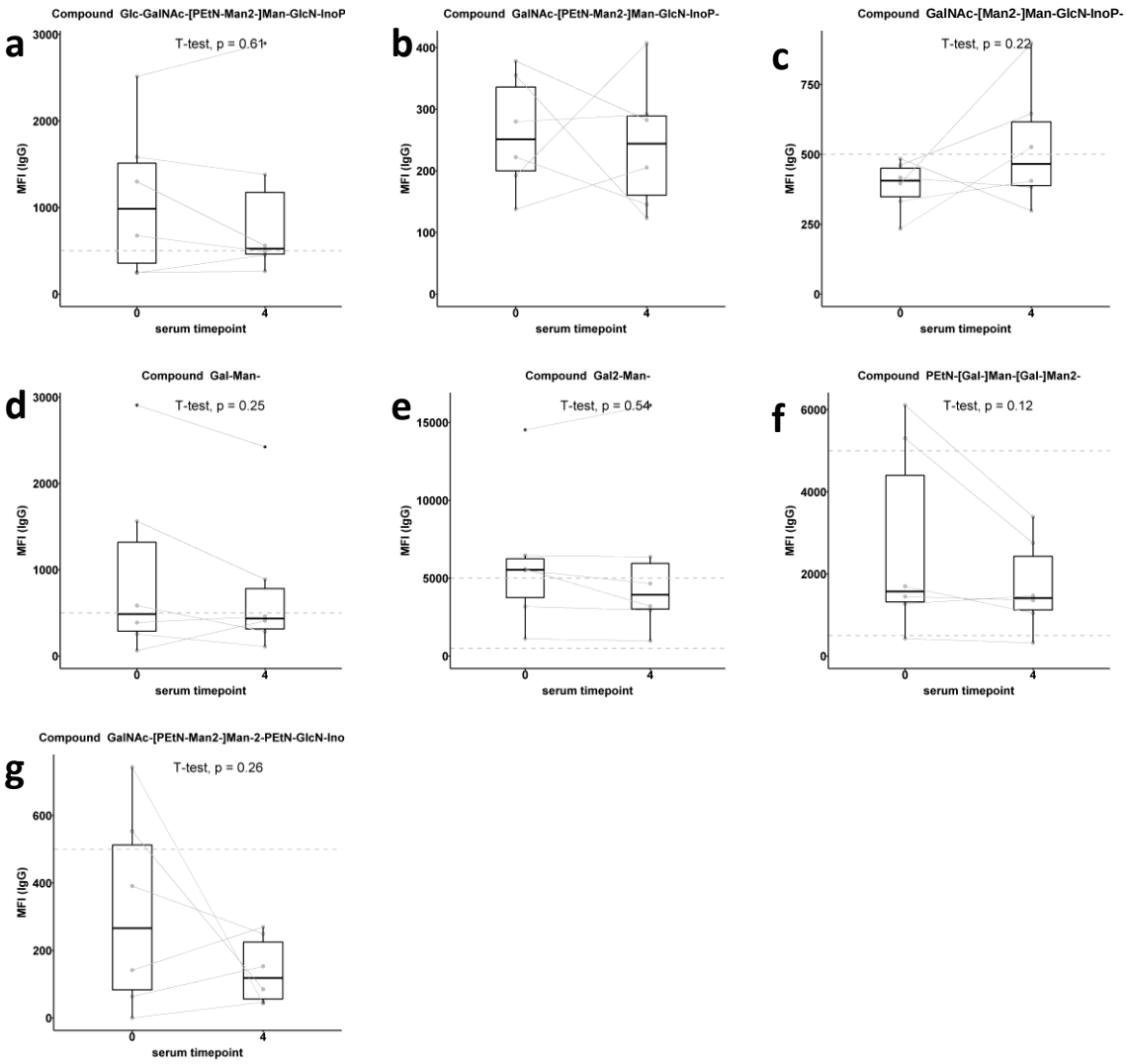

Figure 30: IgG titres against synthetic GPI fragments from other organisms in sera from monkeys experiencing controlled infection. Pre- (serum timepoint 0) and post-infection (serum timepoint 4) IgG titres in sera of monkeys (n=6) were compared using paired T-test. Significant differences ($p<0.05$) indicate that antibodies cross-reactive to the synthetic GPI fragment were induced after infection.

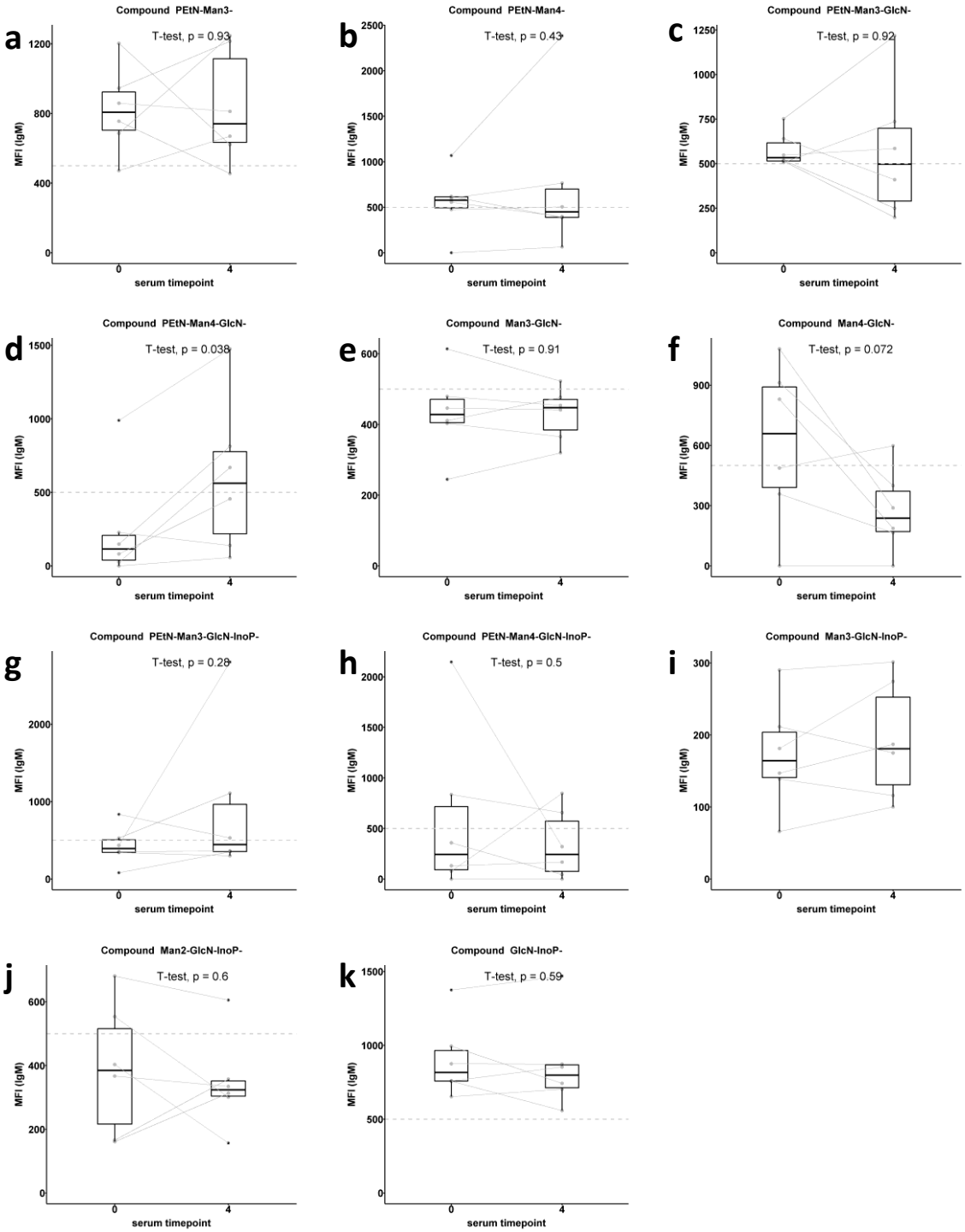

Figure 31: IgM titres against synthetic *P. falciparum* GPI fragments in sera from monkeys experiencing controlled infection. Pre- (serum timepoint 0) and post-infection (serum timepoint 4) IgM titres in sera of monkeys (n=6) were compared using paired T-test. Significant differences ($p<0.05$) indicate that antibodies cross-reactive to the synthetic GPI fragment were induced after infection..

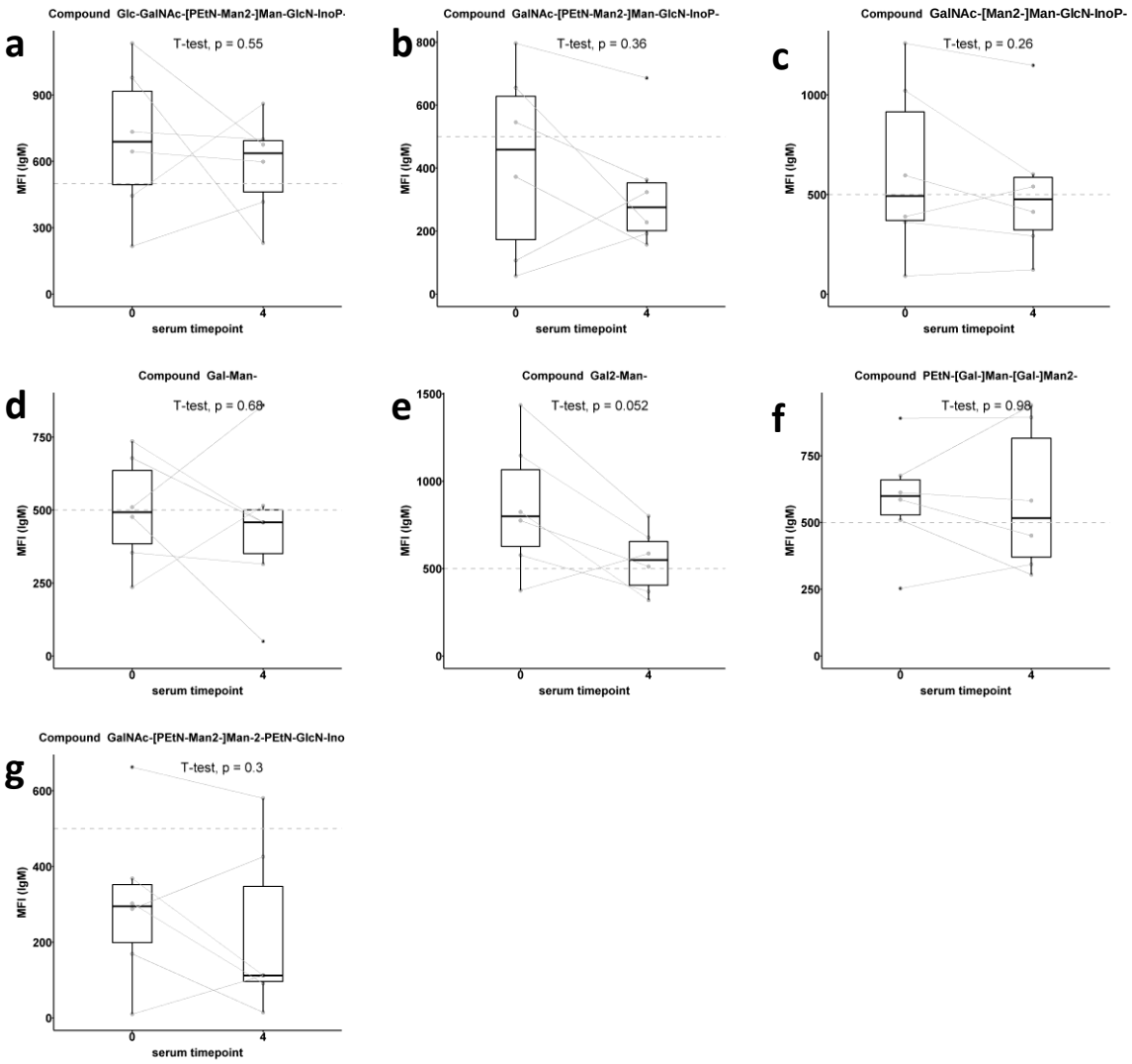

Figure 32: IgG titres against synthetic GPI fragments from other organisms in sera from monkeys experiencing controlled infection. Pre- (serum timepoint 0) and post-infection (serum timepoint 4) IgG titres in sera of monkeys (n=6) were compared using paired T-test. Significant differences ($p<0.05$) indicate that antibodies cross-reactive to the synthetic GPI fragment were induced after infection.

Profiling antibodies in individual human sera

Another approach to confirm whether the synthetic GPI fragments based on *P. falciparum* are specific to antibodies induced by malaria infection employed the use of sera from infected human patients. These sera eliminated the question of possible structural differences in GPI between *Plasmodium spp.* as these patients were reported to be experiencing primary infection with *P. falciparum*.

Sera from individuals experiencing their first malaria infection were sourced from the Charité – Universitätsmedizin Berlin (Department of Internal Medicine with emphasis on Infectiology, Respiratory-, and Critical-Care-Medicine). Sera collected at various timepoints were sorted into early (day 0-4, inclusive) and late (day 7-21, inclusive) timepoint brackets corresponding to before and after the expected induction of class-switched IgG as a result of malaria infection. Sera (diluted 1:50) were screened on the glycan microarray, and for each GPI fragment the minimum titres in the early bracket were compared to the maximum titres in the late bracket using paired T-test. A significantly higher titre in the late bracket suggests that the GPI fragment binds to antibodies induced as a result of natural infection. I expect only *P. falciparum* GPI fragments to show a significant difference indicating IgG induction. Conversely, GPI from other organisms should not show this significant difference. For fragments showing low Ig titres (MFI <500) across all of the serum samples, the T-test analysis was not carried out.

Patients with primary infection show significant differences ($p < 0.05$) in IgG titre between early and late brackets against *P. falciparum* GPI fragments [**Figure 33a-i**]. IgG titres against fragments containing a Man3-GlcN epitope significantly increase after infection [**Figure 33c-i**]. IgG titres against fragments missing Man-III do not significantly increase after infection [**Figure 33j & k**] congruent with previous findings (Kamena, Tamborrini et al. 2008). However, IgG titres against minimal epitope fragments **7** and **8** significantly increase after infection [**Figure 33a & b**], suggesting that neither GlcN nor InoP are required for recognition.

For GPI from other organisms I observed significant IgG titre increase against *T. gondii* GPI that has a truncated side chain [**Figure 34b & c**]. A possible explanation is that induced antibodies recognise the core backbone of GPI [**Figure 33a-i**], and an additional

GalNAc residue on Man-I does not hinder binding to *T. gondii* GPI fragments (Tgon1.2 and Tgon1.3) [**Figure 34b & c**]. However, the additional Glc residue on Tgon1.1 that completes the side chain prevents binding of antibodies to the GPI core Man backbone so that there is no significant difference in early and late IgG titre as a result of infection [**Figure 34a**]. I did not observe significant antibody induction for any other GPI fragments that are not derived from *P. falciparum*. Early and late IgM titres do not present a significant difference [**Figure 37** & **Figure 38**]. The early induction and fall in IgM titre may occur before the first sera collection.

Serum samples from a small sample of patients who had lifelong malaria exposure were also collected during a time of re-infection with *P. falciparum*. IgG titres against synthetic GPI fragments at early and late timepoints were not significantly different [**Figure 35 & Figure 36**], except for a non-*P.falciparum* GPI fragment at comparatively low IgG titre [**Figure 36d**]. This suggests that the induction of the IgG specific antibodies happens at primary infection, but not during re-infection. Differences in IgM titre are similarly non-significant [**Figure 39 & Figure 40**], except for non-*P.falciparum* GPI fragments at comparatively low IgM titres [**Figure 40c & e**].

Taken together, these data show that antibody titres against the current library of synthetic GPI fragments increase after natural *P. falciparum* primary infection. This indicates that the synthetic GPI fragments are a good representation of native GPI, able to be recognised by antibodies induced by native GPI molecules. The epitope important for cross-reactive antibody recognition appears to be the unmodified core Man backbone specific to *P. falciparum*. GlcN and InoP, immunogenic when included in glycoconjugate antigens, are again shown to be irrelevant to the binding of naturally-occurring GPI antibodies. Furthermore, the minimal epitope fragments **7** and **8** that were designed to induce antibodies specific to the non-reducing terminus of GPI are recognised by the naturally-occurring antibodies. Thus, antibodies induced by glycoconjugates of **7** and **8** may better resemble the specificity of naturally occurring antibodies, compared to antibodies induced by synthetic antigens containing GlcN and InoP.

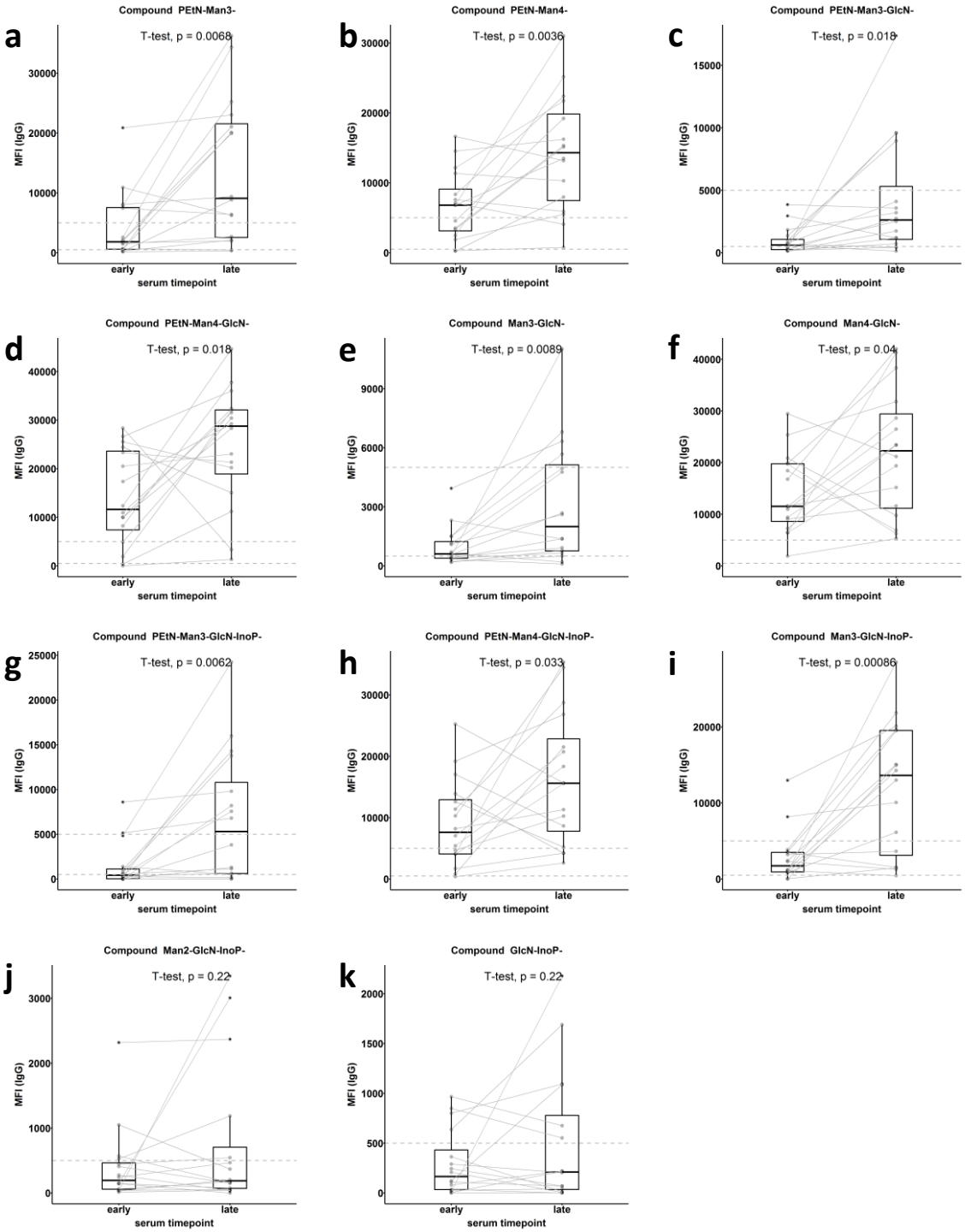

Figure 33: IgG titres in sera from naïve patients experiencing primary infection against synthetic *P. falciparum* GPI fragments. Early and late IgG titres in sera of patients (n=16) were compared using paired T-test. Significant differences ($p<0.05$) indicate that antibodies cross-reactive to the synthetic GPI fragment were induced after infection.

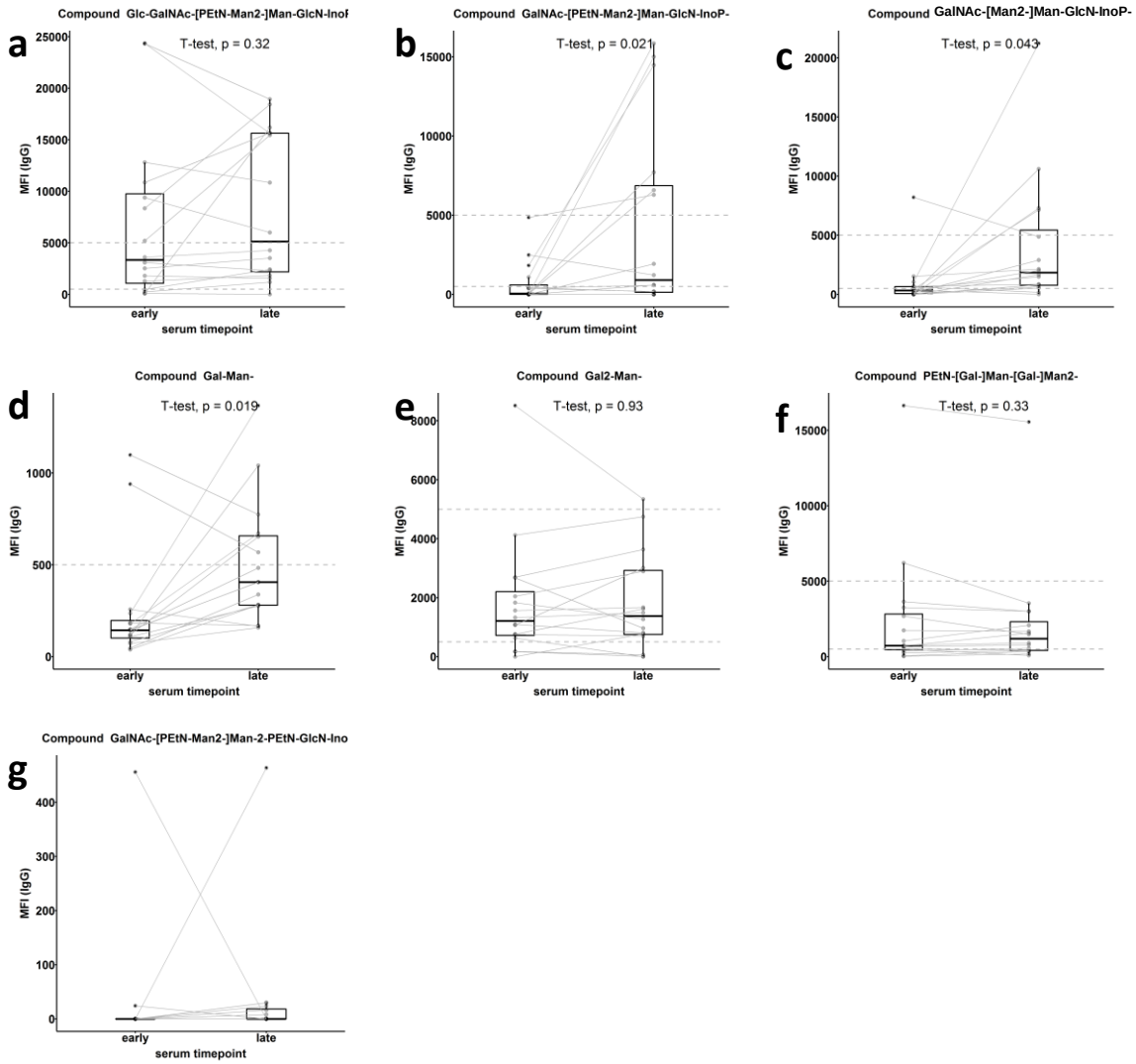

Figure 34: IgG titres in sera from naïve patients experiencing primary infection against synthetic GPI fragments from other organisms. Early and late IgG titres in sera of patients (n=16) were compared using paired T-test. Significant differences ($p<0.05$) indicate that antibodies cross-reactive to the synthetic GPI fragment were induced after infection.

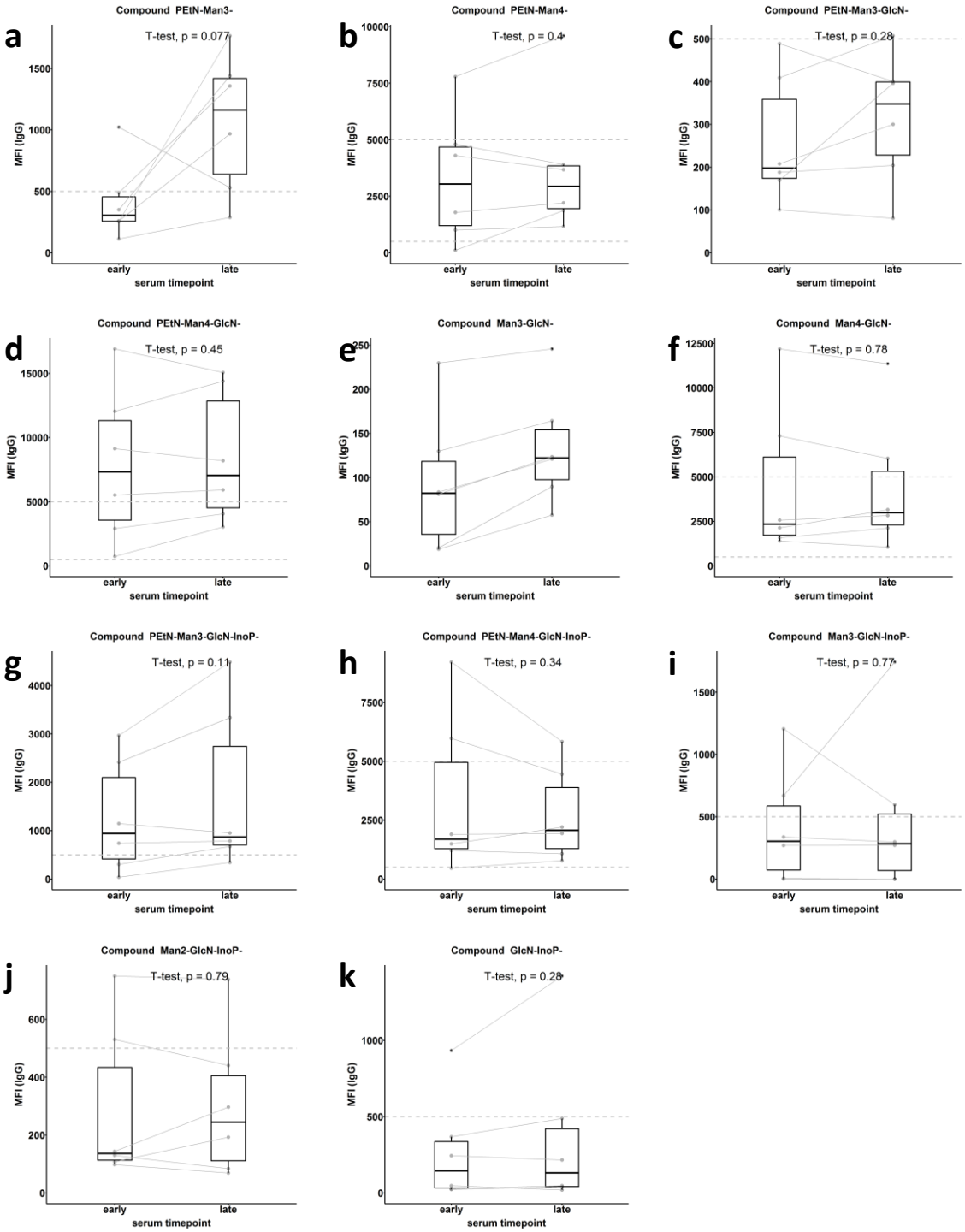

Figure 35: IgG titres in sera from patients with previous exposure against synthetic *P. falciparum* **GPI fragments.** Early and late IgG titres in sera of patients (n=6) were compared using paired T-test. Significant differences ($p<0.05$) indicate that antibodies cross-reactive to the synthetic GPI fragment were induced after infection.

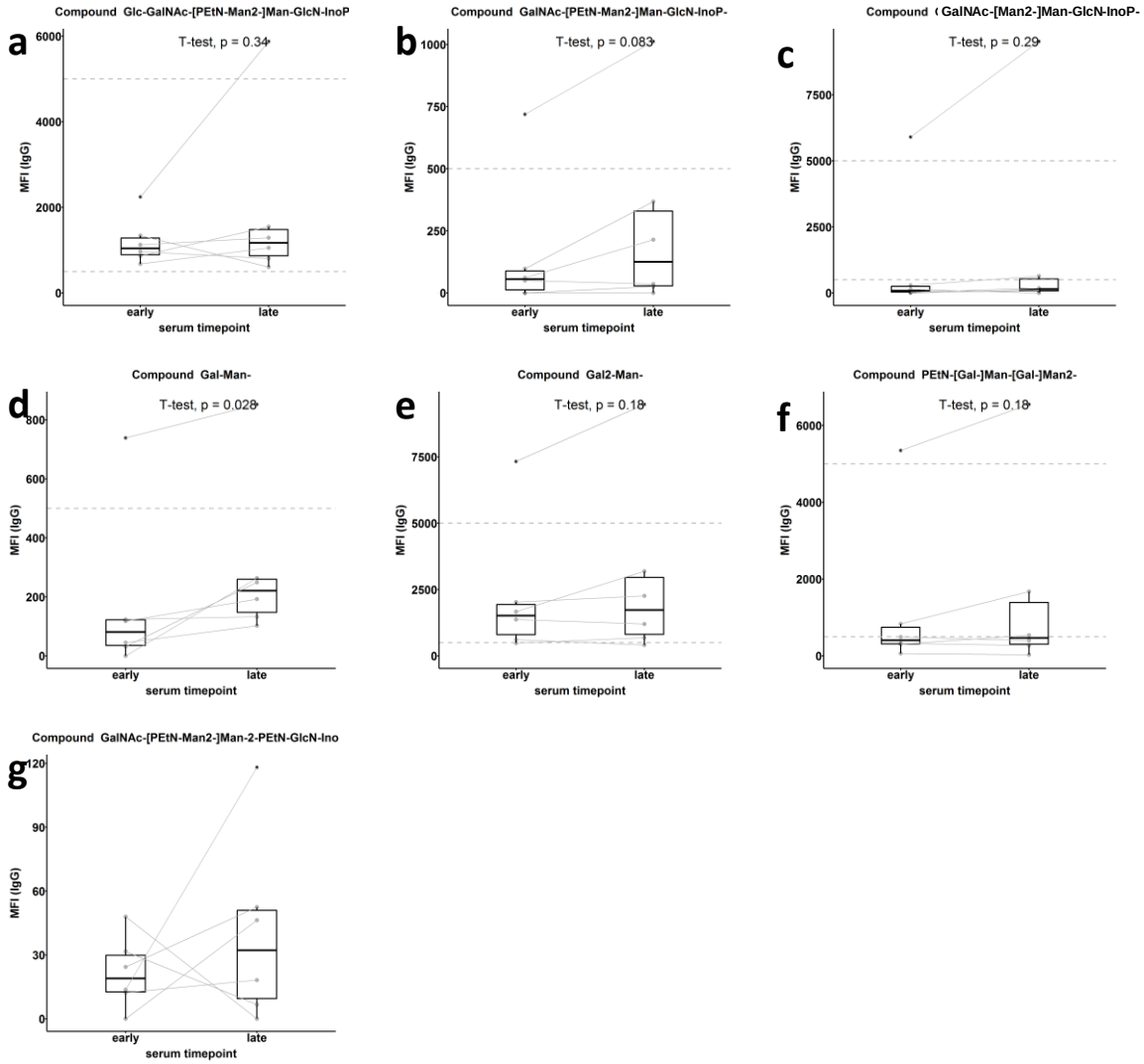

Figure 36: IgG titres in sera from patients with previous exposure against synthetic GPI fragments from other organisms. Early and late IgG titres in sera of patients (n=6) were compared using paired T-test. Significant differences ($p<0.05$) indicate that antibodies cross-reactive to the synthetic GPI fragment were induced after infection.

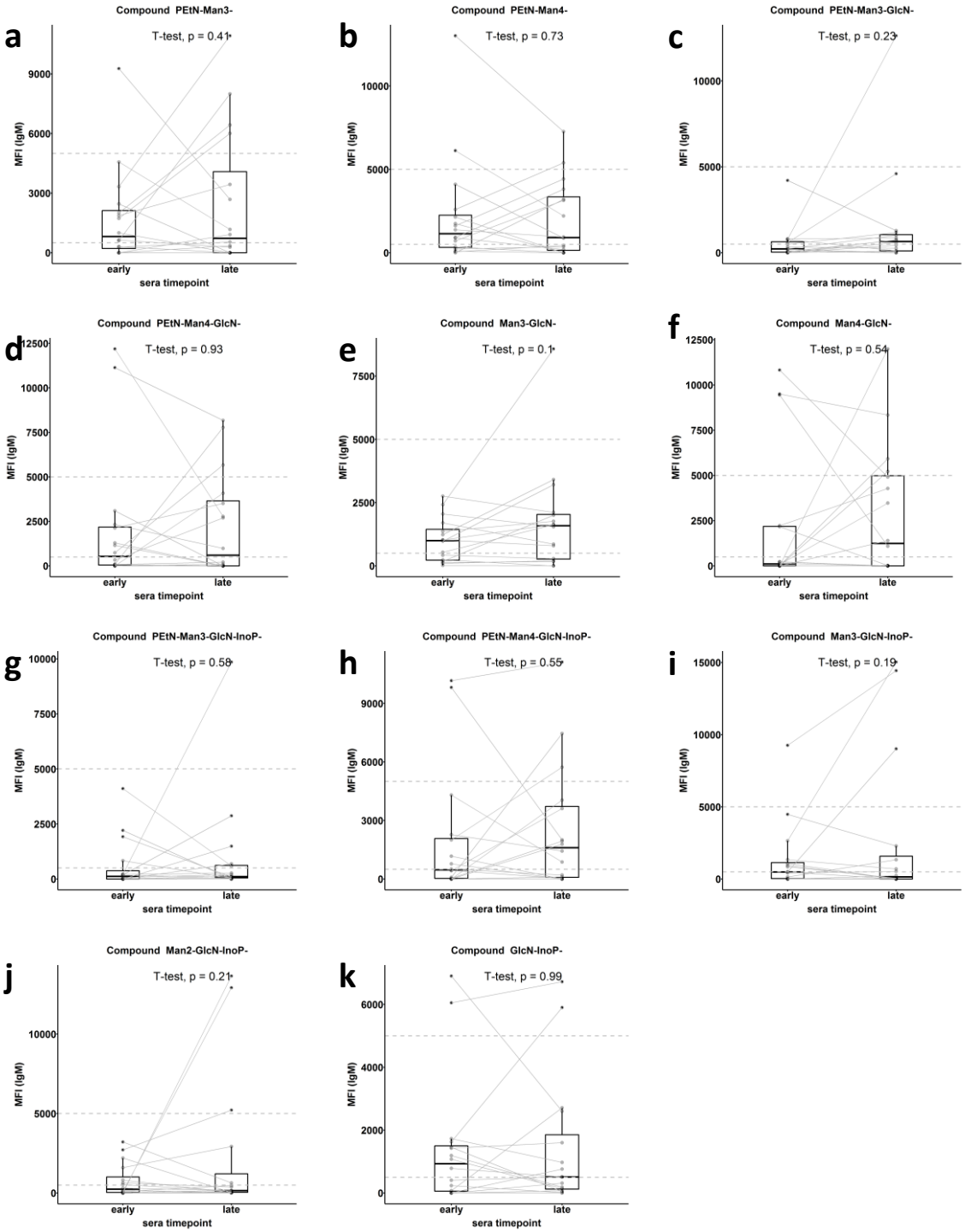

Figure 37: IgM titres in sera from naïve patients experiencing primary infection against synthetic *P. falciparum* **GPI fragments.** Early and late IgM titres in sera of patients (n=16) were compared using paired T-test. Significant differences ($p<0.05$) indicate that antibodies cross-reactive to the synthetic GPI fragment were induced after infection.

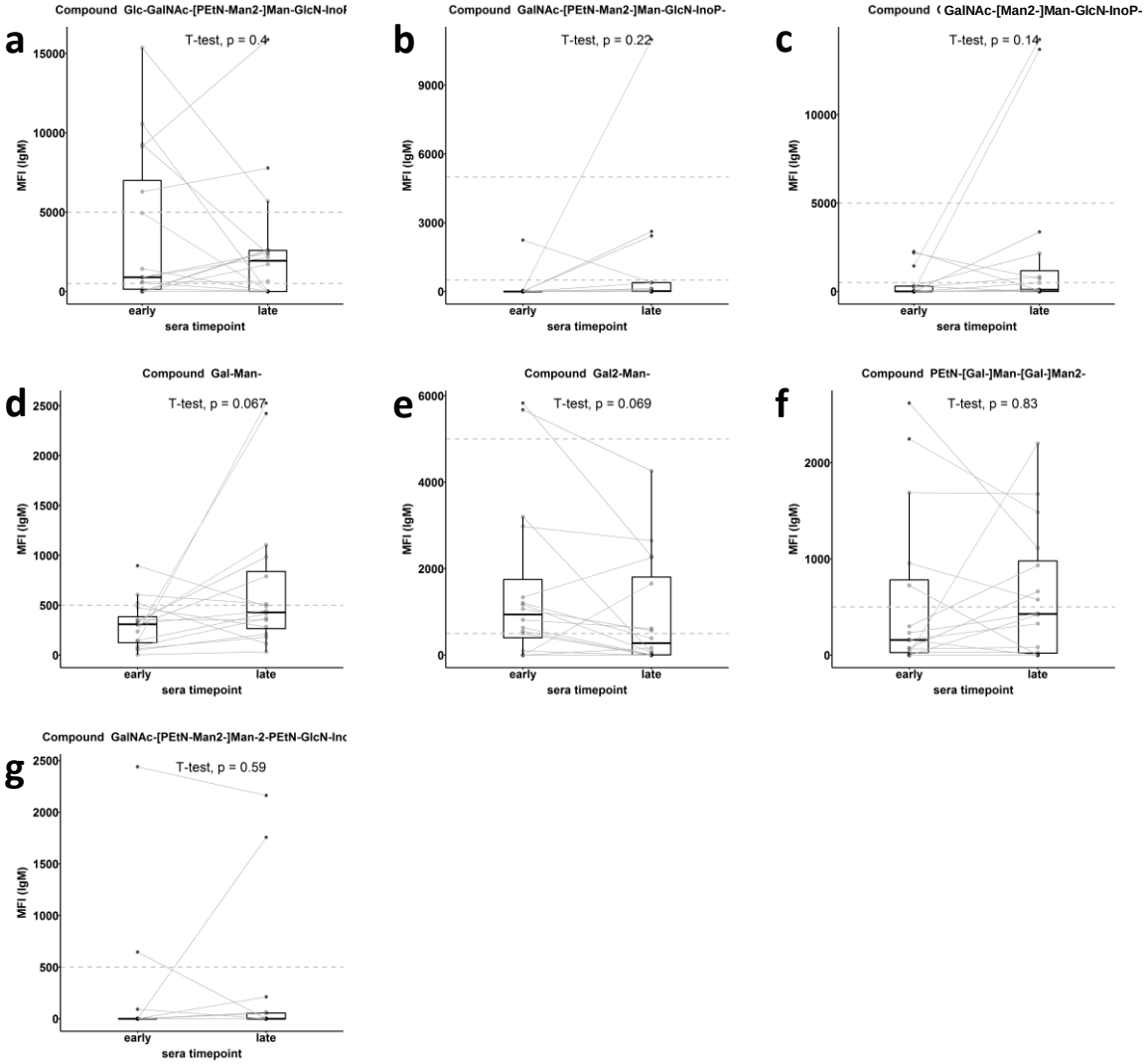

Figure 38: IgM titres in sera from naïve patients experiencing primary infection against synthetic GPI fragments from other organisms. Early and late IgM titres in sera of patients (n=16) were compared using paired T-test. Significant differences ($p<0.05$) indicate that antibodies cross-reactive to the synthetic GPI fragment were induced after infection.

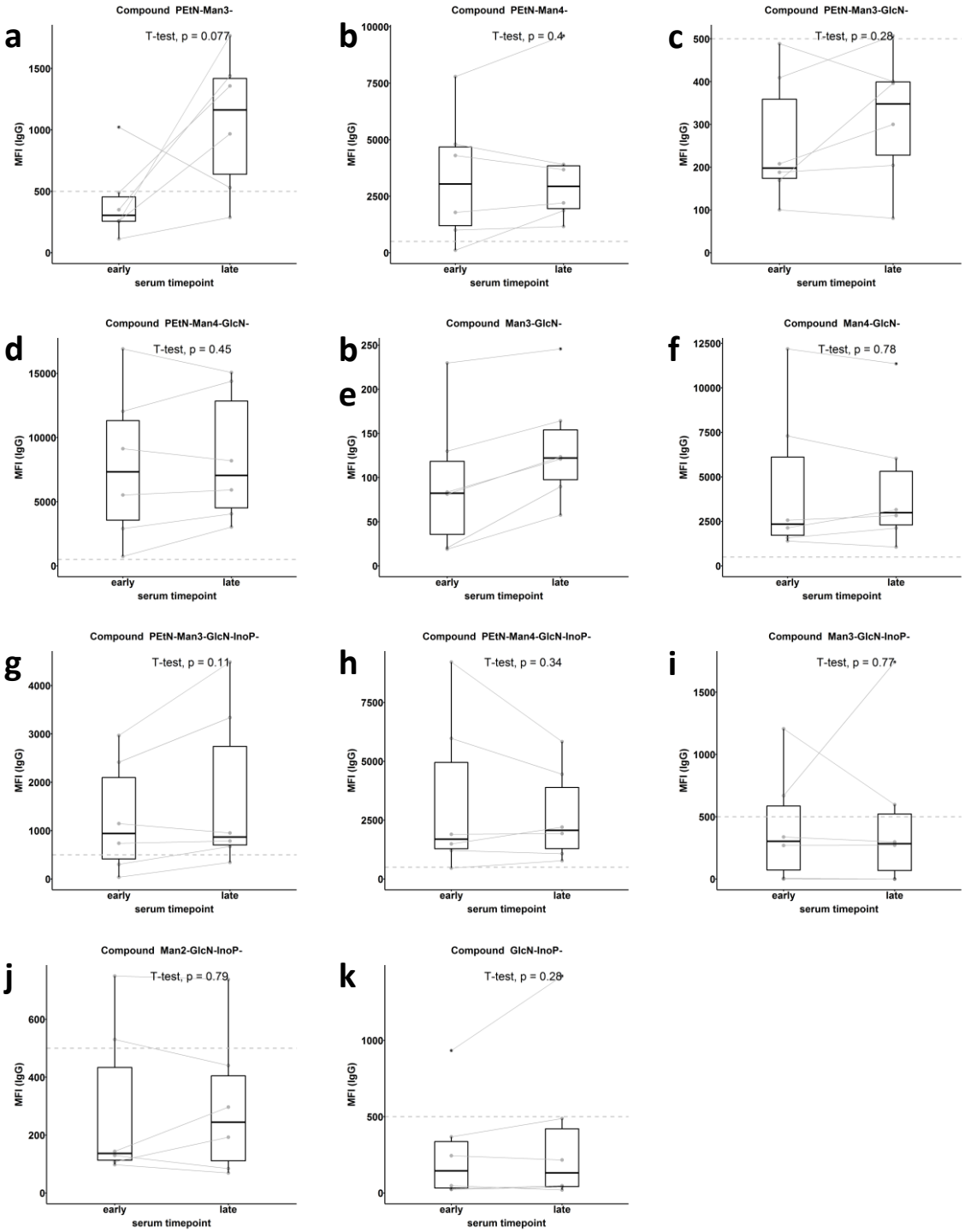

Figure 39: IgM titres in sera from patients with previous exposure against synthetic *P. falciparum* GPI fragments. Early and late IgM titres in sera of patients (n=6) were compared using paired T-test. Significant differences ($p<0.05$) indicate that antibodies cross-reactive to the synthetic GPI fragment were induced after infection.

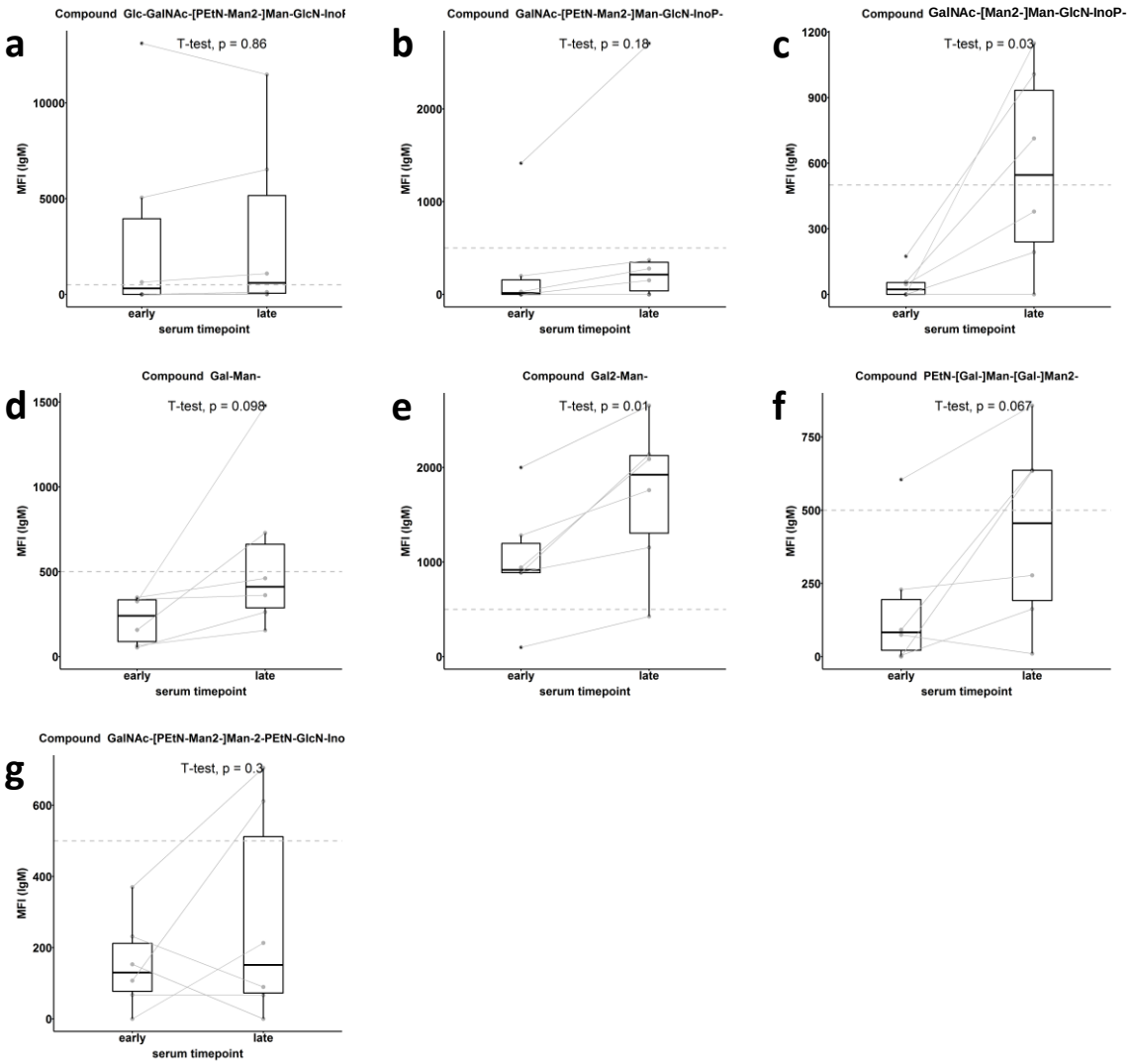

Figure 40: IgM titres in sera from patients with previous exposure against synthetic GPI fragments from other organisms. Early and late IgM titres in sera of patients (n=6) were compared using paired T-test. Significant differences ($p<0.05$) indicate that antibodies cross-reactive to the synthetic GPI fragment were induced after infection.

3.4 Inducing antibodies to epitopes of the GPI terminus

The minimal epitope fragments **7** and **8** were designed to induce antibodies specific to epitopes on the non-reducing terminus of GPI distal to the phospholipid. The design of **7** and **8** came from an understanding of the immunogenic GPI residues, and the non-reducing terminus of GPI was the chosen epitope to explore whether it is the target of protective antibodies. To test whether the designed GPI fragments do indeed induce antibodies to the target terminal epitope, mice were immunised with glycoconjugates of **7** and **8** and their induced antibody titres profiled on glycan microarray.

Minimum dose of glycoconjugate required

To determine how much glycoconjugate of **7** and **8** would be required for immunisation and challenge study experiments, I identified the minimum glycan dose required that could still induces antibodies against the antigen used. Glycoconjugate of **1**, previously produced in our lab, was used as the model antigen to determine the minimum dose. C57BL/6 mice were subcutaneously injected with glycoconjugate of **1** at varying concentrations in a prime-boost-boost regime at two week intervals. Groups of mice (n=3) were characterised by each glycan dose administered at 0.1, 0.4, 1 and 1.8 µg total glycan amount. A control group was immunized with CRM197 only, corresponding to 0 µg of glycan.

Sera (diluted 1:50) up to day 35 post-prime immunisation were screened on the synthetic GPI microarray. Epitope-specific antibody titres induced against each GPI fragment were compared across different immunisation doses [**Figure 41 & Figure 42**]. IgG titres against fragment **1** were induced in all mice across all glycan doses, however antibody titres were not as consistently high in the group of mice immunised with 0.1 µg glycan [**Figure 41a**]. High IgG titres against fragments **2**, **4**, and **5** were induced with 0.4 µg glycan [**Figure 41b, c & e**]. IgG titres against fragment **4** were highest at the maximum 1.8 µg glycan dose [**Figure 41d**]. IgG titres against fragment **6** were negligible [**Figure 41f**].

IgM titres against fragment **1** were consistently induced in all mice across all glycan doses [**Figure 42a**]. Highest IgM titres against fragments **1**, **2**, **4**, and **5** were induced with 0.4 µg glycan [**Figure 42a, b, c & e**]. As seen with IgG, IgM titres against fragment **4** were

highest at the maximum 1.8 µg glycan dose [**Figure 42d**], and IgM titres against fragment **6** were negligible [**Figure 42f**].

Antibodies against the GPI epitopes could be induced across all glycan doses tested. Consistently high antibody titres were induced with as little as 0.4 µg glycan, however inconsistent induction of antibodies was observed at 0.1 µg glycan. A glycan dose to be used for further immunisation and challenge experiments was set as 0.4 µg glycan for the mouse model of glycoconjugate immunisation. This newly established dose uses less glycan than previous immunisation schemes, which used up to 5 µg synthetic GPI per immunising dose. A reduction in dose results in less glycoconjugate that would need to be produced, reducing the amount of synthetic glycan that needs to be used for glycoconjugate production.

Glycoconjugates of **2** and **5**, previously produced in our lab, were then used to immunise mice at the 0.4 µg dose. C57BL/6 mice were subcutaneously injected in a prime-boost-boost regime at two week intervals. Groups of mice (n=4) were characterised by the glycoconjugate used. Sera (diluted 1:50) at day 35 post-prime immunisation were screened on the synthetic GPI microarray. Epitope-specific antibody titres were detected after immunisation [**Appendix, Figure 41 & Figure 42**].

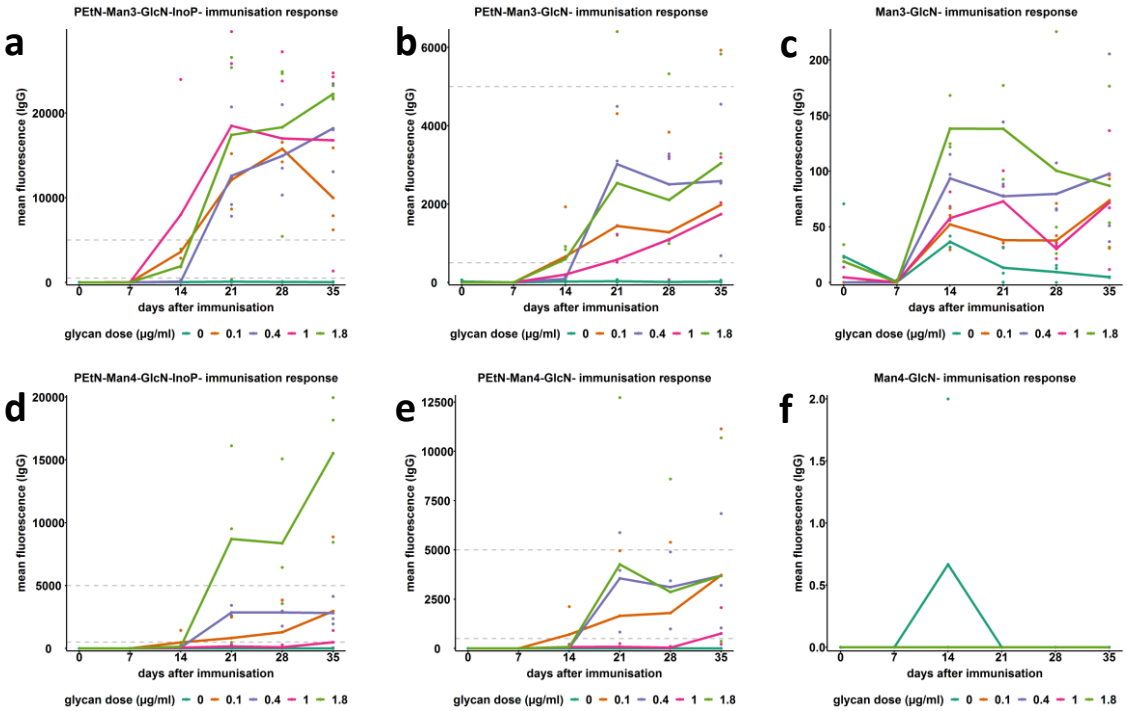

Figure 41: IgG titres against synthetic GPI fragments in sera at day 42. Group size n=3, classified by glycan antigen dose. **Top panel (a-c)** IgG titres after immunisation with glycoconjugates of **1**-**3** lacking the fourth Man. **Bottom panel (d-f)** IgG titres after immunisation with glycoconjugates of **4**-**6** containing the fourth Man.

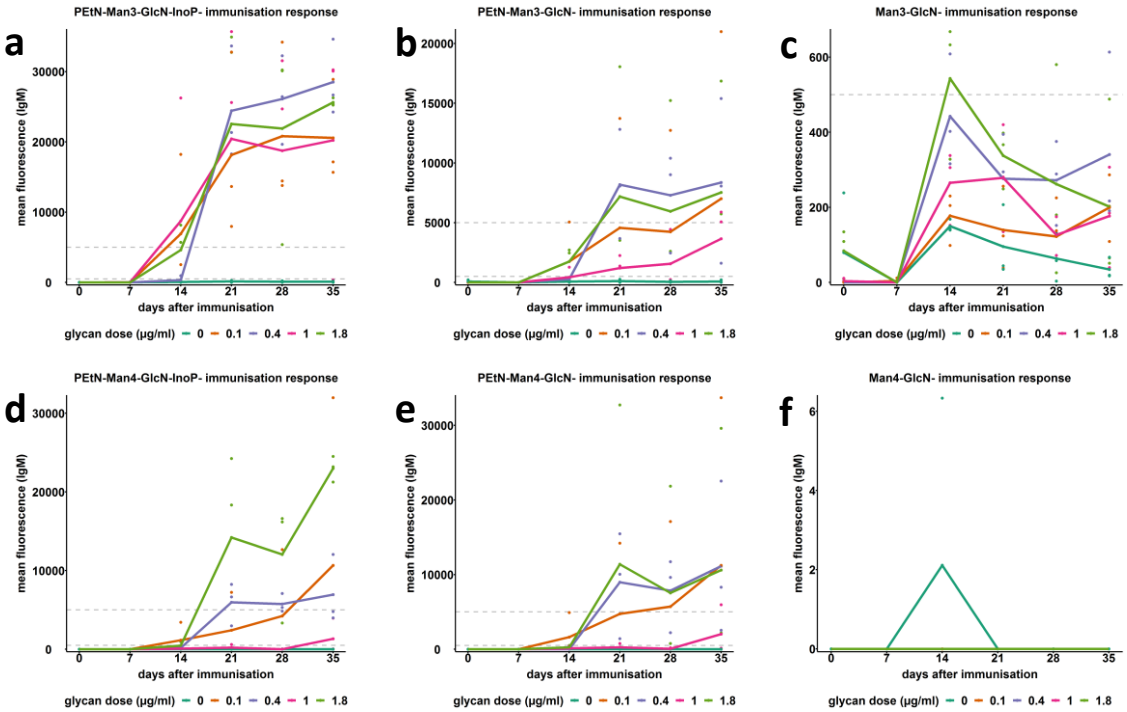

Figure 42: IgM titres against synthetic GPI fragments in sera at day 42. Group size n=3, classified by glycan antigen dose. **Top panel (a-c)** IgM titres after immunisation with glycoconjugates of **1**-**3** lacking the fourth Man. **Bottom panel (d-f)** IgM titres after immunisation with glycoconjugates of **4**-**6** containing the fourth Man.

Preparation of glycoconjugates using the minimal epitope antigens

With the dose and required amount of glycoconjugate confirmed, glycoconjugates of **7** and **8** were prepared by conjugation to CRM197 carrier protein. This carrier was chosen as it used in licensed human vaccines (Astronomo and Burton 2010). MALDI-TOF analysis [**Appendix, Figure 70 & Figure 71**] determined an average loading of 5.26 for glycoconjugate of **7**, and 6.2 for glycoconjugate of **8**. Just before use, SDS-PAGE analysis of the glycoconjugates showed higher mass shift compared to non-conjugated CRM197 [**Figure 43**]. The increase in mass corresponds to synthetic glycans still conjugated to the carrier protein after storage.

When ready to use, the glycoconjugates were adsorbed to aluminium hydroxide adjuvant, which is also approved for human use (Astronomo and Burton 2010). Glycoconjugates adsorb to the adjuvant in order to enhance immunogenicity of the glycoconjugate (De Gregorio, Tritto et al. 2008, Clapp, Siebert et al. 2011). After overnight incubation with adjuvant, adsorption of glycoconjugate was shown to be over 95% as determined by adsorption assay [**Table 3**], comparable to other semi-synthetic glycoconjugates using CRM197 (Broecker, Martin et al. 2016).

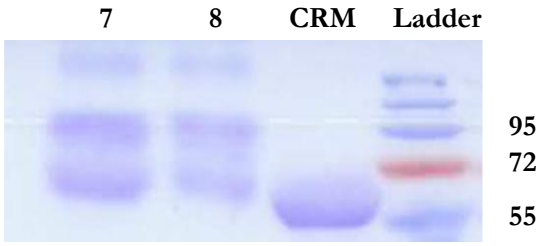

Figure 43: SDS-PAGE analysis of glycoconjugates of 7 & 8. Bands are compared to non-conjguated **CRM197** and molecular weight **ladder**. Numbers to the right indicate the molecular weight of marker bands in kDa.

CRM197 concentration (µg/mL)	Conjugate of 7	Conjugate of 8
before absorption	8.2	6.2
after absorption	0.3	0.3
% conjugate adsorption to adjuvant	96.6	95.8

Table 3: Adsorption values for glycoconjugates of **7** and **8**.

Profiling antibodies induced by minimal epitope antigens

Glycoconjugates of **7** and **8** were tested for their ability to induce antibodies specific to the non-reducing terminus of *P. falciparum* GPI. After overnight adsorption to adjuvant, subcutaneous immunisations in C57BL/6 mice with one of either glycoconjugate formulation were administered. Immunisations followed a prime-boost-boost regime at two week intervals, with each dose containing 0.4 µg of synthetic carbohydrate antigen. After a preliminary immunisation study showed the antigens were immunogenic [**Appendix, Figure 76 - Figure 79**], a larger immunisation study using more animals was carried out. Antibody titres against GPI fragments were assessed using glycan microarray in sera (diluted 1:50) collected every week from the prime immunisation (n=10 per group, classified by the immunising glycoconjugate) [**Appendix, Figure 82 – Figure 105**].

Both glycoconjugates induced IgG1 by day 42, predominantly against fragments **7** and **8** [**Figure 44a** and **Figure 45a**]. A similar profile for IgG2a titres was observed, albeit at a lower intensity [**Figure 44b** and **Figure 45b**]. Highest titres were measured against **7**, closely followed by **8**. Antibodies recognising larger GPI fragments containing a PEtN-Man_3 epitope also showed similarly high titres. Glycoconjugates of **7** & **8** induced similar IgG1 and IgG2a binding profiles, suggesting that the fourth Man only gives a marginal contribution to immunogenicity, confirming previous observations (Naik, Krishnegowda et al. 2006). Antibodies were not induced toward the GlcN-InoP epitope, owing to the fact that these residues were missing from the minimal epitope antigens.

Antibody titres to synthetic GPI fragments based on other organisms were measured [**Figure 46** and **Figure 47]**. Notably, immunisation with glycoconjugates of **7** and **8** induce moderately high IgG1 titres to *T. gondii* and mammalian GPI [**Figure 46a** and **Figure 47a**] likely facilitated by PEtN. Although glycoconjugate of **8** induces high IgG3 titres against *P. falciparum*-specific GPI fragments [**Figure 45c**], IgG3 titre is even higher against GPI from other organisms [**Figure 47c**]. This indicates that IgG3 induced by glycoconjugate of **8** is not specific to *P. falciparum* GPI.

IgM titres peak as early as day 7 against **7** and **8**, then wanes [**Figure 48a & d**]. Meanwhile, IgG1 was observed at day 14 and titres continue to increase until the immunisation schedule's end, typical of a primary antibody response [**Figure 48b & e**].

IgG2a titres peak at day 21 then declines to baseline titres just above the IgM response [**Figure 48c & f**].

These findings show that glycoconjugates of **7** and **8** are consistently immunogenic across all immunised mice, despite the small size of the synthetic glycan antigen. As predicted according to their design, the glycoconjugates could induce antibodies specific to the non-reducing terminus of *P. falciparum* GPI. In this case, the specific antibodies are of the IgG1 and IgG2a isotype. Since the design of the minimal epitope antigens stemmed from earlier analyses, it is demonstrated that understanding residue immunogenicity in synthetic glycan antigens can aid in designing new ones.

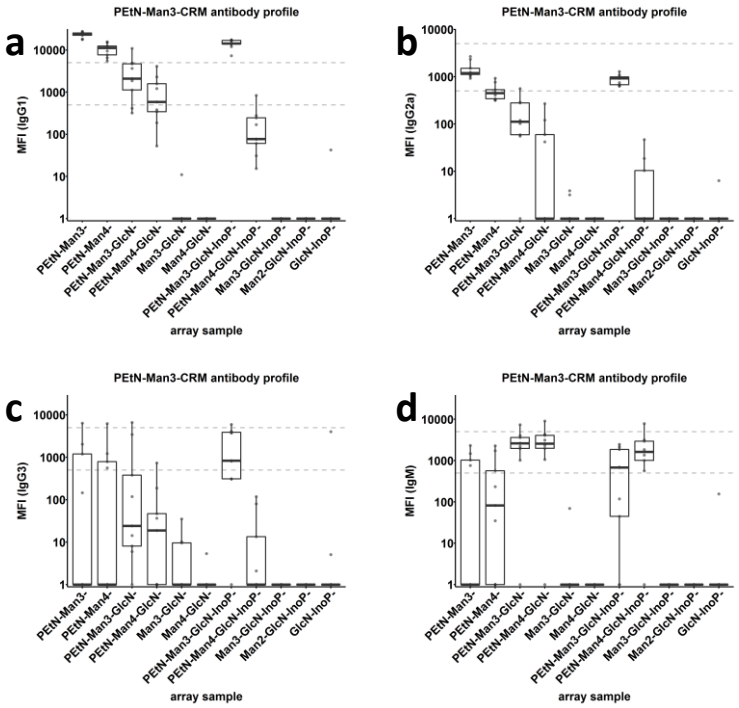

Figure 44: Antibody titres against synthetic *P. falciparum* GPI fragments in sera at day 42. Group size n=10, immunised with glycoconjugate of **7**. **Top panel (a-b)** IgG1 and IgG2a titres. **Bottom panel (c-d)** IgG3 and IgM titres.

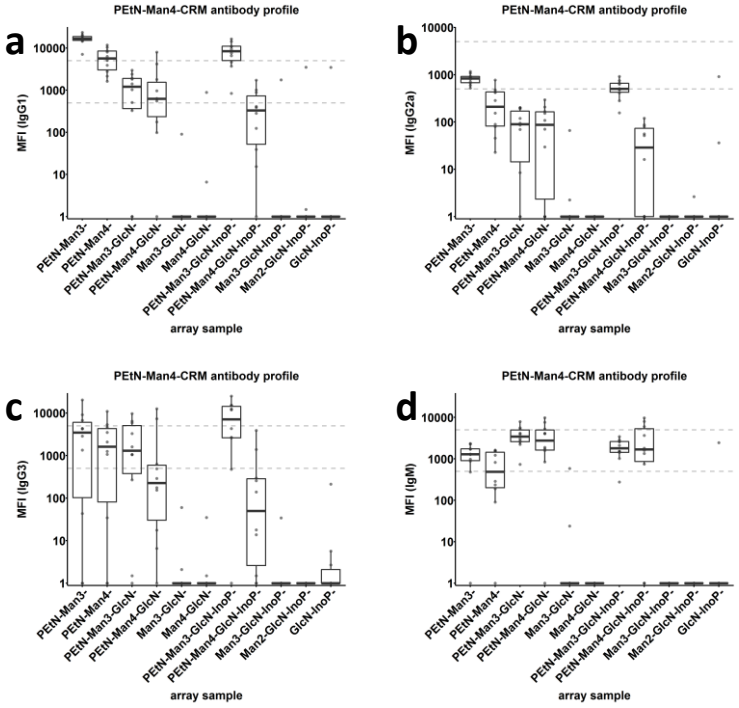

Figure 45: Antibody titres against synthetic *P. falciparum* GPI fragments in sera at day 42. Group size n=10, immunised with glycoconjugate of **8**. **Top panel (a-b)** IgG1 and IgG2a titres. **Bottom panel (c-d)** IgG3 and IgM titres.

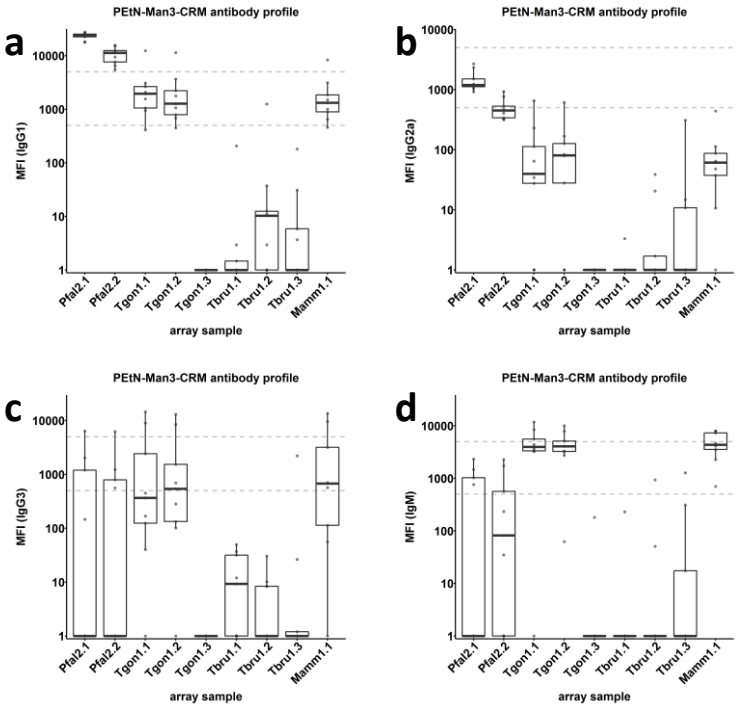

Figure 46: Antibody titres against synthetic GPI fragments from other organisms in sera at day 42. Group size n=10, immunised with glycoconjugate of **7**. **Top panel (a-b)** IgG1 and IgG2a titres. **Bottom panel (c-d)** IgG3 and IgM titres.

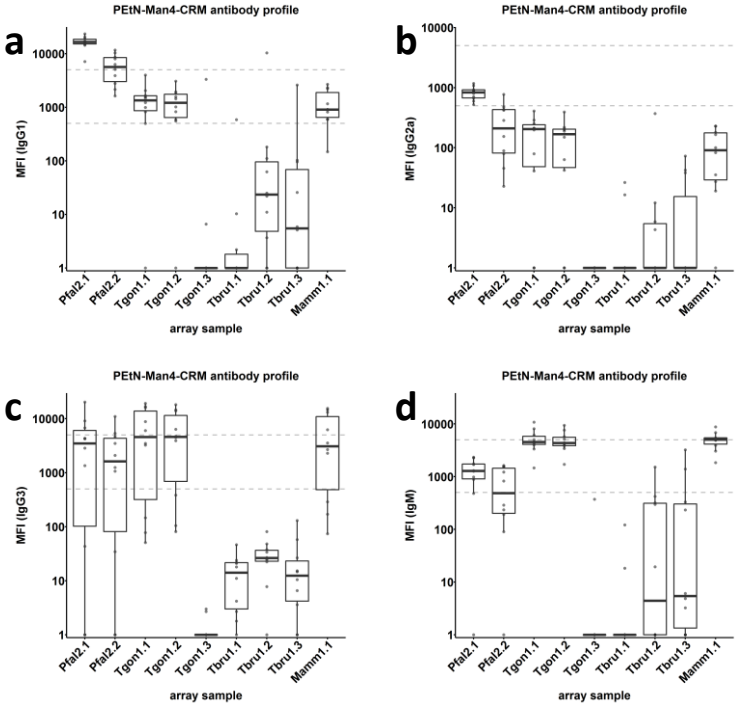

Figure 47: Antibody titres against synthetic GPI fragments from other organisms in sera at day 42. Group size n=10, immunised with glycoconjugate of **8**. **Top panel (a-b)** IgG1 and IgG2a titres. **Bottom panel (c-d)** IgG3 and IgM titres.

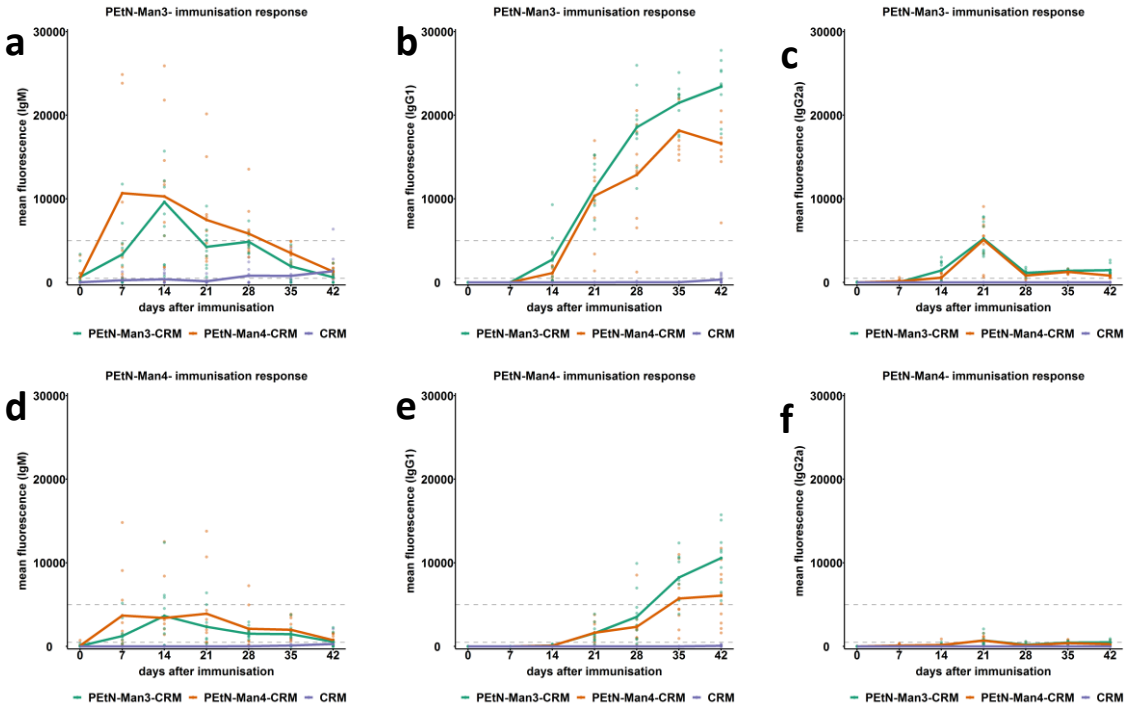

Figure 48: Antibody titres in sera from mice immunised with 7 [green], 8 [orange], or CRM197 only [blue]. IgM titres increase early, while IgG titres arise later, typical of a primary antibody response. **Top panel (a-c)** Antibody titres against fragment **7**. **Bottom panel (d-f)** Antibody titres against fragment **8**.

Isotype ratios to determine Th1 or Th2 biases

IgG2a is a surrogate marker for Th1 responses typically associated with cell-mediated immunity and inflammation. Conversely, IgG1 is indicative of Th2 responses inhibiting inflammatory responses (Rostamian, Sohrabi et al. 2017). Following immunisation, IgG1/IgG2a ratios have been used in mice to determine Th1 or Th2 biases (Broecker, Hanske et al. 2016).

IgG1/IgG2a titre ratios were plotted to compare Th1 or Th2 biases. Immunisation with glycoconjugates **7** and **8** produced more IgG1 than IgG2a, [**Figure 49g & h**] compared to immunisation with glycoconjugates **1**-**6** [**Figure 49a-f**], suggesting a Th2 bias. Especially hyper-inflammatory responses to free GPI are implicated in severe malaria pathogenesis (Gowda 2007). Thus, immunisation with glycoconjugates of **7** and **8**, that induce a Th2 bias, may protect against severe hyper-inflammation in malaria.

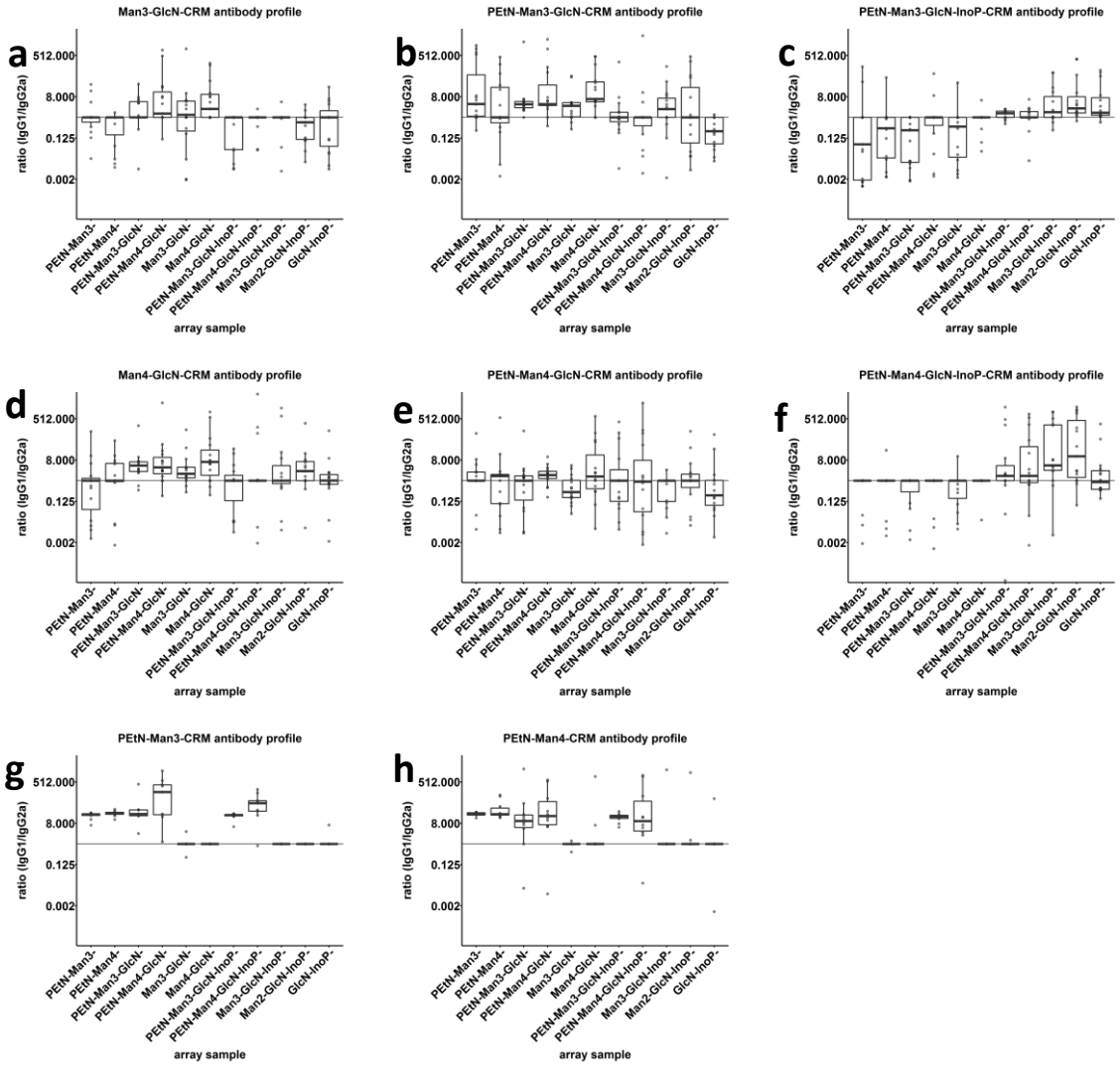

Figure 49: IgG1/IgG2a titre ratios in sera at day 42. Top panel (a-f) Average titre ratios after immunisation with glycoconjugates **1**-**6**. **Bottom panel (g-h)** Average titre ratios after immunisation with glycoconjugates of **7** and **8** suggest an IgG1/Th2 bias.

3.5 ECM challenge study

Antigens can be considered promising vaccine candidates if they are recognised by naturally occurring antibodies, and if glycoconjugates of these antigens are immunogenic in mice (Broecker, Hanske et al. 2016). The minimal epitope antigens **7** and **8** fulfil these requirements. Additionally, they induce antibodies to the non-reducing terminus of GPI, which may be the epitope for protective antibodies.

A series of experiments were planned (with consultancy from Vakzine Projekt Management GmbH, Hannover, Germany) to demonstrate whether immunisation with the glycoconjugates could protect against severe malaria. In this case, the experiments would employ the ECM mouse model of cerebral malaria. I would first determine protection from ECM pathology by immunising 10 mice per group with glycoconjugate at the highest immunisation dose of 0.4 µg glycan. Following this, dose response studies would be carried out to determine the minimum protective dose for the glycoconjugate. Co-formulation studies would also be carried out if the vaccine candidates continue to show promise. Finally, immune cell profiling would be carried out in immunised mice to determine cellular responses shortly after parasite challenge.

Immunisation did not affect experiment cerebral malaria outcome

To determine protection from ECM pathology, CB57BL/6 mice that were immunised with glycoconjugates of **7** and **8**, were subsequently infected with *P. berghei* ANKA at day 42. Mice were weighed [**Appendix, Figure 106**], and cerebral malaria incidence was observed. ECM incidence for mice immunised with either glycoconjugate did not differ from the CRM197 only group [**Figure 50**]. A negligible 0-10% of animals did not develop neurological symptoms. Therefore, glycoconjugate immunisation which induces terminal epitope-specific IgG1 is not protective in the ECM mouse model. It is possible that our induced GPI-specific antibodies confer some level of protection, however a balanced response that is not Th2 biased may be more beneficial (Bouharountayoun and Druilhe 1992). In particular Th1 lymphocytes could produce inflammatory cytokines like IFN-γ which are disruptive to intracellular parasite function (Rostamian, Sohrabi et al. 2017). These cytokines may work in concert with GPI-specific antibodies that limit the systemic inflammatory response and confer overall better protection in ECM. An additional

observation was significantly lower parasitemia at day 6 post-infection for mice immunised with glycoconjugate of **8** compared to mice immunised with CRM197 only, suggesting an inherent anti-parasite activity in these antibodies [**Figure 51**] that is considered to be beneficial.

Surprisingly, glycoconjugates of **7** and **8** did not recapitulate the 75% protection against ECM, previously reported by immunisation with synthetic hexasaccharide GPI (Schofield, Hewitt et al. 2002). In addition to the differing antigens, there are other differences from the previous study that may contribute to this outcome. I used Alum adjuvant, which is approved for human use (Marrack, Mckee et al. 2009) and induces a strong Th2 bias (Grun and Maurer 1989). CFA/IFA adjuvant used in the previous study can induce some Th1 responses (Billiau and Matthys 2001) which could contribute anti-parasitic effects that ameliorate downstream ECM pathology. Adjuvants that potently induce both Th1 and Th2 may be a solution. For example, MF59 adjuvant is approved for human use and induces a more potent Th1 and Th2 response compared to Alum (O'Hagan 2007). Moreover CRM197, as opposed to KLH, was used to mimic glycoconjugate formulations approved for human use as close as possible (Cavallari and De Libero 2017).

Since the synthetic glycoconjugates in the current formulation did not confer protection against ECM, follow up studies employing the ECM model were cancelled. Thus, dose responses, co-formulation and cellular responses were not studied with respect to immunisation with glycoconjugates of **7** and **8**. Though the synthetic glycoconjugates in the current formulation did not confer protection against ECM, severe malaria is often also characterized by severe malarial anaemia incidence (Snow, Omumbo et al. 1997). Emphasis is currently placed on combating severe malarial anaemia because of its negative impact, particularly on children and pregnant women (WHO 2018). Mouse models, such as *P. chabaudi* infection of BALB/c mice, could be used to test whether the synthetic GPI fragments can be used to immunise against severe malarial anaemia (Lamb and Langhorne 2008).

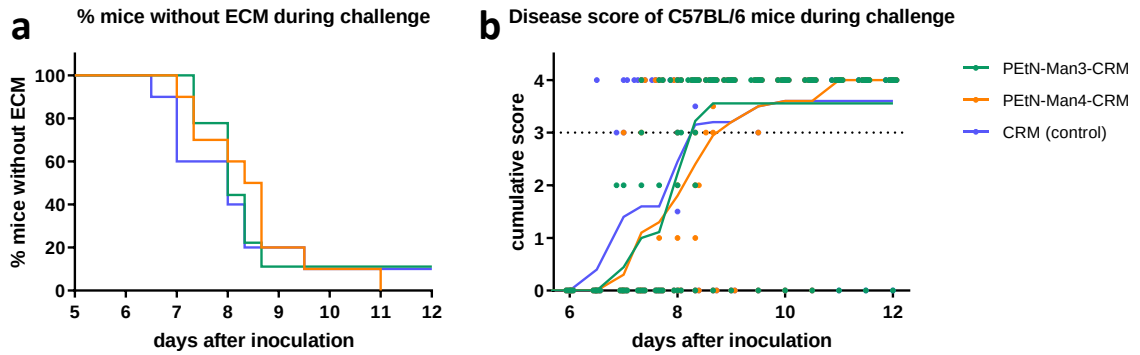

Figure 50: ECM challenge shows no difference between immunised groups. a) Glycoconjugate immunisation did not affect development of neurological symptoms compared to CRM197 control group. **b)** Glycoconjugate immunisation did not affect the disease score during infection compared to CRM197 control group. Mice were euthanized at a cumulative disease score of 3, and were assigned a score of 4 thereafter, increasing the disease score.

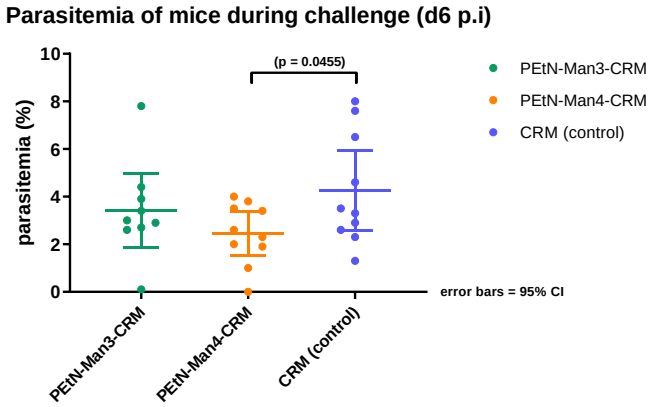

Figure 51: Parasitemia of mice at day 6 post-infection. A significant difference between mice immunised with glycoconjugate of **8** and CRM197 only was observed.

3.6 *In vitro* analysis of terminal epitope-specific antibodies

Binding of antibodies to *P. falciparum*

It was shown that fragments **7** and **8** interact with naturally occurring antibodies, and induced antibodies bind strongly to these fragments on glycan array. Here, efforts were made to evaluate whether antibodies induced by immunisation with glycoconjugates of **7** or **8** could interact with the parasite *in vitro*.

Pooled sera of mice before immunisation (day 0) and after immunisation (day 42) were incubated with fixed iRBCs containing merozoites, labelled for bound IgG, and visualised under confocal microscopy. Immunisation with glycoconjugate of **8** induced IgG that bound to merozoites within iRBCs [**Figure 52d**]. Immunisation with glycoconjugate of **7** also induced binding IgG to a lesser extent [**Figure 52b**]. This binding is likely via recognition of terminal epitopes of GPI on *P. falciparum*. Immunisation with the CRM197 control, and pre-immunised mouse sera do not show IgG binding to merozoites [**Figure 52f, a, c, & e**]. There is no IgG binding to RBCs before or after immunisation, indicating that immunisation with glycoconjugates induced antibodies that can distinguish between mammalian and *P. falciparum* GPI.

Pooled sera of mice early after immunisation (day 7) and late after immunisation (day 35) were incubated with fixed iRBC, labelled for bound IgG, and analysed via flow cytometry. Immunisation with glycoconjugate of **8** induced IgG that bound to iRBCs [**Figure 53b, blue**]. Immunisation with glycoconjugate of **7** also induced binding IgG to a lesser extent [**Figure 53b, orange**]. Immunisation with CRM197 control resulted in a minimal shift from baseline [**Figure 53b, grey**].

The microscopy and flow cytometry results suggest that glycoconjugate of **8** induces antibodies that more strongly recognise naturally occurring *P. falciparum* GPI than glycoconjugate of **7**. Given that glycoconjugate of **8** contains the *P. falciparum*-specific fourth Man, the induced antibodies may have an additional affinity to naturally occurring GPI containing the fourth Man, increasing overall signal. This remains unclear, since glycan microarray analysis did not show a clear difference in induced antibody titre

profiles against synthetic GPI fragments between immunised groups [**Figure 44 & Figure 45**].

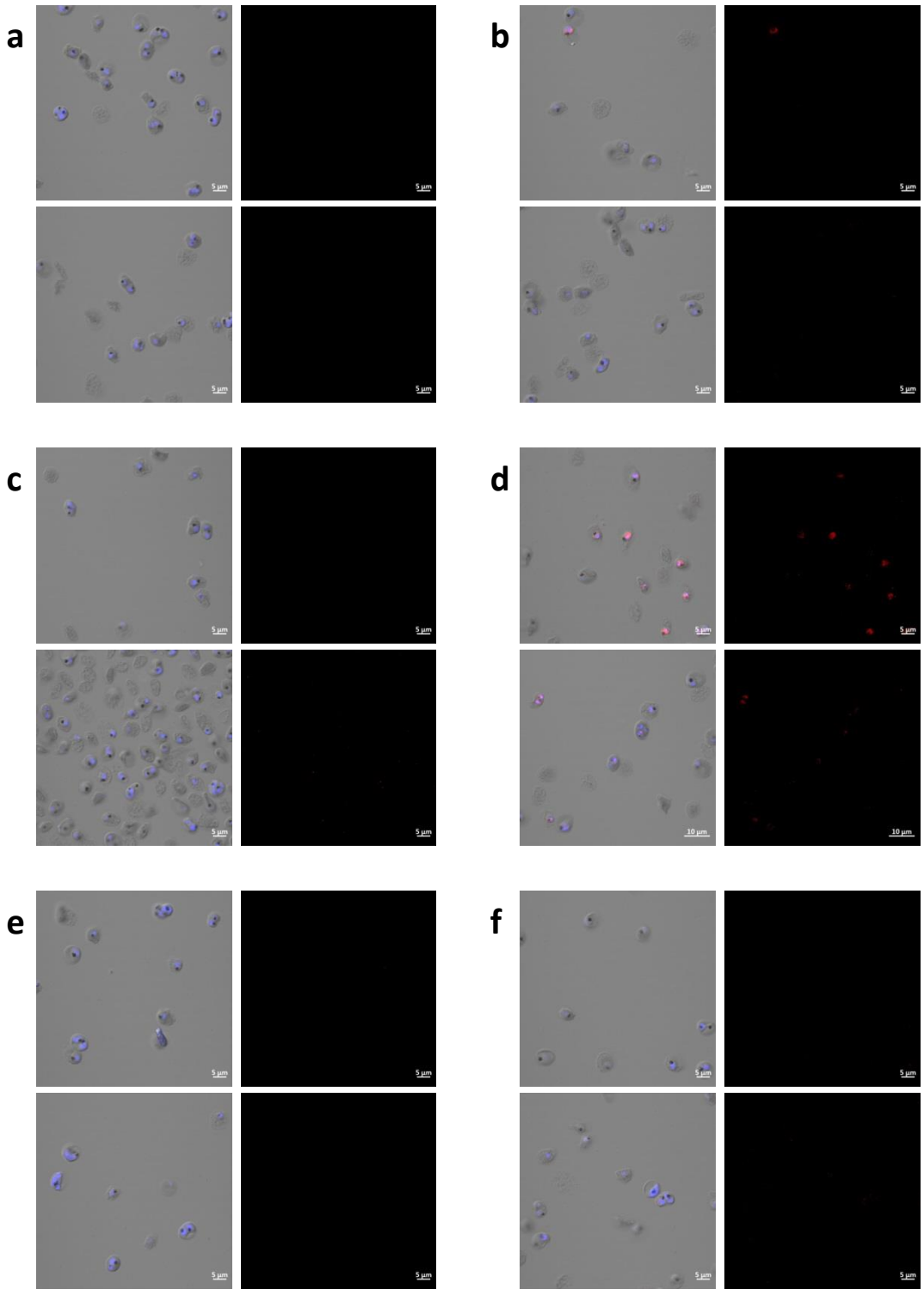

Figure 52: Binding of IgG against merozoites of iRBCs. Fixed iRBCs were incubated with pooled mouse sera and then labelled to show DNA [blue] and bound IgG [red]. **a)** Day 0, before glycoconjugate of **7** immunisation. **b)** Day 42, after glycoconjugate of **7** immunisation. **c)** Day 0, before glycoconjugate of **8** immunisation. **d)** Day 42 after glycoconjugate of **8** immunisation. **e)** Day 0 before CRM197 control immunisation. **f)** Day 42 after CRM197 control immunisation.

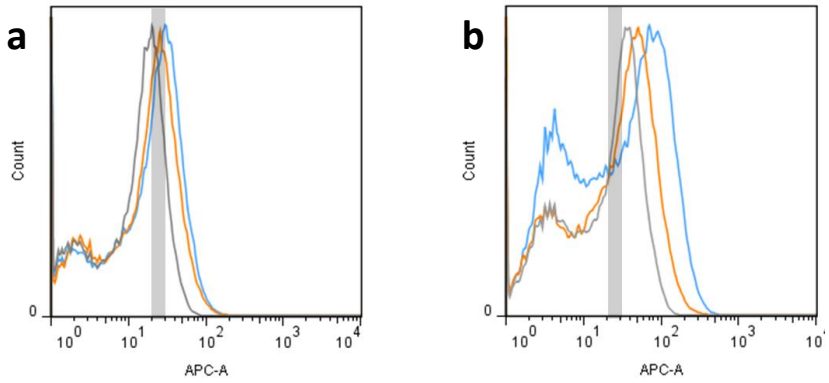

Figure 53: Binding of IgG against merozoites. Mice immunised with glycoconjugate of **7** [orange], **8** [blue], or CRM197 control [grey] were compared in flow cytometry. Increased titre of bound IgG to iRBCs is represented by an increased APC-A peak shift away from day 7 baseline [grey bar]. **a)** Day 7, early after immunisation. **b)** Day 35, late after immunisation.

Effect of antibodies on merozoite-induced TNF-α release

Pooled sera of mice before immunisation (day 0) and after immunisation (day 42) were added at various dilutions to cultures of RAW264.7 murine macrophages and merozoites. Supernatant concentrations of TNF-α were determined by ELISA. Immunisation with glycoconjugate of **7** or CRM197 control did not reduce TNF-α levels to a comparable level [**Figure 54a & c**]. The lowest concentration of TNF-α was found in reaction wells containing sera (diluted 10-fold) from mice immunised with glycoconjugate of **8**, significantly different to TNF-α levels in wells containing sera from the same mice before immunisation. However, higher dilutions of sera did not show clear differences in TNF-α levels [**Figure 54b**]. Glycoconjugate of **8** contains the *P. falciparum*-specific fourth Man, inducing antibodies that, at high concentrations, may affect the ability for naturally occurring GPI to induce inflammation in the reaction well.

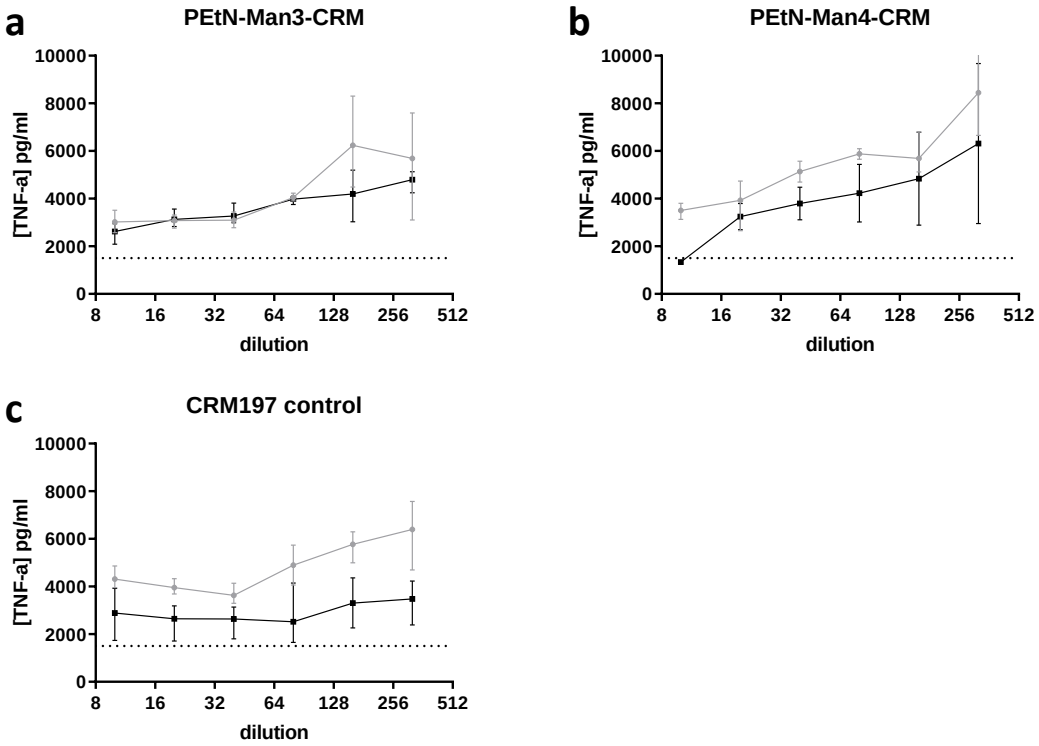

Figure 54: TNF-α concentrations in reaction wells with pooled sera of mice before and after immunisation at varying dilutions. Sera from mice at day 0 before immunisation (grey) were compared to sera from mice at day 42 after immunisation (black). Dotted line indicates the lowest level of TNF-α release achieved. Error bars indicate 95% CI. **a)** Group immunised with glycoconjugate **7**. **b)** Group immunised with glycoconjugate **8**. **c)** Group immunised with CRM197 control.

Binding of antibodies to *L. mexicana*

The antibodies may be cross-reactive to GPI from other protozoan parasites given that free GPI shares structural homology. Pooled sera of mice before immunisation (day 0) and after immunisation (day 42) were incubated with fixed *L. mexicana* amastigotes, labelled for bound IgG, and visualised by confocal microscopy. Immunisation with glycoconjugate of **7** induced IgG that bound to *L. mexicana* parasites [**Figure 55b**]. This binding is likely via recognition of terminal epitopes of GIPL on *Leishmania spp.* which shares the same structure as free GPI on *P. falciparum*, and is the structure of fragment **7** which induced antibodies showing the highest binding. Immunisation with CRM197 control, and pre-immunised mouse sera do not show IgG binding to amastigotes [**Figure 55a & c**].

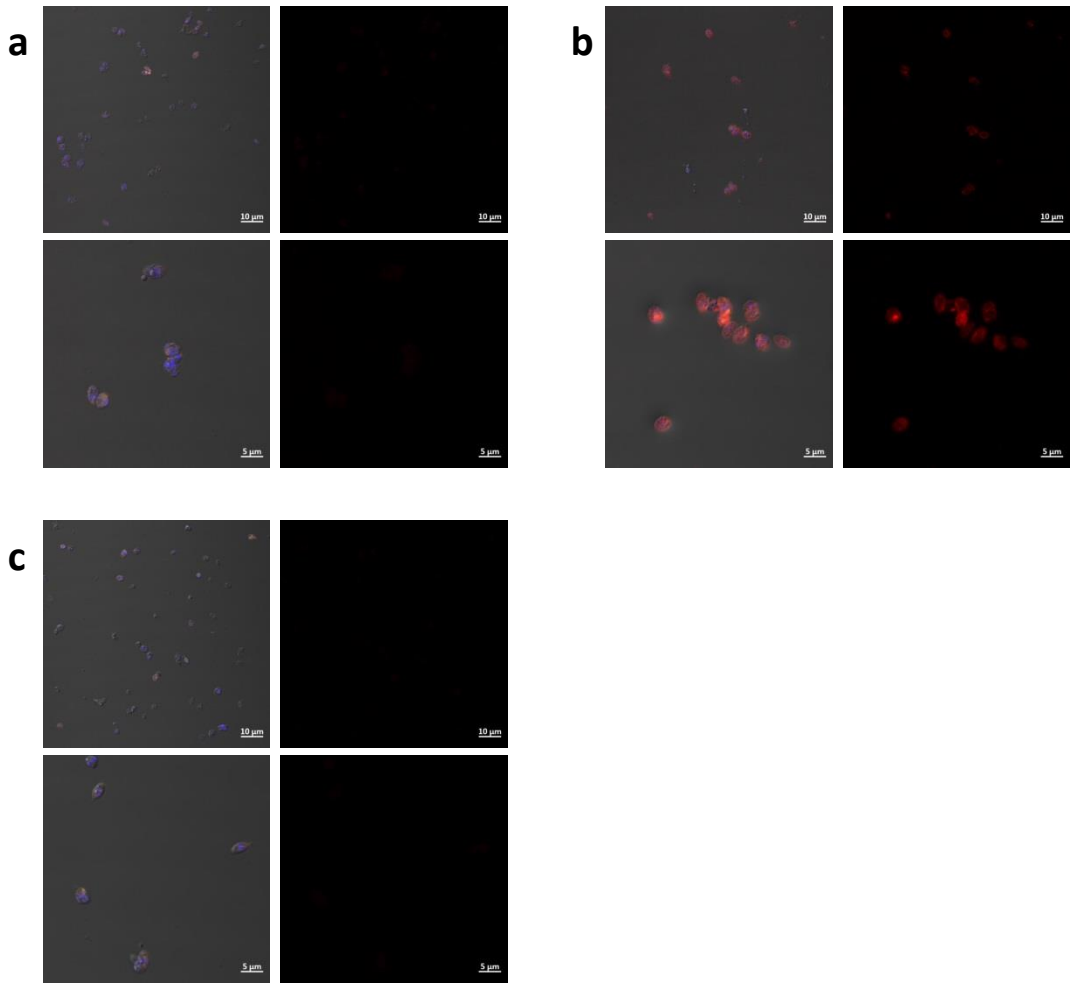

Figure 55: Binding of IgG against *L. mexicana*. Fixed *L. mexicana* parasites were incubated with pooled mouse sera and then labelled to show DNA [blue] and bound IgG [red]. **a)** Day 0, before glycoconjugate of **7** immunisation. **b)** Day 42, after glycoconjugate of **7** immunisation. **c)** Day 42, after CRM197 control immunisation.

3.7 Monoclonal antibody specific to the GPI terminus

Immunisation of mice and subsequent antibody profiling

To further clarify the role of antibodies specific to the non-reducing terminus of GPI, I generated a monoclonal antibody specific to the epitope. Here, mice were immunised with glycoconjugate of **7** (n=2) or **2** (n=4) to generate mice that produce GPI epitope-specific antibodies. More mice were included in the glycoconjugate **2** group since fewer mice were able to produce the desired epitope-specific antibody response. Subcutaneous immunisations in C57BL/6 mice with one of either glycoconjugate were administered in a prime-boost-boost regime at two week intervals, each containing only 0.4 µg of synthetic carbohydrate antigen. I screened sera (diluted 1:100) at day 42 post-prime immunisation and found that antibodies were induced against the desired epitope in one mouse immunised with glycoconjugate of **7** [**Figure 56a-d**] and one mouse immunised with glycoconjugate of **2** [**Figure 56e-h**].

The spleens of these mice were harvested for downstream hybridoma fusion. Interestingly, isotype analysis showed that immunisation with glycoconjugate of **7** generated a very strong IgG1 response almost exclusively to GPI fragment **7**, with only weak antibody responses to larger substructures containing the PEtN-Man3 epitope [**Figure 56a**], and very weak responses to synthetic GPI fragments from other organisms [**Figure 57a**]. Conversely, glycoconjugate of **2** was only weakly immunogenic in IgG1 [**Figure 56e**], but induced high IgG2a titres response against GPI fragment **7** and larger substructures containing PEtN-Man epitopes [**Figure 56f**], and even some non-*P. falciparum* GPI fragments [**Figure 57f**], suggesting that the inclusion of GlcN induced an IgG2a bias.

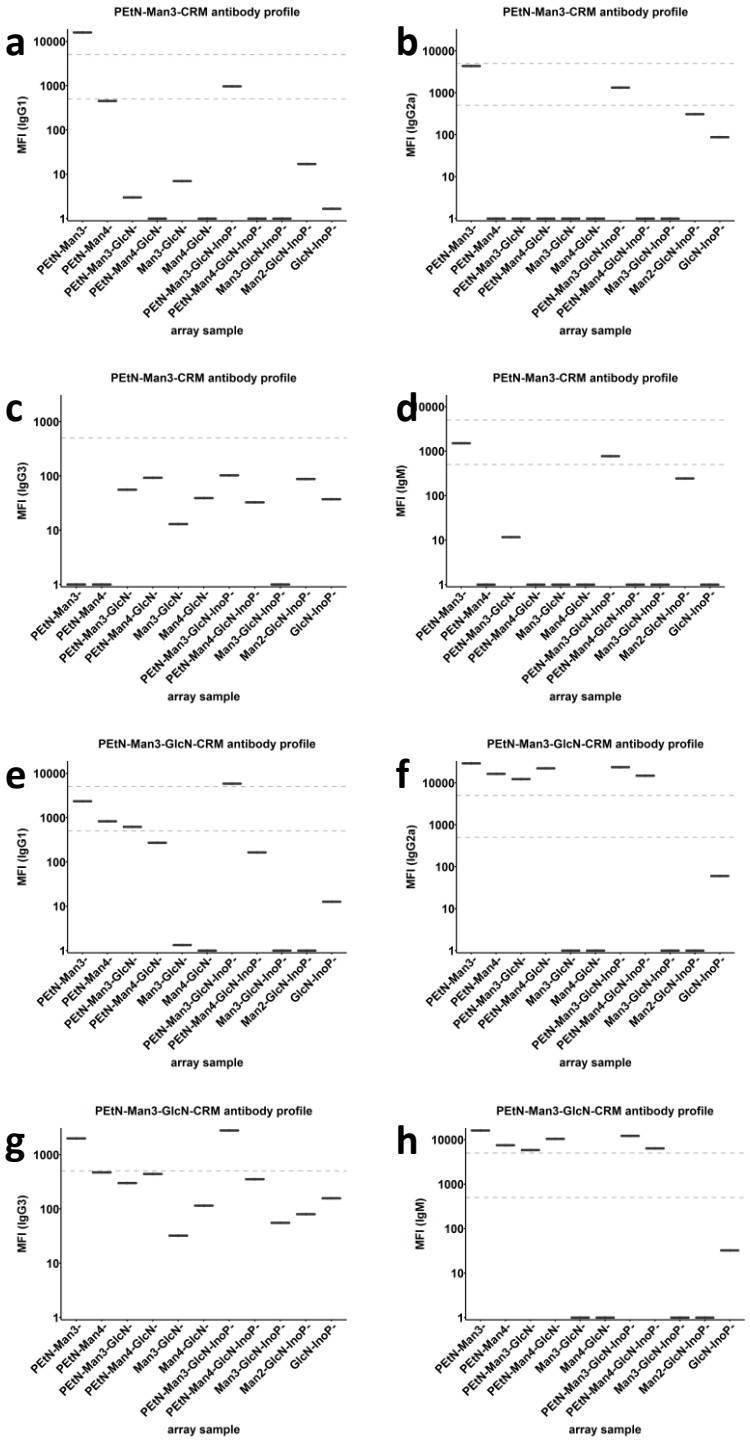

Figure 56: Antibody titres in sera at day 35 against synthetic *P falciparum* GPI fragments. Top panel (a-d) Antibody titres after immunisation with glycoconjugate of **7**. **Bottom panel (e-h)** Antibody titres after immunisation with glycoconjugate of **2**.

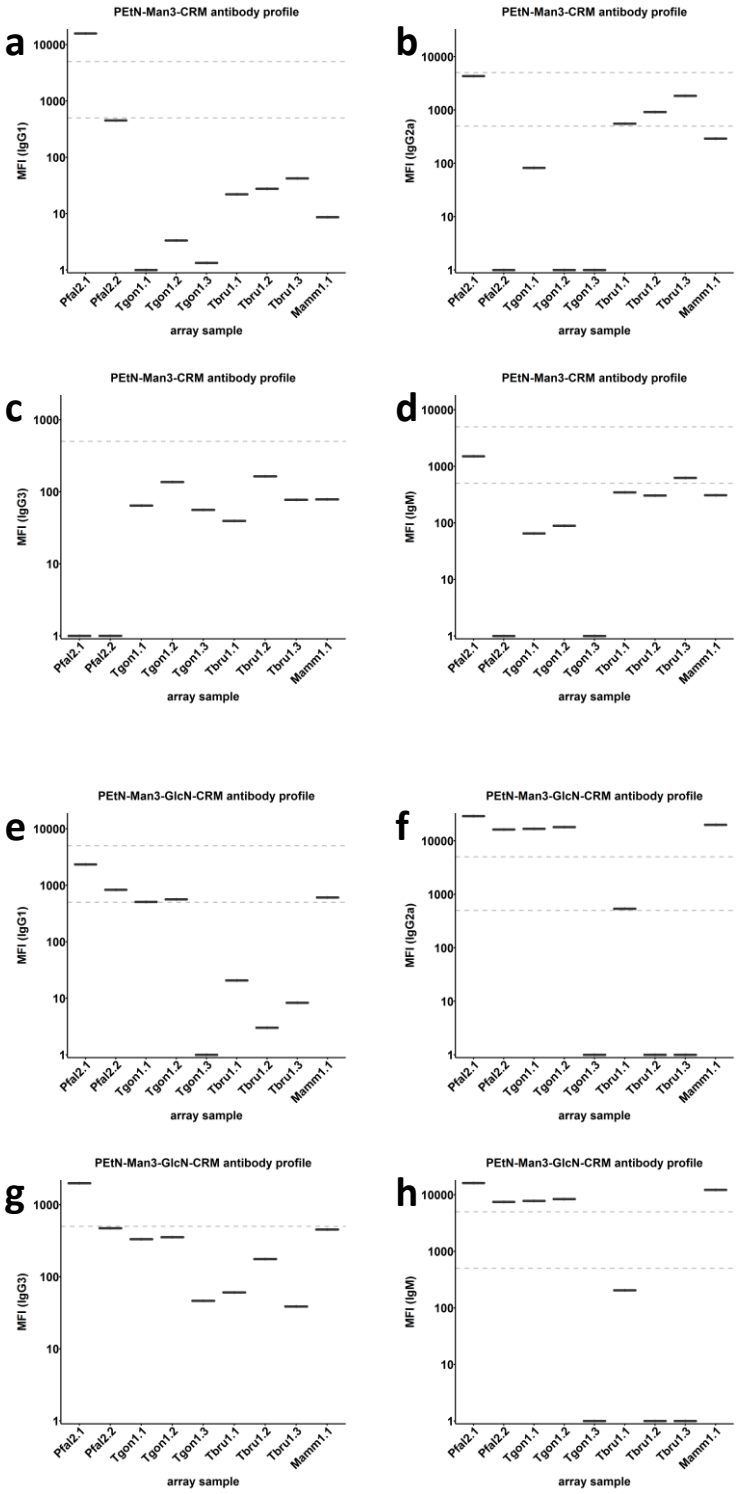

Figure 57: Antibody titres in sera at day 35 against synthetic GPI fragments from other organisms. Top panel (a-d) Antibody titres after immunisation with glycoconjugate of **7**. **Bottom panel (e-h)** Antibody titres after immunisation with glycoconjugate of **2**.

mAb binds to the minimal epitope

Hybridoma cell lines producing terminal epitope-specific antibodies were established from spleens immunized with glycoconjugate of **2** or **7**, according to glycan microarray analysis [**Figure 58a & b, respectively**]. However, these hybridoma stopped producing after expanded cell culturing. A stable, expanded hybridoma from spleen immunized with glycoconjugate of **7** produced IgM specific to the terminal epitope [**Figure 58c,** labelled 2D10D2C6]. The binding profile is similar to the antibody titre profiles in the polyclonal sera of the mouse from which the hybridoma was derived [**Figure 56a**], in that highest binding is against fragment **7**.

Purified mAb 2D10D2C6 at various concentrations was analysed on the GPI epitope microarray. Highest binding for 2D10D2C6mAb was against GPI fragments **7**, **2**, and **1**. Moderate binding against tetramannose substructures **8**, **5** and **4** is observed. Fragments lacking an intact Man backbone showed negligible binding by antibodies [**Figure 59a-c**]. 2D10D2C6 mAb recognises *T. gondii* and mammalian GPI [**Figure 59d-f**] fragments. This recognition is lower than that for fragments containing PEtN-Man3 epitope, but higher than that for fragments containing PEtN-Man4 epitope. Thus, binding is likely facilitated by PEtN.

Binding of 2D10D2C6 mAb at varying concentrations reinforces fragment **7** as the preferred epitope, followed by fragments containing a PEtN-Man3 epitope. Half-max binding is achieved at 284, 286 and 307 ng/mL against fragment **7**, **2** and **1** [**Figure 60a, b & c, respectively]**. The slight increase in half-max binding may be due to residues that hinder access to the PEtN-Man3 epitope. Additionally, the displacement of PEtN on **1** may also contribute to lower mAb affinity. Half-max binding to GPI from other organisms is even higher, achieved at 515, 692 and 494 ng/mL against Tgon1.1, Tgon1.2 and Mamm1.1 [**Figure 60d, e & f, respectively**]. The increased half-max binding is likely due to further modifications to the core GPI that hinder access to the PEtN-Man3 epitope that is specific to free GPI.

The specific binding of mAb 2D10D2C6 to native *P. falciparum* GPI was validated using Western blot analysis. Native GPI was isolated from *P. falciparum* 3D7 merozoites. The GPI was conjugated to polypeptide before transfer to a western blot membrane. Secondary

mouse anti-IgM antibody staining of the membrane showed that mAb binds the GPI-conjugated polypeptide, whereas the polypeptide alone was not bound [**Figure 61**].

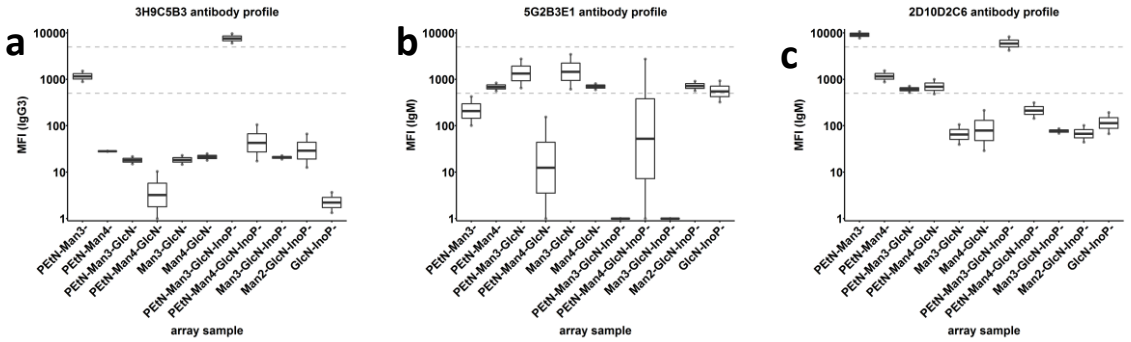

Figure 58: Monoclonal antibody binding specificities against synthetic *P falciparum* GPI fragments in supernatant of expanded clones. (a-b) Antibody titres after immunisation with glycoconjugate of **2**. **(c)** Antibody titres after immunisation with glycoconjugate of **7**.

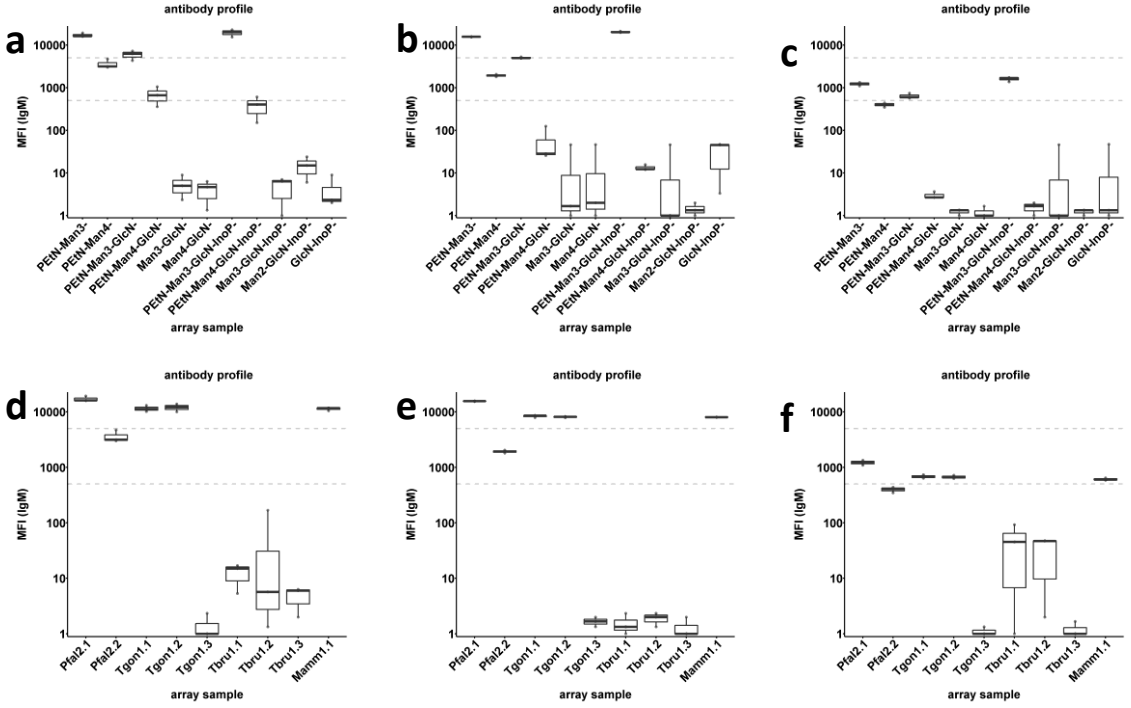

Figure 59: 2D10D2C6 mAb titres against synthetic GPI fragments. Top panel (a-c) mAb binding against *P. falciparum* GPI. **a)** 40 μg/mL **b)** 1.25 μg/mL **c)** 0.0391 μg/mL. **Bottom panel (d-f)** mAb binding against GPI from other organisms. **d)** 40 μg/mL **e)** 1.25 μg/mL **f)** 0.0391 μg/mL.

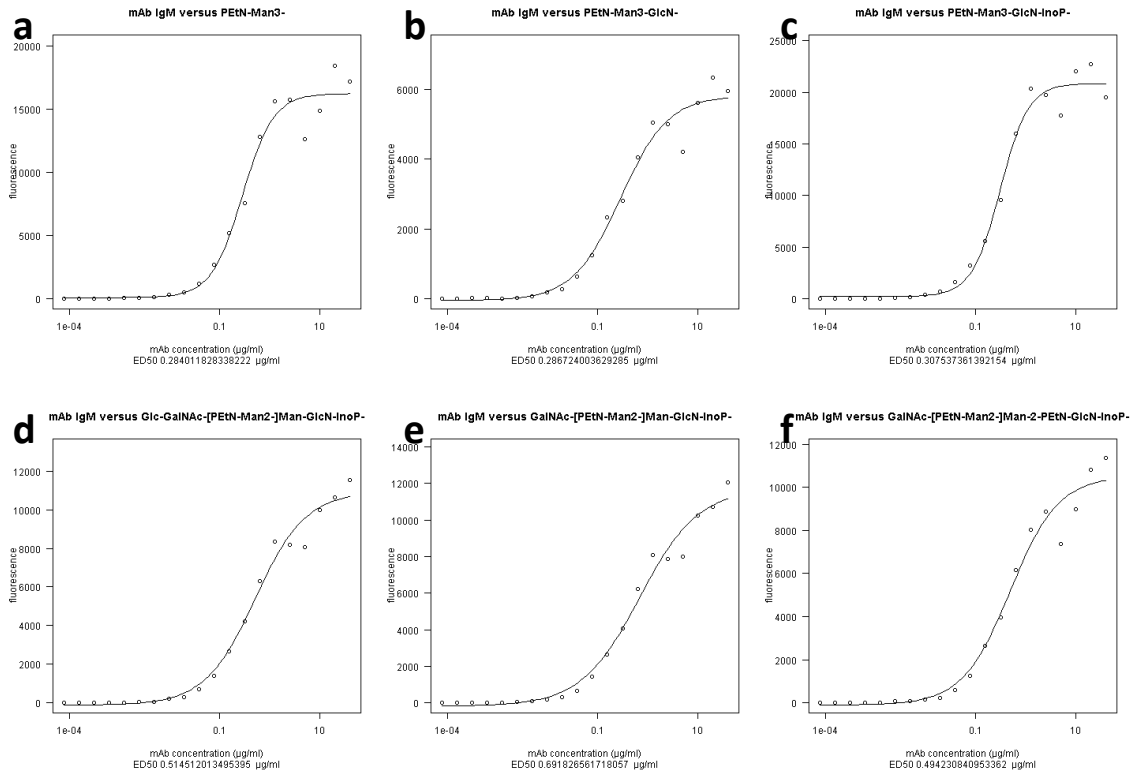

Figure 60: Binding concentration curves of mAb against specific GPI fragments. Top panel (a-c) mAb binding against *P. falciparum* GPI. **a)** Fragment **7**. **b)** Fragment **2**. **c)** Fragment **1**. **Bottom panel (d-f)** mAb binding against GPI from other organisms. **d)** Fragment **Tgon1.1**. **e)** Fragment **Tgon1.2**. **f)** Fragment **Mamm1.1**.

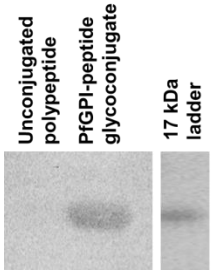

Figure 61: mAb raised by glycoconjugate of 7 bind to GPI isolated from *P. falciparum*. Image courtesy of S. Khilji.

Effect of mAb on *in vitro* parasitemia and TNF-α release

If protective effects of the mAb can be convincingly demonstrated *in vitro*, then passive immunisation studies using the mAb can be considered. To explore this possibility, I tested whether the mAb can reduce parasitemia *in vitro*, as an inherent anti-parasite activity is considered to be beneficial. The addition of mAb did not reduce parasitemia after one [**Figure 62a**] or two cycles of replication [**Figure 62b**]. This reflects what is seen *in vivo* for the ECM mouse model, where immunisation with synthetic GPI glycoconjugates did not lead to parasite clearance.

I also tested whether mAb can reduce the merozoite-induced release of TNF-α in RAW264.7 macrophages. I reasoned the mAb could sequester free GPI molecules by binding the PEtN-Man epitope, preventing the inflammatory effect of the entire GPI molecule *in vitro*. However, the merozoite-induced release of TNF-α by macrophages was not significantly affected by the presence of the monoclonal antibody [**Figure 63**].

As protective effects of the mAb could not be demonstrated *in vitro*, passive immunisation using the mAb was not pursued.

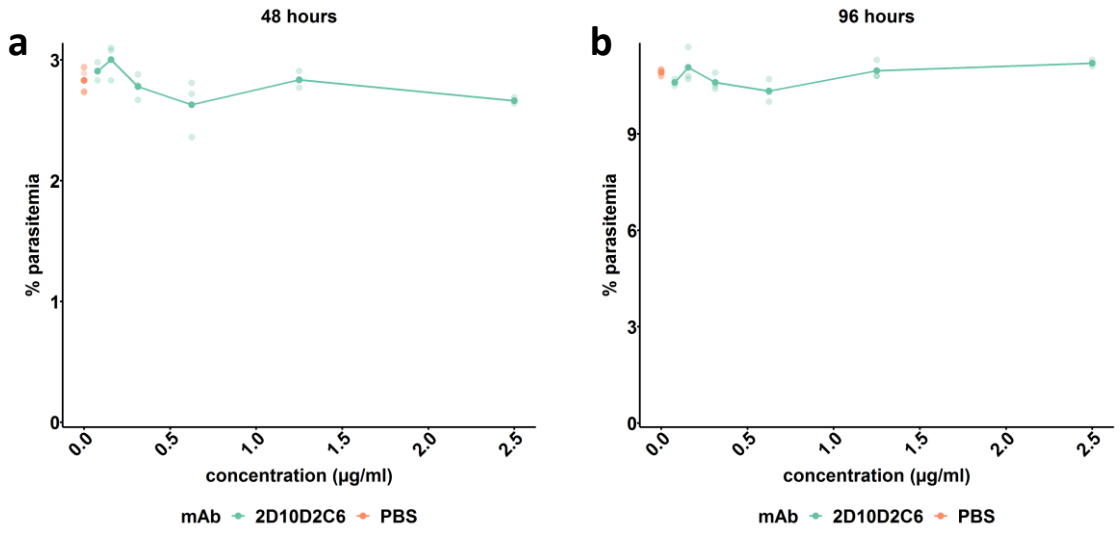

Figure 62: Parasitemia in cell culture with varying amounts of 2D10D2C6 mAb. a) After 1 cycle, at 48 hours. **b)** After 2 cycles, at 96 hours.

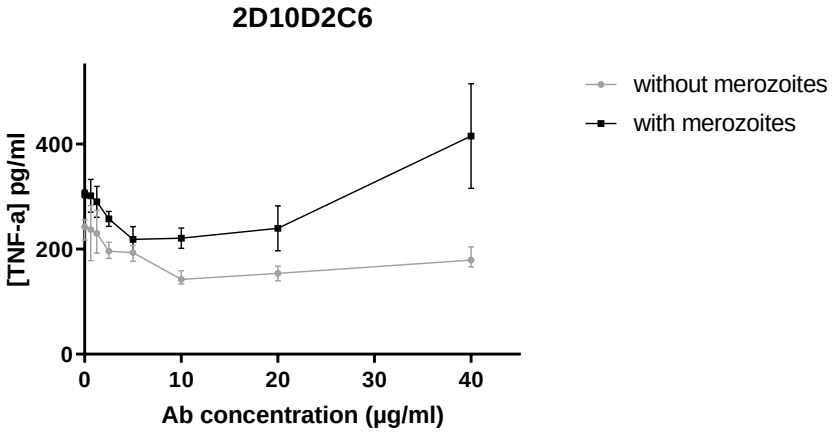

Figure 63: Dose-dependent TNF-α release. Concentration of 2D10D2C6 mAb, up to 40 µg/mL, compared to TNF-α concentration in cell culture.

Binding of mAb to *L. mexicana*

mAb 2D10D2C6 may be cross-reactive to GPI from other protozoan parasites similar to polyclonal antibodies from immunised mice, given that free GPI shares structural homology. mAb 2D10D2C6 was incubated at varying concentrations with fixed *L. mexicana* amastigotes, labelled for bound IgM, and visualised by confocal microscopy. 2D10D2C6 mAb bound to *L. mexicana* amastigotes at 0.1 µg/mL or higher [**Figure 64a-c**]. This binding is likely via recognition of terminal epitopes of GIPL on *Leishmania spp.* which shares the same structure as free GPI on *P. falciparum*, and is the structure of fragment **7** was used for immunisation to generate the mAb. Incubation with control IgM or no mAb did not show binding to amastigotes [**Figure 65a-d**].

mAb 2D10D2C6 at varying concentrations were incubated with fixed *L. mexicana* promastigotes, labelled for bound IgM, and visualised under confocal microscopy. mAb 2D10D2C6 bound to *L. mexicana* promastigotes at 0.1 µg/mL or higher [**Figure 66a-c**]. Again, this binding is likely via recognition of terminal epitopes of GIPL. Incubation with control IgM or no mAb showed minimal or no binding to promastigotes [**Figure 67a-d**].

In retrospect, I found that the binding studies with *Leishmania* were reproducible and consistent. This was in contrast to in vitro studies using *P. falciparum*, where difficulty was encountered when trying to reproduce the optimal conditions that showed antibody interaction.

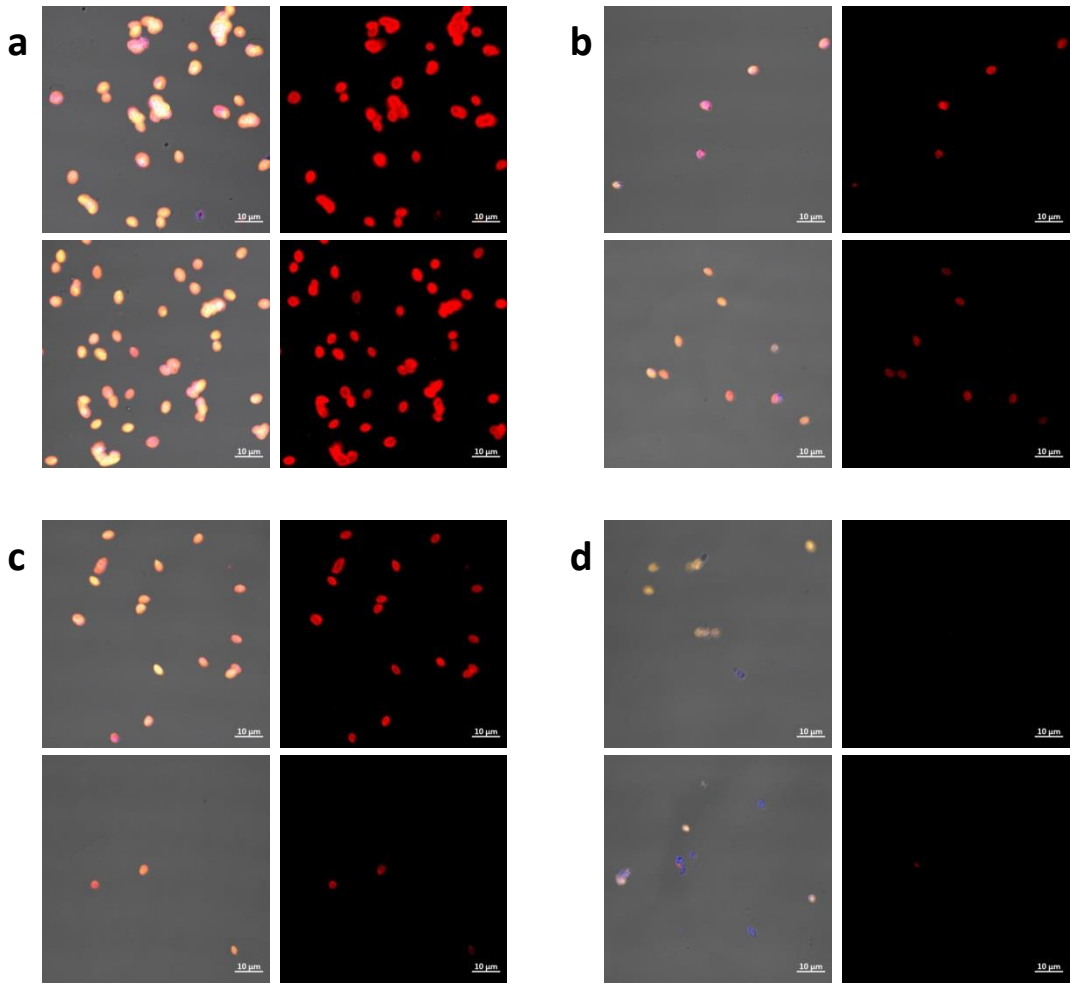

Figure 64: Binding of mAb against *L. mexicana*. Fixed *L. mexicana* amastigotes expressing DsRed [orange] were incubated with 2D10D2C6 mAb and then labelled to show DNA [blue] and bound IgM [red]. 2D10D2C6 mAb added at **a)** 10 μg/mL, **b)** 1 μg/mL, **c)** 0.1 μg/mL, **d)** 0.01 μg/mL.

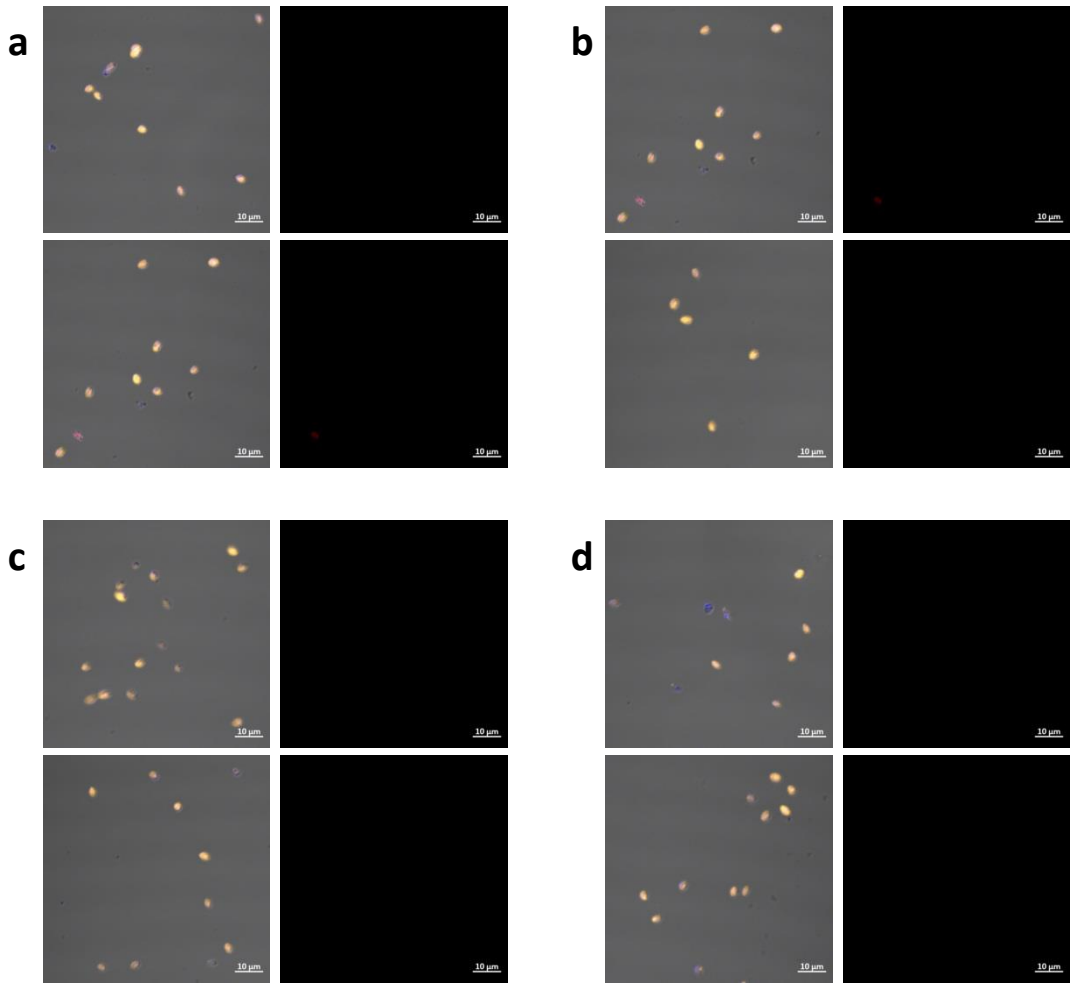

Figure 65: Binding of control IgM mAb against *L. mexicana*. Fixed *L. mexicana* amastigotes expressing DsRed [orange] were incubated with control IgM mAb and then labelled to show DNA [blue] and bound IgM [red]. Control IgM mAb added at **a)** 10 μg/mL, **b)** 1 μg/mL, **c)** 0.1 μg/mL. **d)** No mAb added.

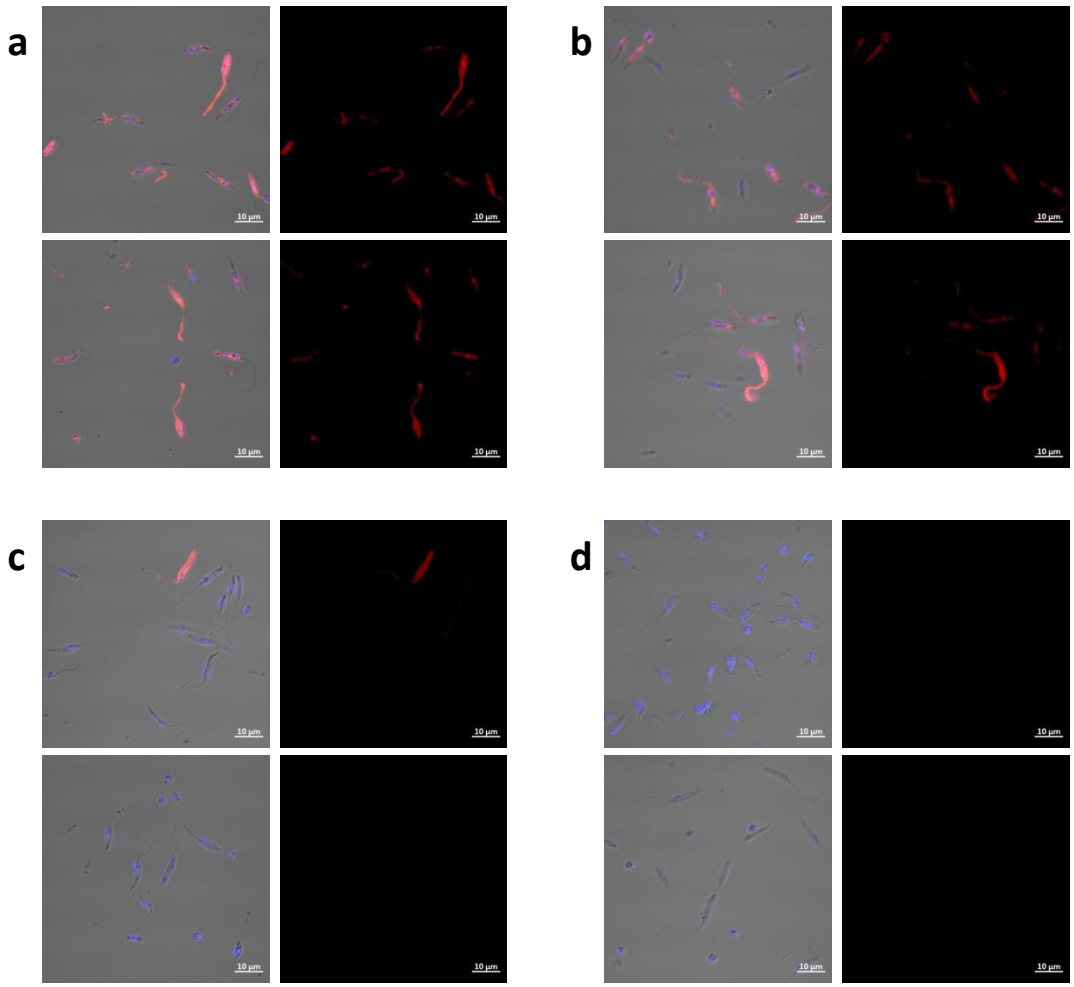

Figure 66: Binding of mAb against *L. mexicana*. Fixed *L. mexicana* promastigotes were incubated with 2D10D2C6 mAb and then labelled to show DNA [blue] and bound IgM [red]. 2D10D2C6 mAb added at **a)** 10 μg/mL, **b)** 1 μg/mL, **c)** 0.1 μg/mL, **d)** 0.01 μg/mL.

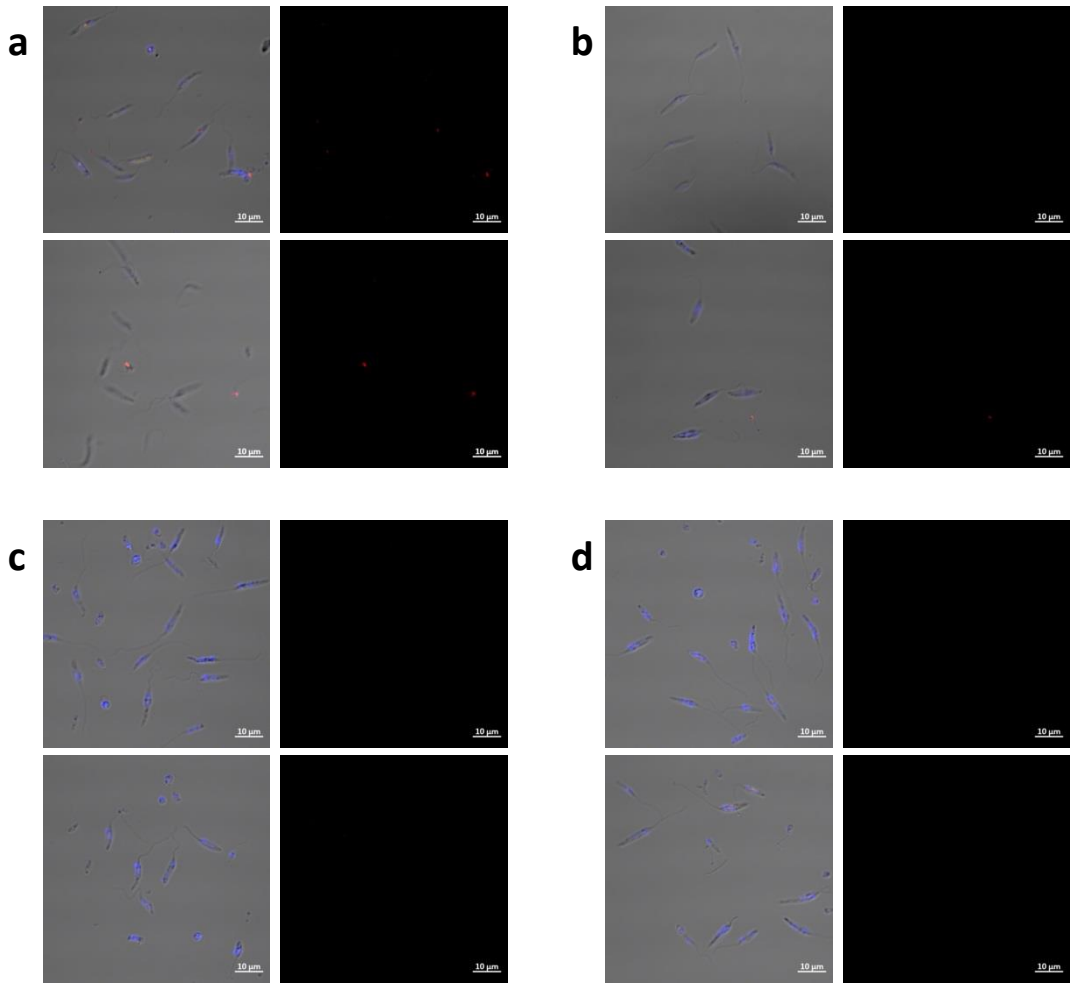

Figure 67: Binding of control IgM against *L. mexicana*. Fixed *L. mexicana* promastigotes were incubated with control IgM mAb and then labelled to show DNA [blue] and bound IgM [red]. Control IgM mAb added at **a)** 10 μg/mL, **b)** 1 μg/mL, **c)** 0.1 μg/mL. **d)** No mAb added.

4 Conclusions & Outlook

This thesis describes the selection of a *P. falciparum*-specific GPI epitope hypothesised to be the target of antibodies protective against severe malaria. I designed an antigen that predictably induces antibodies specific to this epitope, and characterised these antibodies regarding their possible protective effects.

First, I investigated how certain GPI residues affect the epitope specificity of induced antibodies. Polyclonal serum antibodies and monoclonal antibodies from previous synthetic GPI immunisation studies were screened on microarrays furnished with a synthetic GPI epitope library. InoP and GlcN were identified as the immunodominant residues facilitating the induction of antibodies specific to the GlcN-InoP epitope, followed by PEtN. However, analysis of sera from naturally infected individuals showed that InoP and GlcN are only immunodominant when included in synthetic GPI fragments that are used for immunisation, but do not appear similarly immunodominant as a part of native GPI antigen structures. Rather, naturally-occurring GPI-specific antibodies from malaria-infected patients recognize the non-reducing end of the GPI. Therefore, synthetic GPI antigens lacking InoP could induce antibodies more akin to naturally occurring GPI-specific antibodies. Moreover, the immunogenic PEtN should be included to maintain antigen immunogenicity in the absence of InoP.

Rationalising residue-dependent GPI immunogenicity aided in the design of minimal epitope antigens **7** and **8**. These antigens were designed to induce antibodies specific to epitopes on the non-reducing terminus of GPI distal to the phospholipid. This terminal epitope was targeted as it is specific to *P. falciparum* GPI, could induce antibodies more akin to naturally occurring GPI-specific antibodies, and should effectively mask the GPI molecule to thereby block inflammation. Furthermore, the antigens could induce epitope-specific antibodies that have likely not been explored by earlier glycoconjugates of synthetic GPI. As predicted, glycoconjugates of **7** and **8** could consistently induce antibodies specific to the non-reducing terminus of *P. falciparum* GPI, with a Th2 bias. Induced antibodies bound to merozoites likely via the terminal GPI epitope.

I then employed the ECM mouse model of cerebral malaria to elucidate whether immunisation with the glycoconjugates is protective. Immunisation, and subsequent induction of terminal specific antibodies, did not protect against neurological symptoms in ECM as envisioned. Follow-up studies investigating dose responses, co-formulation and immune cell profiles in the context of the ECM model were cancelled as a result.

To further characterise the effect of antibodies specific to the terminal epitope, I successfully generated a mAb derived from mice immunised with glycoconjugate of **7**. Similar to the polyclonal sera of immunised mice, the mAb was highly specific to fragment **7** representing the terminal epitope. However, as the monoclonal antibody did not show any effect in reducing GPI-induced inflammation or inhibit parasitemia *in vitro*, passive immunisation with the monoclonal antibody to protect against severe malaria was not considered.

Various methods showed polyclonal and monoclonal antibody binding to native GPI of *P. falciparum*, likely by recognition of the non-reducing terminus of GPI. Since this unmodified core backbone is structurally similar to GPI of other protozoan parasites, I investigated binding to *L. mexicana*, a parasite species responsible for leishmaniasis. Polyclonal and monoclonal antibodies similarly bound to *L. mexicana* amastigotes, and mAb also showed limited binding to promastigotes. Meanwhile, sera from unimmunised mice, control immunised mice, or unrelated mAb did not show binding to either parasite. The current *in vitro* observations across both parasites gives strong evidence that native GPI are recognised by antibodies, likely via recognition of shared terminal epitopes of free GPI on *P. falciparum* and GIPL on *Leishmania* species. Whereas antibody binding is consistently reproducible against *L. mexicana*, reproducible results for *P. falciparum* are elusive. This might be due to difficulties to reproduce the required fixation conditions. Consequently, optimal conditions required when handling *P. falciparum* for reproducible *in vitro* analysis should be determined. Furthermore, given the demonstrated cross-reactivity of epitope-specific polyclonal and monoclonal antibodies to *Leishmania*, protective effects of immunisation against other protozoan diseases could be explored.

This thesis demonstrated that antigen design is strengthened by understanding the immunogenic properties of individual residues in semi-synthetic glycoconjugates. This

understanding was achieved by profiling antibody responses against synthetic epitope fragments of a larger carbohydrate. This workflow, though effective, is not widely available to research laboratories. Although individual reports can be found, there is no widely accessible resource providing an overview of glycan residue immunogenicity. On the contrary for protein-related antigens, the Immune Epitope Database is an up-to-date resource that contains information on peptide antigens (Peters, Sidney et al. 2005) and includes tools to identify possible T cell and B cell epitopes to predict peptide antigen immunogenicity. A similar database for glycan antigens would be a logical next step to improve antigen design for carbohydrate vaccines.

Glycoconjugates that induce terminal-epitope GPI-specific antibodies, using vaccine formulations approved for human use, were successfully realised. A monoclonal antibody, specific to the terminal epitope (**7**) was also generated, and is successfully used as a positive GPI-binding control in other studies. The monoclonal antibody is also currently being explored as a potential diagnostic and therapeutic tool to combat malaria and other parasite related diseases. However, the definitive identity and epitope specificity of antibodies that protect against severe malaria remains ambiguous. This dissertation reports only limited success in the development of a vaccine against the neuropathology of the ECM mouse model using the chosen glycoconjugates. Different glycoconjugate formulations using the antigens could be investigated, if a modified T cell response away from the Th2 bias is required to be protective in ECM. Moreover, protective effects as a result of immunisation may be demonstrated in other models of severe malaria if a Th2 bias is needed. A better understanding of how free GPI affects ECM neuropathology could improve the use of the ECM model of malaria (Lepenies, Cramer et al. 2008). Potentially other severe malaria mouse models could be investigated, such as models of severe malarial anaemia, to check if our glycoconjugates protect against other manifestations of disease. Additionally, new animal models of severe malaria need to be developed in order to better represent the human condition (Craig, Grau et al. 2012). It is also worth investigating whether our current understanding of the role of GPI in severe malaria is complete, or if the GPI toxin hypothesis itself needs further development.

Bibliography

Adamo, R., M. R. Romano, F. Berti, R. Leuzzi, M. Tontini, E. Danieli, E. Cappelletti, O. S. Cakici, E. Swennen, V. Pinto, B. Brogioni, D. Proietti, C. L. Galeotti, L. Lay, M. A. Monteiro, M. Scarselli and P. Costantino (2012). "Phosphorylation of the Synthetic Hexasaccharide Repeating Unit Is Essential for the Induction of Antibodies to Clostridium difficile PSII Cell Wall Polysaccharide." Acs Chemical Biology **7**(8): 1420-1428.

Amante, F. H., A. C. Stanley, L. M. Randall, Y. H. Zhou, A. Haque, K. McSweeney, A. P. Waters, C. J. Janse, M. F. Good, G. R. Hill and C. R. Engwerda (2007). "A role for natural regulatory T cells in the pathogenesis of experimental cerebral malaria." American Journal of Pathology **171**(2): 548-559.

Antinori, S., L. Galimberti, L. Milazzo and M. Corbellino (2013). "Plasmodium knowlesi: The emerging zoonotic malaria parasite." Acta Tropica **125**(2): 191-201.

Astronomo, R. D. and D. R. Burton (2010). "Carbohydrate vaccines: developing sweet solutions to sticky situations?" Nat Rev Drug Discov **9**(4): 308-324.

Ayimba, E., J. Hegewald, A. Y. Segbena, R. G. Gantin, C. J. Lechner, A. Agosssou, M. Banla and P. T. Soboslay (2011). "Proinflammatory and regulatory cytokines and chemokines in infants with uncomplicated and severe Plasmodium falciparum malaria." Clinical and Experimental Immunology **166**(2): 218-226.

Banerjee, P., M. Wehle, R. Lipowsky and M. Santer (2018). "A molecular dynamics model for glycosylphosphatidyl-inositol anchors: "flop down" or "lollipop"?" Physical Chemistry Chemical Physics **20**(46): 29314-29324.

Berhe, S., L. Schofield, R. T. Schwarz and P. Gerold (1999). "Conservation of structure among glycosylphosphatidylinositol toxins from different geographic isolates of Plasmodium falciparum." Molecular and Biochemical Parasitology **103**(2): 273-278.

Billiau, A. and P. Matthys (2001). "Modes of action of Freund's adjuvants in experimental models of autoimmune diseases." Journal of Leukocyte Biology **70**(6): 849-860.

Bouchaud, O., M. Cot, S. Kony, R. Durand, R. Schiemann, P. Ralaimazava, J. P. Coulaud, J. Le Bras and P. Deloron (2005). "Do African immigrants living in France have long-term malarial immunity?" American Journal of Tropical Medicine and Hygiene **72**(1): 21-25.

Bouharountayoun, H., P. Attanath, A. Sabchareon, T. Chongsuphajaisiddhi and P. Druilhe (1990). "Antibodies That Protect Humans against Plasmodium-Falciparum Blood Stages Do Not on Their Own Inhibit Parasite Growth and Invasion Invitro, but Act in Cooperation with Monocytes." Journal of Experimental Medicine **172**(6): 1633-1641.

Bouharountayoun, H. and P. Druilhe (1992). "Plasmodium-Falciparum Malaria - Evidence for an Isotype Imbalance Which May Be Responsible for Delayed Acquisition of Protective Immunity." Infection and Immunity **60**(4): 1473-1481.

Boutlis, C. S., D. C. Gowda, R. S. Naik, G. P. Maguire, C. S. Mgone, M. J. Bockarie, M. Lagog, E. Ibam, K. Lorry and N. M. Anstey (2002). "Antibodies to Plasmodium falciparum glycosylphosphatidylinositols: inverse association with tolerance of parasitemia in Papua New Guinean children and adults." Infect Immun **70**(9): 5052-5057.

Broecker, F., J. Aretz, Y. Yang, J. Hanske, X. Q. Guo, A. Reinhardt, A. Wahlbrink, C. Rademacher, C. Anish and P. H. Seeberger (2014). "Epitope Recognition of Antibodies against a Yersinia pestis Lipopolysaccharide Trisaccharide Component." Acs Chemical Biology **9**(4): 867-873.

Broecker, F., J. Hanske, C. E. Martin, J. Y. Baek, A. Wahlbrink, F. Wojcik, L. Hartmann, C. Rademacher, C. Anish and P. H. Seeberger (2016). "Multivalent display of minimal Clostridium difficile glycan epitopes mimics antigenic properties of larger glycans." Nature Communications **7**.

Broecker, F., C. E. Martin, E. Wegner, J. Mattner, J. Y. Baek, C. L. Pereira, C. Anish and P. H. Seeberger (2016). "Synthetic Lipoteichoic Acid Glycans Are Potential Vaccine Candidates to Protect from Clostridium difficile Infections." Cell Chemical Biology **23**(8): 1014-1022.

Bunn, A., R. Escombe, M. Armstrong, C. J. M. Whitty and J. F. Doherty (2004). "Falciparum malaria in malaria-naive travellers and African visitors." Qjm-an International Journal of Medicine **97**(10): 645-649.

Caro, H. N., N. A. Sheikh, J. Taverne, J. H. L. Playfair and T. W. Rademacher (1996). "Structural similarities among malaria toxins, insulin second messengers, and bacterial endotoxin." Infection and Immunity **64**(8): 3438-3441.

Carter, R. and K. N. Mendis (2002). "Evolutionary and historical aspects of the burden of malaria." Clinical Microbiology Reviews **15**(4): 564-+.

Castelli, F., A. Matteelli, S. Caligaris, M. Gulletta, I. El-Hamad, C. Scolari, G. Chatel and G. Carosi (1999). "Malaria in migrants." Parassitologia, Vol 41, Nos 1-3, September 1999: 261-265.

Cavallari, M. and G. De Libero (2017). "From Immunologically Archaic to Neoteric Glycovaccines." Vaccines **5**(1): 4.

CDC (2019). Treatment of Malaria (Guidelines for Clinicians).

Charoenvit, Y., M. Sedegah, L. F. Yuan, M. Gross, C. Cole, R. Bechara, M. F. Leef, F. A. Robey, G. H. Lowell, R. L. Beaudoin and S. L. Hoffman (1990). "Active and Passive-Immunization against Plasmodium-Yoelii Sporozoites." Bulletin of the World Health Organization **68**: 26-32.

Cissoko, Y., M. Daou, K. E. Lyke, A. Dicko, I. Diarra, A. Kone, A. Guindo, K. Traore, G. Krishnegowda, D. A. Diallo, O. K. Doumbo, C. V. Plowe, C. Gowda and M. B. Sztein (2006). "Serum antibody levels to glycosylphosphatidylinositols in specimens derived from matched Malian children with severe or uncomplicated Plasmodium falciparum

malaria and healthy controls." American Journal of Tropical Medicine and Hygiene **75**(2): 199-204.

Clapp, T., P. Siebert, D. X. Chen and L. J. Braun (2011). "Vaccines with Aluminum-containing Adjuvants: Optimizing Vaccine Efficacy and Thermal Stability." Journal of Pharmaceutical Sciences **100**(2): 388-401.

Clark, I. A. and K. A. Rockett (1994). "The Cytokine Theory of Human Cerebral Malaria." Parasitology Today **10**(10): 410-412.

Clyde, D. F., V. C. Mccarthy, R. M. Miller and W. E. Woodward (1975). "Immunization of Man against Falciparum and Vivax Malaria by Use of Attenuated Sporozoites." American Journal of Tropical Medicine and Hygiene **24**(3): 397-401.

Cohen, S., S. Carrington and I. A. Mcgregor (1961). "Gamma-Globulin and Acquired Immunity to Human Malaria." Nature **192**(480): 733-&.

Collins, A. M. (2016). "IgG subclass co-expression brings harmony to the quartet model of murine IgG function." Immunology and Cell Biology **94**(10): 949-954.

Couper, K. N., T. Barnes, J. C. R. Hafalla, V. Combes, B. Ryffel, T. Secher, G. E. Grau, E. M. Riley and J. B. de Souza (2010). "Parasite-Derived Plasma Microparticles Contribute Significantly to Malaria Infection-Induced Inflammation through Potent Macrophage Stimulation." Plos Pathogens **6**(1).

Cowman, A. F., D. Berry and J. Baum (2012). "The cellular and molecular basis for malaria parasite invasion of the human red blood cell." Journal of Cell Biology **198**(6): 961-971.

Cowman, A. F. and B. S. Crabb (2006). "Invasion of red blood cells by malaria parasites." Cell **124**(4): 755-766.

Craig, A. G., G. E. Grau, C. Janse, J. W. Kazura, D. Milner, J. W. Barnwell, G. Turner, J. Langhorne and H. R. M. A. Model (2012). "The Role of Animal Models for Research on Severe Malaria." Plos Pathogens **8**(2).

Day, N. P., T. T. Hien, T. Schollaardt, P. P. Loc, L. V. Chuong, T. T. Chau, N. T. Mai, N. H. Phu, D. X. Sinh, N. J. White and M. Ho (1999). "The prognostic and pathophysiologic role of pro- and antiinflammatory cytokines in severe malaria." J Infect Dis **180**(4): 1288-1297.

Day, N. P. J., T. T. Hien, T. Schollaardt, P. P. Loc, L. Van Chuong, T. T. H. Chau, N. T. H. Mai, N. H. Phu, D. X. Sinh, N. J. White and M. Ho (1999). "The prognostic and pathophysiologic role of pro- and antiiflammatory cytokines in severe malaria." Journal of Infectious Diseases **180**(4): 1288-1297.

De Gregorio, E., E. Tritto and R. Rappuoli (2008). "Alum adjuvanticity: Unraveling a century old mystery." European Journal of Immunology **38**(8): 2068-2071.

de Souza, J. B. and E. M. Riley (2002). "Cerebral malaria: the contribution of studies in animal models to our understanding of immunopathogenesis." Microbes and Infection **4**(3): 291-300.

de Souza, J. B., M. Runglall, P. H. Corran, L. C. Okell, S. Kumar, D. C. Gowda, K. N. Couper and E. M. Riley (2010). "Neutralization of malaria glycosylphosphatidylinositol in vitro by serum IgG from malaria-exposed individuals." Infect Immun **78**(9): 3920-3929.

de Souza, J. B., J. Todd, G. Krishegowda, D. C. Gowda, D. Kwiatkowski and E. M. Riley (2002). "Prevalence and boosting of antibodies to Plasmodium falciparum glycosylphosphatidylinositols and evaluation of their association with protection from mild and severe clinical malaria." Infect Immun **70**(9): 5045-5051.

Delorenzi, M., A. Sexton, H. Shams-Eldin, R. T. Schwarz, T. Speed and L. Schofield (2002). "Genes for glycosylphosphatidylinositol toxin biosynthesis in Plasmodium falciparum." Infection and Immunity **70**(8): 4510-4522.

Diez-Silva, M., Y. Park, S. Huang, H. Bow, O. Mercereau-Puijalon, G. Deplaine, C. Lavazec, S. Perrot, S. Bonnefoy, M. S. Feld, J. Han, M. Dao and S. Suresh (2012). "Pf155/RESA protein influences the dynamic microcirculatory behavior of ring-stage Plasmodium falciparum infected red blood cells." Scientific Reports **2**.

Dondorp, A. M., S. J. Lee, M. A. Faiz, S. Mishra, R. Price, E. Tjitra, M. Than, Y. Htut, S. Mohanty, E. Bin Yunus, R. Rahman, F. Nosten, N. M. Anstey, N. P. J. Day and N. J. White (2008). "The relationship between age and the manifestations of and mortality associated with severe malaria." Clinical Infectious Diseases **47**(2): 151-157.

Doolan, D. L., C. Dobano and J. K. Baird (2009). "Acquired immunity to malaria." Clin Microbiol Rev **22**(1): 13-36, Table of Contents.

Douglas, A. D., G. C. Baldeviano, C. M. Lucas, L. A. Lugo-Roman, C. Crosnier, S. J. Bartholdson, A. Diouf, K. Miura, L. E. Lambert, J. A. Ventocilla, K. P. Leiva, K. H. Milne, J. J. Illingworth, A. J. Spencer, K. A. Hjerrild, D. G. W. Alanine, A. V. Turner, J. T. Moorhead, K. A. Edgel, Y. M. Wu, C. A. Long, G. J. Wright, A. G. Lescano and S. J. Draper (2015). "A PfRH5-Based Vaccine Is Efficacious against Heterologous Strain Blood-Stage Plasmodium falciparum Infection in Aotus Monkeys." Cell Host & Microbe **17**(1): 130-139.

Drew, D. R., D. W. Wilson, S. R. Elliott, N. Cross, U. Terheggen, A. N. Hodder, P. M. Siba, K. Chelimo, A. E. Dent, J. W. Kazura, I. Mueller and J. G. Beeson (2016). "A novel approach to identifying patterns of human invasion-inhibitory antibodies guides the design of malaria vaccines incorporating polymorphic antigens." Bmc Medicine **14**.

Dutta, S. and P. Sengupta (2016). "Men and mice: Relating their ages." Life Sciences **152**: 244-248.

Dvorak, J. A., L. H. Miller, W. C. Whitehouse and T. Shiroishi (1975). "Invasion of Erythrocytes by Malaria Merozoites." Science **187**(4178): 748-750.

Eisenhaber, B., P. Bork and F. Eisenhaber (2001). "Post-translational GPI lipid anchor modification of proteins in kingdoms of life: analysis of protein sequence data from complete genomes." Protein Engineering **14**(1): 17-25.

Esen, M., P. G. Kremsner, R. Schleucher, M. Gassler, E. B. Imoukhuede, N. Imbault, O. Leroy, S. Jepsen, B. W. Knudsen, M. Schumm, J. Knobloch, M. Theisen and B. Mordmuller (2009). "Safety and immunogenicity of GMZ2-a MSP3-GLURP fusion protein malaria vaccine candidate." Vaccine **27**(49): 6862-6868.

Farnert, A., K. Wyss, S. Dashti and P. Naucler (2015). "Duration of residency in a non-endemic area and risk of severe malaria in African immigrants." Clinical Microbiology and Infection **21**(5): 494-501.

Ferguson, M. A. J., S. W. Homans, R. A. Dwek and T. W. Rademacher (1988). "Glycosyl-Phosphatidylinositol Moiety That Anchors Trypanosoma-Brucei Variant Surface Glycoprotein to the Membrane." Science **239**(4841): 753-759.

French, D., E. Fischberg, S. Buhl and M. D. Scharff (1986). "The Production of More Useful Monoclonal-Antibodies .1. Modifications of the Basic Technology." Immunology Today **7**(11): 344-346.

Fried, M. and P. E. Duffy (1996). "Adherence of Plasmodium falciparum to chondroitin sulfate A in the human placenta." Science **272**(5267): 1502-1504.

Gazzinelli, R. T., P. Kalantari, K. A. Fitzgerald and D. T. Golenbock (2014). "Innate sensing of malaria parasites." Nature Reviews Immunology **14**(11): 744-757.

Geissner, A., C. Anish and P. H. Seeberger (2014). "Glycan arrays as tools for infectious disease research." Curr Opin Chem Biol **18**: 38-45.

Geissner, A., C. L. Pereira, M. Leddermann, C. Anish and P. H. Seeberger (2016). "Deciphering Antigenic Determinants of Streptococcus pneumoniae Serotype 4 Capsular Polysaccharide using Synthetic Oligosaccharides." Acs Chemical Biology **11**(2): 335-344.

Geissner, A., A. Reinhardt, C. Rademacher, T. Johannssen, J. Monteiro, B. Lepenies, M. Thepaut, F. Fieschi, J. Mrazkova, M. Wimmerova, F. Schuhmacher, S. Gotze, D. Grunstein, X. Q. Guo, H. S. Hahm, J. Kandasamy, D. Leonori, C. E. Martin, S. G. Parameswarappa, S. Pasari, M. K. Schlegel, H. Tanaka, G. Z. Xiao, Y. Yang, C. L. Pereira, C. Anish and P. H. Seeberger (2019). "Microbe-focused glycan array screening platform." Proceedings of the National Academy of Sciences of the United States of America **116**(6): 1958-1967.

Gerold, P., A. Dieckmann-Schuppert and R. T. Schwarz (1994). "Glycosylphosphatidylinositols synthesized by asexual erythrocytic stages of the malarial parasite, Plasmodium falciparum. Candidates for plasmodial glycosylphosphatidylinositol membrane anchor precursors and pathogenicity factors." J Biol Chem **269**(4): 2597-2606.

Gething, P. W., I. R. F. Elyazar, C. L. Moyes, D. L. Smith, K. E. Battle, C. A. Guerra, A. P. Patil, A. J. Tatem, R. E. Howes, M. F. Myers, D. B. George, P. Horby, H. F. L. Wertheim, R. N. Price, I. Mueller, K. Baird and S. I. Hay (2012). "A Long Neglected

World Malaria Map: Plasmodium vivax Endemicity in 2010." Plos Neglected Tropical Diseases **6**(9).

Gilson, P. R. and B. S. Crabb (2009). "Morphology and kinetics of the three distinct phases of red blood cell invasion by Plasmodium falciparum merozoites." International Journal for Parasitology **39**(1): 91-96.

Gilson, P. R., T. Nebl, D. Vukcevic, R. L. Moritz, T. Sargeant, T. P. Speed, L. Schofield and B. S. Crabb (2006). "Identification and stoichiometry of glycosylphosphatidylinositol-anchored membrane proteins of the human malaria parasite Plasmodium falciparum." Mol Cell Proteomics **5**(7): 1286-1299.

Gomes, L. R., P. R. Totino, M. C. Sanchez, E. P. Daniel, C. S. Macedo, F. Fortes, J. R. Coura, S. M. Santi, G. L. Werneck, M. C. Suarez-Mutis, F. Ferreira-da-Cruz Mde and C. T. Daniel-Ribeiro (2013). "Asymptomatic infection in individuals from the municipality of Barcelos (Brazilian Amazon) is not associated with the anti-Plasmodium falciparum glycosylphosphatidylinositol antibody response." Mem Inst Oswaldo Cruz **108**(6): 796-800.

Gosling, R. and L. von Seidlein (2016). "The Future of the RTS, S/AS01 Malaria Vaccine: An Alternative Development Plan." Plos Medicine **13**(4).

Götze, S., N. Azzouz, Y. H. Tsai, U. Gross, A. Reinhardt, C. Anish, P. H. Seeberger and D. Varon Silva (2014). "Diagnosis of toxoplasmosis using a synthetic glycosylphosphatidylinositol glycan." Angew Chem Int Ed Engl **53**(50): 13701-13705.

Götze, S., A. Reinhardt, A. Geissner, N. Azzouz, Y. H. Tsai, R. Kurucz, D. Varon Silva and P. H. Seeberger (2015). "Investigation of the protective properties of glycosylphosphatidylinositol-based vaccine candidates in a Toxoplasma gondii mouse challenge model." Glycobiology **25**(9): 984-991.

Gowda, D. C. (2002). "Structure and activity of glycosylphosphatidylinositol anchors of Plasmodium falciparum." Microbes and Infection **4**(9): 983-990.

Gowda, D. C. (2007). "TLR-mediated cell signaling by malaria GPIs." Trends Parasitol **23**(12): 596-604.

Gowda, D. C., P. Gupta and E. A. Davidson (1997). "Glycosylphosphatidylinositol anchors represent the major carbohydrate modification in proteins of intraerythrocytic stage Plasmodium falciparum." Journal of Biological Chemistry **272**(10): 6428-6439.

Grau, G. E., P. F. Piguet, P. Vassalli and P. H. Lambert (1989). "Tumor-Necrosis Factor and Other Cytokines in Cerebral Malaria - Experimental and Clinical-Data." Immunological Reviews **112**: 49-70.

Greenfield, E. A. (2018). "Polyethylene Glycol Fusion for Hybridoma Production." Cold Spring Harb Protoc **2018**(3): pdb prot103176.

Grun, J. L. and P. H. Maurer (1989). "Different T-Helper Cell Subsets Elicited in Mice Utilizing 2 Different Adjuvant Vehicles - the Role of Endogenous Interleukin-1 in Proliferative Responses." Cellular Immunology **121**(1): 134-145.

Guevara-Patino, J. A., A. A. Holder, J. S. McBride and M. J. Blackman (1997). "Antibodies that inhibit malaria merozoite surface protein-1 processing and erythrocyte invasion are blocked by naturally acquired human antibodies." Journal of Experimental Medicine **186**(10): 1689-1699.

Hecht, M. L., P. Stallforth, D. V. Silva, A. Adibekian and P. H. Seeberger (2009). "Recent advances in carbohydrate-based vaccines." Current Opinion in Chemical Biology **13**(3): 354-359.

Ho, M. M., B. Bolgiano and M. J. Corbel (2000). "Assessment of the stability and immunogenicity of meningococcal oligosaccharide C-CRM197 conjugate vaccines." Vaccine **19**(7-8): 716-725.

Hodder, A. N., P. E. Czabotar, A. D. Uboldi, O. B. Clarke, C. S. Lin, J. Healer, B. J. Smith and A. F. Cowman (2012). "Insights into Duffy Binding-like Domains through the Crystal Structure and Function of the Merozoite Surface Protein MSPDBL2 from Plasmodium falciparum." Journal of Biological Chemistry **287**(39): 32922-32939.

Hoffman, S. L., J. Vekemans, T. L. Richie and P. E. Duffy (2015). "The march toward malaria vaccines." Vaccine **33**: D13-D23.

Hommel, M. (1993). "Amplification of Cytoadherence in Cerebral Malaria - Towards a More Rational Explanation of Disease Pathophysiology." Annals of Tropical Medicine and Parasitology **87**(6): 627-635.

Hunt, N. H. and G. E. Grau (2003). "Cytokines: accelerators and brakes in the pathogenesis of cerebral malaria." Trends in Immunology **24**(9): 491-499.

Jakobsen, P. H., L. Baek and S. Jepsen (1988). "Demonstration of Soluble Plasmodium-Falciparum Antigens Reactive with Limulus Amebocyte Lysate and Polymyxin-B." Parasite Immunology **10**(6): 593-606.

Jaurigue, J. A. and P. H. Seeberger (2017). "Parasite Carbohydrate Vaccines." Frontiers in Cellular and Infection Microbiology **7**.

Jelinek, T., C. Schulte, R. Behrens, M. P. Grobusch, J. P. Coulaud, Z. Bisoffi, A. Matteelli, J. Clerinx, M. Corachan, S. Puente, I. Gjorup, G. Harms, H. Kollaritsch, A. Kotlowski, A. Bjorkmann, J. P. Delmont, J. Knobloch, L. N. Nielsen, J. Cuadros, C. Hatz, J. Beran, M. L. Schmid, M. Schulze, R. Lopez-Velez, K. Fleischer, A. Kapaun, P. McWhinney, P. Kern, J. Atougia, G. Fry, S. da Cunha, G. Boecken and E. N. S. Imp (2002). "Imported falciparum malaria in europe: Sentinel surveillance data from the European network on surveillance of imported infectious diseases." Clinical Infectious Diseases **34**(5): 572-576.

Jennings, R. M., J. B. De Souza, J. E. Todd, M. Armstrong, K. L. Flanagan, E. M. Riley and J. F. Doherty (2006). "Imported Plasmodium falciparum malaria: Are patients

originating from disease-endemic areas less likely to develop severe disease? A prospective, observational study." American Journal of Tropical Medicine and Hygiene **75**(6): 1195-1199.

John, C. C., A. J. Tande, A. M. Moormann, P. O. Sumba, D. E. Lanar, X. M. Min and J. W. Kazura (2008). "Antibodies to pre-erythrocytic Plasmodium falciparum antigens and risk of clinical malaria in Kenyan children." Journal of Infectious Diseases **197**(4): 519-526.

Kalantari, P., R. B. DeOliveira, J. Chan, Y. Corbett, V. Rathinam, A. Stutz, E. Latz, R. T. Gazzinelli, D. T. Golenbock and K. A. Fitzgerald (2014). "Dual Engagement of the NLRP3 and AIM2 Inflammasomes by Plasmodium-Derived Hemozoin and DNA during Malaria." Cell Reports **6**(1): 196-210.

Kamena, F., M. Tamborrini, X. Liu, Y. U. Kwon, F. Thompson, G. Pluschke and P. H. Seeberger (2008). "Synthetic GPI array to study antitoxic malaria response." Nat Chem Biol **4**(4): 238-240.

Kaneko, A., G. Taleo, M. Kalkoa, S. Yamar, T. Kobayakawa and A. Bjorkman (2000). "Malaria eradication on islands." Lancet **356**(9241): 1560-1564.

Keenihan, S. N. H., S. Ratiwayanto, S. Soebianto, Krisin, H. Marwoto, G. Krishnegowda, D. C. Gowda, M. J. Bangs, D. J. Fryauff, T. L. Richie, S. Kumar and J. K. Baird (2003). "Age-dependent impairment of IgG responses to glycosylphosphatidylinositol with equal exposure to Plasmodium falciparum among Javanese migrants to Papua, Indonesia." American Journal of Tropical Medicine and Hygiene **69**(1): 36-41.

Kohler, G. and C. Milstein (1975). "Continuous Cultures of Fused Cells Secreting Antibody of Predefined Specificity." Nature **256**(5517): 495-497.

Krishnegowda, G., A. M. Hajjar, J. Zhu, E. J. Douglass, S. Uematsu, S. Akira, A. S. Woods and D. C. Gowda (2005). "Induction of proinflammatory responses in macrophages by the glycosylphosphatidylinositols of Plasmodium falciparum: cell signaling receptors, glycosylphosphatidylinositol (GPI) structural requirement, and regulation of GPI activity." J Biol Chem **280**(9): 8606-8616.

Laemmli, U. K. (1970). "Cleavage of Structural Proteins during Assembly of Head of Bacteriophage-T4." Nature **227**(5259): 680-+.

Lamb, T. J. and J. Langhorne (2008). "The severity of malarial anaemia in Plasmodium chabaudi infections of BALB/c mice is determined independently of the number of circulating parasites." Malaria Journal **7**.

Lepenies, B., J. P. Cramer, G. D. Burchard, H. Wagner, C. J. Kirschning and T. Jacobs (2008). "Induction of experimental cerebral malaria is independent of TLR2/4/9." Medical Microbiology and Immunology **197**(1): 39-44.

Lepenies, B. and P. H. Seeberger (2010). "The promise of glycomics, glycan arrays and carbohydrate-based vaccines." Immunopharmacology and Immunotoxicology **32**(2): 196-207.

Maier, A. G., M. Rug, M. T. O'Neill, M. Brown, S. Chakravorty, T. Szestak, J. Chesson, Y. Wu, K. Hughes, R. L. Coppel, C. Newbold, J. G. Beeson, A. Craig, B. S. Crabb and A. F. Cowman (2008). "Exported proteins required for virulence and rigidity of Plasmodium falciparum-infected human erythrocytes." Cell **134**(1): 48-61.

Marrack, P., A. S. Mckee and M. W. Munks (2009). "Towards an understanding of the adjuvant action of aluminium." Nature Reviews Immunology **9**(4): 287-293.

Martin, C. E., F. Broecker, M. A. Oberli, J. Komor, J. Mattner, C. Anish and P. H. Seeberger (2013). "Immunological Evaluation of a Synthetic Clostridium difficile Oligosaccharide Conjugate Vaccine Candidate and Identification of a Minimal Epitope." Journal of the American Chemical Society **135**(26): 9713-9722.

Mbengue, B., B. Niang, M. S. Niang, M. L. Varela, B. Fall, M. M. Fall, R. N. Diallo, B. Diatta, D. C. Gowda, A. Dieye and R. Perraut (2016). "Inflammatory cytokine and humoral responses toPlasmodium falciparumglycosylphosphatidylinositols correlates with malaria immunity and pathogenesis." Immunity, Inflammation and Disease **4**(1): 24-34.

Mejia, P., M. Diez-Silva, F. Kamena, F. Lu, S. M. Fernandes, P. H. Seeberger, A. E. Davis, 3rd and J. R. Mitchell (2016). "Human C1-Inhibitor Suppresses Malaria Parasite Invasion and Cytoadhesion via Binding to Parasite Glycosylphosphatidylinositol and Host Cell Receptors." J Infect Dis **213**(1): 80-89.

Mendis, K., B. J. Sina, P. Marchesini and R. Carter (2001). "The neglected burden of Plasmodium vivax malaria." American Journal of Tropical Medicine and Hygiene **64**(1-2): 97-106.

Miller, L. H., D. I. Baruch, K. Marsh and O. K. Doumbo (2002). "The pathogenic basis of malaria." Nature **415**(6872): 673-679.

Molyneux, M. E., T. E. Taylor, J. J. Wirima and G. E. Grau (1991). "Tumor-Necrosis-Factor, Interleukin-6, and Malaria." Lancet **337**(8749): 1098-1098.

Murray, C. J. L., L. C. Rosenfeld, S. S. Lim, K. G. Andrews, K. J. Foreman, D. Haring, N. Fullman, M. Naghavi, R. Lozano and A. D. Lopez (2012). "Global malaria mortality between 1980 and 2010: a systematic analysis." Lancet **379**(9814): 413-431.

Naik, R. S., O. H. Branch, A. S. Woods, M. Vijaykumar, D. J. Perkins, B. L. Nahlen, A. A. Lal, R. J. Cotter, C. E. Costello, C. F. Ockenhouse, E. A. Davidson and D. C. Gowda (2000). "Glycosylphosphatidylinositol anchors of Plasmodium falciparum: molecular characterization and naturally elicited antibody response that may provide immunity to malaria pathogenesis." J Exp Med **192**(11): 1563-1576.

Naik, R. S., G. Krishnegowda, C. F. Ockenhouse and D. C. Gowda (2006). "Naturally Elicited Antibodies to Glycosylphosphatidylinositols (GPIs) of Plasmodium falciparum Require Intact GPI Structures for Binding and Are Directed Primarily against the Conserved Glycan Moiety." Infection and Immunity **74**(2): 1412-1415.

Neafsey, D. E., M. Juraska, T. Bedford, D. Benkeser, C. Valim, A. Griggs, M. Lievens, S. Abdulla, S. Adjei, T. Agbenyega, S. T. Agnandji, P. Aide, S. Anderson, D. Ansong, J. J.

Aponte, K. P. Asante, P. Bejon, A. J. Birkett, M. Bruls, K. M. Connolly, U. D'Alessandro, C. Dobano, S. Gesase, B. Greenwood, J. Grimsby, H. Tinto, M. J. Hamel, I. Hoffman, P. Kamthunzi, S. Kariuki, P. G. Kremsner, A. Leach, B. Lell, N. J. Lennon, J. Lusingu, K. Marsh, F. Martinson, J. T. Molel, E. L. Moss, P. Njuguna, C. F. Ockenhouse, B. R. Ogutu, W. Otieno, L. Otieno, K. Otieno, S. Owusu-Agyei, D. J. Park, K. Pelle, D. Robbins, C. Russ, E. M. Ryan, J. Sacarlal, B. Sogoloff, H. Sorgho, M. Tanner, T. Theander, I. Valea, S. K. Volkman, Q. Yu, D. Lapierre, B. W. Birren, P. B. Gilbert and D. F. Wirth (2015). "Genetic Diversity and Protective Efficacy of the RTS, S/AS01 Malaria Vaccine." New England Journal of Medicine **373**(21): 2025-2037.

Newby, G., J. Hwang, K. Koita, I. Chen, B. Greenwood, L. von Seidlein, G. D. Shanks, L. M. Slutsker, S. P. Kachur, J. Wegbreit, M. M. Ippolito, E. Poirot and R. Gosling (2015). "Review of Mass Drug Administration for Malaria and Its Operational Challenges." American Journal of Tropical Medicine and Hygiene **93**(1): 125-134.

Nyame, A. K., Z. S. Kawar and R. D. Cummings (2004). "Antigenic glycans in parasitic infections: implications for vaccines and diagnostics." Archives of Biochemistry and Biophysics **426**(2): 182-200.

O'Hagan, D. T. (2007). "MF59 is a safe and potent vaccine adjuvant that enhances protection against influenza virus infection." Expert Review of Vaccines **6**(5): 699-710.

Oberli, M. A., M. Tamborrini, Y. H. Tsai, D. B. Werz, T. Horlacher, A. Adibekian, D. Gauss, H. M. Moller, G. Pluschke and P. H. Seeberger (2010). "Molecular Analysis of Carbohydrate-Antibody Interactions: Case Study Using a Bacillus anthracis Tetrasaccharide." Journal of the American Chemical Society **132**(30): 10239-10241.

Okitsu, S. L., O. Silvie, N. Westerfeld, M. Curcic, A. R. Kammer, M. S. Mueller, R. W. Sauerwein, J. A. Robinson, B. Genton, D. Mazier, R. Zurbriggen and G. Pluschke (2007). "A Virosomal Malaria Peptide Vaccine Elicits a Long-Lasting Sporozoite-Inhibitory Antibody Response in a Phase 1a Clinical Trial." Plos One **2**(12).

Orengo, J. M., A. Leliwa-Sytek, J. E. Evans, B. Evans, D. van de Hoef, M. Nyako, K. Day and A. Rodriguez (2009). "Uric Acid Is a Mediator of the Plasmodium falciparum-Induced Inflammatory Response." Plos One **4**(4).

Panda, A. K., B. K. Das, A. Panda, R. Tripathy, S. S. Pattnaik, H. Mahto, S. Pied, S. Pathak, S. Sharma and B. Ravindran (2016). "Heterozygous mutants of TIRAP (S180L) polymorphism protect adult patients with Plasmodium falciparum infection against severe disease and mortality." Infection, Genetics and Evolution.

Patel, S. N., Z. Lu, K. Ayi, L. Serghides, D. C. Gowda and K. C. Kain (2007). "Disruption of CD36 Impairs Cytokine Response to Plasmodium falciparum Glycosylphosphatidylinositol and Confers Susceptibility to Severe and Fatal Malaria In Vivo." The Journal of Immunology **178**(6): 3954-3961.

Perraut, R., B. Diatta, L. Marrama, O. Garraud, R. Jambou, S. Longacre, G. Krishnegowda, A. Dieye and D. C. Gowda (2005). "Differential antibody responses to

Plasmodium falciparum glycosylphosphatidylinositol anchors in patients with cerebral and mild malaria." Microbes and Infection **7**(4): 682-687.

Persson, K. E. M., F. J. McCallum, L. Reiling, N. A. Lister, J. Stubbs, A. F. Cowman, K. Marsh and J. G. Beeson (2008). "Variation in use of erythrocyte invasion pathways by Plasmodium falciparum mediates evasion of human inhibitory antibodies." Journal of Clinical Investigation **118**(1): 342-351.

Peters, B., J. Sidney, P. Bourne, H. H. Bui, S. Buus, G. Doh, W. Fleri, M. Kronenberg, R. Kubo, O. Lund, D. Nemazee, J. V. Ponomarenko, M. Sathiamurthy, S. Schoenberger, S. Stewart, P. Surko, S. Way, S. Wilson and A. Sette (2005). "The immune epitope database and analysis resource: From vision to blueprint." Plos Biology **3**(3): 379-381.

Phillips, A., P. Bassett, S. Zeki, S. Newman and G. Pasvol (2009). "Risk Factors for Severe Disease in Adults with Falciparum Malaria." Clinical Infectious Diseases **48**(7): 871-878.

Pinder, M., V. S. Moorthy, B. D. Akanmori, B. Genton and G. V. Brown (2010). "MALVAC 2009: Progress and Challenges in Development of Whole Organism Malaria Vaccines for Endemic Countries, 3-4 June 2009, Dakar, Senegal." Vaccine **28**(30): 4695-4702.

Pistone, T., A. Diallo, M. Mechain, M. C. Receveur and D. Malvy (2014). "Epidemiology of imported malaria give support to the hypothesis of 'long-term' semi-immunity to malaria in sub-Saharan African migrants living in France." Travel Medicine and Infectious Disease **12**(1): 48-53.

Playfair, J. H. L., J. Taverne, C. A. W. Bate and J. Brian de Souza (1990). "The malaria vaccine: anti-parasite or anti-disease?" Immunology Today **11**: 25-27.

Plebanski, M., E. A. M. Lee, C. M. Hannan, K. L. Flanagan, S. C. Gilbert, M. B. Gravenor and A. V. S. Hill (1999). "Altered peptide ligands narrow the repertoire of cellular immune responses by interfering with T-cell priming." Nature Medicine **5**(5): 565-571.

Pongponratn, E., G. D. H. Turner, N. P. J. Day, N. H. Phu, J. A. Simpson, K. Stepniewska, N. T. H. Mai, P. Viriyavejakul, S. Looareesuwan, T. T. Hien, D. J. P. Ferguson and N. J. White (2003). "An ultrastructural study of the brain in fatal Plasmodium falciparum malaria." American Journal of Tropical Medicine and Hygiene **69**(4): 345-359.

Radfar, A., D. Mendez, C. Moneriz, M. Linares, P. Marin-Garcia, A. Puyet, A. Diez and J. M. Bautista (2009). "Synchronous culture of Plasmodium falciparum at high parasitemia levels." Nat Protoc **4**(12): 1899-1915.

Remarque, E. J., B. W. Faber, C. H. M. Kocken and A. W. Thomas (2008). "Apical membrane antigen 1: a malaria vaccine candidate in review." Trends in Parasitology **24**(2): 74-84.

Renar, K. S., J. Iskra and I. Krizaj (2016). "Understanding malarial toxins." Toxicon **119**: 319-329.

Renia, L. and Y. S. Goh (2016). "Malaria Parasites: The Great Escape." Frontiers in Immunology **7**.

Riglar, D. T., D. Richard, D. W. Wilson, M. J. Boyle, C. Dekiwadia, L. Turnbull, F. Angrisano, D. S. Marapana, K. L. Rogers, C. B. Whitchurch, J. G. Beeson, A. F. Cowman, S. A. Ralph and J. Baum (2011). "Super-Resolution Dissection of Coordinated Events during Malaria Parasite Invasion of the Human Erythrocyte." Cell Host & Microbe **9**(1): 9-20.

Roberts, D. J., A. G. Craig, A. R. Berendt, R. Pinches, G. Nash, K. Marsh and C. I. Newbold (1992). "Rapid Switching to Multiple Antigenic and Adhesive Phenotypes in Malaria." Nature **357**(6380): 689-692.

Rostamian, M., S. Sohrabi, H. Kavosifard and H. M. Niknam (2017). "Lower levels of IgG1 in comparison with IgG2a are associated with protective immunity against Leishmania tropica infection in BALB/c mice." Journal of Microbiology Immunology and Infection **50**(2): 160-166.

Sarthou, J. L., G. Angel, G. Aribot, C. Rogier, A. Dieye, A. T. Balde, B. Diatta, P. Seignot and C. Roussilhon (1997). "Prognostic value of anti-Plasmodium falciparum specific immunoglobulin G3, cytokines, and their soluble receptors in West African patients with severe malaria." Infection and Immunity **65**(8): 3271-3276.

Schofield, L. (2007). "Rational approaches to developing an anti-disease vaccine against malaria." Microbes and Infection **9**(6): 784-791.

Schofield, L. and G. E. Grau (2005). "Immunological processes in malaria pathogenesis." Nature Reviews Immunology **5**(9): 722-735.

Schofield, L. and F. Hackett (1993). "Signal transduction in host cells by a glycosylphosphatidylinositol toxin of malaria parasites." J Exp Med **177**(1): 145-153.

Schofield, L., M. C. Hewitt, K. Evans, M. A. Siomos and P. H. Seeberger (2002). "Synthetic GPI as a candidate anti-toxic vaccine in a model of malaria." Nature **418**(6899): 785-789.

Schofield, L., S. Novakovic, P. Gerold, R. T. Schwarz, M. J. McConville and S. D. Tachado (1996). "Glycosylphosphatidylinositol toxin of Plasmodium up-regulates intercellular adhesion molecule-1, vascular cell adhesion molecule-1, and E-selectin expression in vascular endothelial cells and increases leukocyte and parasite cytoadherence via tyrosine kinase-dependent signal transduction." Journal of Immunology **156**(5): 1886-1896.

Schofield, L., L. Vivas, F. Hackett, P. Gerold, R. T. Schwarz and S. Tachado (1993). "Neutralizing monoclonal antibodies to glycosylphosphatidylinositol, the dominant TNF-alpha-inducing toxin of Plasmodium falciparum: prospects for the immunotherapy of severe malaria." Ann Trop Med Parasitol **87**(6): 617-626.

Schumann, B., H. S. Hahm, S. G. Parameswarappa, K. Reppe, A. Wahlbrink, S. Govindan, P. Kaplonek, L. A. Pirofski, M. Witzenrath, C. Anish, C. L. Pereira and P. H.

Seeberger (2017). "A semisynthetic Streptococcus pneumoniae serotype 8 glycoconjugate vaccine." Science Translational Medicine **9**(380).

Sedegah, M., C. Tamminga, S. McGrath, B. House, H. Ganeshan, J. Lejano, E. Abot, G. J. Banania, R. Sayo, F. Farooq, M. Belmonte, N. Manohar, N. O. Richie, C. Wood, C. A. Long, D. Regis, F. T. Williams, M. Shi, I. Chuang, M. Spring, J. E. Epstein, J. Mendoza-Silveiras, K. Limbach, N. B. Patterson, J. T. Bruder, D. L. Doolan, C. R. King, L. Soisson, C. Diggs, D. Carucci, S. Dutta, M. R. Hollingdale, C. F. Ockenhouse and T. L. Richie (2011). "Adenovirus 5-Vectored P. falciparum Vaccine Expressing CSP and AMA1. Part A: Safety and Immunogenicity in Seronegative Adults." Plos One **6**(10).

Seder, R. A., L. J. Chang, M. E. Enama, K. L. Zephir, U. N. Sarwar, I. J. Gordon, L. A. Holman, E. R. James, P. F. Billingsley, A. Gunasekera, A. Richman, S. Chakravarty, A. Manoj, S. Velmurugan, M. L. Li, A. J. Ruben, T. Li, A. G. Eappen, R. E. Stafford, S. H. Plummer, C. S. Hendel, L. Novik, P. J. M. Costner, F. H. Mendoza, J. G. Saunders, M. C. Nason, J. H. Richardson, J. Murphy, S. A. Davidson, T. L. Richie, M. Sedegah, A. Sutamihardja, G. A. Fahle, K. E. Lyke, M. B. Laurens, M. Roederer, K. Tewari, J. E. Epstein, B. K. L. Sim, J. E. Ledgerwood, B. S. Graham, S. L. Hoffman and V. S. Team (2013). "Protection Against Malaria by Intravenous Immunization with a Nonreplicating Sporozoite Vaccine." Science **341**(6152): 1359-1365.

Seeberger, P. H. and D. B. Werz (2007). "Synthesis and medical applications of oligosaccharides." Nature **446**(7139): 1046-1051.

Simon, N., E. Lasonder, M. Scheuermayer, A. Kuehn, S. Tews, R. Fischer, P. F. Zipfel, C. Skerka and G. Pradel (2013). "Malaria Parasites Co-opt Human Factor H to Prevent Complement-Mediated Lysis in the Mosquito Midgut." Cell Host & Microbe **13**(1): 29-41.

Snow, R. W., J. A. Omumbo, B. Lowe, C. S. Molyneux, J. O. Obiero, A. Palmer, M. W. Weber, M. Pinder, B. Nahlen, C. Obonyo, C. Newbold, S. Gupta and K. Marsh (1997). "Relation between severe malaria morbidity in children and level of Plasmodium falciparum transmission in Africa." Lancet **349**(9066): 1650-1654.

Sturm, A., R. Amino, C. van de Sand, T. Regen, S. Retzlaff, A. Rennenberg, A. Krueger, J. M. Pollok, R. Menard and V. T. Heussler (2006). "Manipulation of host hepatocytes by the malaria parasite for delivery into liver sinusoids." Science **313**(5791): 1287-1290.

Tachado, S. D., P. Gerold, M. J. McConville, T. Baldwin, D. Quilici, R. T. Schwarz and L. Schofield (1996). "Glycosylphosphatidylinositol toxin of Plasmodium induces nitric oxide synthase expression in macrophages and vascular endothelial cells by a protein tyrosine kinase-dependent and protein kinase C-dependent signaling pathway." Journal of Immunology **156**(5): 1897-1907.

Tachado, S. D., P. Gerold, R. Schwarz, S. Novakovic, M. McConville and L. Schofield (1997). "Signal transduction in macrophages by glycosylphosphatidylinositols of Plasmodium, Trypanosoma, and Leishmania: Activation of protein tyrosine kinases and protein kinase C by inositolglycan and diacylglycerol moieties." Proceedings of the National Academy of Sciences of the United States of America **94**(8): 4022-4027.

Tamborrini, M. (2009). Use of Synthetic Carbohydrates as Vaccine Components and Biomedical Research Tools.

Tamborrini, M., X. Liu, J. P. Mugasa, Y. U. Kwon, F. Kamena, P. H. Seeberger and G. Pluschke (2010). "Synthetic glycosylphosphatidylinositol microarray reveals differential antibody levels and fine specificities in children with mild and severe malaria." Bioorg Med Chem **18**(11): 3747-3752.

Teo, A., G. Feng, G. V. Brown, J. G. Beeson and S. J. Rogerson (2016). "Functional Antibodies and Protection against Blood-stage Malaria."

Thompson, F. M., D. W. Porter, S. L. Okitsu, N. Westerfeld, D. Vogel, S. Todryk, I. Poulton, S. Correa, C. Hutchings, T. Berthoud, S. Dunachie, L. Andrews, J. L. Williams, R. Sinden, S. C. Gilbert, G. Pluschke, R. Zurbriggen and A. V. S. Hill (2008). "Evidence of Blood Stage Efficacy with a Virosomal Malaria Vaccine in a Phase IIa Clinical Trial." Plos One **3**(1).

Tinto, H., U. D'Alessandro, H. Sorgho, I. Valea, M. C. Tahita, W. Kabore, F. Kiemde, P. Lompo, S. Ouedraogo, K. Derra, F. Ouedraogo, J. B. Ouedraogo, W. R. Ballou, J. Cohen, Y. Guerra, D. Heerwegh, E. Jongert, D. Lapierre, A. Leach, M. Lievens, O. Ofori-Anyinam, A. Olivier, J. Vekemans, S. T. Agnandji, B. Lell, J. F. Fernandes, B. P. Abossolo, A. L. Kabwende, A. A. Adegnika, B. Mordmuller, S. Issifou, P. G. Kremsner, M. M. Loembe, E. Bache, A. Alabi, S. Owusu-Agyei, K. P. Asante, O. Boahen, D. Dosoo, I. Asante, Z. Yidana, J. Anim, E. Adeniji, A. K. Yawson, K. Kayan, D. Chandramohan, B. Greenwood, D. Ansong, T. Agbenyega, S. Adjei, H. O. Boateng, T. Rettig, J. Sylverken, D. Sambian, A. Badu-Prepah, A. Kotey, P. Buabeng, V. Paintsil, A. Enimil, M. J. Hamel, S. Kariuki, M. Oneko, C. Odero, K. Otieno, N. Awino, V. Muturi-Kioi, J. Omoto, T. Sang, S. Odhiambo, K. F. Laserson, L. Slutsker, W. Otieno, L. Otieno, N. Otsyula, S. Gondi, J. Ochola, G. Okoth, D. C. Mabunde, A. Wangwe, A. Otieno, J. Oyieko, J. Cowden, B. Ogutu, P. Njuguna, K. Marsh, P. Akoo, C. Kerubo, C. Maingi, P. Bejon, A. Olotu, R. Chilengi, B. Tsofa, T. Lang, J. Gitaka, K. Awuondo, F. Martinson, I. Hoffman, T. Mvalo, P. Kamthunzi, R. Nkomo, T. Tembo, G. Tegha, C. Chawinga, T. Banda, S. Khan, S. Mwambakulu, E. Mzembe, J. Sacarlal, P. Aide, L. Madrid, S. Mandjate, J. J. Aponte, H. Bulo, S. Massora, E. Varela, E. Macete, P. Alonso, J. Lusingu, S. Gesase, A. Malabeja, O. Abdul, C. Mahende, E. Liheluka, M. Lemnge, T. G. Theander, C. Drakeley, J. Mbwana, R. Olomi, B. Mmbando, S. Abdulla, N. Salim, A. Mtoro, S. Ahmed, A. Hamad, S. Kafuruki, R. Minja, M. Tanner, M. Maganga, A. Mdemu, C. Gwandu, A. Mohammed, D. Kaslow, D. Leboulleux, B. Savarese, D. Schellenberg and R. S. C. T. Partnership (2015). "Efficacy and safety of RTS,S/AS01 malaria vaccine with or without a booster dose in infants and children in Africa: final results of a phase 3, individually randomised, controlled trial." Lancet **386**(9988): 31-45.

Torre, D., F. Speranza and R. Martegani (2002). "Role of proinflammatory and anti-inflammatory cytokines in the immune response to Plasmodium falciparum malaria." Lancet Infectious Diseases **2**(12): 719-720.

Tsai, Y. H., S. Götze, I. Vilotijevic, M. Grube, D. V. Silva and P. H. Seeberger (2013). "A general and convergent synthesis of diverse glycosylphosphatidylinositol glycolipids." Chemical Science **4**(1): 468-481.

Tsai, Y. H., X. Y. Liu and P. H. Seeberger (2012). "Chemical Biology of Glycosylphosphatidylinositol Anchors." Angewandte Chemie-International Edition **51**(46): 11438-11456.

Vidarsson, G., G. Dekkers and T. Rispens (2014). "IgG subclasses and allotypes: from structure to effector functions." Frontiers in Immunology **5**.

Vijaykumar, M., R. S. Naik and D. C. Gowda (2001). "Plasmodium falciparum glycosylphosphatidylinositol-induced TNF-alpha secretion by macrophages is mediated without membrane insertion or endocytosis." Journal of Biological Chemistry **276**(10): 6909-6912.

von Seidlein, L. and A. Dondorp (2015). "Fighting fire with fire: mass antimalarial drug administrations in an era of antimalarial resistance." Expert Review of Anti-Infective Therapy **13**(6): 715-730.

von Seidlein, L. and B. M. Greenwood (2003). "Mass administrations of antimalarial drugs." Trends in Parasitology **19**(10): 452-460.

White, N. J. (2011). "Determinants of relapse periodicity in Plasmodium vivax malaria." Malaria Journal **10**.

White, N. J., S. Pukrittayakamee, T. T. Hien, M. A. Faiz, O. A. Mokuolu and A. M. Dondorp (2014). "Malaria." Lancet **383**(9918): 723-735.

WHO (2013). World Malaria Report 2013. World Malaria Report 2013**:** 1-255.

WHO (2014). World Malaria Report 2014.

WHO (2015). Guidelines for the Treatment of Malaria.

WHO (2016). Malaria Vaccine: WHO position paper - January 2016.

WHO (2018). Artemisinin resistance and artemisinin-based combination therapy efficacy

WHO (2018). World malaria report 2018.

Wu, X. Z., N. M. Gowda, S. Kumar and D. C. Gowda (2010). "Protein-DNA Complex Is the Exclusive Malaria Parasite Component That Activates Dendritic Cells and Triggers Innate Immune Responses." Journal of Immunology **184**(8): 4338-4348.

Zhu, J. Z., G. Krishnegowda and D. C. Gowda (2005). "Induction of proinflammatory responses in macrophages by the Glycosylphosphatidylinositols of Plasmodium falciparum - The requirement of extracellular signal-regulated kinase, p38, c-Jun N-terminal kinase and NF-kappa B pathways for the expression of proinflammatory cytokines and nitric oxide." Journal of Biological Chemistry **280**(9): 8617-8627.

Publications

Scientific articles

Jaurigue JA, Seeberger PH. Parasite Carbohydrate Vaccines. *Frontiers in Cellular and Infection Microbiology*. 2017;7:248. doi:10.3389/fcimb.2017.00248.

Jaurigue JA, Malik A, Steinbeis F, Lepenies B, Varón Silva D, Seeberger PH. Designed synthetic antigens induce antibody responses to the non-reducing terminus of P. falciparum GPI. *Manuscript in preparation.*

Conferences

28th Annual Meeting of the German Society for Parasitology (**Oral presentation**)

Development of an anti-toxin vaccine against *P. falciparum* malaria

March 2018, Berlin, Germany

Ringberg Conference (**Oral presentation**)

Development of an anti-toxin vaccine against *P. falciparum* malaria

September 2017, Bavarian Alps, Germany

21th Annual Woods Hole Immunoparasitology Meeting (**Poster**)

Synthetic anti-toxin vaccines against *P. falciparum*

April 2017, Massachusetts, USA

RIKEN IMS Summer Program (**Oral presentation and poster**)

P. falciparum glycans in adaptive immune recognition and their vaccine potential

June 2016, Kyoto, Japan

27th Annual Meeting of the German Society for Parasitology (**Poster**)

P. falciparum glycans in adaptive immune recognition and their vaccine potential

March 2016, Göttingen, Germany

Ringberg Conference (**Oral presentation**)

Principles of glycan arrays

September 2015, Bavarian Alps, Germany

Research Training Group presentations

ZIBI Graduate School Retreat (**Oral presentation**)

Development of an anti-toxin vaccine against P. falciparum malaria

April 2018, Berlin.

ZIBI Graduate School Students' Day (**Oral presentation**)

Development of an anti-toxin vaccine against P. falciparum malaria

January 2018, Berlin.

GRK2046 retreat (**Oral presentation**)

Development of an anti-toxin vaccine against P. falciparum malaria

September 2017, Berlin.

ZIBI Graduate School Retreat (**Poster**)

P. falciparum glycans in adaptive immune recognition and their vaccine potential

March 2017, Berlin.

GRK2046 retreat (**Oral presentation**)

P. falciparum glycans in adaptive immune recognition and their vaccine potential

September 2016, Berlin.

ZIBI Graduate School Retreat (**Poster**)

P. falciparum glycans in adaptive immune recognition and their vaccine potential

March 2016, Berlin.

ZIBI Graduate School Students' Day (**Oral presentation**)

P. falciparum glycans in adaptive immune recognition and their vaccine potential

February 2016, Berlin

GRK2046 retreat (**Oral presentation**)

P. falciparum glycans in adaptive immune recognition and their vaccine potential

November 2015, Berlin.

Appendix

Minimal dosing test for glycoconjugates of 2 and 5

Glycoconjugates of **2** and **5**, previously produced in our lab, were used to immunise mice at the 0.4 µg dose. C57BL/6 mice were subcutaneously injected in a prime-boost-boost regime at two week intervals. Groups of mice (n=4) were characterised by the glycoconjugate used. Sera (diluted 1:50) at day 35 post-prime immunisation were screened on the synthetic GPI microarray. Epitope-specific antibody titres were detected after immunisation.

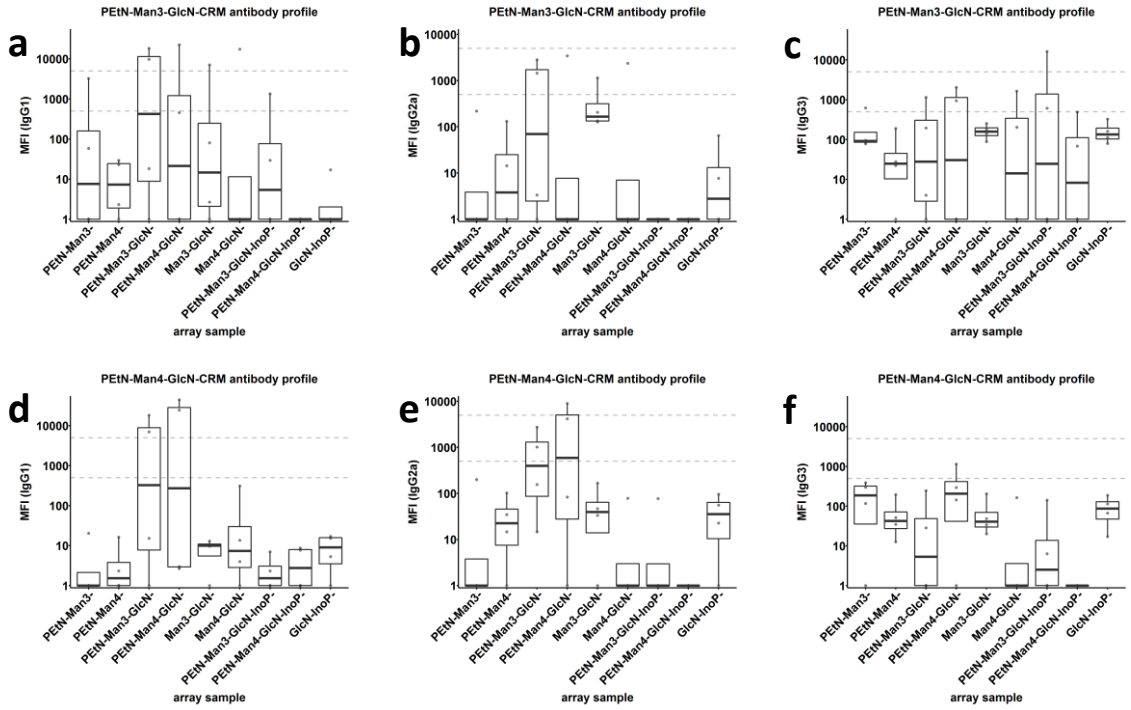

Figure 68: Antibody titres against synthetic GPI fragments in sera at day 35. Group size n=4. **Top panel (a-c)** IgG isotype titres of mice immunised with glycoconjugate of **2**. **Bottom panel (d-f)** IgG isotype titres of mice immunised with glycoconjugate of **5**.

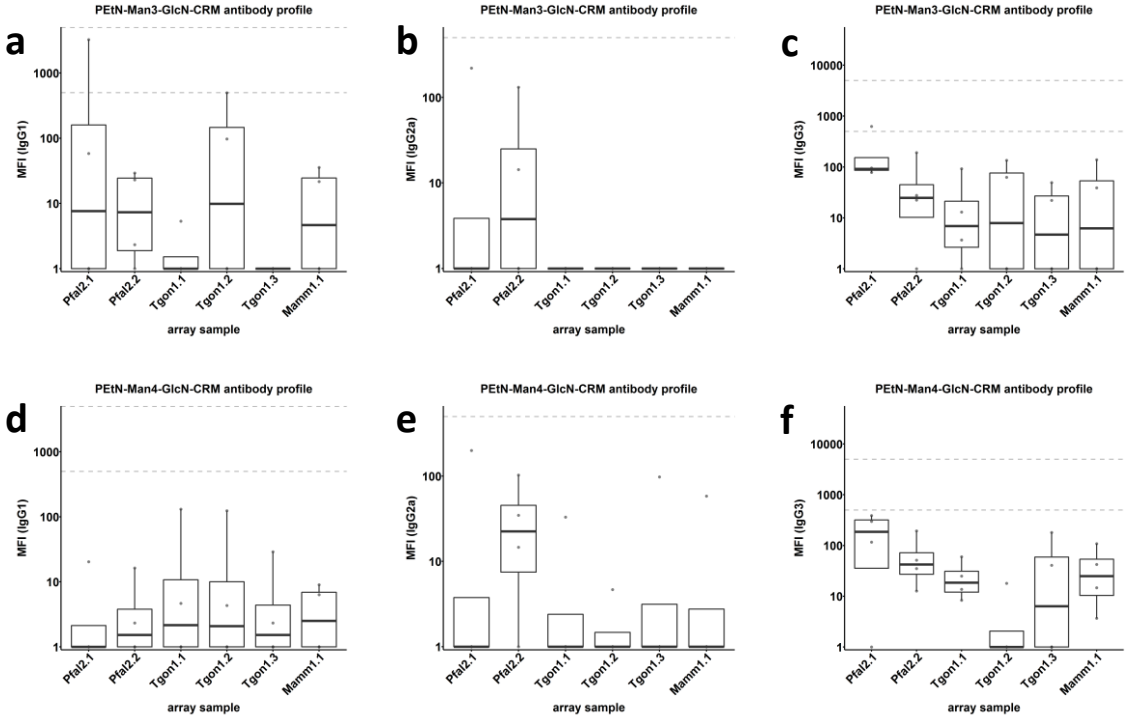

Figure 69: Antibody titres against synthetic GPI fragments in other organisms in sera at day 35. Group size n=4. **Top panel (a-c)** IgG isotype titres of mice immunised with glycoconjugate of **2**. **Bottom panel (d-f)** IgG isotype titres of mice immunised with glycoconjugate of **5**.

MALDI-TOF spectra for glycoconjugates of 7 and 8

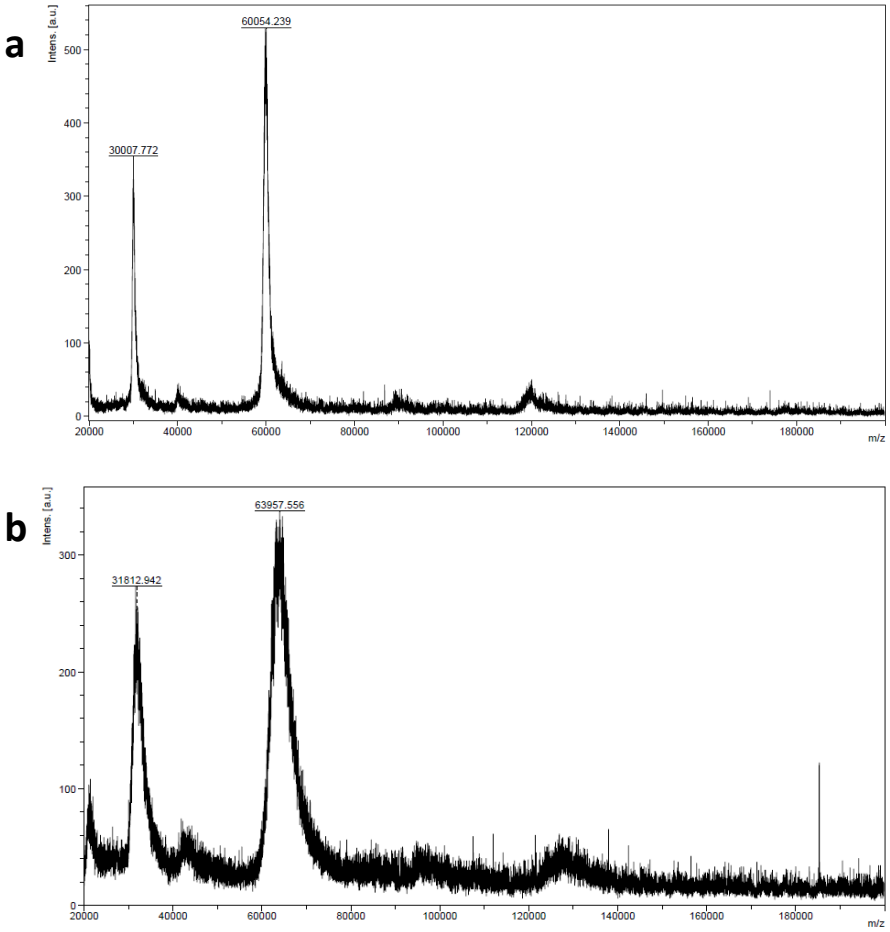

Figure 70: MALDI-TOF spectra for glycoconjugate of 7. a) Activated CRM197 before conjugation to fragment **7**. Mass reported as 60054 Da. **b)** Activated CRM197 conjugated to fragment **7.** Mass reported as 63958 Da.

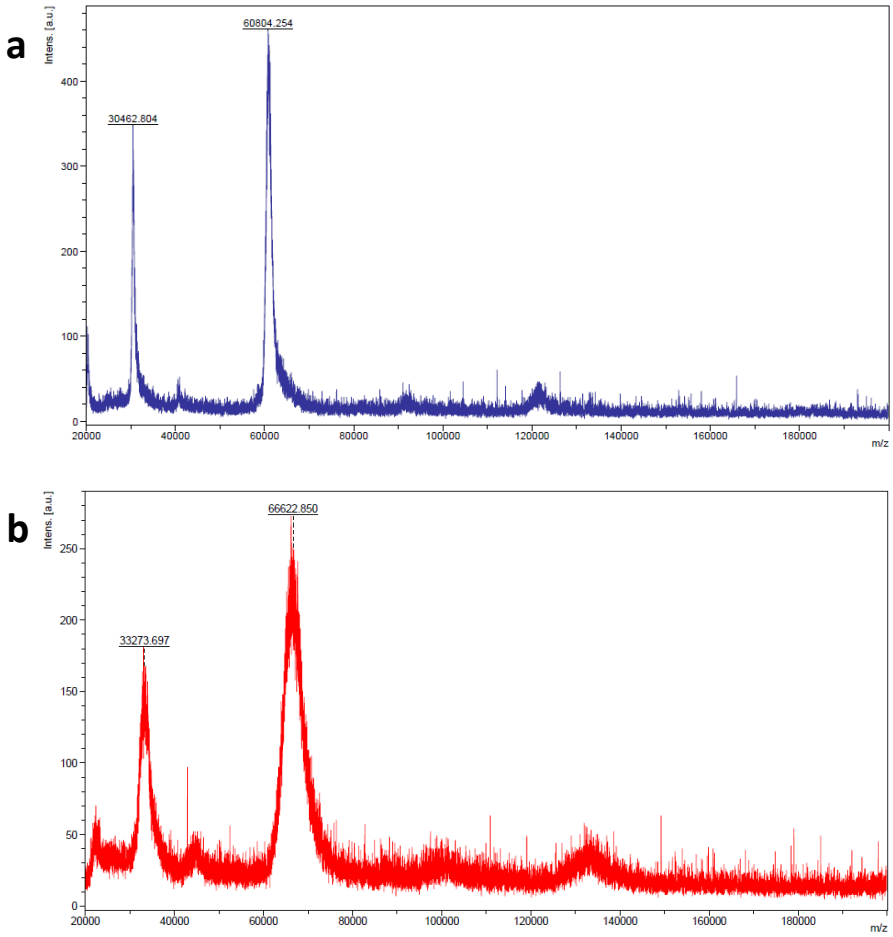

Figure 71: MALDI-TOF spectra for glycoconjugate of 8. a) Activated CRM197 before conjugation to fragment **8**. Mass reported as 60804 Da. **b)** Activated CRM197 conjugated to fragment **8**. Mass reported as 66623 Da.

Determining that the stabilates mice work on Janvier C57B/6 mice

Inbred mice at the MPICI were not susceptible to the prepared *P. berghei* ANKA stabilate. In order to establish a susceptible mouse model, mice (n=10) sourced from Janvier Labs (Le Genest-Saint-Isle, France) were infected with *P. berghei* ANKA and monitored for mass, parasitemia, and development of neurological symptoms. This study indicates that the stabilates were effective in these mice. Following this, the ECM challenge study against mice immunised with glycoconjugates of **7** and **8** was carried out using mice sourced from Janvier Labs.

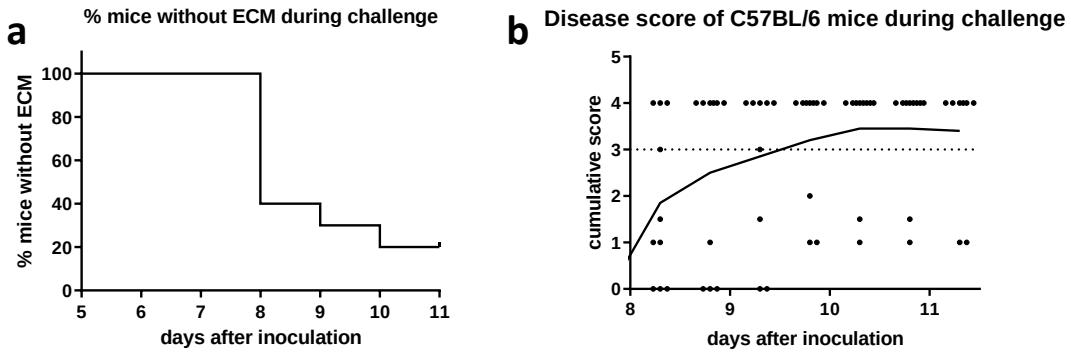

Figure 72: ECM challenge shows mice develop neurological symptoms. a) Inoculation leads to development of neurological symptoms. **b)** Inoculation leads to a rise in disease score. Mice were euthanized at a cumulative disease score of 3, and were assigned a score of 4 thereafter, increasing the disease score.

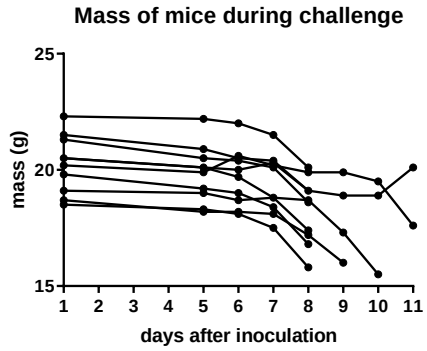

Figure 73: Mass of mice during challenge. Consistent with the model, mice lost weight after the challenge inoculation. Mice that were euthanised mice were as a result of neurological symptom development, before the other endpoint of extreme weight loss occurred.

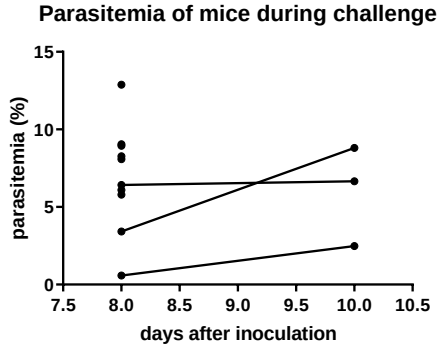

Figure 74: Parasitemia of mice after inoculation. Parasitemia confirms that injection with the stabilates lead to infection.

Determining that glycoconjugates remain intact after freezing

For long term storage, conjugates were frozen at -80°C (Ho, Bolgiano et al. 2000). To initially test whether freezing of the glycoconjugates is viable, an aliquot of each glycoconjugate was frozen. When thawed, the glycoconjugates were assessed on SDS-PAGE to determine whether the conjugates remained intact. The glycoconjugates showed higher mass shift compared to non-conjugated CRM197 [**Appendix, Figure 75**]. The increase in mass corresponds to synthetic glycans still conjugated to the carrier protein after storage. MALDI-TOF analysis (by Dr. Ankita Malik) also confirmed the glycoconjugates remained intact.

After overnight adsorption to adjuvant, adsorption of glycoconjugate was determined by adsorption assay [**Appendix, Table 4**] and showed that that adsorption still occurred after freezing the glycoconjugate.

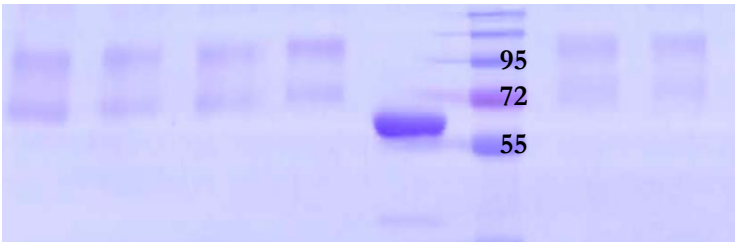

Figure 75: SDS-PAGE analysis of glycoconjugates of 1 – 6. Bands are compared to non-conjguated **CRM197** and molecular weight **ladder**. Numbers indicate the molecular weight of marker bands in kDa. Samples from left to right as follows: **3**, **2**, **6**, **5**, CRM197, ladder, **1**, **4**.

#	structure	pre-adsorption [CRM µg/mL]	post-adsorption [CRM µg/mL]	% adsorbed
1	PEt-Man3-GlcN-InoP	2.8	0.0	**100.0**
2	PEt-Man3-GlcN	3.2	0.0	**100.0**
3	Man3-GlcN	0.4	0.0	**100.0**
4	PEt-Man4-GlcN-InoP	2.7	0.1	**96.0**
5	PEt-Man4-GlcN	1.7	0.0	**100.0**
6	Man4-GlcN	1.6	0.6	**65.4**
	CRM-Gal	3.6	0.4	**88.7**
	CRM	5.8	0.2	**95.7**

Table 4: Adsorption values for glycoconjugates of **1 – 6**.

Preliminary immunisation study for glycoconjugates of 7 and 8

To test their ability for inducing specific antibodies against epitopes at the non-reducing terminus of *P. falciparum* GPI, glycoconjugates of **7** and **8** were prepared by conjugation to CRM197 carrier protein for immunisation. Subcutaneous immunisations in C57BL/6 mice with one of either glycoconjugate (n=4, classified by the immunising glycoconjugate) were administered in a prime-boost-boost regime at two week intervals, each containing only 0.4 μg of synthetic carbohydrate antigen. A control group was immunized with CRM197 only.

Sera (diluted 1:100) were screened on glycan microarray. Immunisation with glycoconjugates of **7** [**Figure 76**] and **8** [**Figure 77**] induced IgG1 by day 35 predominantly against fragments **7** and **8**. A similar profile for IgG2a titres was observed, albeit at a lower intensity. Highest titres were measured against **7**, closely followed by **8**. Immunisation with glycoconjugates of **7** and **8** induce moderately high IgG1 titres to *T. gondii* and mammalian GPI [**Figure 78**a and **Figure 79a**] likely facilitated by PEtN. Comparing IgM titres versus IgG titres suggests that class-switching was important for creating antibodies more specific to *P. falciparum* GPI.

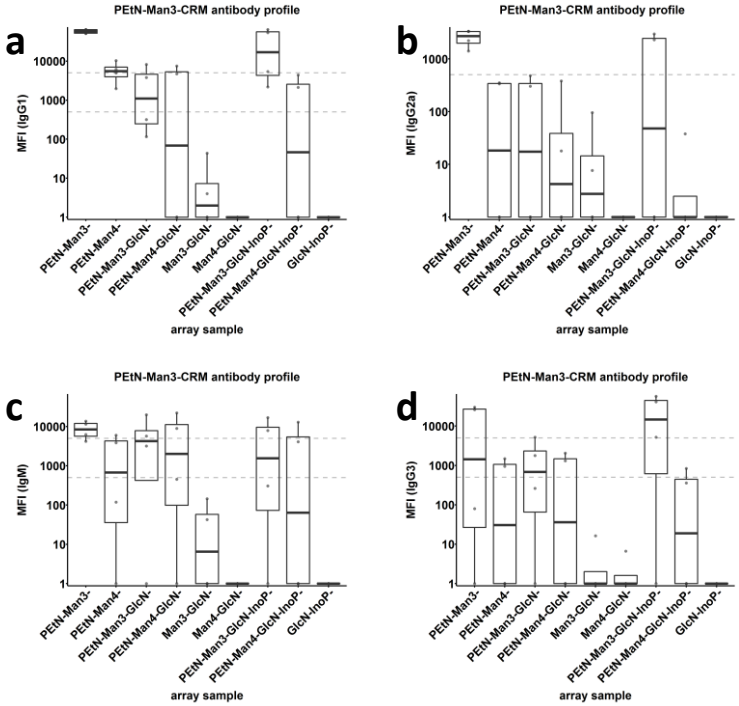

Figure 76: Antibody titres in sera at day 35 against synthetic GPI fragments. Group size n=4, immunised with glycoconjugate **7**. **Top panel (a-b)** IgG1 and IgG2a titres. **Bottom panel (c-d)** IgG3 and IgM titres.

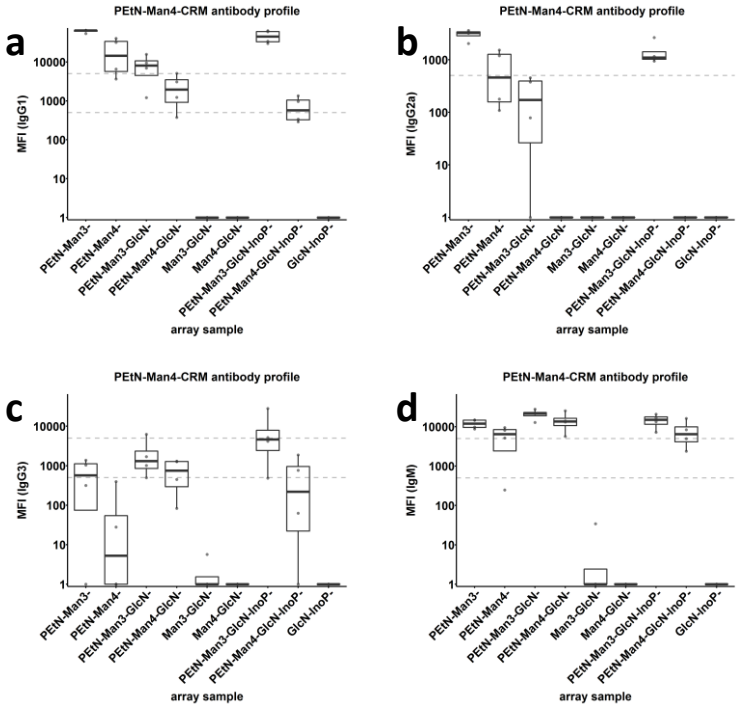

Figure 77: Antibody titres in sera at day 35 against synthetic GPI fragments. Group size n=4, immunised with glycoconjugate **8**. **Top panel (a-b)** IgG1 and IgG2a titres. **Bottom panel (c-d)** IgG3 and IgM titres.

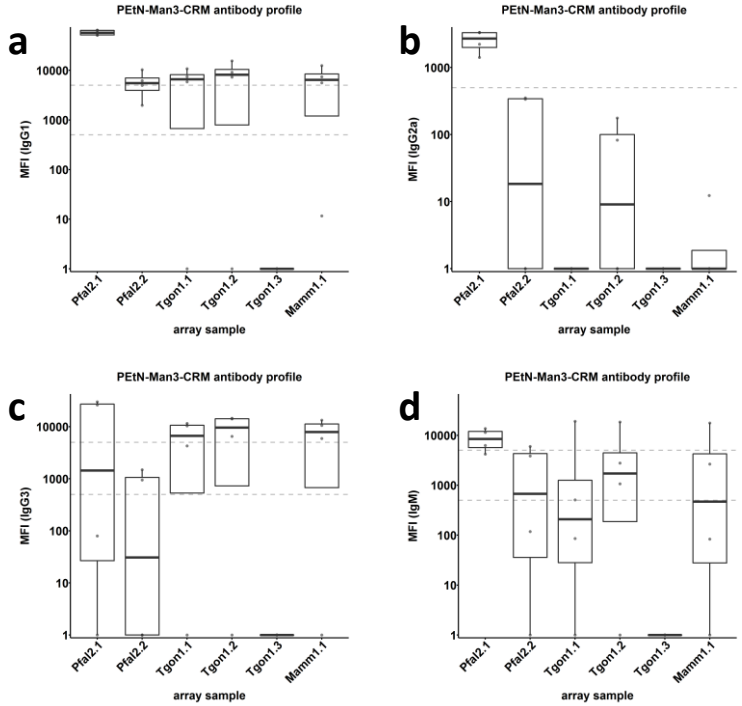

Figure 78: Antibody titres in sera at day 35 against synthetic GPI fragments in other organisms. Group size n=4, immunised with glycoconjugate **7**. **Top panel (a-b)** IgG1 and IgG2a titres. **Bottom panel (c-d)** IgG3 and IgM titres.

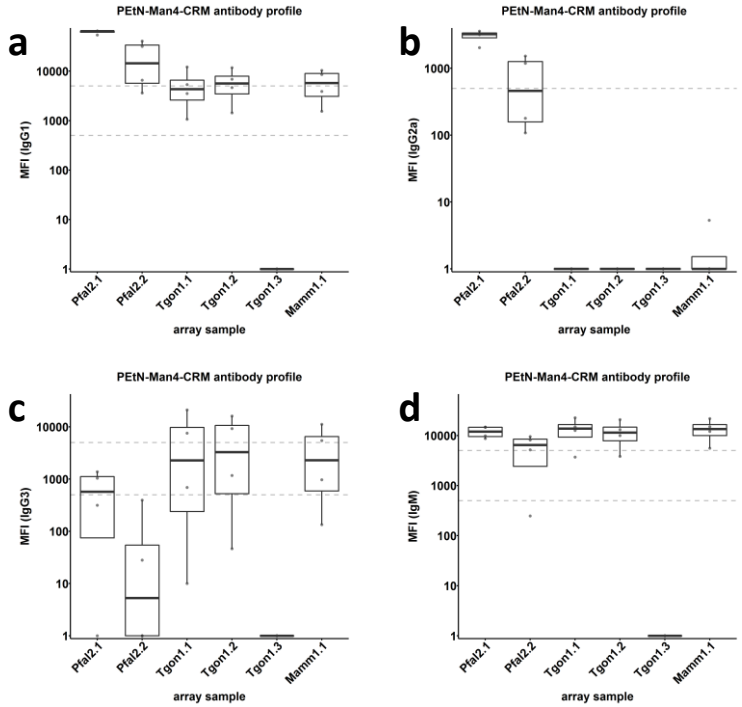

Figure 79: Antibody titres in sera at day 35 against synthetic GPI fragments in other organisms. Group size n=4, immunised with glycoconjugate **8**. **Top panel (a-b)** IgG1 and IgG2a titres. **Bottom panel (c-d)** IgG3 and IgM titres.

Immunisation with a synthetic hexasaccharide glycoconjgugate

A hexasaccharide [**Appendix**, **Figure 80**] was synthesised and conjugated to CRM197 carrier protein (using PNP method, where the glycan is activated instead of the carrier protein) by Dr. Ankita Malik. MALDI-TOF analysis [**Appendix, Figure 81**] determined an average glycan loading of 4.2. Notably, the glycans were attached to carrier protein via PEtN, rather than a thiol linker positioned at InoP. This conjugation at the non-reducing terminus was similar to previously published conjugation strategies, in order to determine their induced antibody specificities.

Glycoconjugate of the hexasaccharide was tested for its ability to induce antibodies against synthetic *P. falciparum* GPI epitopes. After overnight adsorption to adjuvant, subcutaneous immunisations in C57BL/6 mice with one of either glycoconjugate formulation were administered. Immunisations followed a prime-boost-boost regime at two week intervals, with each dose containing 0.4 µg of synthetic carbohydrate antigen. Antibody titres against GPI fragments were assessed using glycan microarray in sera (diluted 1:50) collected every week from the prime immunisation (n=4). It was revealed that this glycoconjugate did not induce antibody production against the synthetic GPI epitopes. As the glycoconjugate was not immunogenic, further work was not pursued.

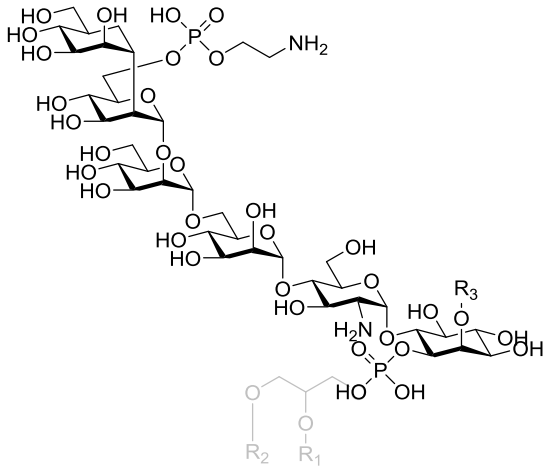

Figure 80: The hexasaccharide antigen. The full GPI is shown in grey for context.

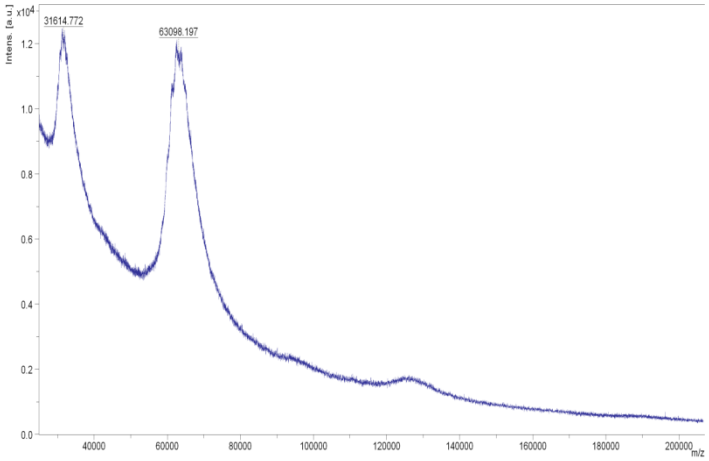

Figure 81: MALDI-TOF spectra for glycoconjugate of hexasaccharide. Observed change is 5098 Da.

Additional glycan array data during the immunisation study

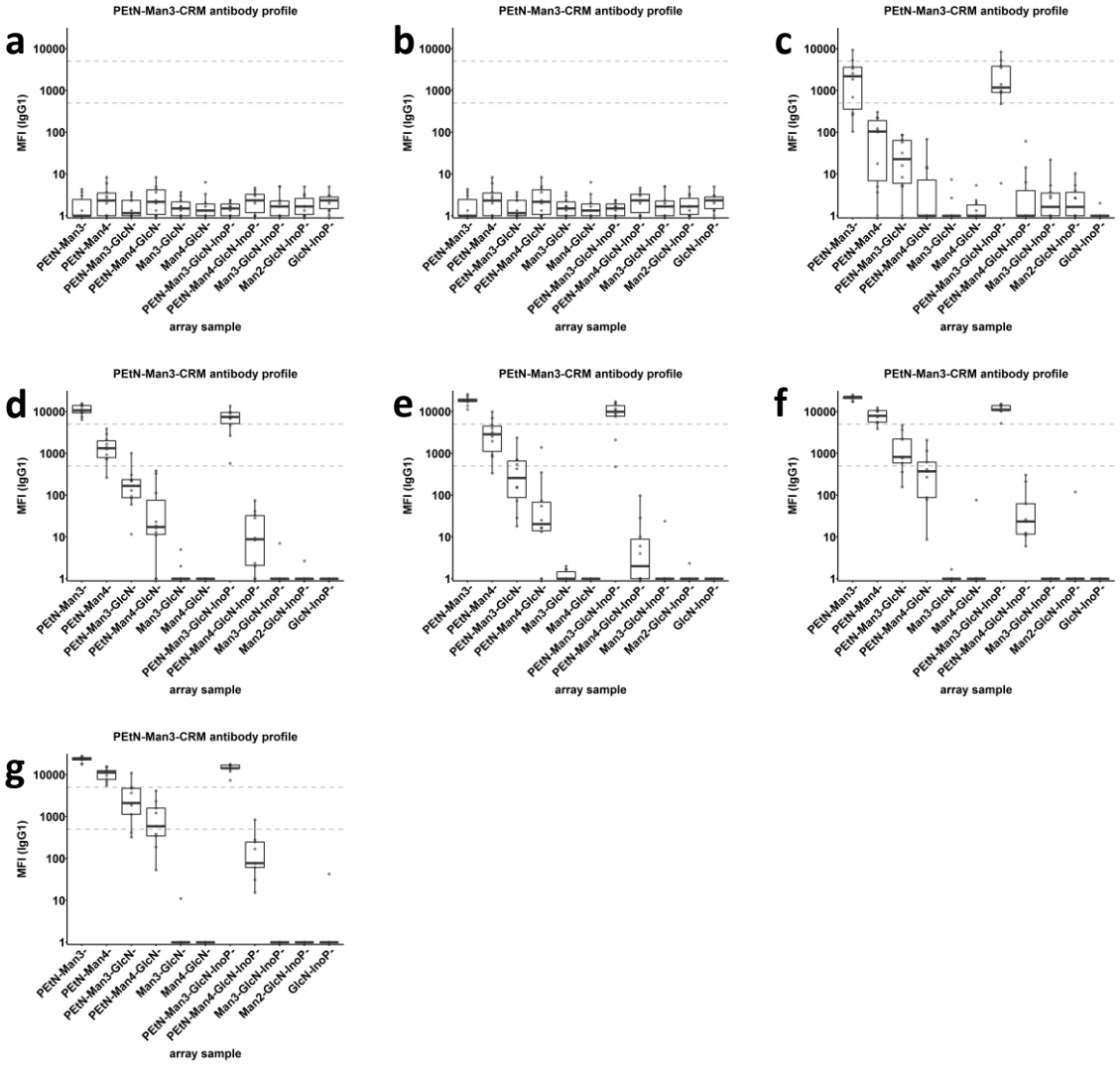

Figure 82: IgG1 titres against synthetic GPI fragments in sera of mice immunised with glycoconjugate of 7. Group size n=10, classified by the immunising glycoconjugate. Titres at day **a)** 0, **b)** 7, **c)** 14, **d)** 21, **e)** 28, **f)** 35, **g)** 42.

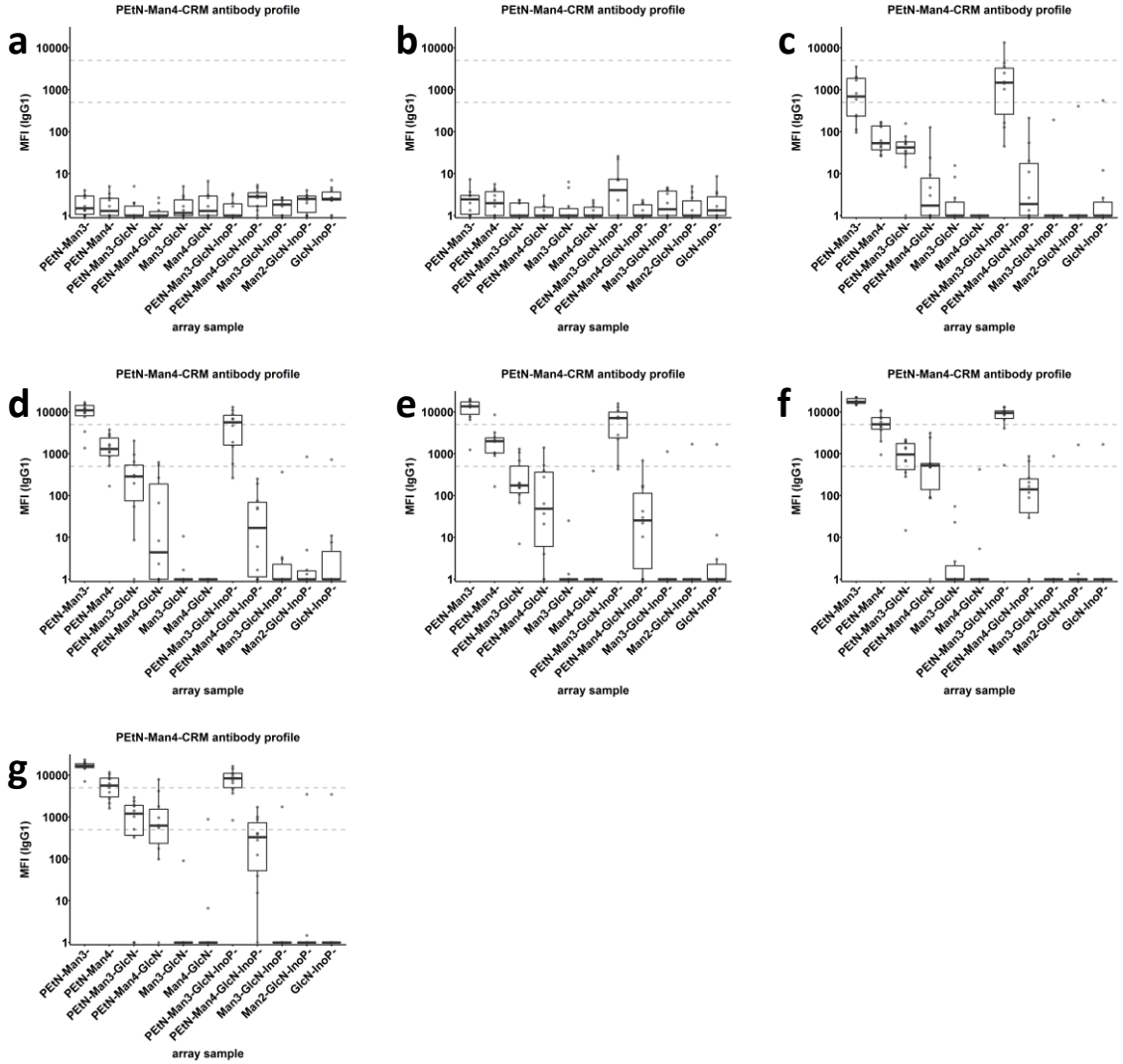

Figure 83: IgG1 titres against synthetic GPI fragments in sera of mice immunised with glycoconjugate of 8. Group size n=10, classified by the immunising glycoconjugate. Titres at day **a)** 0, **b)** 7, **c)** 14, **d)** 21, **e)** 28, **f)** 35, **g)** 42.

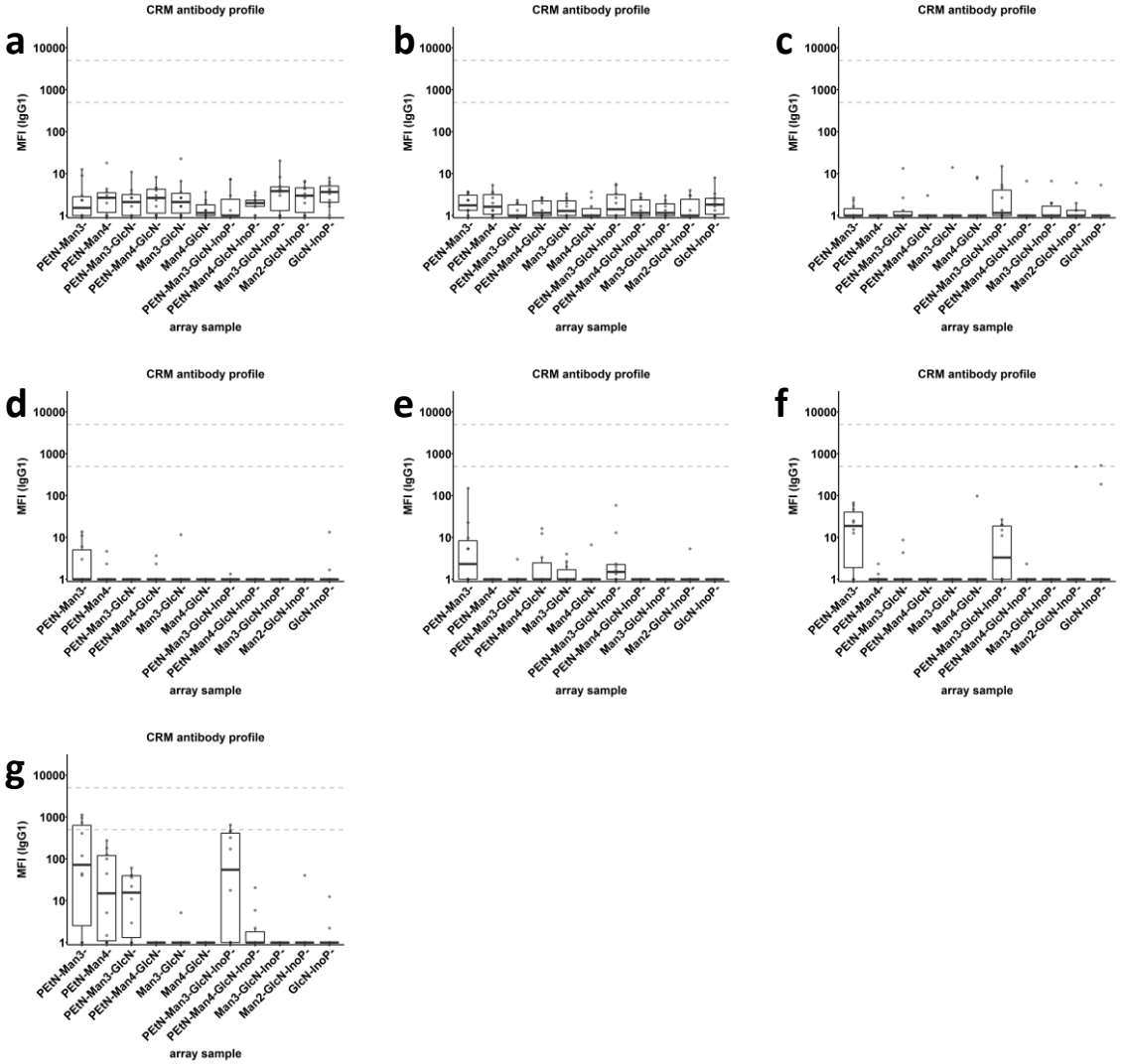

Figure 84: IgG1 titres against synthetic GPI fragments in sera of mice immunised with CRM197 control. Group size n=10, classified by the immunising glycoconjugate. Titres at day **a)** 0, **b)** 7, **c)** 14, **d)** 21, **e)** 28, **f)** 35, **g)** 42.

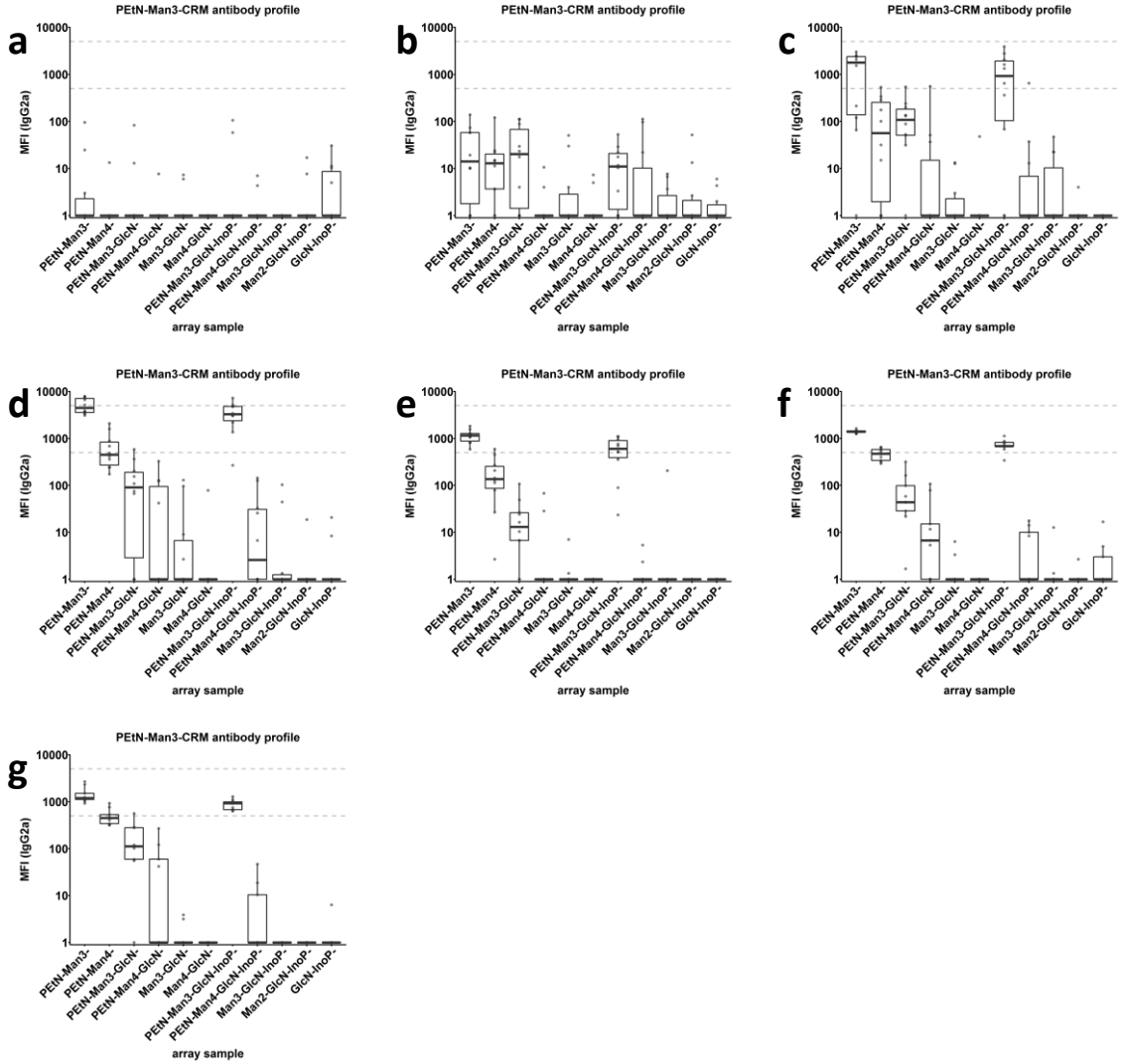

Figure 85: IgG2a titres against synthetic GPI fragments in sera of mice immunised with glycoconjugate of 7. Group size n=10, classified by the immunising glycoconjugate. Titres at day **a)** 0, **b)** 7, **c)** 14, **d)** 21, **e)** 28, **f)** 35, **g)** 42.

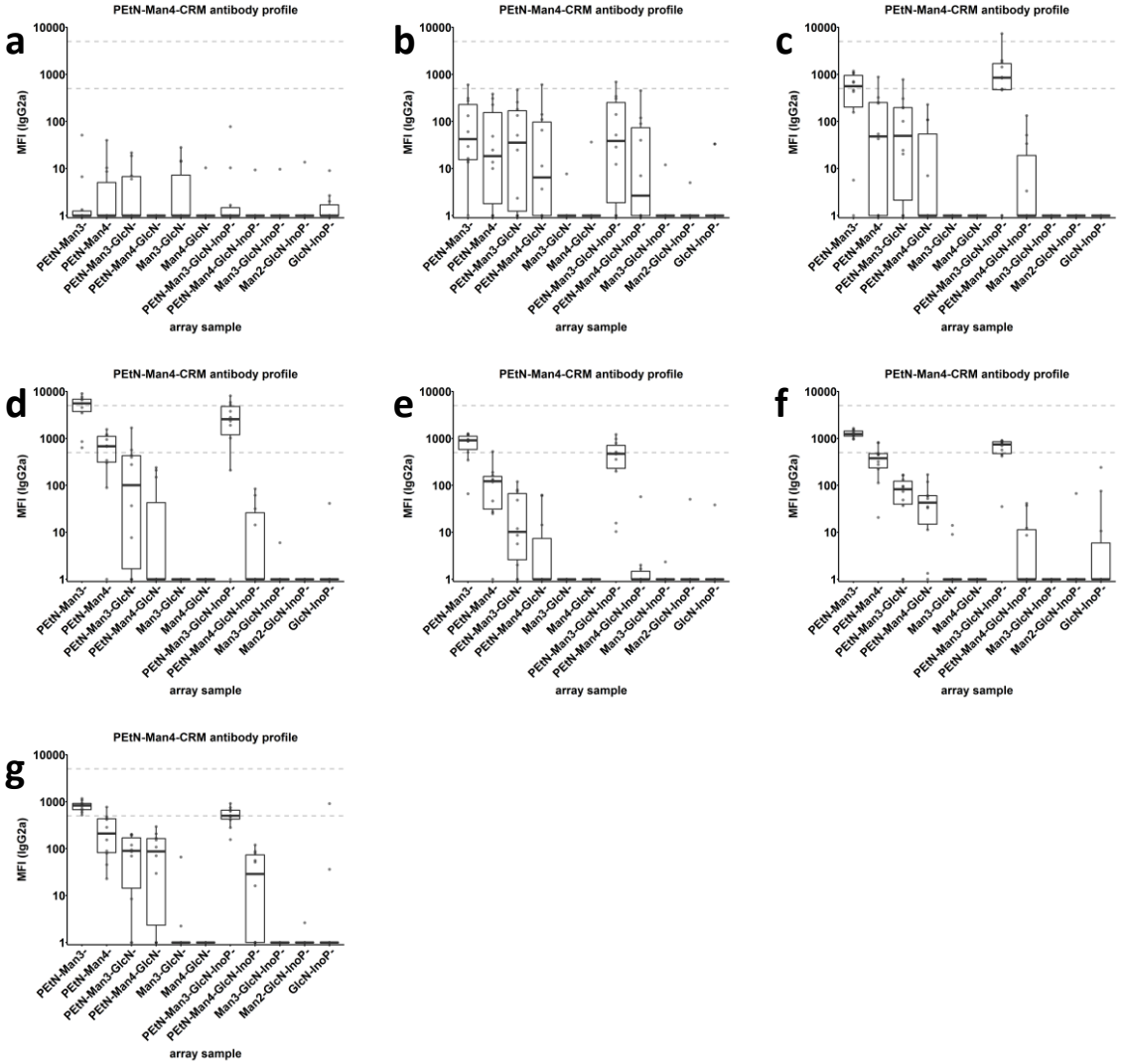

Figure 86: IgG2a titres against synthetic GPI fragments in sera of mice immunised with glycoconjugate of 8. Group size n=10, classified by the immunising glycoconjugate. Titres at day **a)** 0, **b)** 7, **c)** 14, **d)** 21, **e)** 28, **f)** 35, **g)** 42.

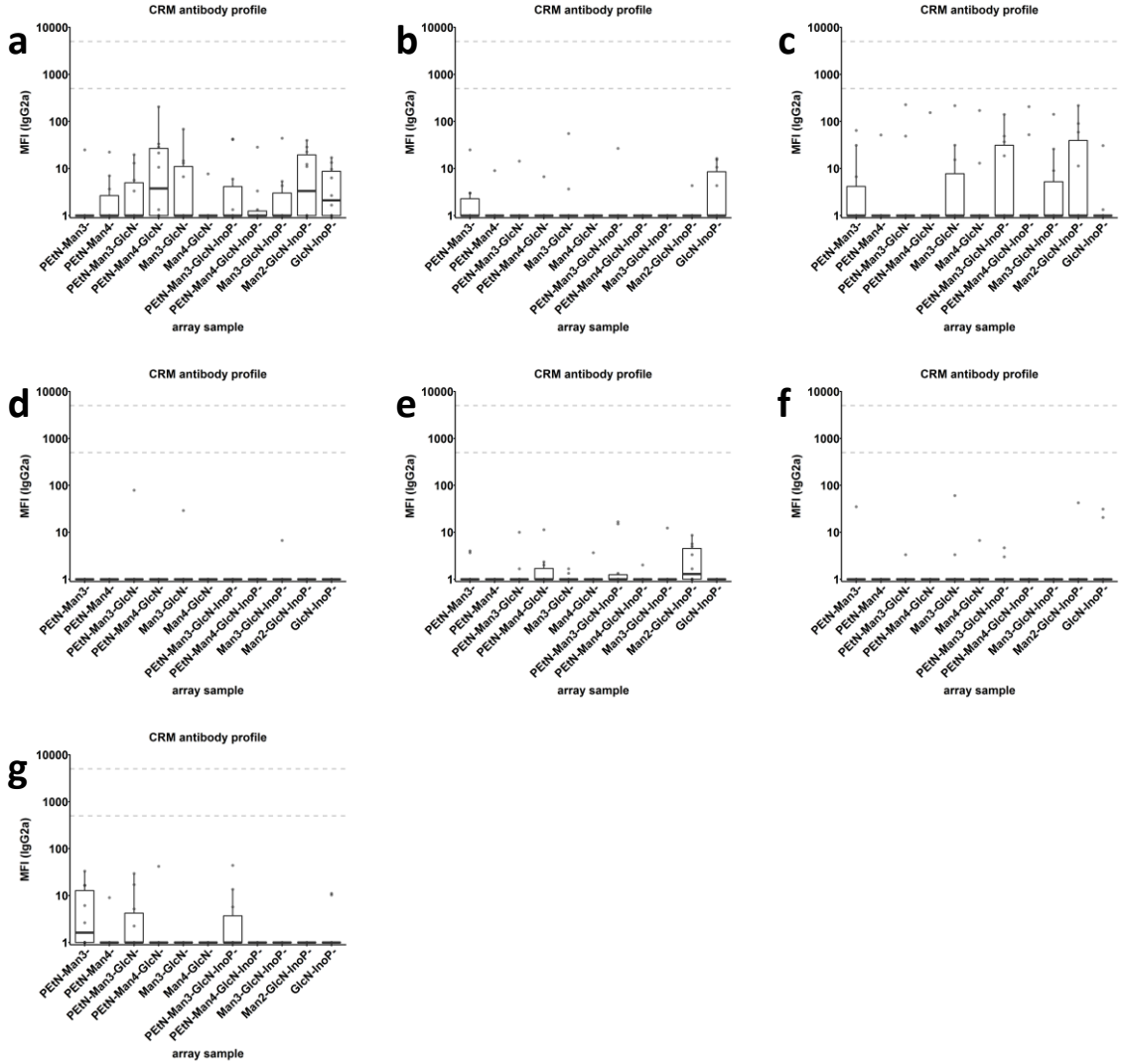

Figure 87: IgG2a titres against synthetic GPI fragments in sera of mice immunised with CRM197 control. Group size n=10, classified by the immunising glycoconjugate. Titres at day **a)** 0, **b)** 7, **c)** 14, **d)** 21, **e)** 28, **f)** 35, **g)** 42.

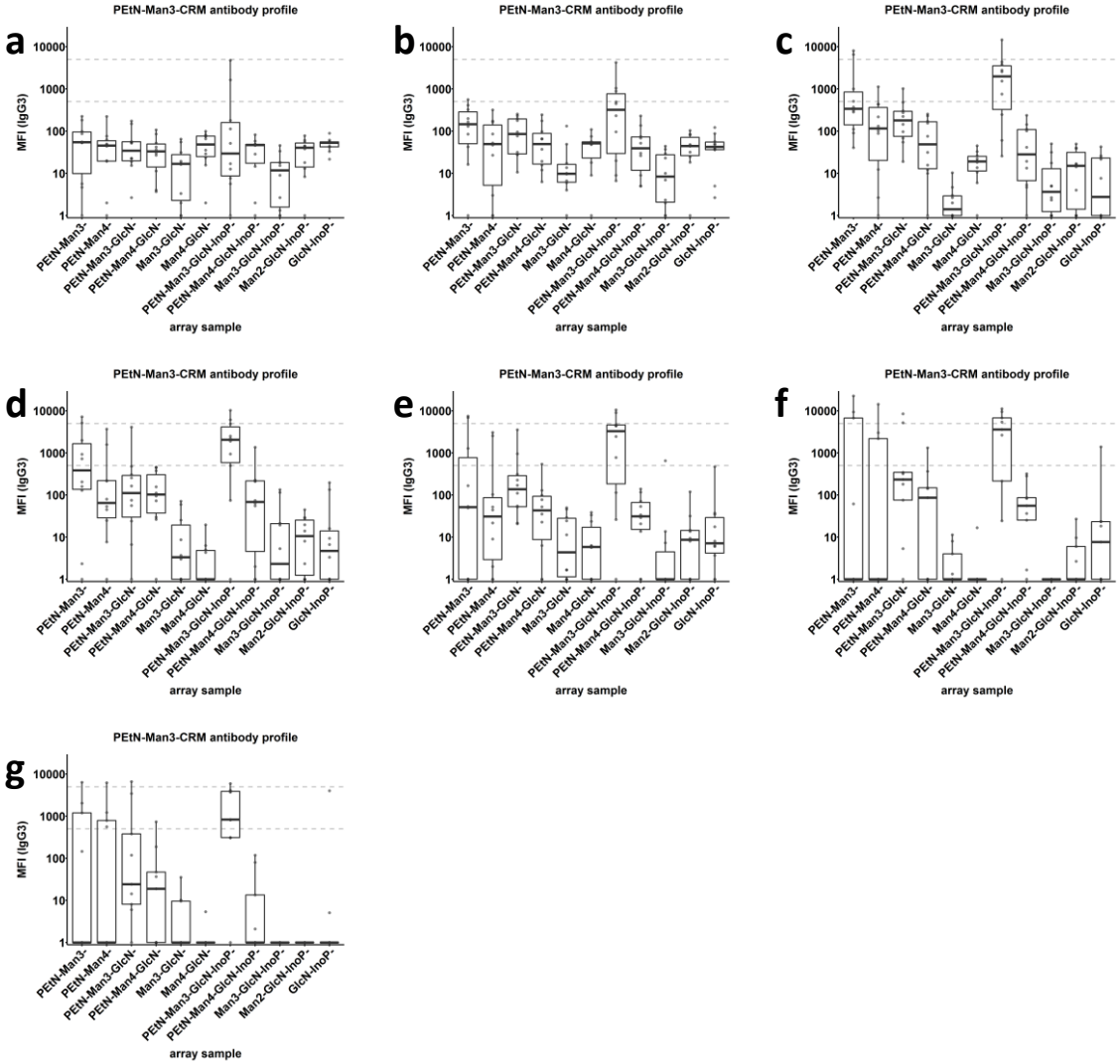

Figure 88: IgG3 titres against synthetic GPI fragments in sera of mice immunised with glycoconjugate of 7. Group size n=10, classified by the immunising glycoconjugate. Titres at day **a)** 0, **b)** 7, **c)** 14, **d)** 21, **e)** 28, **f)** 35, **g)** 42.

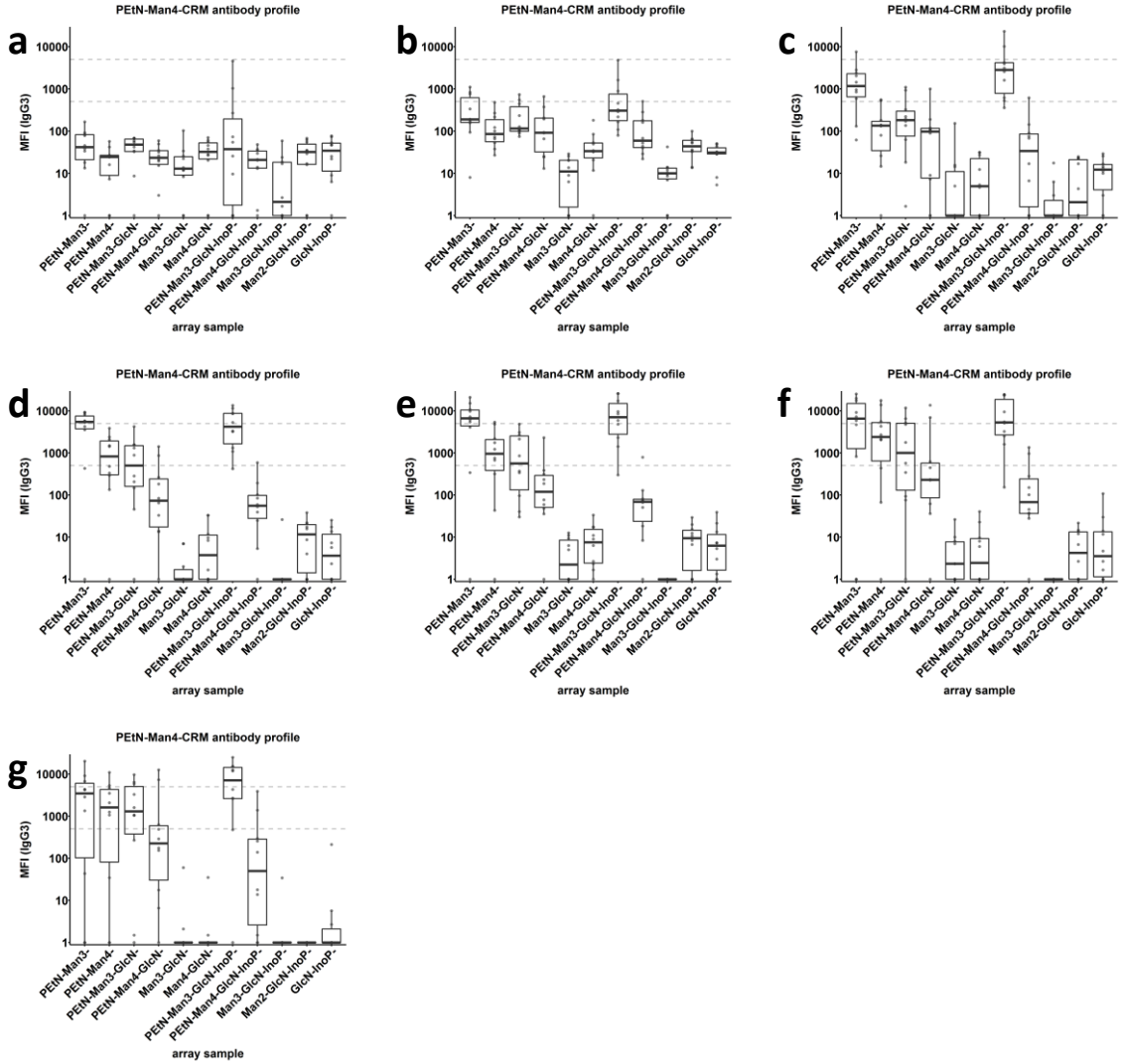

Figure 89: IgG3 titres against synthetic GPI fragments in sera of mice immunised with glycoconjugate of 8. Group size n=10, classified by the immunising glycoconjugate. Titres at day **a)** 0, **b)** 7, **c)** 14, **d)** 21, **e)** 28, **f)** 35, **g)** 42.

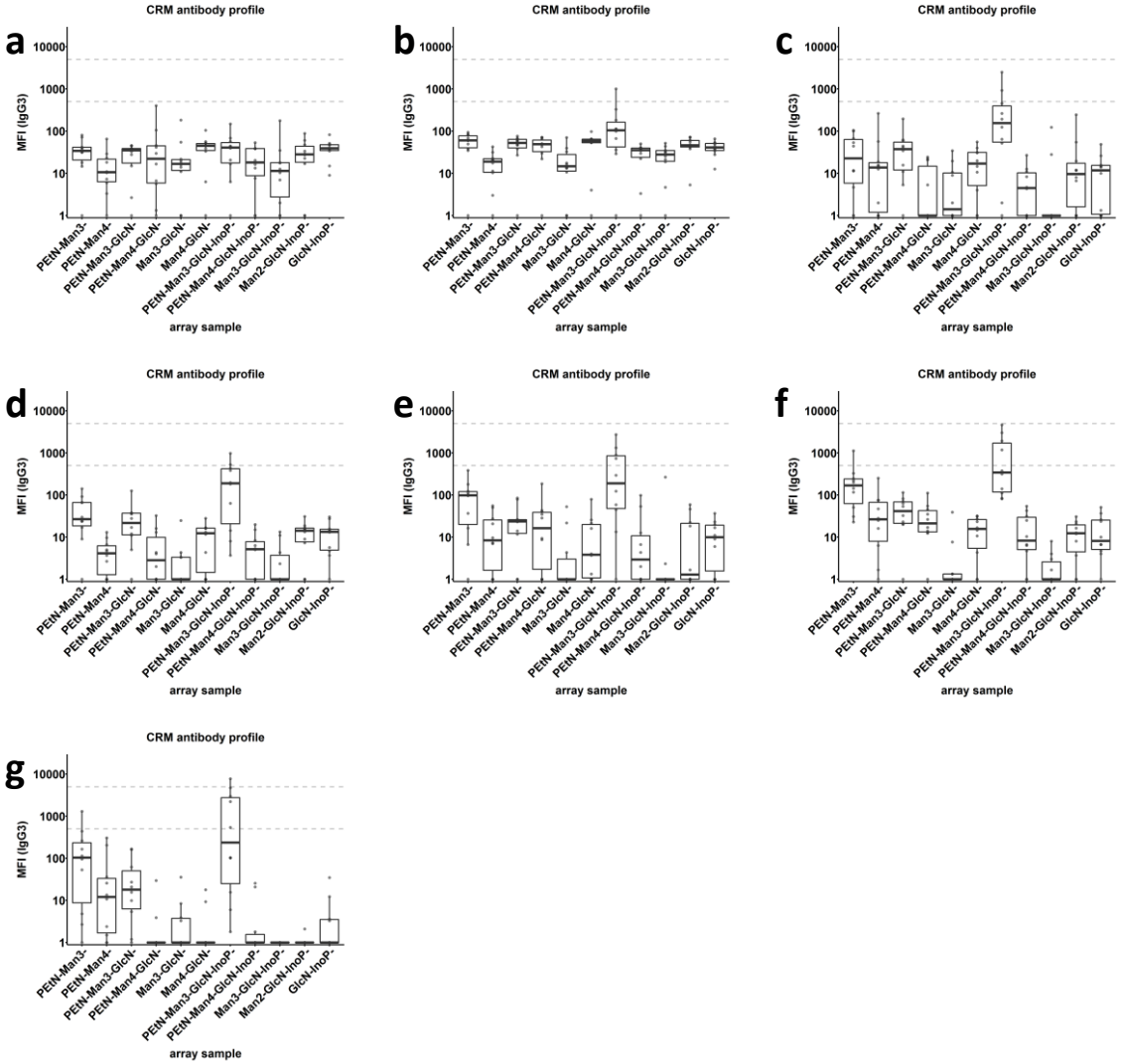

Figure 90: IgG3 titres against synthetic GPI fragments in sera of mice immunised with CRM197 control. Group size n=10, classified by the immunising glycoconjugate. Titres at day **a)** 0, **b)** 7, **c)** 14, **d)** 21, **e)** 28, **f)** 35, **g)** 42.

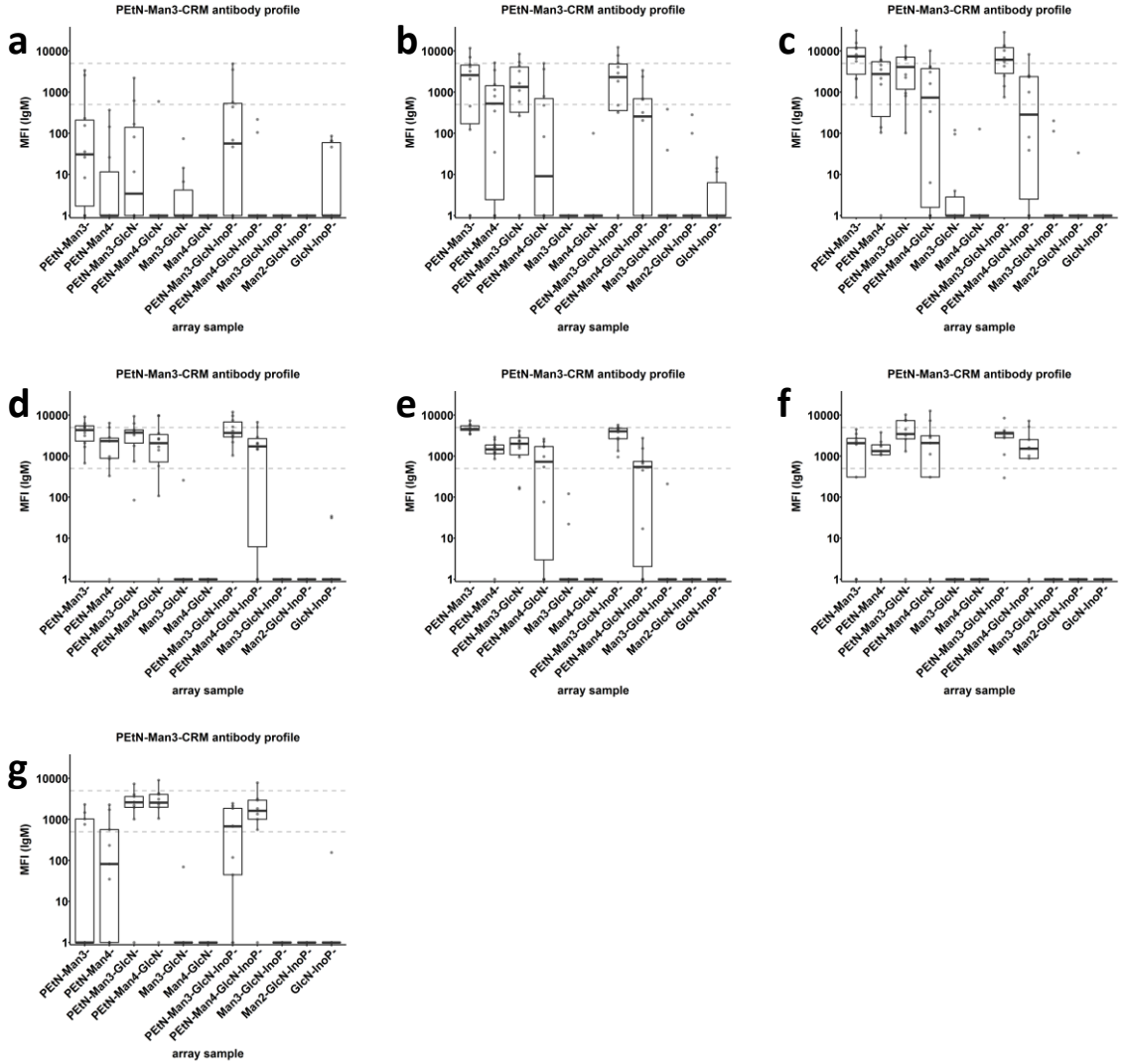

Figure 91: IgM titres against synthetic GPI fragments in sera of mice immunised with glycoconjugate of 7. Group size n=10, classified by the immunising glycoconjugate. Titres at day **a)** 0, **b)** 7, **c)** 14, **d)** 21, **e)** 28, **f)** 35, **g)** 42.

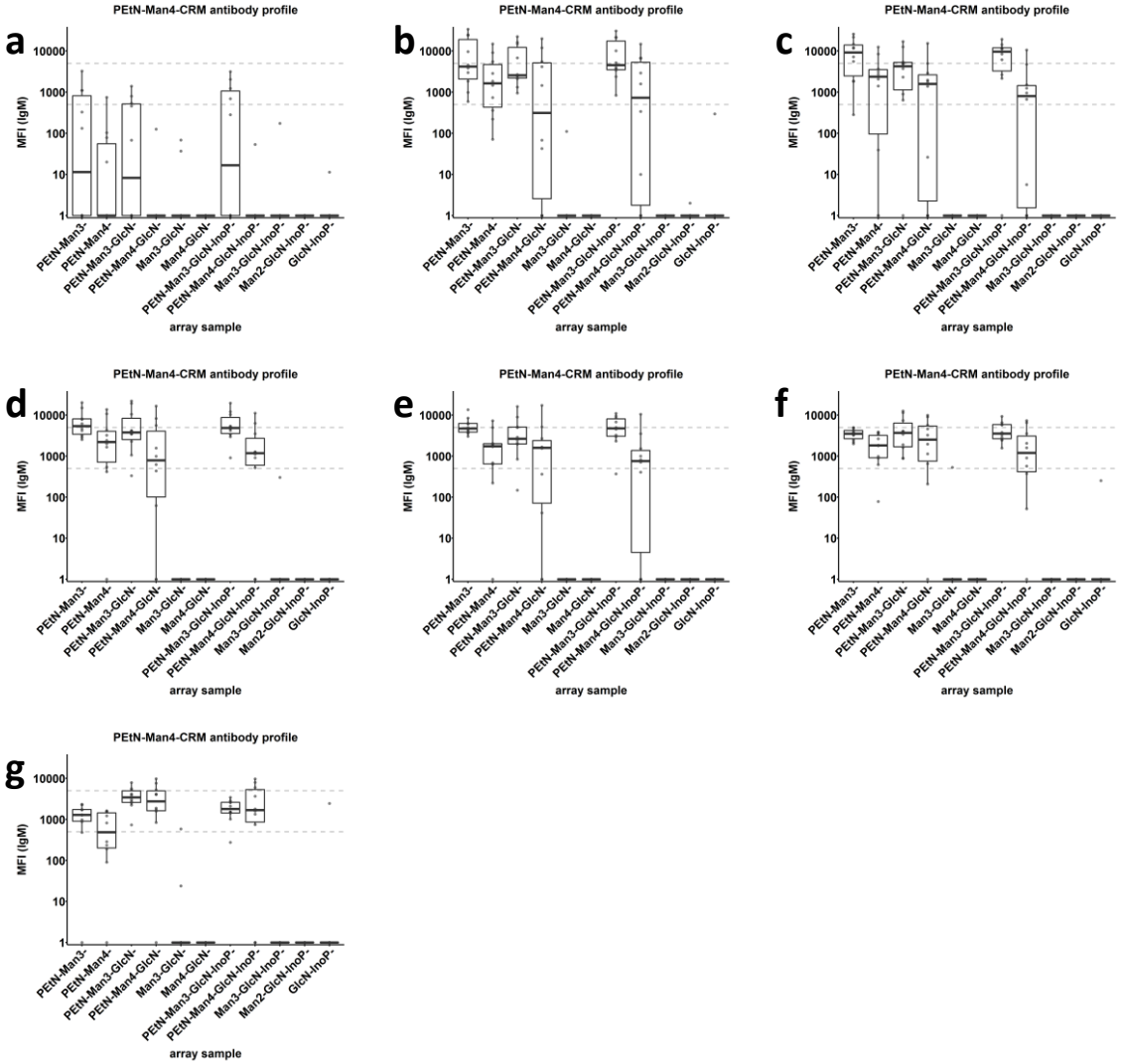

Figure 92: IgM titres against synthetic GPI fragments in sera of mice immunised with glycoconjugate of 8. Group size n=10, classified by the immunising glycoconjugate. Titres at day **a)** 0, **b)** 7, **c)** 14, **d)** 21, **e)** 28, **f)** 35, **g)** 42.

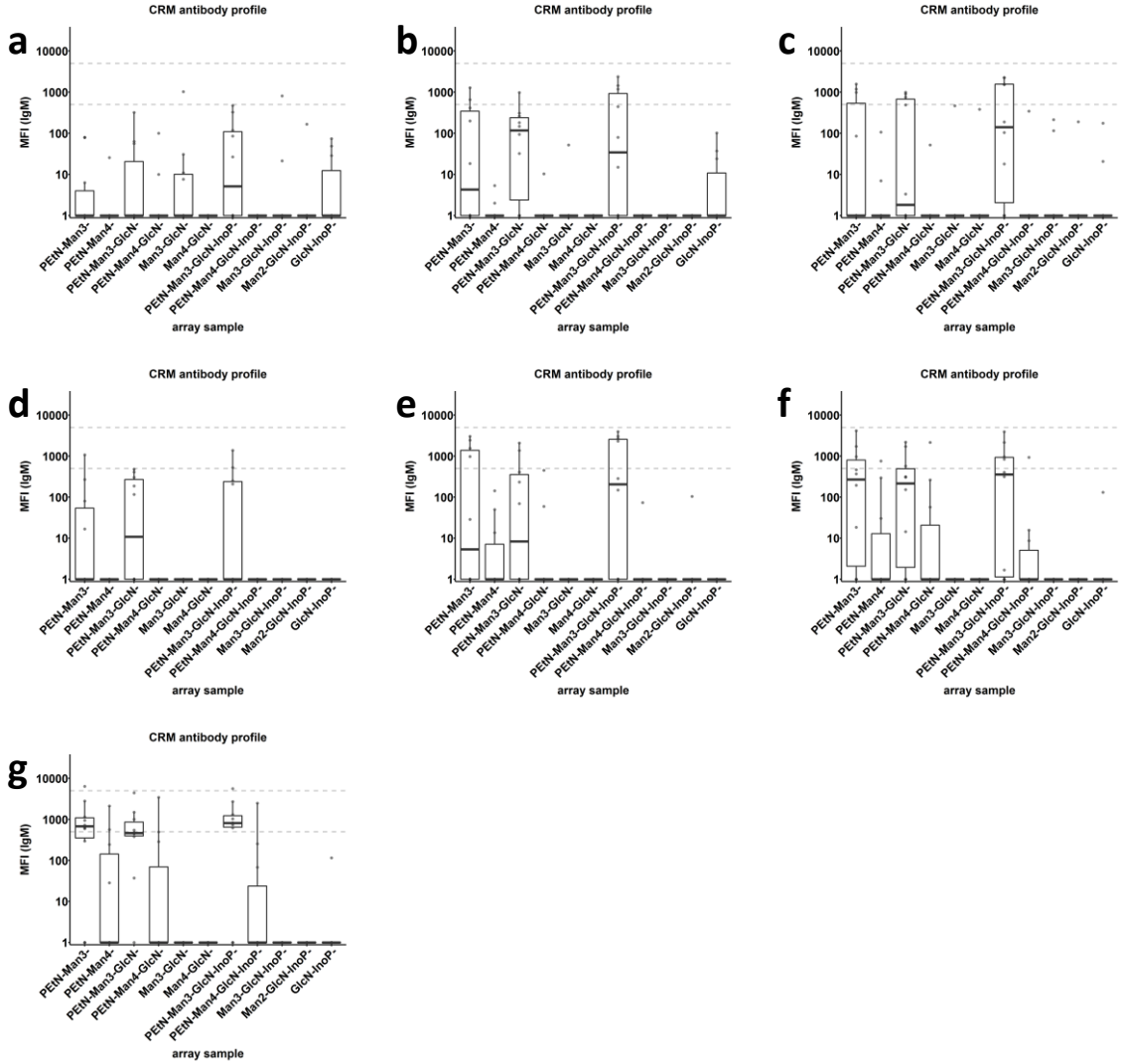

Figure 93: IgM titres against synthetic GPI fragments in sera of mice immunised with CRM197 control. Group size n=10, classified by the immunising glycoconjugate. Titres at day **a)** 0, **b)** 7, **c)** 14, **d)** 21, **e)** 28, **f)** 35, **g)** 42.

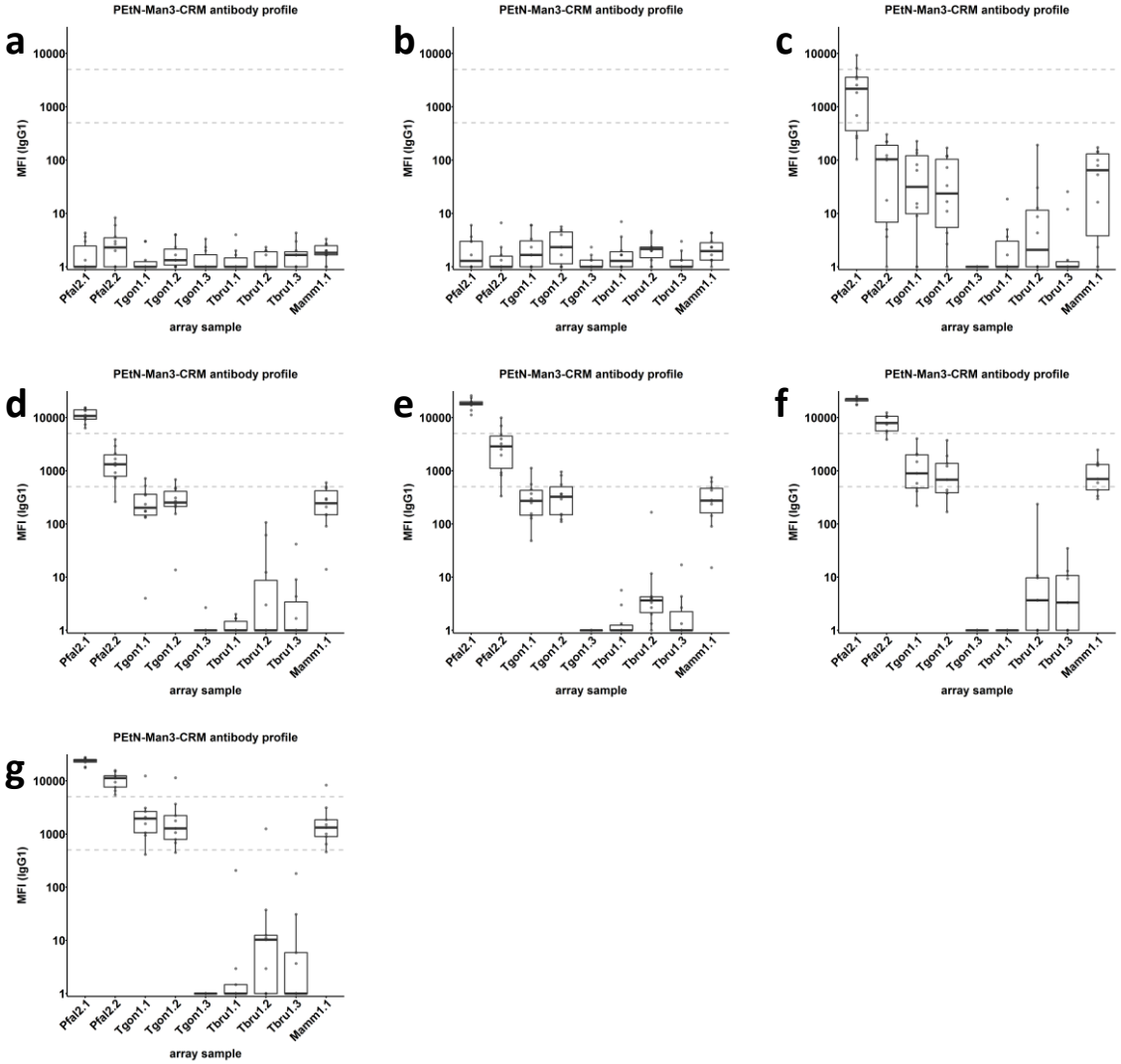

Figure 94: IgG1 titres against synthetic GPI fragments from other organisms in sera of mice immunised with glycoconjugate of 7. Group size n=10, classified by the immunising glycoconjugate. Titres at day **a)** 0, **b)** 7, **c)** 14, **d)** 21, **e)** 28, **f)** 35, **g)** 42.

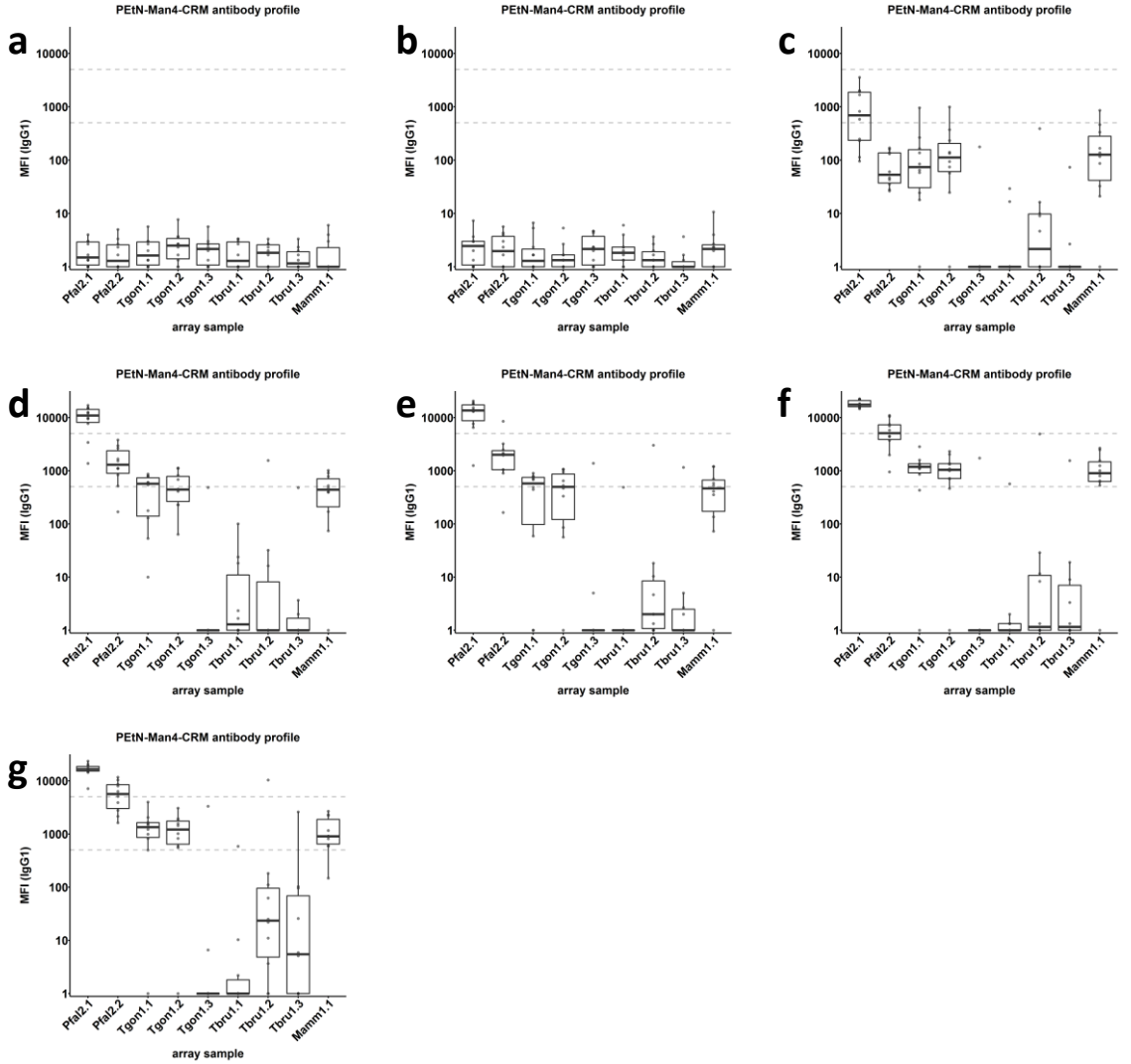

Figure 95: IgG1 titres against synthetic GPI fragments from other organisms in sera of mice immunised with glycoconjugate of 8. Group size n=10, classified by the immunising glycoconjugate. Titres at day **a)** 0, **b)** 7, **c)** 14, **d)** 21, **e)** 28, **f)** 35, **g)** 42.

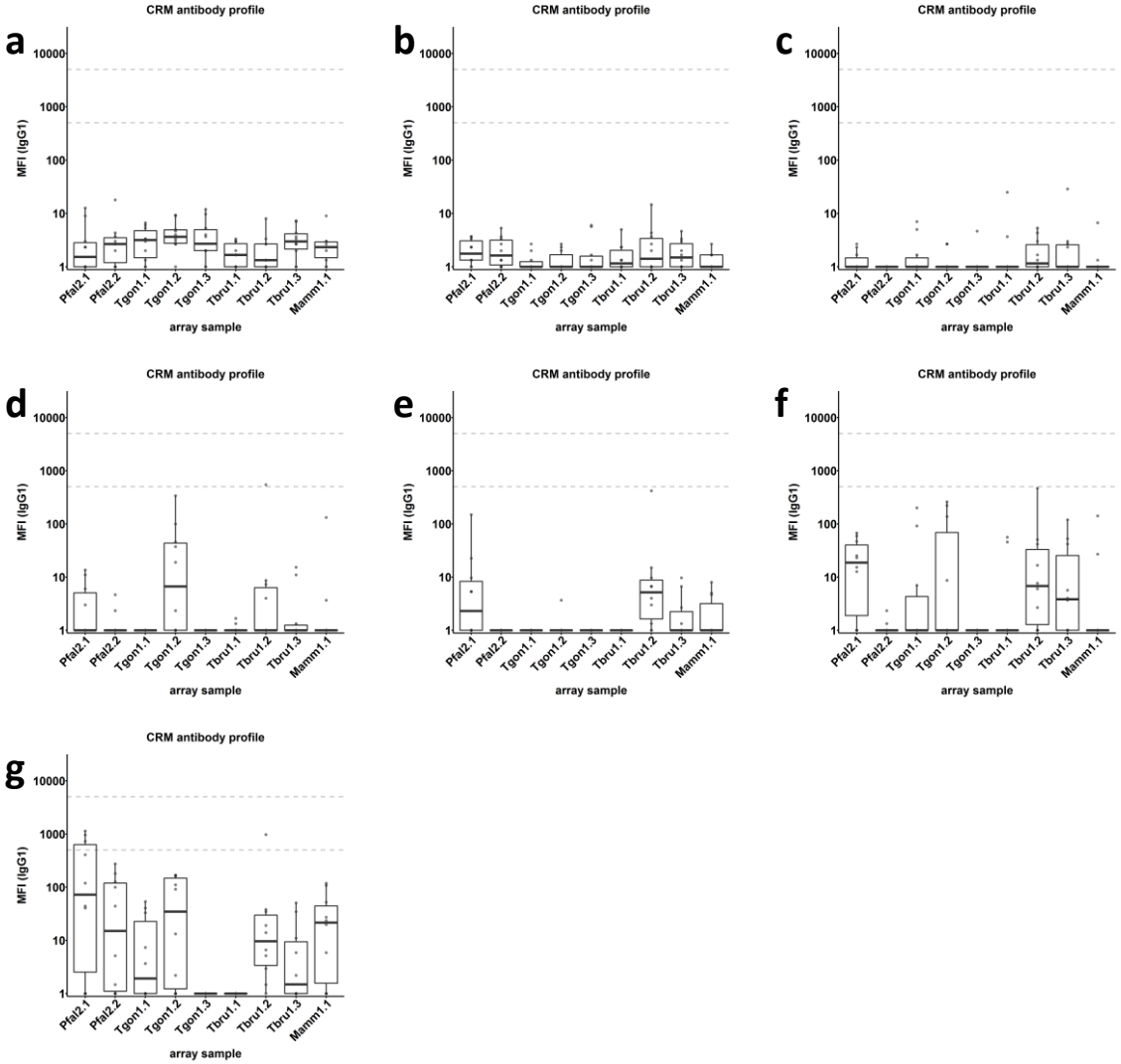

Figure 96: IgG1 titres against synthetic GPI fragments from other organisms in sera of mice immunised with CRM197 control. Group size n=10, classified by the immunising glycoconjugate. Titres at day **a)** 0, **b)** 7, **c)** 14, **d)** 21, **e)** 28, **f)** 35, **g)** 42.

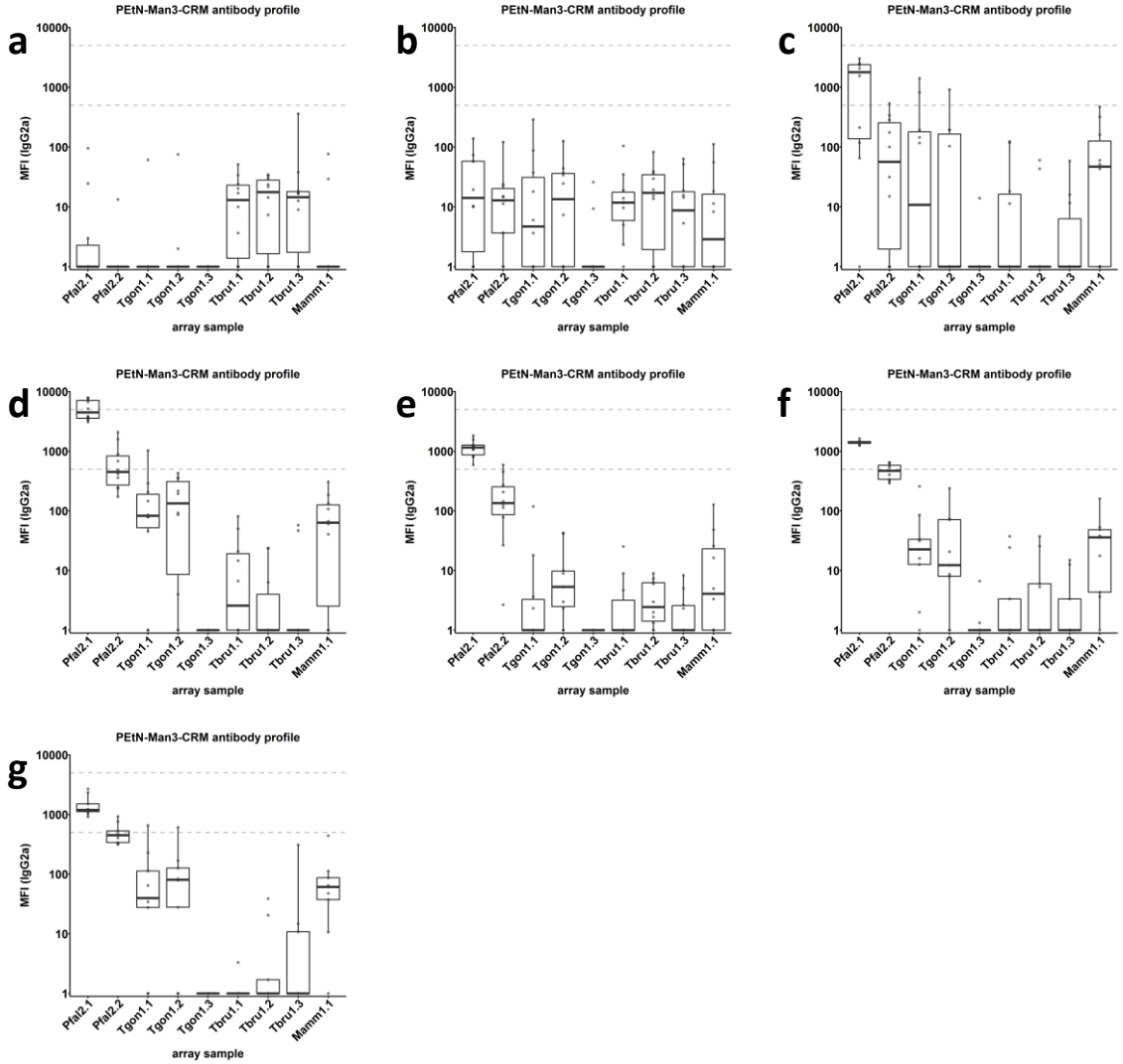

Figure 97: IgG2a titres against synthetic GPI fragments from other organisms in sera of mice immunised with glycoconjugate of 7. Group size n=10, classified by the immunising glycoconjugate. Titres at day **a)** 0, **b)** 7, **c)** 14, **d)** 21, **e)** 28, **f)** 35, **g)** 42.

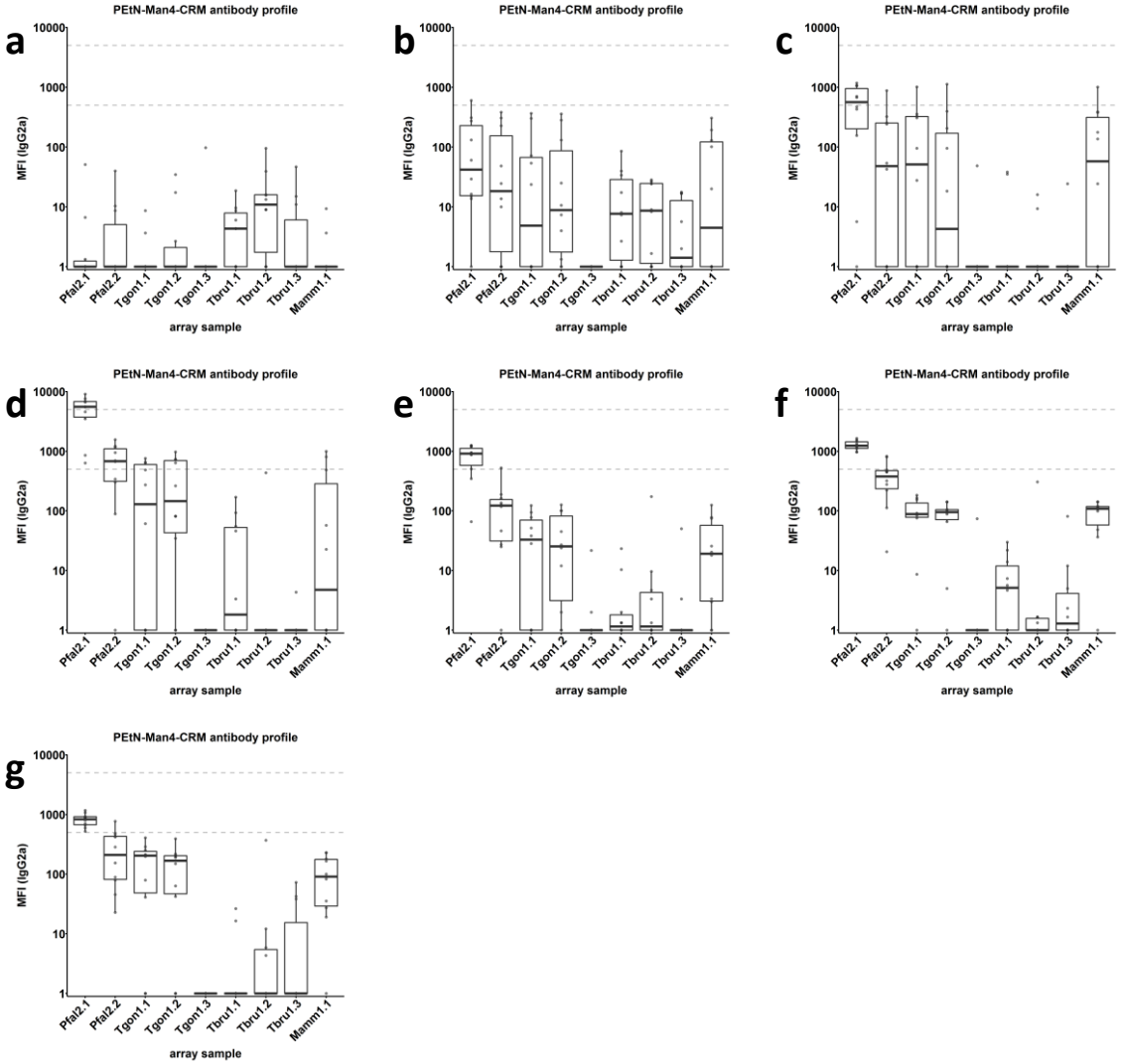

Figure 98: IgG2a titres against synthetic GPI fragments from other organisms in sera of mice immunised with glycoconjugate of 8. Group size n=10, classified by the immunising glycoconjugate. Titres at day **a)** 0, **b)** 7, **c)** 14, **d)** 21, **e)** 28, **f)** 35, **g)** 42.

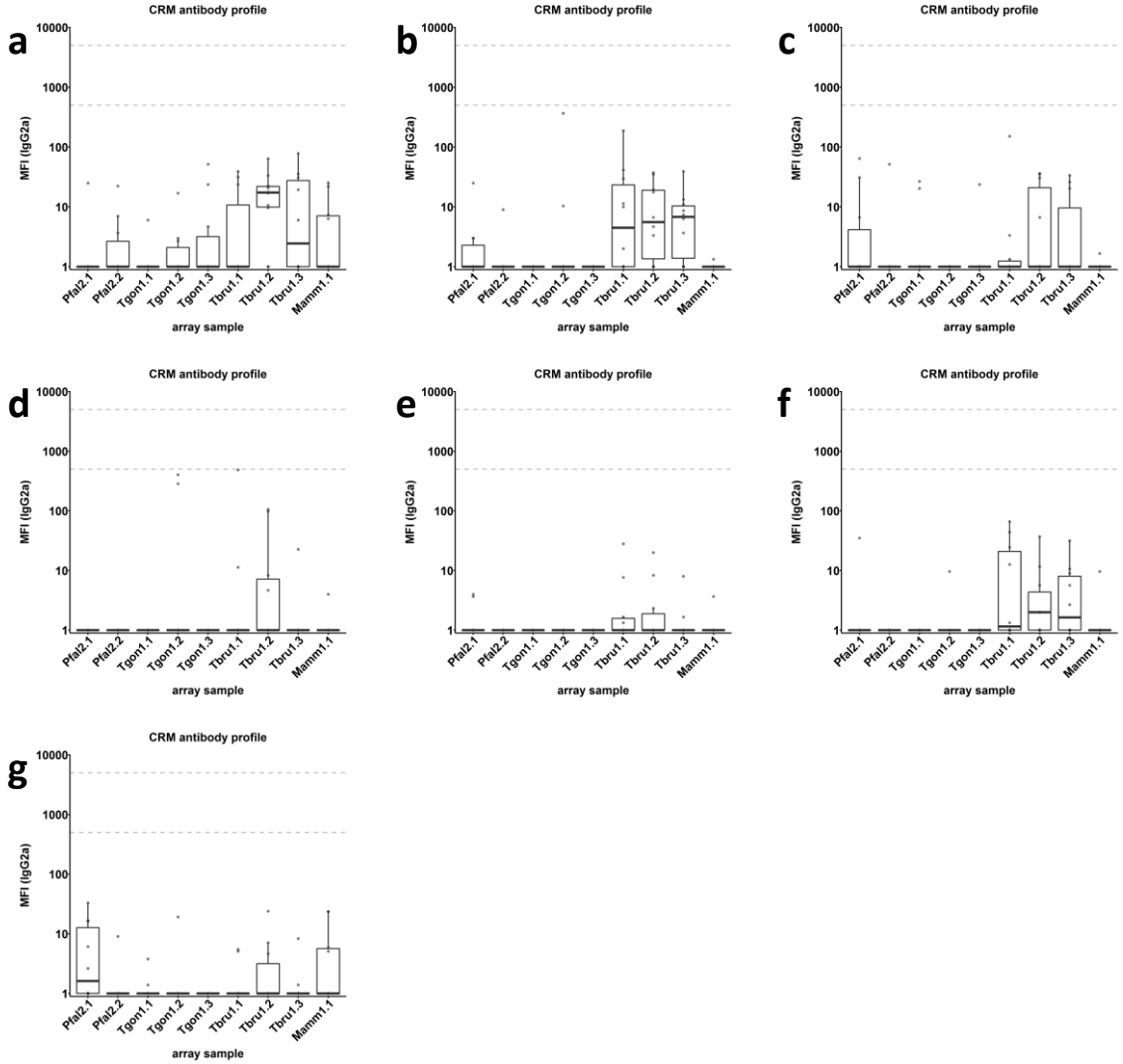

Figure 99: IgG2a titres against synthetic GPI fragments from other organisms in sera of mice immunised with CRM197 control. Group size n=10, classified by the immunising glycoconjugate. Titres at day **a)** 0, **b)** 7, **c)** 14, **d)** 21, **e)** 28, **f)** 35, **g)** 42.

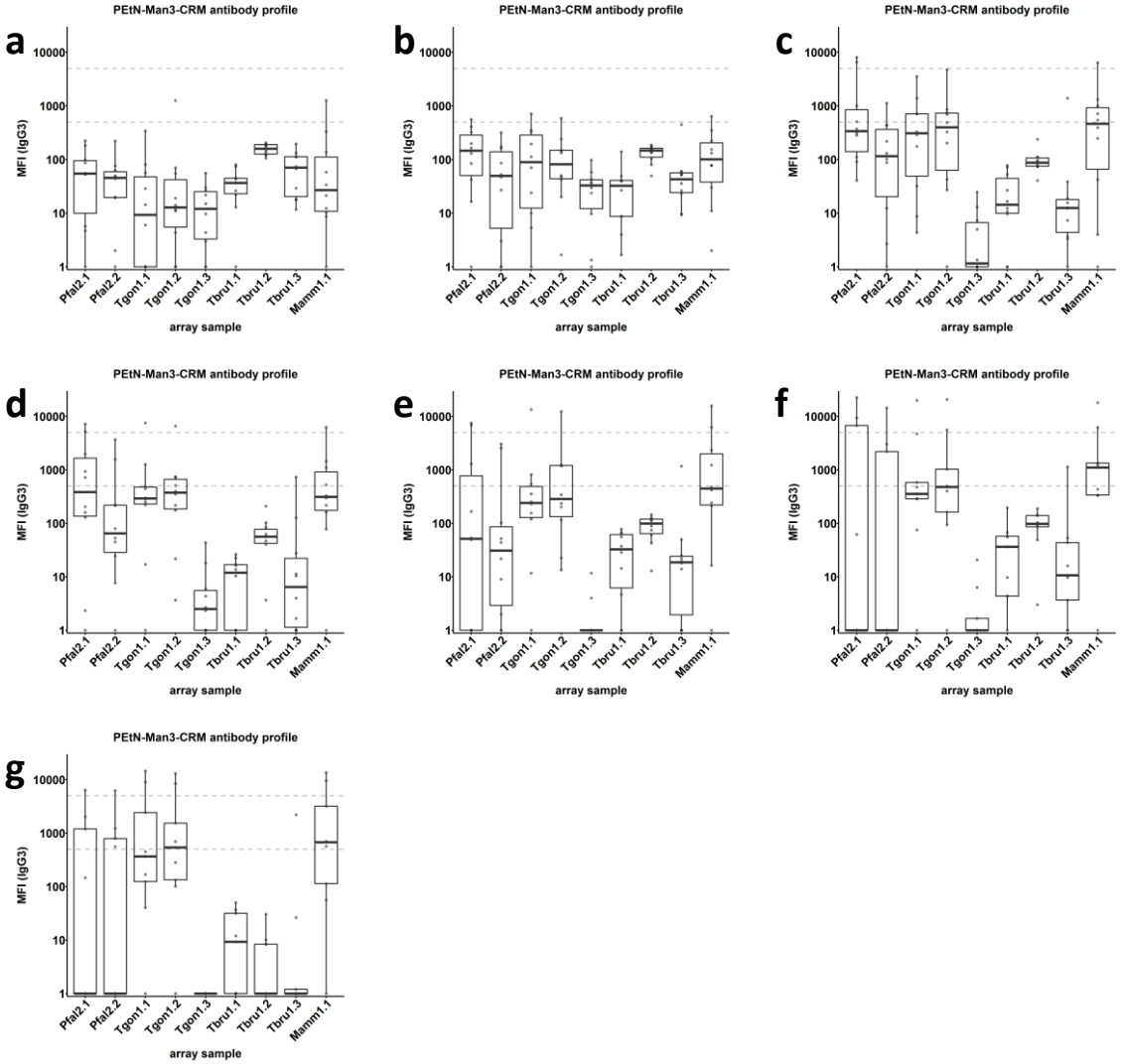

Figure 100: IgG3 titres against synthetic GPI fragments from other organisms in sera of mice immunised with glycoconjugate of 7. Group size n=10, classified by the immunising glycoconjugate. Titres at day **a)** 0, **b)** 7, **c)** 14, **d)** 21, **e)** 28, **f)** 35, **g)** 42.

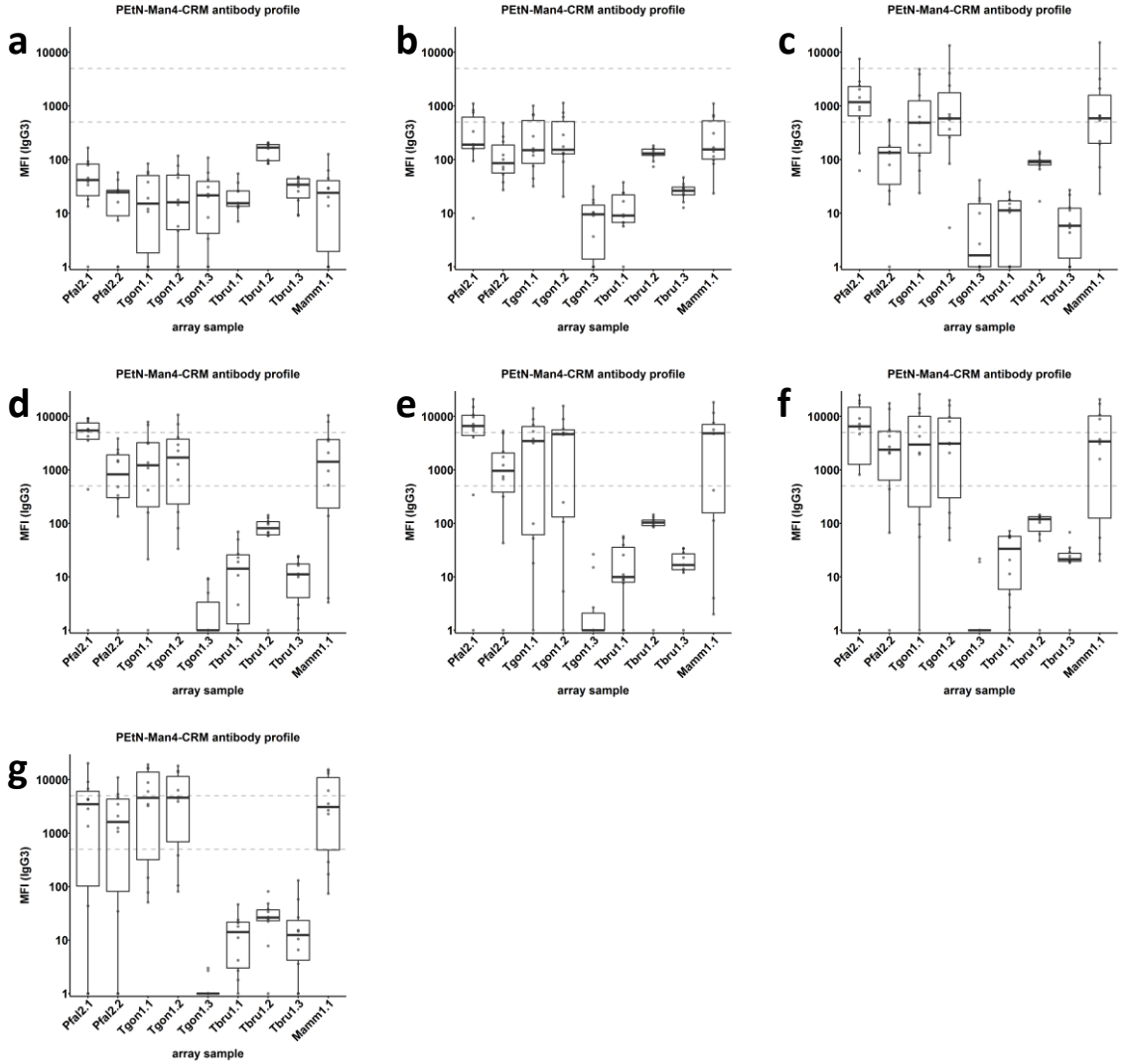

Figure 101: IgG3 titres against synthetic GPI fragments from other organisms in sera of mice immunised with glycoconjugate of 8. Group size n=10, classified by the immunising glycoconjugate. Titres at day **a)** 0, **b)** 7, **c)** 14, **d)** 21, **e)** 28, **f)** 35, **g)** 42.

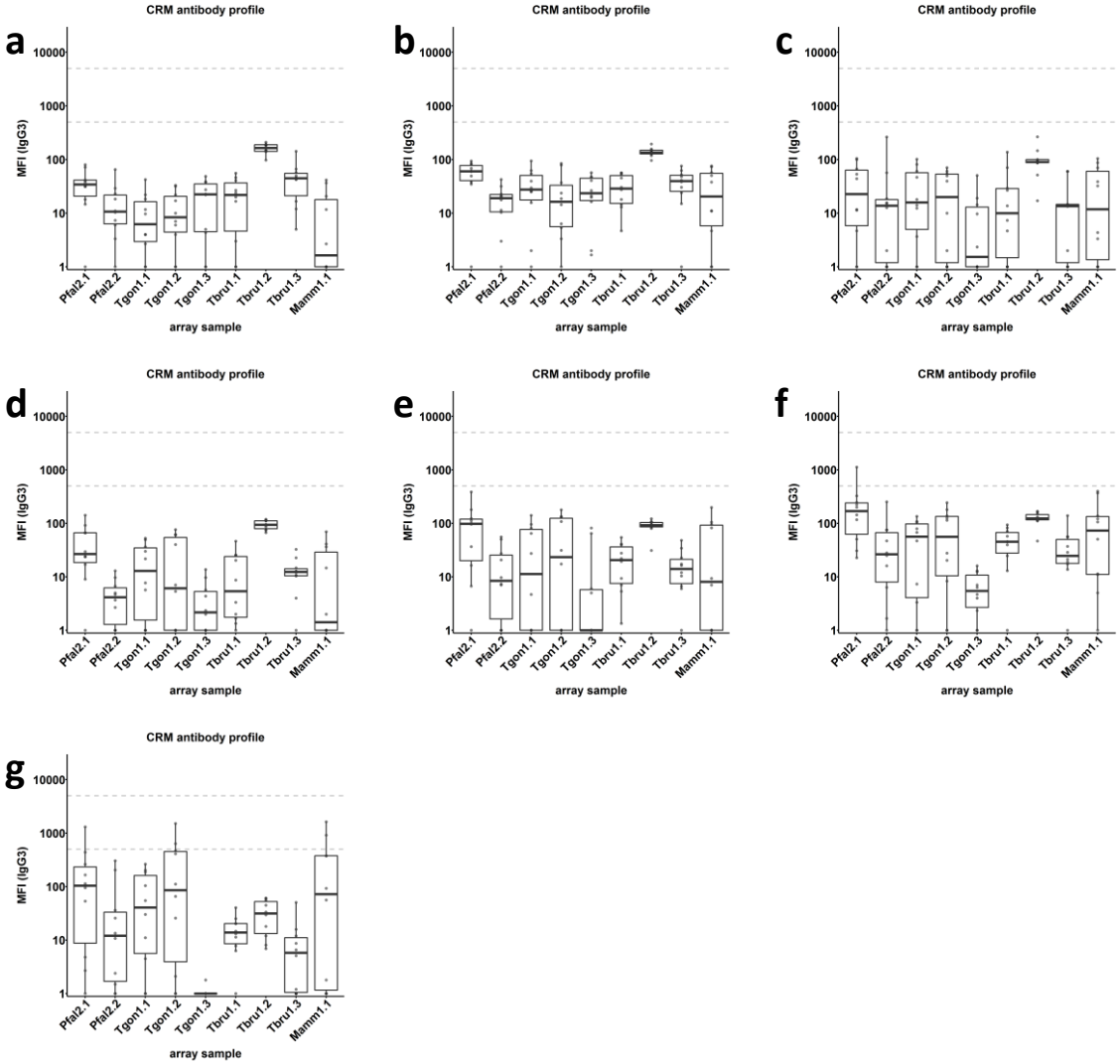

Figure 102: IgG3 titres against synthetic GPI fragments from other organisms in sera of mice immunised with CRM197 control. Group size n=10, classified by the immunising glycoconjugate. Titres at day **a)** 0, **b)** 7, **c)** 14, **d)** 21, **e)** 28, **f)** 35, **g)** 42.

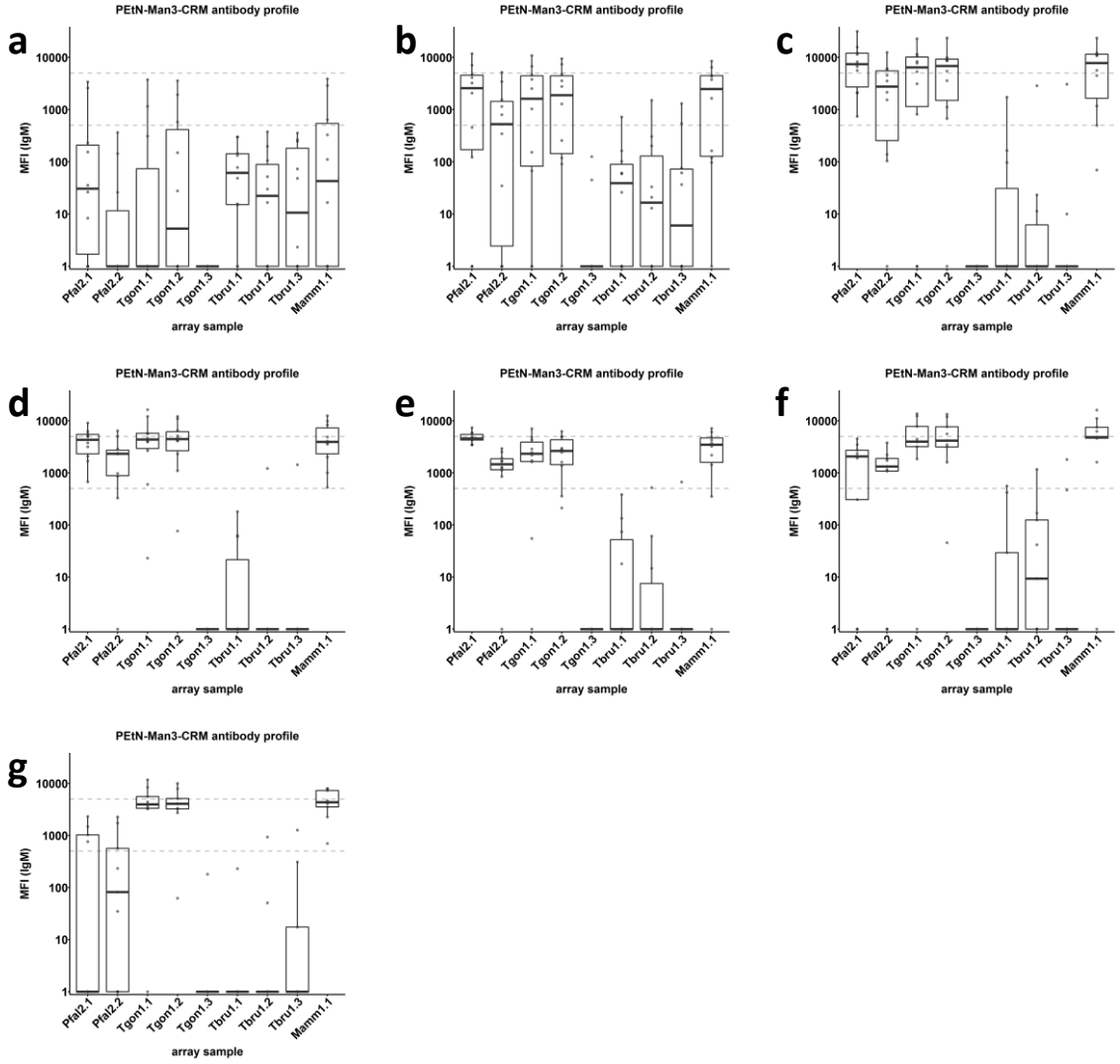

Figure 103: IgM titres against synthetic GPI fragments from other organisms in sera of mice immunised with glycoconjugate of 7. Group size n=10, classified by the immunising glycoconjugate. Titres at day **a)** 0, **b)** 7, **c)** 14, **d)** 21, **e)** 28, **f)** 35, **g)** 42.

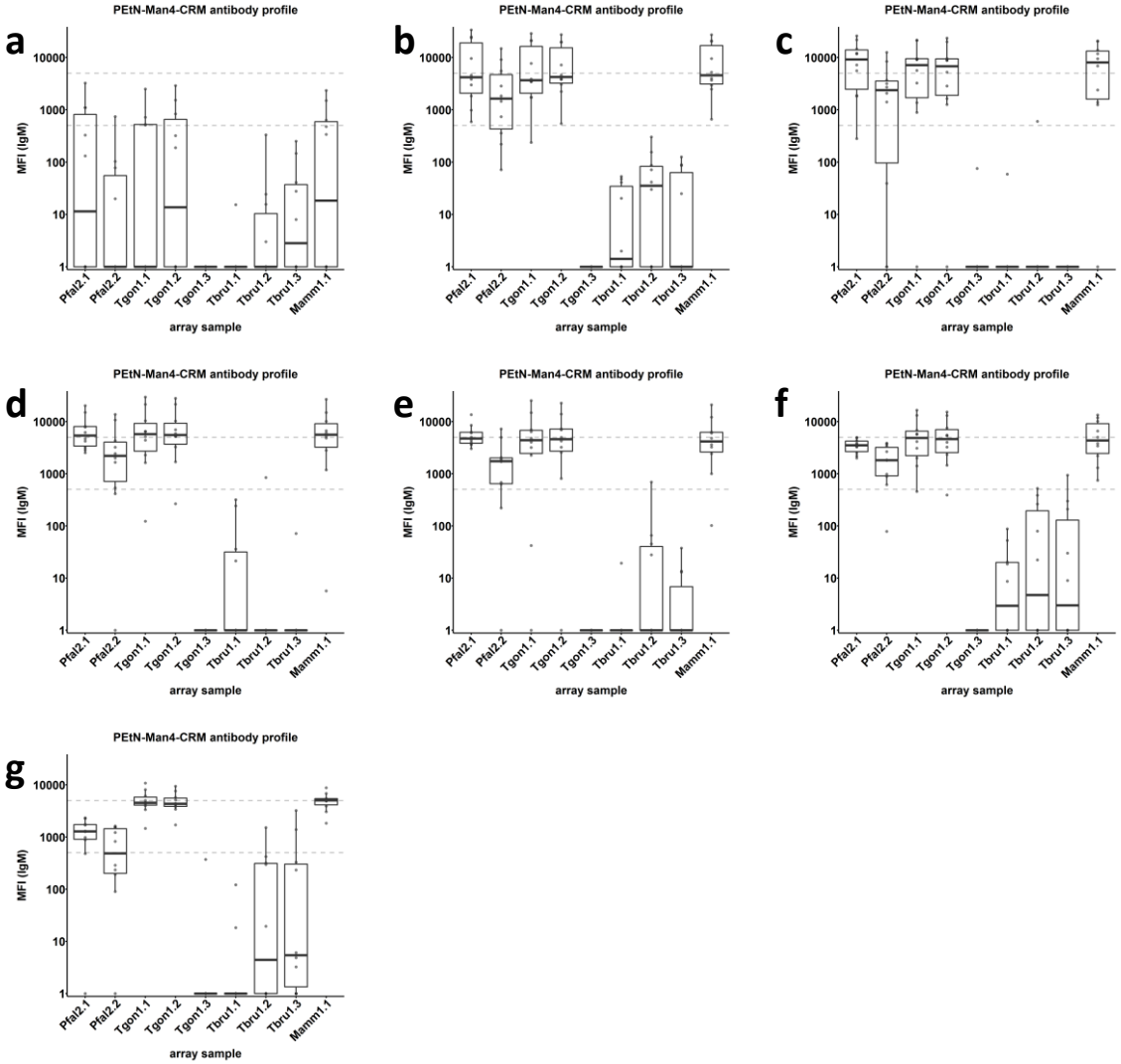

Figure 104: IgM titres against synthetic GPI fragments from other organisms in sera of mice immunised with glycoconjugate of 8. Group size n=10, classified by the immunising glycoconjugate. Titres at day **a)** 0, **b)** 7, **c)** 14, **d)** 21, **e)** 28, **f)** 35, **g)** 42.

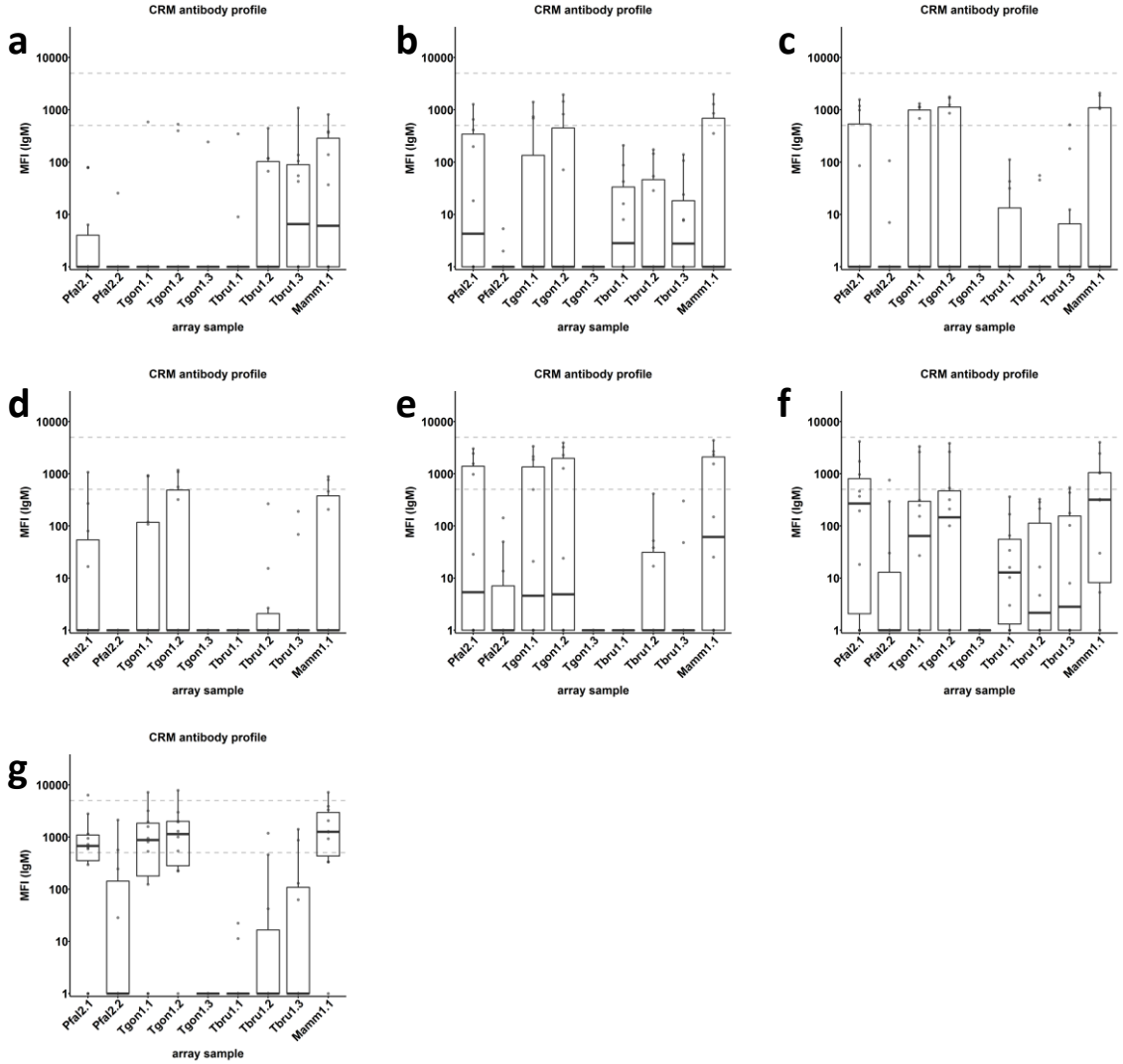

Figure 105: IgM titres against synthetic GPI fragments from other organisms in sera of mice immunised with CRM197 control. Group size n=10, classified by the immunising glycoconjugate. Titres at day **a)** 0, **b)** 7, **c)** 14, **d)** 21, **e)** 28, **f)** 35, **g)** 42.

Additional mouse data during the ECM challenge study

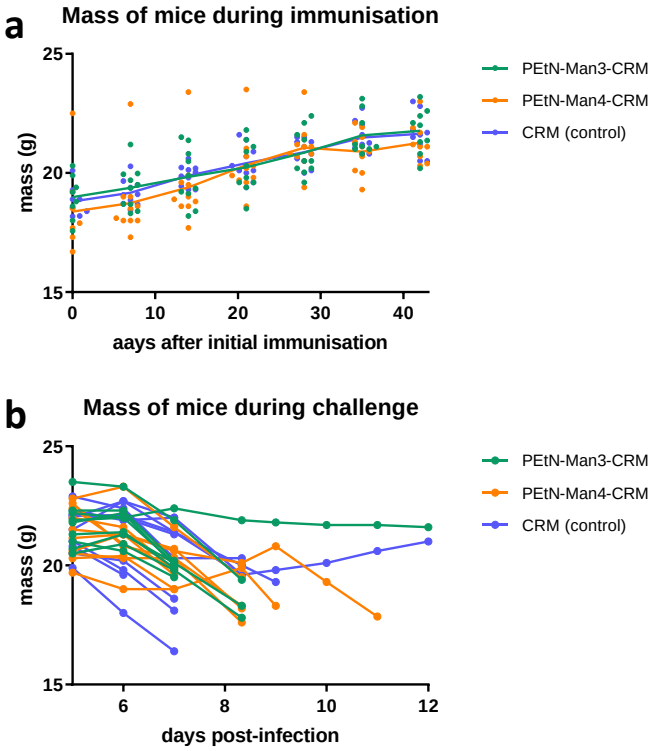

Figure 106: Mass of mice a) during immunisation and b) during challenge. Consistent with the model, mice lost weight after the challenge inoculation. Mice that were euthanised mice were as a result of neurological symptom development, before the other endpoint of extreme weight loss occurred.

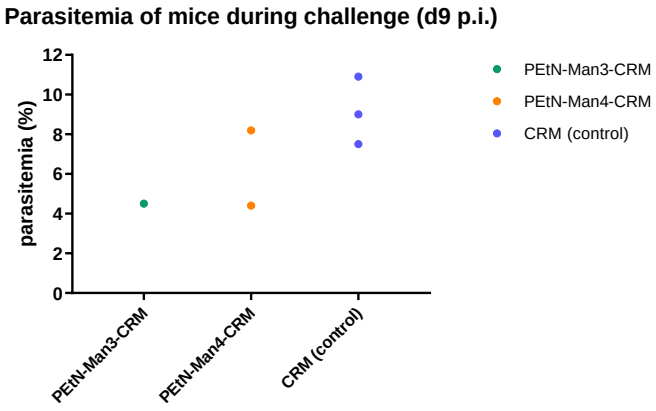

Figure 107: Parasitemia of mice at day 9 post-infection. Parasitemia appears lower at day 9 post-infection for surviving mice immunised with glycoconjugate of **7** and **8** compared to mice immunised with CRM197 only, however not enough mice are sampled to draw a conclusion.

Curriculum Vitae

[For reasons of data protection, the curriculum vitae is not published in the electronic version.]

[For reasons of data protection, the curriculum vitae is not published in the electronic version.]

[For reasons of data protection, the curriculum vitae is not published in the electronic version.]